

PINE CREEK CONSERVATION AREA

2013 MAPPING AND MONITORING REPORT



Eric M. Nielsen, Matthew D. Noone, James S. Kagan, and Matthew T. Lee
Institute for Natural Resources, Portland State University.



Acknowledgments

This project was completed through the effort and dedication of many individuals. Jason van Warmerdam and Michael Conroy led the 2011 field collection effort, with assistance from Berta Youtie, Rachel Brunner, and this report's coauthors. Treg Christopher assisted during the 2012 field collection effort, and Nick Bard graciously transcribed the field data collected that year. Lindsey Wise and Theresa Burcsu assisted with project management. Brigette Whipple, cultural resources manager for the Confederate Tribes of Warm Springs, provided valuable introductions to the cultural aspects of Pine Creek's ecology. Finally, we would have been unable to complete this work without the extraordinary hospitality of Rick Hayes, manager of the Pine Creek Conservation Area. Thanks to Rick for his patient instruction and for helping to make our time at the ranch comfortable.

Please cite this publication as:

Nielsen, E.M., M.D. Noone, J.S. Kagan, and M.T. Lee. 2013. Pine Creek Conservation Area Mapping and Monitoring Report. Institute for Natural Resources, Portland State University. Portland, Oregon. 138 pp., including attachments and appendices.

Contact information: Institute for Natural Resources – Portland
Portland State University
P.O. Box 751
Portland, OR 97207

OUTLINE

1. Introduction
 - 1.1. Project Area
 - 1.2. First Mapping Effort
 - 1.3. Current Mapping and Monitoring Effort

2. Project Organization
 - 2.1. Land-Cover Base Mapping
 - 2.2. Change Estimation
 - 2.2.1. Juniper Change Modeling
 - 2.2.2. Photo-Interpretation Sampling
 - 2.2.3. Vegetation Transects
 - 2.3. Cultural Plants Habitat Mapping

3. Discussion
 - 3.1. Current Conditions
 - 3.1.1. Western Juniper
 - 3.1.2. Big Sagebrush
 - 3.1.3. Riparian Woody Vegetation
 - 3.1.4. Other Shrubs
 - 3.1.5. Native Grasses
 - 3.1.6. Exotic Grasses
 - 3.1.7. Exotic Forbs
 - 3.2. Recent Change
 - 3.2.1. Western Juniper
 - 3.2.2. Big Sagebrush
 - 3.2.3. Riparian Woody Vegetation
 - 3.2.4. Other Shrubs
 - 3.2.5. Bunchgrasses
 - 3.2.6. Native Forbs
 - 3.2.7. Exotics
 - 3.3. Management Recommendations

4. Literature Cited
 - Attachment 1: Land-Cover Base Mapping
 - Attachment 2: Juniper Change Modeling
 - Attachment 3: Photo-Interpretation Sampling
 - Attachment 4: Vegetation Transects
 - Attachment 5: Mapping and Modeling Plants of Tribal Interest

1. INTRODUCTION

1.1. Project Area

Pine Creek Conservation Area (PCCA), just northeast of the John Day River in Wheeler County, Oregon, was acquired in 1999-2001 by the Confederate Tribes of Warm Springs with support from the Bonneville Power Administration (BPA), to mitigate for wildlife losses created by the large, hydropower Columbia River Dams, particularly the Bonneville, Dalles and John Day Dams. Many thousands of acres of grassland, shrub steppe and riparian habitats were lost due to inundation, and the objectives of the acquisition included restoration of similar habitats.

The majority of the approximately 35,000-acre conservation area was historically native grassland, dominated by bluebunch wheatgrass (*Pseudoroegneria spicata* ssp. *spicata*), Idaho fescue (*Festuca idahoensis*), sand dropseed (*Sporobolus cryptandrus*) and Thurber's needlegrass (*Achnatherum thurberianum*) and some patches of sagebrush steppe with Wyoming sagebrush (*Artemisia tridentata* ssp. *wyomingensis*). The bottomlands along Pine Creek had extensive bottomland hardwood forests and woodlands, riparian shrublands, mixed shrublands with black greasewood (*Sarcobatus vermiculatus*), basin big sagebrush (*Artemisia tridentata* ssp. *tridentata*) and Great Basin wildrye (*Leymus cinereus*). However, following years of management as a private ranch with fire suppression and altered fire regimes, much of the site has transitioned to woodlands of western juniper (*Juniperus occidentalis*). At the highest elevations there are small patches of Douglas-fir (*Pseudotsuga menziesii*) and Ponderosa pine (*Pinus ponderosa*) forests. The management objectives upon the property's acquisition were to restore as much as possible to the historic mix of grasslands, shrub steppe and riparian habitats.

The nearly 18,000 acres of adjacent public lands administered by the Department of the Interior (DOI), including the Clarno Unit of the John Day Fossil Beds National Monument and the Spring Basin Wilderness Area of the Bureau of Land Management, enhance Pine Creek's conservation value. Since the management objectives for conservation should be informed by knowledge of the condition of the surrounding public lands, we felt it important to incorporate those areas in our assessments. For most aspects of this report, therefore, the project area is defined as the conservation area itself in combination with the adjacent DOI land (Figure 1), approximately 52,500 acres in total.

1.2. First Mapping Effort

As part of an interagency agreement created in 2002, the Oregon Natural Heritage Information Center established a baseline monitoring program in 2002. This effort included the establishment of permanent monitoring plots to allow for a detailed assessment of vegetation change in the plant communities occurring at the site. It also included the development of an existing vegetation map, hopefully to allow for an analysis of overall vegetation change across the conservation area. The map showed the distribution of western juniper, native grasslands, big sagebrush, and weed-dominated areas at the site.

1.3. Current Mapping and Monitoring Effort

In the eight years since the original map was made, a series of management actions, including juniper clearing, prescribed fires, and riparian restoration activities have significantly changed the vegetation at PCCA. In the spring and summer of 2010, the Oregon Natural Heritage Information Center, now the Oregon Biodiversity Information Center at Portland State University, visited the area to assist the land manager in developing a strategy for meeting the information needs of the Tribes and BPA in evaluating the success of the first decade of restoration. This report details that effort, which incorporated a combination of field inspection, photo-interpretation, and remote sensing-based mapping to assess change since the establishment of the conservation area, to lay a new baseline against which to measure future change, and most importantly to provide detailed information useful for land management decision-making in the continuing restoration efforts.

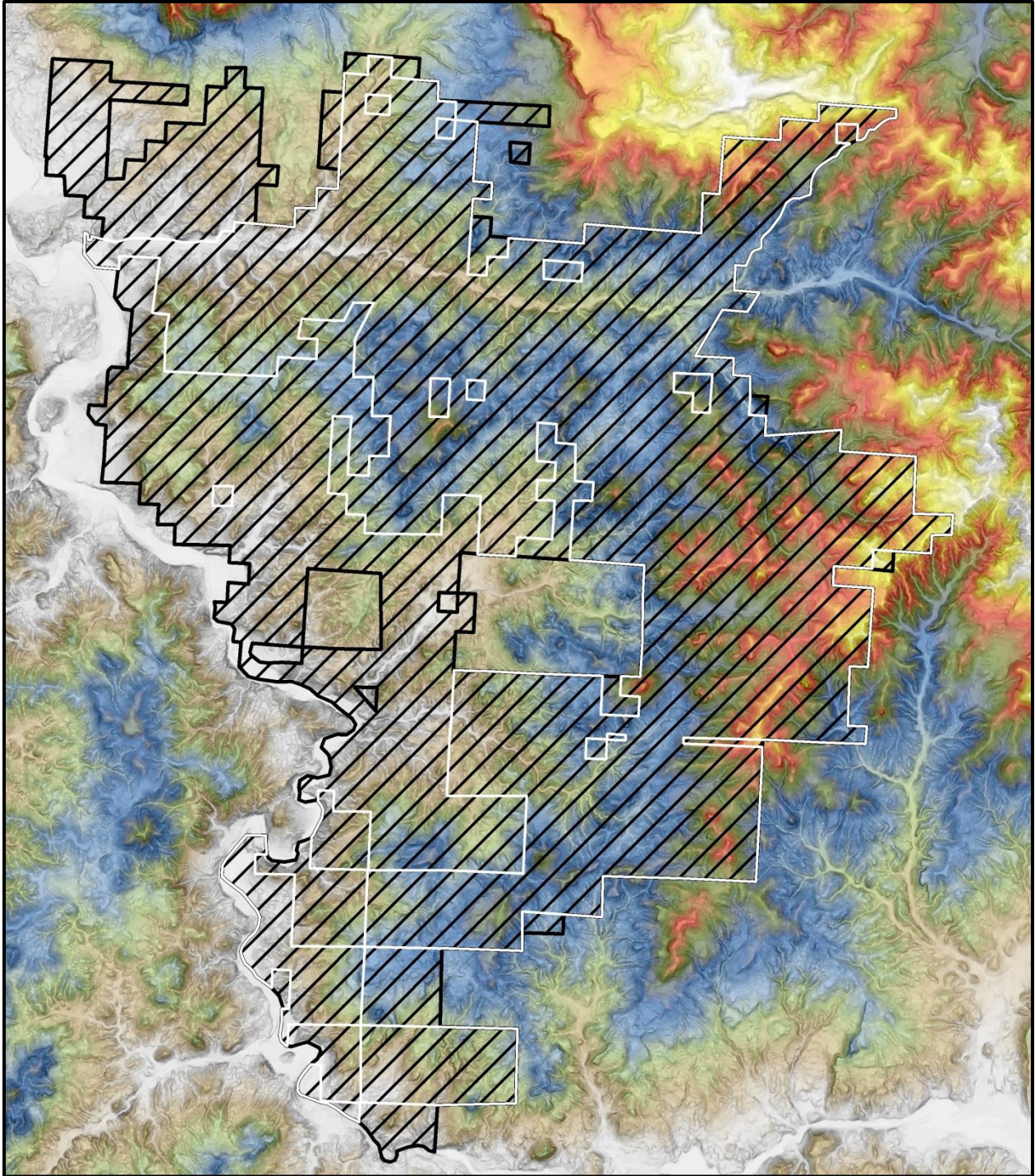


Figure 1. The Pine Creek Conservation Area boundary is shown in white; the hatched area represents the project and analysis area including adjacent public lands. Background layer is elevation.

2. PROJECT ORGANIZATION

2.1. Land-Cover Base Mapping (Attachment 1)

Constructing a new baseline vegetation map at 10-meter resolution using remote sensing mapping techniques was the central activity of the project. Rather than using a classification system to assign all locations in the project area to a single land-cover class, we broke land-cover down into 19 major categories, and produced percent cover maps for each. The resulting maps have much greater flexibility for supporting management activities and future remote sensing change detection work at PCCA. The accuracy level of the maps were enhanced by a LiDAR data collection flown in spring 2011, which greatly improved the spatial resolution of topographic data and also provided information on the height of vegetation canopies. The map modeling process was supported by the collection of cover data at 331 unique field plots, supplementing those with over 100 additional photo-interpreted (PI) plots.

Presence of most land-cover categories was modeled at accuracies between 80-90%, and cover modeling was also accurate for most categories. The resulting maps were used to make estimates of the area occupied and the total percent cover of each land-cover category over PCCA, the project area incorporating the adjacent DOI lands, and over an area including a 5-kilometer buffer around the boundary of PCCA. These area estimates will be useful in determining future change, even if the next iteration of monitoring is sample-based rather than relying on remote sensing. The main utility of the cover maps, however, will be to provide a flexible base on which to plan a wide variety of ongoing conservation management activities.

An extensive hydrological analysis was performed as an intermediate step in the land-cover mapping process, which the LiDAR data made possible. The delineated channel networks and potential riparian habitat, calibrated in the field, should also be helpful data in supporting future management work, assessing recovery of riparian systems, and supporting analysis of wildlife habitat.

2.2. Change Estimation

The original plan to derive decadal change estimates by comparing the maps produced in the 2002 effort to current conditions did not turn out as hoped. The accuracy levels of the previous map, made with a poor aerial photography dataset, were not sufficient to support comparison with the current map. Instead, we used three very different techniques to make change estimates for land-cover types of interest. The only technique of the three that produced a wall-to-wall change estimation map was an image-based change detection for western juniper. Change in big sagebrush, riparian woody vegetation, exotics, and other vegetation types relied on sample-based approaches, either from PI of current and historic aerial photography, or from the permanent vegetation transects installed in 2002.

2.2.1. Juniper Change Modeling (Attachment 2)

We used a remote sensing cover estimation approach to map cover of western juniper in 2002 and 2011, and differenced the images to determine areas of significant increase or decrease. Although LiDAR data was not available from 2002, we used the current LiDAR collection to train models to accurately predict juniper cover from aerial photography. The techniques we developed work reliably even with older photography of varying specifications. In addition to providing information about how much juniper change has occurred and where, we used the modeled change results to produce metrics describing the topographic settings in which juniper cover is increasing and decreasing.

2.2.2. Photo-Interpretation Sampling (Attachment 3)

Remote sensing-based approaches to change detection for land-cover types other than western juniper were not possible within our timeframe, given the poor accuracy of the 2002 map. However, despite not being able to produce a wall-to-wall map showing where changes had occurred, we were able to make

statistically sound estimates of change in the area occupied by big sagebrush stands, riparian woody vegetation, and western juniper through a photo-interpreted sampling exercise. 1000 randomly selected points were manually assessed for western juniper cover in 2002 and 2011 aerial photography; over 2400 points were assessed for riparian woody vegetation in the same two years. The methods differed for big sagebrush, which could not always be reliably distinguished in the older air photos. For big sagebrush we produced an estimate the coverage of big sagebrush stands in 2009, and a proportional change estimate from 2002 to 2009 based on those stands that could be confidently assigned in the 2002 photos. The PI results are the only estimates we have for change in big sagebrush and riparian woody vegetation; for western juniper they provide an alternate approach and a check on the remote sensing change modeling results.

2.2.3. Vegetation Transects (Attachment 4)

Most permanent vegetation transects installed in 2002 were revisited in 2011. Although they were not randomly located and were not enough in number to support reliable estimates of change across the conservation area, they provide important snapshots into change processes occurring at particular locations, and give context for understanding the other change results.

2.3. Cultural Plants Habitat Mapping (Attachment 5)

The final major product detailed in this report is an exercise in mapping habitat for two culturally important plants, bitterroot (*Lewisia rediviva*) and cous biscuitroot (*Lomatium cous*). We used field-generated presence and absence data, supplemented with additional locations determined in the office with reference to air photos and topography, to model potential habitat for both species. Although the model does not predict whether or not the habitat will be occupied, the maps produced provide a useful starting point in seeking new populations of these species.

3. DISCUSSION

3.1. Current Conditions

We used two main approaches to establish current conditions for various aspects of land-cover in the project area. The land-cover mapping process produced estimates of total area occupied and percent cover for each of 19 categories of land-cover (see Attachment 1). This method made use of all available data, and the models constructed were generally of high accuracy. For the land-cover types modeled at high accuracy (including western juniper, big sagebrush, and riparian woody vegetation), the primary caveat in their use is that they are calibrated to field estimates of cover which are not always accurate. It is possible that systematic biases toward higher or lower cover estimates exist within the maps depending on how accurately crews were able to visually estimate true cover in the field.

Photo-interpretation of aerial photography was used to estimate cover for several land-cover types (big sagebrush stands, riparian woody vegetation, and western juniper). The random sampling approach used for these assessments allows confidence intervals to be established and provides statistically defensible estimates. However, PI of tree cover can yield overestimates due to oblique viewing angles and the presence of shadows which can be difficult to distinguish from crowns.

3.1.1. Western Juniper (base mapping, juniper modeling)

The base map for coniferous trees (see Attachment 1, Table 10) indicated that western juniper is present over approximately 45% of the project area at greater than trace amounts (52% of PCCA land). The total projected canopy cover of juniper trees was estimated at 7.3% (8.9% at PCCA); the average juniper occurrence has about 16% canopy cover. More acres of juniper occurrence were found on west-facing aspects (see Attachment 2) but that may be due to the fact that the project area generally rises in

elevation to the east away from the John Day River. Lower canopy cover stands tend to occur more often on south-facing slopes, while north-facing slopes often support stands with greater canopy cover. Higher canopy cover stands also occur at higher elevations, generally over about 700 meters.

We chose to use the relationship between the land-cover mapping estimate of total juniper cover and the photo-interpreted juniper cover to derive a correction factor to compensate for cover overestimation, allowing accurate change estimates to be made from the photo-interpreted data. However, this meant that the photo-interpreted results no longer constituted an independent assessment of juniper cover for purposes of estimating current conditions.

3.1.2. Big Sagebrush (base mapping, photo-interpretation sampling)

The base map for big sagebrush (see Attachment 1, Table 10) indicated that big sagebrush is present over approximately 7.4% of the project area at greater than trace amounts (6.8% of PCCA land). The total projected canopy cover of big sagebrush was estimated at 0.72%, with an average occurrence having about 10% canopy cover. The PI resulted in an estimate that about 1.6% of all land in the project area was occupied by recognizable sagebrush stands. These estimates are compatible, as the stands recognizable in imagery were likely only the largest and densest sagebrush occurrences.

3.1.3. Riparian Woody Vegetation (base mapping, photo-interpretation sampling)

The base map for riparian woody vegetation (RWV, see Attachment 1, Table 10) indicated presence over approximately 190 acres (77 hectares) in the project area, nearly all of it on PCCA land. The photo-interpreted estimate was a total of 143 acres, but this did not consider all streams in the project area (though it did consider the major ones), and it also left out some RWV along the John Day River that was included in the base map. The estimates are in good agreement.

3.1.4. Other Shrubs (base mapping)

The base map for other shrubs—including mountain mahogany (*Cercocarpus ledifolius*), antelope bitterbrush (*Purshia tridentata*), gray and green rabbitbrushes (*Ericameria nauseosus* and *Chrysothamnus viscidiflorus*), broom snakeweed (*Gutierrezia sarothrae*), and others; see Attachment 1, Table 10—indicated a combined projected cover total of approximately 4%. The majority is made up of various shrubs tolerant of disturbance in rangeland environments (e.g., broom snakeweed, rabbitbrushes), and it is likely that most cover in this category consists of broom snakeweed, which may not be as beneficial to wildlife as some of the other shrubs. Mountain mahogany, antelope bitterbrush, and rigid sagebrush (*Artemisia rigida*) are all fairly uncommon, being present at only 1.2%, 3.5%, and 0.5% of sites in the project area at greater than trace amounts, amounting to projected cover totals of only 0.20%, 0.18%, and 0.10% respectively.

3.1.5. Native Grasses (base mapping)

The dominant bunchgrass at PCCA, bluebunch wheatgrass, is extremely widespread, being present at 87% of sites in the project area at greater than trace amounts, with a total projected cover of 15.5%. Idaho fescue is more restricted to cool slopes, but still occurs in meaningful amounts at 38% of sites for a total projected cover of 6.7%. Of the less widespread natives, sand dropseed occurs over 7.8% of the project area with a projected cover of 0.95%. Most of these occurrences are on DOI lands; it is much less common at PCCA. Needlegrasses, primarily Thurber's needlegrass, occur over 7.1% of sites but at lower density, and total only 0.5% in projected cover.

3.1.6 Exotic Grasses (base mapping)

The base map for exotic grasses (see Attachment 1, Table 11) indicated their presence over 87% of sites in the project area. Typical cover amounts were approximately 25%, resulting in a total projected

cover of about 22%. Both numbers were slightly lower at PCCA than on the adjacent DOI lands. Though these numbers are high, the combined projected cover of bluebunch wheatgrass and Idaho fescue was slightly higher than that of exotic grasses.

3.1.7 Exotic Forbs (base mapping)

The base map for exotic forbs (see Attachment 1, Table 11) indicated their presence over 27% of the project area (34% on DOI lands, but only 24% at PCCA). They generally occur at lower cover amounts than exotic grasses, and have total projected cover estimated at 2.5% (3.0% on DOI lands, but just 2.2% at PCCA).

3.2. Recent Change

We used three quite different approaches to make assessments of change over the period of time since the initial PCCA survey effort in 2002. As the different methods each have their strengths and weaknesses, it is valuable to consider their results together.

The permanent plot transects established in 2002 were revisited and resampled in 2011, yielding a non-random but representative set of species cover and diversity estimates (see Attachment 4). 52 transects were resampled, producing a total of 2600 point intercept samples and 5200m² of area sampled for species diversity. Although the utility of the datasets produced for statistical analysis is limited by the relatively small sample size and non-random sample locations, they do cover a variety of the habitats at PCCA, and the in-depth information they provide about species diversity and cover of individual plants is not available from any other source. The resulting datasets are available only in tabular form, as the small sample size does not allow any spatial conclusions to be drawn.

PI of aerial photography was used to compare the cover change since 2002 of western juniper individuals, big sagebrush stands, and riparian woody vegetation (RWV) (see Attachment 3). Although all these vegetation types are included in the 2011 vegetation base map (Attachment 1), that map relied on data sources (e.g., LiDAR) that were not available in 2002, so estimating change from historic conditions required another approach. The fine spatial scale needed to assess these types required that we rely on aerial photography rather than coarser resolution satellite data. We used a random sampling approach to estimate cover of these types for both 2002 and more recently (2009 for sagebrush stands, 2011 for juniper and RWV). The random sampling approach used for these assessments allows confidence intervals to be established and provides the most statistically defensible estimates. However, there are possible data quality issues involved in using air photos, due both to the effects on apparent surface cover resulting from varying geometry across individual photos and to difficulties in interpretation itself. The latter was a greater issue for sagebrush stand sampling than for juniper or RWV. Despite these difficulties, the PI methodology provides the most reliable change estimates, and while continuous maps cannot be produced, visualizing the outcomes of the samples themselves in map form can be informative (see Attachment 3, Figures 4-6).

A remote sensing modeling technique was used to produce continuous maps of western juniper cover in 2002 and 2011, and of change occurring in the intervening time (see Attachment 2). This method relied on an automated analysis of both air photos and medium resolution Landsat TM imagery from both dates, and was calibrated using high quality maps of juniper distribution derived from the 2011 LiDAR collection. Although this approach was not feasible with any other vegetation type than western juniper and the results are not as amenable to statistical interpretation as the random sampling approach, the spatially-explicit outputs are very informative regarding the patterns of juniper change and will be key for planning future management activities.

In brief, all of the methods concurred that cover amounts of both western juniper and big sagebrush have declined over the monitoring period. Riparian woody vegetation was found via PI to have increased. The permanent plots indicated an increase in bunchgrasses and mesic habitat shrubs, especially at higher

elevations, and a decrease in most exotic vegetation. Native forbs were found to have decreased in cover, but that was likely due to differences in sampling date necessitated by weather conditions in 2011. Greater detail is given about each of these vegetation categories below.

3.2.1. Western Juniper (*juniper modeling, photo-interpretation sampling, permanent plots*)

All approaches registered a significant decline in western juniper cover on both PCCA and DOI lands, with fractional decreases on DOI land greater than on PCCA land. Juniper elimination was partially offset by expansion, which occurred at about 20% the rate of elimination overall. Continued expansion is a significant issue on PCCA land, where it occurred at about 25% the rate of elimination. Monitoring on permanent plots indicated that in general the elimination of juniper is accompanied by improvement in ecological conditions, although fires can have negative (but likely temporary) impacts on other native species.

The change detection modeling approach estimated that about 4300 acres of juniper stands were lost between 2000 and 2011, fairly evenly split between PCCA (about 2500 acres) and DOI (about 1800 acres). Because of the much greater amount of juniper on PCCA land to begin with, the loss constituted a much larger portion of the total DOI juniper acreage (32%) than of the PCCA acreage (11%). Overall, there was a relative decrease of about 16% in juniper stand acreage from 2000 to 2011 across the entire project area, with about three-quarters of this decrease occurring on northwestern, northern, and northeastern aspects.

Photo-interpreted results, based on individual tree crown cover rather than woodland extents, were consistent with the modeled results. A total of about 800 acres of trees were eliminated between 2002 and 2011, ~520 acres from PCCA land and ~290 acres from DOI land. This was partially offset by expansion of juniper on about 170 acres, mostly on PCCA land (~130 acres vs. ~34 acres on DOI land). This resulted in a net decrease of ~640 acres of juniper trees (14% of the total 2002 cover), with ~380 acres of decrease estimated on PCCA land (11% of the total 2002 cover), and ~250 acres of decrease estimated on DOI land (24% of the total 2002 cover). Assuming that an average juniper stand has approximately 15-20% canopy closure, the change modeling and PI results are in nearly perfect agreement.

Decreases in juniper cover were likewise observed on the permanent plots, where 12 of the 22 plots classes as juniper plots in 2002 exhibited measurable, and often complete, declines. This rate of decrease is very high compared to the estimates based on the above approaches, either due to chance resulting from the low sample size, or due to the non-random distribution of the transects and disproportionately sampled effects of particular fires. Half of the 2002 juniper plots showed improved ecological conditions, while only three of the plots worsened. Some plots where juniper was reduced showed poorer conditions, due to fire impacts on bunchgrasses and native forbs and increases in non-native plants. These negative impacts are likely not permanent.

Juniper expansion occurred on some of the permanent plots, where two of the 19 grassland plots were significantly invaded and are now properly classified as juniper-dominated. The total juniper crown cover estimated via point intercept sampling was 7.4% in 2002, and just under 5% in 2011. This represents a 34% relative decrease, almost entirely due to wildfires on PCCA land. Again, this represents a significant overestimate of decline compared to the results yielded by the more rigorous methods above.

3.2.2. Big Sagebrush (*photo-interpretation sampling, permanent plots*)

Both approaches registered a significant decrease in big sagebrush cover over the time period 2002 - 2009, or 2002 - 2011. Although the PI sampling estimated the extent of sagebrush stands rather than crown cover of individual plants, and the permanent plots provided limited precision due to the small sample size, the results of the two methods were nevertheless in good agreement. The decrease occurred on both PCCA and DOI lands, but fractional decrease was somewhat greater on PCCA land. In large part,

sagebrush decrease seems to have resulted from fire, which presents a downside to the use of fire as a management tool for controlling or reversing juniper expansion.

PI of change in big sagebrush was done on the basis of recognizable stands of sagebrush rather than individual plants, which were not reliably distinguishable in air photos. Due to the poorer quality of older photography, it was impossible to estimate increase in sagebrush stand extent. To arrive at a change estimate, it was necessary to assume a rate of sagebrush stand expansion. Making the fairly generous assumption that sagebrush stand expansion since 2002 accounted for 10% of existing sagebrush stands in 2009, we estimated that the fractional cover of sagebrush stands on PCCA lands declined from 2.5% in 2002 to 1.6% in 2009. On all land in the project area, the decline was from 2.3% in 2002 to 1.6% in 2009. Most of the sagebrush area lost came from reduction of the extent of persisting stands, although a significant number of stands were eliminated completely. Sagebrush loss occurred in numerous portions of the project area, and mostly seemed to result from fire. However, juniper encroachment also contributed significantly, and was responsible for reducing the size of many persisting sagebrush stands.

Decreases in big sagebrush cover were likewise observed on the permanent plots, mostly in response to wildfires. Out of eight shrubland plots with big sagebrush in 2002, the 2011 sampling indicated that sagebrush had disappeared completely from four of them and declined in two others. The impact of juniper expansion was also felt: out of the four juniper plots with big sagebrush as a stand component in 2002, three no longer had sagebrush in 2011. The total big sagebrush crown cover estimated via point intercept sampling was 2.2% in 2002, and only 1.3% in 2011.

3.2.3. Riparian Woody Vegetation (photo-interpretation sampling, permanent plots)

No RWV was observed in the permanent plots, so our conclusions here come completely from PI sampling. RWV increased over both the eastern and western portions of Pine Creek, as well as all the other riparian zones in the project area considered cumulatively. The relative increase was particularly large on the western portion of Pine Creek, where the RWV cover in 2002 was significantly lower than on the eastern portion. We estimated an RWV increase on western Pine Creek from 10.6 acres in 2002 to 15.8 acres in 2011, on eastern Pine Creek from 22.2 acres to 26.7 acres, and on all other riparian zones from 48.9 acres to 63.6 acres. The total RWV increase over the entire project area was estimated to be from 105.3 acres in 2002 to 142.8 acres in 2011.

3.2.4. Other Shrubs (permanent plots)

The permanent plots indicated a cover increase for mountain mahogany, antelope bitterbrush, snowberry (*Symphoricarpos albus*), and native roses (*Rosa* spp.). All mesic shrubs increased at higher elevations, due to livestock removal. However, small weedy native shrubs, including broom snakeweed and green rabbitbrush, declined from 2.5% to 1.5% cover over the monitoring interval.

3.2.5. Bunchgrasses (permanent plots)

The permanent plots indicated an increase in most native bunchgrasses, especially for those most sensitive to livestock impacts such as Idaho fescue, bluebunch wheatgrass, and Thurber's needlegrass. Sand dropseed also increased, possibly due to the adaptive advantage of its C4 photosynthetic pathway in a warming climate. On the other hand, declines were observed in smaller, more disturbance-tolerant native grasses such as Sandberg bluegrass (*Poa secunda*), needle-and-thread (*Hesperostipa comata*), Indian ricegrass (*Achnatherum hymenoides*), and squirreltail (*Elymus elymoides*), likely due to increased competition with the rebounding larger bunchgrasses.

3.2.6. Native Forbs (permanent plots)

The permanent plots indicated that native forbs generally declined in cover, likely due to the later sampling date in 2011 as compared to 2002. Increasing bunchgrass cover, short-term impacts of fire, and

variability in spring and early summer rainfall might also have played a role, however, Cover changes were minor, and overall diversity did not appear to be significantly altered.

3.2.7. Exotics (permanent plots)

The permanent plots indicated decreases in most exotic plants, other than medusahead (*Taeniatherum caput-medusae*), which increased from 2.4% to 3.4% overall cover and became established across the conservation area. Other increasing exotics were teasel (*Dipsacus fullonum*) and common mullein (*Verbascum thapsus*). These biennials were not present in 2002 but have now appeared, although they are primarily limited to riparian areas. Their appearance may be due to either rising water tables or late season flooding. Ventenata (*Ventenata dubia*) also has been increasing in the region, but only appeared in a single plot. Annual bromes, including cheatgrass (*Bromus tectorum*), declined from 2002 levels but remained very high, at 24% overall cover in 2011. Introduced thistles (*Cirsium* spp.) dropped from 0.15% cover in 2002 to a mere 0.04% in 2011.

3.3. Management Recommendations

Based on the 2011 and 2012 surveys and the different analyses of change since the Pine Creek Conservation Area was acquired in 2001, existing management plans and activities appear to have been remarkably effective in meeting the objectives of the conservation area. Overall, the amount of western juniper in PCCA has declined, the area dominated by native bunchgrasses appears to have increased, and there is remarkable recovery in some of the riparian areas. However, there are some recommendations which this work, and similar research in central Oregon, indicate might improve the overall recovery rate.

Recommendation 1. Continue with efforts to manually restore areas that had been previously farmed or had been heavily impacted by livestock due to salt or water placement.

While recovery appears to be occurring throughout much of PCCA, there has been almost no recovery of native species in these heavily impacted areas. They provide a concentration of exotic species and they are sources of seeds that can impact adjacent areas if burned. The plans being developed by the U.S. Forest Service to restore the formerly farmed areas along Pine Creek and Highway 218 will address the largest areas of these habitats. However, if these methods are effective, it would certainly be beneficial if they could be applied to the other large disturbance patches at the site, perhaps with an initial focus on areas dominated by medusahead.

Recommendation 2. Use sand dropseed, Thurber's needlegrass and Great Basin wildrye in restoration.

Based on our observations, these three species seem to be increasing and able to compete with the introduced species present at PCCA. They occur in the types of habitats most in need of restoration, and are likely to persist over time. Sandberg bluegrass is often recommended because it grows and establishes quickly, but given the steep declines at the site, it probably should be avoided. Native seed sources are available from local vendors.

Recommendation 3. Expand the capacity to use wildfire as a management technique.

There is strong circumstantial evidence that declines in western juniper cover at PCCA resulted from the combination of livestock exclusion and the fortuitous occurrence of multiple wildfires in areas where understory fuels and native grasses were present. In addition, while the most productive grasslands at PCCA are on north-facing slopes, recovery appears to be occurring on all aspects and slope positions; and on almost all soil types. Because of the terrain, prescribed fire is difficult to use in most locations at PCCA, but expanding the conditions under which wildfire is permitted across the site is recommended. This might include expanding work with the BLM to increase the ability to use the John Day River and Pine Creek as meaningful fire barriers on the north, west and southern boundaries of PCCA, creating some barrier to spread on the west, and acquiring the large private inholding, already a priority.

Recommendation 4. Explore the use of early spring prescribed fire in consecutive years to address western juniper and invasive species on south slopes.

While the research from PCCA and Rowe Creek indicate the best opportunities for meaningful restoration and juniper control occur on the more productive north or northeast slopes, there are some low gradient south-facing slopes and toe slopes that appear to support significant bunchgrass and native forb vegetation. However, some of these locations have had very heavy invasions of annual grasses following wildfires. The best example of this are the slopes and the lower ridges around Cove Creek. This area is currently has high cover of many invasive annual grasses, but also has sufficient native forbs and grasses that recovery is likely possible. Cool season burns are effective ways of significantly reducing the annual grass seed bank as well as removing some juniper-related fuels in a less damaging way than hot fires. Assuring that livestock is kept away from the area is critical if this type of restoration is undertaken, but significantly reducing the annual seed inputs to the Pine Creek bottomlands could provide additional benefits.

Recommendation 5. Protect or insulate the large remaining sagebrush or other shrub patches from late-season, hot wildfires.

It may be very difficult to do this for sagebrush, although many of the remaining large patches of sagebrush are located near the John Day River where it may be possible to establish natural fire breaks, or use cool season burns to reduce flashy fuels. Bitterbrush and mountain mahogany may be higher priority wildlife habitats at PCCA despite occurring at high cover in only limited parts of the conservation area. The large patches of these species should be protected as well, although their habitat (especially for mountain mahogany) provides some natural protection from fire.

Recommendation 6. Consider experimental removals of some very dense juniper patches, through fire or cutting.

Current thinking is that the best places to focus juniper removal are those places with lower cover of juniper and higher cover of native bunchgrasses. The mapping results indicate that most juniper stands at PCCA have 20% or lower juniper cover. For these areas, wildfires are likely to lead to significant recovery of the prior type which occurred at the site. However, there are some very dense stands present as well, with juniper cover over 35%. It would be useful to know, at least on a local basis, whether or not recovery can occur in these areas if livestock is not present.

Recommendation 7. Remove isolated junipers by cutting in areas where a wildfire has already removed most of the trees.

There are some large areas of PCCA where western juniper has been almost entirely eradicated by wildfire. However, isolated trees remain on many of the deep-soiled north slopes, where trees were able to survive the fire. While juniper is easily spread by birds over large distances, most seed dispersal occurs locally, and these isolated trees are a continual source of seeds. In slopes where natural rocky juniper habitats do not occur uphill, removal of isolated junipers may be able to slow the reinvasion of juniper into the local sites, and make repeated fires unnecessary, potentially allowing for more rapid regeneration of bitterbrush and sagebrush.

Recommendation 8. Collect data on the distribution of ventenata, and identify biological control methods if possible.

While there is no direct evidence that ventenata is likely to spread throughout PCCA, including areas where livestock is excluded, the potential should not be ignored. The species has shown abilities to invade natural grasslands and shrub steppe in a number of Research Natural Areas with excluded livestock. Most of the spread of ventenata has been at higher elevation and more mesic sites, and it is possible that the majority of PCCA is too hot and dry to support the species. However, monitoring the spread is probably wise, given the potential damage the species may be able to cause.

4. LITERATURE CITED

- Berry, M. 2006. Pine Creek Conservation Area Monitoring Report. Technical Report to BPA, Confederated Tribes of the Warm Springs, Fossil, OR.
- Breiman, L. 2001. Random Forests. *Machine Learning* 45(1):5-32.
- Buechling, A., and C. Tobalske. 2011. Predictive habitat modeling of rare plant species in Pacific Northwest forests. *Western Journal of Applied Forestry* 26: 71-81.
- Chavez, P.S. 1988. An improved dark-object subtraction technique for atmospheric scattering correction of multispectral data. *Remote Sensing of Environment* 24: 459-479.
- Chen, X., L. Vierling, and D. Deering. 2005. A simple and effective radiometric correction method to improve landscape change detection across sensors and across time. *Remote Sensing of Environment* 98: 63-79.
- Congalton, R.G. 1991. A review of assessing the accuracy of classifications of remotely sensed data. *Remote Sensing of Environment* 37:35-46.
- Congalton, R.G., and K. Green. 1999. *Assessing the accuracy of remotely sensed data: Principles and practices*. Lewis Publishers, Boca Raton, Florida.
- Coppin, P.R., and M.E. Bauer. 1994. Processing of multitemporal Landsat TM imagery to optimize extraction of forest cover change features. *IEEE Transactions on Geoscience and Remote Sensing* 32:918-927.
- Crist, E.P., and R.C. Cicone. 1984. A physically-based transformation of thematic mapper data- the TM tasseled cap. *IEEE Transactions on Geoscience and Remote Sensing* GE22(3):256-263.
- Elzinga, C.L., D.W. Salzer, J.W. Willoughby, and J.P. Gibbs. 2001. *Monitoring Plant and Animal Populations: A Handbook for Field Biologists*.
- Franklin, J. 2009. *Mapping Species Distributions: Spatial Inference and Prediction*. Cambridge University Press, New York.
- Hall, D.K., G.A. Riggs, and V.V. Salomonson. 1995. Development of methods for mapping global snow cover using moderate resolution imaging spectroradiometer data. *Remote Sensing of Environment* 54: 127-140.
- Hijmans, R.J., and J. van Etten. 2012. raster: Geographic analysis and modeling with raster data. R package version 1.9-92. <http://cran.r-project.org/package=raster>.
- Jennings, Michael D., Don Faber-Langendoen, Orie L. Loucks, Robert K. Peet, and David Roberts. 2009. Standards for associations and alliances of the U.S. National Vegetation Classification. *Ecological Monographs* 79:173–199. <http://dx.doi.org/10.1890/07-1804.1>
- Jin, S., and S.A. Sader. 2005. Comparison of time series tasseled cap wetness and normalized difference moisture index in detecting forest disturbances. *Remote Sensing of Environment* 94:364-372.
- Keitt, T.H., R. Bivand, E. Pebesma, and B. Rowlingson. 2012. rgdal: Bindings for the Geospatial Data Abstraction Library. R package version 0.7-8. <http://cran.r-project.org/package=rgdal>.
- Lambin, E.F., and A.H. Strahler. 1994. Change-vector analysis in multitemporal space: a tool to detect and categorize land-cover change processes using high temporal-resolution satellite data. *Remote Sensing of Environment* 48: 231-244.
- Liaw, A., and M. Wiener. 2002. Classification and regression by Random Forests. *R News* 2:18-22.
- McCune, B. 2007. Improved estimates of incident radiation and heat load using non-parametric regression against topographic variables. *Journal of Vegetation Science* 18: 751-754.
- Moore, I.D. 1991. Digital terrain modeling: a review of hydrological, geomorphological, and biological applications. *Hydrological Processes* 5: 3-30.
- Nielsen, E.M., J.S. Kagan, L.K. Wise, and C. Copass. In press. Mount Rainier National Park vegetation classification and mapping project report. Natural Resource Report NPS/MORA/NRR. National Park Service, Fort Collins, Colorado.
- Parker, G.G., and M.E. Russ. 2004. The canopy surface and stand development: assessing forest canopy structure and complexity with near-surface altimetry. *Forest Ecology and Management* 189: 307-315.

- Pike, R.J., and S.E. Wilson. 1971. Elevation-relief-ratio, hypsometric integral, and geomorphic area-altitude analysis. *Geological Society of America Bulletin* 82: 1079-1083.
- R Development Core Team. 2012. *R: A language and environment for statistical computing*. R Foundation for Statistical Computing, Vienna, Austria. ISBN 3-900051-07-0. <http://www.r-project.org>.
- Rouse, J.W., R.H. Haas, J.A. Schell, and D.W. Deering. 1973. Monitoring vegetation systems in the Great Plains with ERTS. *Third ERTS Symposium, Vol. I*.
- Royle, J.A., R.B. Chandler, C. Yackulic, and J.D. Nichols. 2012. Likelihood analysis of species occurrence probability from presence-only data for modeling species distributions. *Methods in Ecology and Evolution*. Wiley. 10 pp.
- SAGA-GIS. 2012. System for Automated Geoscientific Analyses. <http://www.saga-gis.org>.
- Shreve, R.L. 1966. Statistical law of stream numbers. *Journal of Geology* 74: 17-37.
- Sing, T., O. Sander, N. Beerenwinkel, and T. Lengauer. 2005. ROCr: visualizing classifier performance in R. *Bioinformatics* 21:3940-3941.
- Stohlgren, T.J., C.S. Jarnevich, W. Esaias, and J.T. Morissette. 2011. Bounding species distribution models. *Current Zoology* 57: 642-647.
- Twele, A. 2006. The effect of stratified topographic correction on land cover classification in tropical mountainous regions. *ISPRS Commission VII Mid-term Symposium: Remote Sensing From Pixels to Processes*. Enschede, the Netherlands.
- Williams, J.N., C. Seo, J. Thorne, J.K. Nelson, S. Erwin, J.M. O'Brien, and M.W. Schwartz. 2009. Using species distribution models to predict new occurrences for rare plants. *Diversity and Distributions* 15: 565-576.
- Wilson, E.H. and S.A. Sader. 2002. Detection of forest harvest type using multiple dates of Landsat TM imagery. *Remote Sensing of Environment* 80: 385-396.



ATTACHMENT 1

LAND-COVER BASE MAP



Eric Nielsen

Institute for Natural Resources, Portland State University

1. INTRODUCTION

The land-cover base map is the core product of this project. The data developed here can be used to support and guide a wide range of management activities at Pine Creek Conservation Area (PCCA) and the surrounding lands. It can also serve as an accurate baseline for change detection in the future. This report section describes the base map products and the methods by which they were developed.

Some changes were made in the products provided compared to those originally proposed. Rather than mapping at a polygon scale with a minimum map unit of one-half hectare, we chose to produce a pixel-based map at much higher resolution. This permits the identification of smaller vegetation patches than would be possible with the originally proposed product. We also had originally planned to produce a classified map by assigning each location to one of 10-12 unique vegetation classes. However, no existing classification appeared to meet the management needs at PCCA, which seemed better served by creating cover maps for a variety of different land-cover elements. Reducing the existing vegetation complexity into a small number of classes would have reduced the flexibility and utility of the map data products considerably, and would also have been much less appropriate as a base for future change detection work.

We originally planned to make change maps for juniper, invasive grasses and forbs, and riparian and upland shrubs. We found that the quality of the 2002 mapping was not sufficient to support this endeavor, and attempted other means of change mapping. The only vegetation type for which we were successful in mapping change was western juniper (see Attachment 2). The variable annual greenup timing and vigor of annual plants, and limited resolution of satellite imagery available from the earlier time period did not permit reliable change mapping for those types. Similar issues of spatial resolution and the difficulty of distinguishing riparian woody vegetation and upland shrubs based on aerial photography alone made accurate change mapping for those classes impossible. As a substitute, reliable cumulative estimates of change in riparian vegetation and big sagebrush were produced through photo-interpretation (see Attachment 3); however, this was not possible for herbaceous plants. The accuracy of the new maps should permit estimates of change in all of the above vegetation types over the next monitoring cycle.

1.1. Mapping Area

The base mapping area was defined as the 2012 PCCA boundary, buffered by five kilometers on all sides. However, field sampling for model training only occurred on PCCA land and adjacent public lands (equivalent to the project area referenced in other sections of this report). Reliability of the map products will decrease with increasing distance from the training area due to the lack of field sampling. However, we felt it was important to provide spatial context for understanding the environment surrounding PCCA.

1.2. Primary Products

In addition to describing the base mapping methodology, the following primary products are presented and discussed in the subsequent pages:

Base Layers – backdrop and reference imagery

- (1) 4-band color-IR aerial photography at 1-meter resolution, from the 2012 Oregon NAIP (National Agricultural Imagery Program) collection
- (2) LiDAR bare earth elevation and vegetation height, at 1-meter resolution

Vegetation Canopy Layers – based on LiDAR vegetation height data

- (1) Percent canopy cover of vegetation over 8' in height, at 10-meter resolution
- (2) Percent canopy cover of vegetation over 3' in height, at 10-meter resolution

- (3) Dominant vegetation height—the height which is equaled or exceeded by only 12.5% of the surrounding 10-meter area

Hydrological Layers – based on LiDAR bare earth data, products field-calibrated

- (1) Delineated perennial channels (including seasonal channels)
- (2) Delineated intermittent channels
- (3) Riparian areas, potentially hosting riparian woody vegetation

Base Map Outputs – vegetation map products produced for 19 separate land-cover categories

- (1) Likelihood of occurrence, at 10-meter resolution
- (2) Predicted percent canopy cover, at 10-meter resolution

Tabular Outputs –

- (1) Rank-based associations between predictor variables and land-cover category cover amounts
- (2) Bootstrapped accuracy assessment for predicted occurrences of each land-cover category
- (3) Bootstrapped R^2 and root-mean-square error of cover models for each land-cover category
- (4) Relative importance of predictor variables in presence and cover Random Forests models for each land-cover category
- (5) Tabular summaries of field cover data collected during 2011 and 2012 sampling efforts

2. METHODS

2.1. Remote Sensing and GIS Data

2.1.1. Data Selection and Acquisition

2.1.1.1. LiDAR Data

Light Detection and Ranging (LiDAR) data were collected and processed for the majority of PCCA and some adjacent lands by Watershed Sciences of Portland, Oregon in the spring of 2011. We used the standard 1-meter gridded product for the bare earth and highest hit elevation layers. Return intensity was used only to a limited degree, due to inconsistencies between flight lines. We did not evaluate the point cloud data as the gridded product appeared sufficient for our needs.

2.1.1.2. Aerial Photography

Two orthorectified 4-band color-IR air photo collections were used during the project. Both were collected through the National Agriculture Imagery Program (NAIP); the 2009 collection at half-meter resolution, and the 2012 collection at 1-meter resolution. The 2009 imagery served as the basis for field site selection, field map sheet production, and early mapping exercises. When the 2012 imagery became available, it was substituted for the 2009 collection despite its coarser resolution. This was done in order to produce a map more closely resembling current conditions. Both NAIP datasets were obtained as full resolution, uncompressed tiles.

2.1.1.3. Satellite Imagery

Several SPOT-5 images over the mapping area became available during the course of a standing request kept open during the duration of the project. An adequate image from May 2010 was used to make initial decisions about land-cover categories for mapping and to guide field sampling. Excellent cloud-free images from August 2, 2010 and May 10, 2012 became available later and were used as the

primary satellite data sources for mapping. Because the images were collected in different seasons, they illustrate different aspects of vegetation phenology and jointly contain significantly more information than would be available from a single image.

Five Landsat TM images (August 13, 1998; August 14, 2010; April 21, 2009; June 24, 2009; June 27, 2010) were used for field site selection. The anniversary images from 1998 and 2010 were used to provide a stratification for field sampling of changed areas; the other three images, exhibiting different aspects of vegetation phenology, were used to stratify sampling for base mapping. The Landsat data were not used for predictive modeling due to their coarser spatial resolution.

2.1.1.4. Other Data

The collected LiDAR data did not cover the full extent of the mapping area and were lacking from a small portion of PCCA itself. In order to have topographic metrics available over the full mapping area, we needed to supplement the LiDAR elevation data with conventional elevation data for the missing areas. We downloaded 10-meter resolution elevation data from the USGS National Elevation Dataset (NED) to meet this need.

We digitized the 2012 boundary of PCCA and adjacent federally-owned lands from available maps georeferenced to recognizable features in the aerial photography. Roads and other travel routes in the training area were digitized from the 2009 NAIP photography, supplemented by USGS topographic maps.

We decided against using geology and soils layers for mapping purposes because of the risk of map artifacts due to their coarser resolution and lower spatial accuracy. We also felt that most of the predictive power of these layers was available from metrics derived from the previously discussed datasets.

Table 1. Data sources for predictive modeling layers and their acquisition dates.

Data Type	Spatial Resolution	Data Source	Date
LiDAR Bare Earth and Highest Hit Elevation	1 meter	Watershed Sciences	Spring 2011
Color-IR Aerial Photography	1 meter	NAIP, State of Oregon	Summer 2012
SPOT Satellite Data	10 meter	USGS EROS	Aug. 2, 2010 May 10, 2012
USGS Elevation	10 meter	USGS National Elevation Dataset	---

2.1.2. Data Pre-Processing

All data layers required pre-processing to make the data maximally useful for modeling. The following steps were performed using either ArcGIS 9.3 or ERDAS Imagine 2010.

2.1.2.1. LiDAR Data

The LiDAR bare earth elevation data tiles were reprojected to UTM Zone 11 (NAD83) at 1-meter resolution, mosaicked into a single image, and converted from floating point to integer format with vertical units of quarter-feet for efficiency of data storage and processing. Preliminary topographic metrics such as slope and aspect were produced using the built-in ERDAS functions, after first smoothing the bare earth elevation with a 3x3-cell focal mean filter. The 10-meter NED elevation data were processed similarly to the LiDAR bare earth data.

The height above ground of vegetation and other objects was calculated by subtracting floating point bare earth elevation from highest hit elevation and then converting to integer format with vertical units of centimeters. As we have observed in previous gridded LiDAR datasets, an artifact occurred regularly in steep areas, resulting in invalid height values roughly proportional to the steepness and length of the slope, even in completely barren areas. These errors occurred in linear strips up to 15 meters wide, oriented perpendicularly to the direction of steepest slope. We used an approach we developed previously (Nielsen *et al.*, in press) to flag these locations based on a simultaneous combination of high slope and vegetation height relative to the surrounding area. Height values of these detected artifacts were recoded

as missing data, as were the routes of the power lines crossing the mapping area. Vegetation cover in areas with little remaining valid LiDAR height data were predicted through a different pathway that did not use height information (section 2.5.2).

2.1.2.2. Aerial Photography

The 2009 and 2012 orthorectified air photos were processed similarly. Individual tiles were reprojected to UTM Zone 11 (NAD83) and then mosaicked. The 2009 mosaic was aggregated to 1-meter resolution to reduce overhead in subsequent steps while the 2012 mosaic was kept at its native 1-meter resolution. The datasets coregistered well with the LiDAR data and with each other, although some differences in registration due to orthorectification problems were observed in steep areas. Such artifacts are difficult or impossible to resolve in post-processing. The 2009 NAIP collection was also characterized by occasional discontinuities in the response of the near-infrared band. This impacted the southern portion of the training area; fortunately, the 2012 collection with which final mapping was performed did not have this issue.

2.1.2.3. Satellite Imagery

Both SPOT images were imported from the provided TIF image format, stripped of areas near the image edges where data were missing from some bands, reprojected to UTM Zone 11 (NAD83), and manually coregistered to the 2012 aerial photography. Images were left as digital numbers rather than converting to surface reflectance since no comparison between the images was required. The images were of excellent quality with minimal apparent atmospheric effects.

The Landsat TM data were imported from their native format and converted to exo-atmospheric reflectance using the provided header information. Areas of cloud, shadow, smoke and haze were manually digitized and removed from the images. Atmospheric variability between images was corrected for by applying a dark object subtraction in which the minimum observed reflectance value in each band was subtracted from all pixel values. This simple technique is appropriate when the imaged area includes many pixels corresponding to dark water or cast shadow (Chavez 1988), a valid assumption with several miles of the John Day River in the mapping area. We then applied a relative normalization to the anniversary images from 1998 and 2010 by implementing the “ridge method” discussed in Chen *et al.* (2005).

2.2. Training Data

2.2.1. 2011 Season

2.2.1.1. Field Training Site Selection

Targeted sites for training data acquisition were selected using an automated procedure based on the acquired Landsat TM images. Both the historical change image pair and the selected set of three modern images were used, to ensure that areas of recent change (e.g., burns) and the full spectrum of current conditions were adequately represented in training data. Sites were selected only from areas either within PCCA or on adjacent public lands, and only within 400 meters of the road and trail system.

Sampling of recently changed areas was based on the anniversary image pair. Both images were simplified into two indices, the Normalized Difference Vegetation Index (NDVI, Rouse *et al.* 1973) and the Normalized Difference Moisture Index (NDMI, Wilson and Sader 2002). A change vector analysis procedure (Lambin and Strahler 1994) was then used to identify six distinct types of spectral change over the 1998 – 2010 time interval. 220 points were randomly located within the change areas meeting the accessibility criteria above. Points were created proportionally to the area represented by each of the six change classes.

Sampling of areas with distinct spectral response was based on the three images selected as representative of current conditions. The red, near-infrared, and mid-infrared bands were extracted from the three images and stacked into a single image. An ISODATA unsupervised classification was used to break the training area into 45 classes characterized by similar spectral responses at the three dates. Representation of distinct topographic settings was ensured by additionally intersecting the 45 spectral classes with three classes derived from topographic curvature. The resulting classes were restricted to the accessible regions, and then an automated procedure was used to locate the most spatially homogeneous representative areas from each class. Three to six points were randomly selected from these areas, in rough proportion to their frequency on the landscape. A total of 503 points resulted from this procedure.

Field crews were instructed to sample as wide a variety of the points generated through both procedures as possible, in addition to opportunistic sampling when homogeneous areas of undersampled vegetation types were encountered. To assist field sampling, the randomly selected sampling points were shown on aerial photo map sheets produced from the 2009 aerial photography

2.2.1.2. Field Data Collection

Crews visited accessible locations, attempting to maximize diversity among the sampled classes. If the assigned location was near a vegetation boundary, it was relocated nearer the center of a homogeneous vegetation patch, and a new GPS point was taken. Small patches (less than 90 meters in both dimensions) were only sampled if the vegetation type represented did not occur often in larger patches. In addition, opportunistic plots were taken when unusually homogeneous examples or less common vegetation types were encountered.

Vegetation and ground cover at PCCA were broken into categories that could be assessed quickly in the field, feasibly mapped, and potentially prove valuable for management purposes. Percent coverage at the plots was assessed for 19 land-cover categories: (1) conifers, including western juniper (*Juniperus occidentalis*), Douglas-fir (*Pseudotsuga menziesii*), and ponderosa pine (*Pinus ponderosa*); (2) mountain mahogany (*Cercocarpus ledifolius*, CERLED); (3) big sagebrush (*Artemisia tridentata*, ARTTRI), including subspecies *tridentata* and *wyomingensis*; (4) rigid sagebrush (*Artemisia rigida*, ARTRIG); (5) antelope bitterbrush (*Purshia tridentata*, PURTRI); (6) riparian woody vegetation (RWV); (7) shrubs tolerant of disturbed rangeland (DRS), including rubber rabbitbrush (*Ericameria nauseosa*), green rabbitbrush (*Chrysothamnus viscidiflorus*), broom snakeweed (*Gutierrezia sarothrae*), salt desert shrubs, and other shrubs not incorporated elsewhere; (8) bluebunch wheatgrass (*Pseudoroegneria spicata*, PSESPI); (9) Idaho fescue (*Festuca idahoensis*, FESIDA); (10) needlegrasses (*Achnatherum* spp., ACHSPP), primarily Thurber's needlegrass (*Achnatherum thurberianum*); (11) sand dropseed (*Sporobolus cryptandrus*, SPOCRY); (12) native bluegrasses (*Poa* spp., POANAT), primarily *Poa secunda*; (13) exotic grasses (EXOGRASS), primarily cheatgrass (*Bromus tectorum*), medusahead (*Taeniatherum caput-madusae*), and ventenata (*Ventenata dubia*); (14) exotic forbs (EXOFOR), including common mullein (*Verbascum thapsus*), teasel (*Dipsacus fullonum*), and Scotch thistle (*Onopordum acanthium*); (15) cryptobiotic soils and moss (MOSSCRYP); (16) exposed bedrock (BEDROCK); (17) exposed talus (TALUS); (18) exposed bare soil (SOIL); (19) exposed ash beds (ASH).

All cover assessments were visually estimated, with the aim of producing reasonably accurate estimates at the scale of a 45-meter radius circle plot (approximately 0.65 hectares, or 1.5 acres). Cover was assessed in a single large plot if visibility was adequate to allow that; otherwise, five small 10-meter radius plots were assessed located at the plot centers and 37 meters distant at 45, 135, 225, and 315 degrees. Smaller and/or irregularly shaped patches were assessed over an area determined by the crew and sketched on the map sheets. Live and dead western juniper were distinguished, and all junipers were separated into several size-based age classes. Photos were taken, and a range of other identifying characteristics were collected, mostly to aid in positive plot identification and location for quality control (see Appendix A).

Plot data were entered into an Access database, and polygons drawn for irregularly sized polygons were entered into a GIS system. Plot center locations, GPS error estimates, species cover data, and available notes were exported from the database to a spreadsheet for additional quality control (section 2.2.3).

2.2.2. 2012 Season

The 2012 field season was originally planned as an effort to obtain sufficient additional field data to perform a map-based accuracy assessment using independent data. However, we later determined that insufficient data were available from 2011 to accurately model cover for many of the land-cover categories. Therefore, the 2012 field data were instead used in the model building process, and we used a model-based accuracy assessment process (section 2.6).

2.2.2.1. Field Training Site Selection

Early in 2012, draft land-cover category cover maps at 10-meter pixel resolution were built from the field data collected in 2011, using a process similar to that discussed below. All 19 cover predictions were stacked and passed through a 3x3-cell focal mean filter. An ISODATA unsupervised classification was used to break the stacked cover image into thirty distinct cover type classes. The most homogeneous representatives of each resulting cover type class were determined, and about ten points were randomly located within each of these, subject to the same accessibility constraints used earlier. The resulting 304 points were targeted, again attempting to distribute sampling effort as evenly as possible between the thirty classes.

2.2.2.2. Field Data Collection

By this point in the project, it had become clear that 10-meter resolution SPOT-5 satellite imagery would be used during production of the final map, rather than the coarser resolution Landsat TM imagery. For this reason, and because the 2012 plots were originally intended for accuracy assessment purposes, plot size was reduced to a single 15-meter radius circle, although in heterogeneous areas sketches were made illustrating nearby vegetation types. The categories listed for cover assessment were slightly altered for clarity, but otherwise the protocol remained identical to that used in 2011.

2.2.3. Field Data Quality Control

Plot data from both field efforts were quality checked for category cover calls, spatial accuracy, and internal consistency. This process focused primarily on those plots that modeled poorly in a preliminary Random Forests modeling run (section 2.5.3.1).

Adjustments were made in the circumscription of some of the land-cover categories to make the 2011 and 2012 data completely consistent with one another; for instance, the disturbed rangeland shrubs category now includes broom snakeweed, which was originally lumped with native forbs and sub-shrubs. Where there was substantial doubt about the accuracy of cover calls for any category, the cover call was changed to a token signifying missing data and the plot was not used for modeling that category.

Several plots with poor GPS data, or located near vegetation transitions were manually repositioned with reference to aerial photography, LiDAR data, field notes on topographic setting, and field site photos. Plots for which the correct location could not be positively verified were eliminated, as were those located in active agricultural fields and those that were unintentionally resampled. In addition, plots in locations that appeared to have been disturbed between the dates of field collection and more recently acquired imagery were eliminated.

The quality checked cover data were associated with a polygon coverage, derived from either a 45-meter circle centered on the sample point or a field-sketched polygon (2011 field season) or a 15-meter

radius circle centered on the sample point (2012 field season). A total of 331 plots were available for modeling from the combined 2011 and 2012 field work efforts.

2.2.4. Photointerpreted Training Data

Some land-cover categories were insufficiently sampled in the course of field work to successfully model. Where possible, these categories were supplemented with additional positive training data occurrences created from image interpretation. The mountain mahogany, big sagebrush, rigid sagebrush, riparian woody vegetation, talus, bedrock, and ash bed categories were supplemented in this way. Cover for the category of interest was estimated from aerial photography and LiDAR height images. In addition, some negative occurrence data was added from photointerpretation. Some of these training locations were located in poorly predicted areas where initial model runs were indicating a substantial likelihood of the category's occurrence in a location it was clearly absent from in imagery (this was particularly an issue with RWV and rigid sagebrush). Other negative occurrences were entered for some categories in the course of adding positive cover data for other categories. 112 additional training polygons were digitized, giving a combined total of 443 plots for model training (Figure 1).

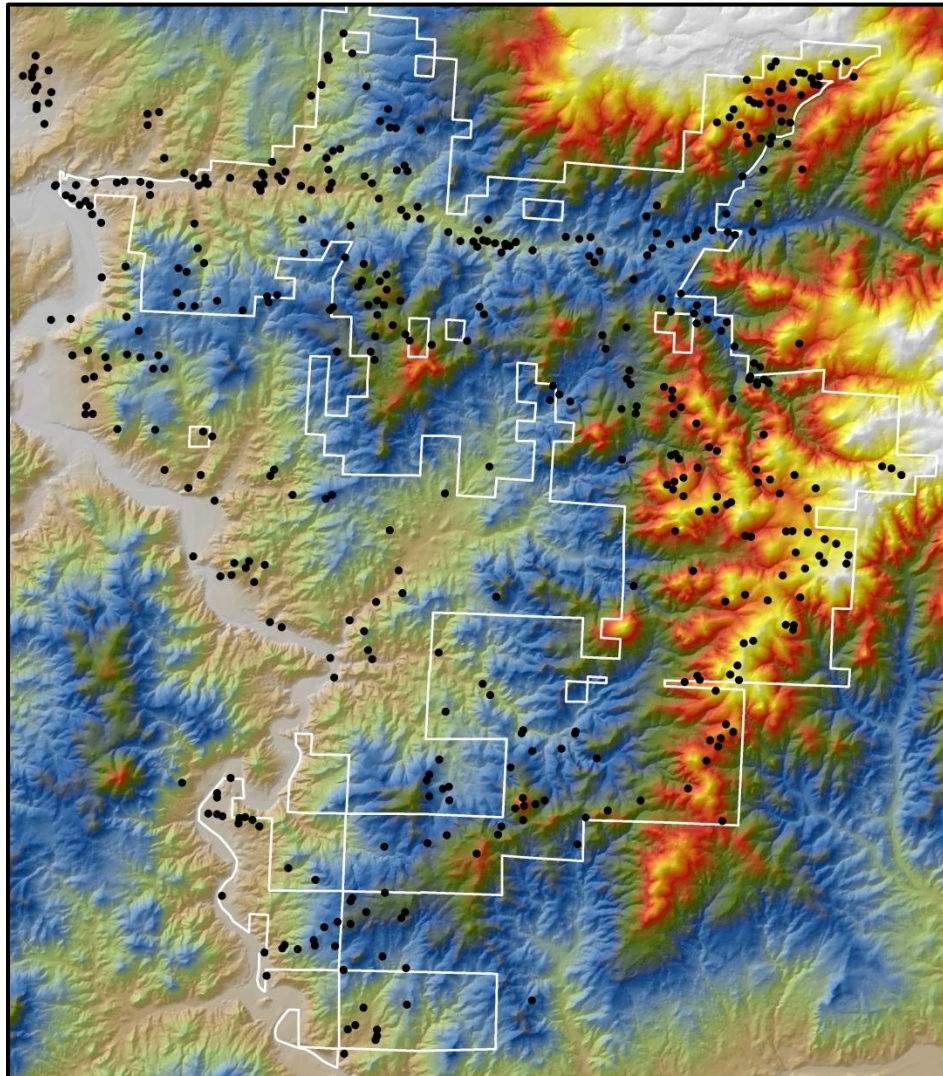


Figure 1. The 443 plot locations used for model training, with Pine Creek Conservation Area boundary superimposed (background is elevation).

2.3. Predictive Metrics

The first step in generating predictive information for modeling was to produce a variety of localized raster data layers from the available remote sensing and GIS data. These metrics are referred to as localized because they depend only on pixel values in an immediate spatial neighborhood, generally defined by a moving window. They fall into four main groups: metrics derived from topographic data, LiDAR vegetation height data, aerial photography, and satellite imagery. Metrics representing hydrological conditions were generated in a landscape perspective since they depend on upstream areas rather than on the immediate neighborhood only. They are described separately in section 2.4 along with the other hydrological processing tasks.

2.3.1. Topographic Data

A variety of distinct metrics describing the range of influences of local topography on growing conditions were calculated. Most metrics were created from both the LiDAR bare earth elevation dataset and the 10-meter NED elevation data, since we needed to map beyond the boundaries of the LiDAR collection.

Table 2. Characteristics of topographic predictors derived from LiDAR and NED elevation data.

Metric Name	Label	Computation Resolution	Description
Bare Earth Elevation	<i>ELEV</i>	1m (LiDAR), 10m (NED)	Bare earth elevation
Slope	<i>SLD</i>	1m (LiDAR), 10m (NED)	Bare earth slope in degrees
Relative Heat Load	<i>HL</i>	1m (LiDAR), 10m (NED)	Relative heat load (McCune method)
Total Curvature	<i>CUR5, CUR10, CUR30, CUR150</i>	5m, 10m, 30m, 150m	Total curvature from elevation aggregated to 5m (LiDAR only), 10m, 30m and 150m resolution
Planimetric Curvature	<i>CPL5, CPL10, CPL30, CPL150</i>	5m, 10m, 30m, 150m	Planimetric curvature from elevation aggregated to 5m (LiDAR only), 10m, 30m and 150m resolution
Profile Curvature	<i>CPR5, CPR10, CPR30, CPR150</i>	5m, 10m, 30m, 150m	Profile curvature from elevation aggregated to 5m (LiDAR only), 10m, 30m and 150m resolution
Topographic Position Percentile	<i>TPP200, TPP800</i>	10m, 40m	Percentile of cell elevation relative to surrounding elevations within 200m and 800m
Topographic Position Difference from Median	<i>TPM200, TPM800</i>	10m, 40m	Difference between cell elevation and median elevation of cells within 200m and 800m
Direct Solar Radiation	<i>RDIR</i>	10m	ArcGIS direct solar radiation across full year
Direct Solar Radiation Duration	<i>RDUR</i>	10m	ArcGIS duration of direct solar radiation across full year

The bare earth elevation (*ELEV*) and degree slope (*SLD*) data layers formed the basis for a variety of other topographic metrics. Slope and aspect were transformed into relative heat load (*HL*) using formulas from McCune (2007). Heat load describes the relative degree of solar heating expected on various slope facets, integrating the influence of slope and aspect on sun incidence angle during the warmest part of the day. It is a biologically meaningful quantity that is more appropriate than aspect for modeling as a continuous variable.

Curvature was computed at a variety of spatial resolutions in order to pick up landscape features occurring at different spatial scales. Bare earth elevation was first degraded to 5-meter, 10-meter, 30-meter, and 150-meter resolutions. The ArcGIS curvature functions were then used to determine total curvature (*CUR*), profile curvature (*CPR*) and planimetric curvature (*CPL*) at each resolution over the surrounding 3x3-cell area.

Two types of relative topographic position metrics were calculated, each at two spatial scales. We defined topographic position percentile (*TPP*) as a cell elevation's percentile ranking relative to the cells surrounding it, and topographic position difference from median (*TPM*) as the difference between the

cell's elevation and the median elevation of the cells surrounding it. The coarse scale metrics used a computation radius of 800 meters, while the fine scale used a radius of 200 meters. For computational feasibility, the coarse scale metrics were calculated at 40-meter pixel resolution, while the fine scale metrics were calculated at 10-meter pixel resolution.

The exposure of each 10-meter pixel to direct solar radiation throughout the year was estimated using the ArcGIS solar modeling tool. This index is substantially different from heat load because it considers topographic shading due to the presence of surrounding slopes, calculated across the course of the sun's trajectory, which can have a major impact in steep, mountainous terrain. Total direct solar radiation (*RDIR*) and the duration of exposure to direct solar radiation (*RDUR*) were computed across a full simulated year, using the "uniform sky" option.

2.3.2. LiDAR Canopy Data

Metrics describing various aspects of vegetation canopy height, density, and variability were created from the LiDAR height data.

Table 3. Characteristics of vegetation canopy predictors.

Predictor Name	Label	Computation Resolution	Description
Dominant Canopy Height	<i>HT88</i>	10m	Height exceeded by only 12.5% of surrounding pixels
75th Percentile Canopy Height	<i>HT75</i>	10m	Height exceeded by 25% of surrounding pixels
Median Canopy Height	<i>HT50</i>	10m	Height exceeded by 50% of surrounding pixels
Median Woody Canopy Height	<i>HTWMD</i>	10m	Local median height of vegetation over 3 feet tall
Median Tree Canopy Height	<i>HTTMD</i>	10m	Local median height of vegetation over 8 feet tall
Normalized Dominant Canopy Height	<i>88NMAX</i>	10m	Ratio of local dominant canopy height to local maximum height
Normalized Mean Canopy Height	<i>MNNMAX</i>	10m	Ratio of local mean canopy height to local maximum height
Canopy Rugosity	<i>FOLDY1, FOLDY2, FOLDY4, FOLDY8</i>	1m, 2m, 4m, 8m	Ratio of summed local canopy height transitions to absolute height. Calculated on heights at 1m, 2m, 4m, and 8m resolution, aggregated by maximum
Normalized Height Standard Deviation	<i>HTA4SD, HTA8SD</i>	4m, 8m	Ratio of local height variability to absolute height. Calculated on heights at 4m and 8m resolution, aggregated by mean
Woody Canopy Cover	<i>CC3F</i>	10m	Fraction of surrounding area with vegetation over 3 feet tall
Tree Canopy Cover	<i>CC8F</i>	10m	Fraction of surrounding area with vegetation over 8 feet tall
Top Layer Canopy Cover	<i>CCTOP</i>	10m	Fraction of surrounding area with vegetation over 90% of the dominant canopy height

The vegetation height data layer with masked cliff artifacts formed the basis for a range of predictors, representing measures of canopy height, canopy roughness or rugosity, and total canopy cover. Many of these predictors can only be calculated at coarser spatial scales, as they integrate the characteristics of a number of finer resolution pixels in order to expose characteristics of a vegetation canopy rather than a single object.

Three predictors are quantile-based descriptors of the 1-meter resolution raw height data, and were formed by repeatedly computing medians on the 1-meter vegetation height cells in each larger 10-meter cell. After calculating the median canopy height (*HT50*) at 10-meter resolution, all 1-meter cells with heights less than the local *HT50* were set to missing data. The median of the cells that remained was taken, resulting in the 75th percentile height (*HT75*). The same procedure was repeated once more,

resulting in a measure of the dominant canopy height (HT_{88}). HT_{88} provides a good estimate of the typical overall canopy height of the dominant vegetation present at most sites. If the highest vegetation layer at a site has cover of less than 12.5%, it will be ignored, and HT_{88} will instead represent the height of the dominant vegetation layer. Therefore, HT_{88} is useful for discriminating between vegetation types defined on the basis of dominance.

The median tree height ($HTTMD$) was determined by first eliminating all 1-meter cells with height values less than eight feet, and taking the median of the values remaining in each 10-meter cell. Rather than indicating the height of the dominant vegetation, $HTTMD$ describes the height of the tree layer present (if any), no matter how sparse it is. The median height of woody vegetation ($HTWMD$) was computed similarly, but used a threshold of three feet, on the assumption that most height values over that limit at PCCA should correspond to woody vegetation.

Two additional descriptors of vertical canopy structure were derived, both based on the elevation relief ratio of Pike and Wilson (1971). The normalized mean canopy height ($MNNMAX$) specifies the fractional vertical distance of the mean canopy height between the minimum (usually zero) and maximum heights in the 10-meter pixel, while the normalized dominant canopy height ($88NMAX$) specifies the same for the dominant canopy height instead of the mean height. They were computed by:

$$MNNMAX = \frac{HT_{mean} - HT_{min}}{HT_{max} - HT_{min}}$$

$$88NMAX = \frac{HT_{88} - HT_{min}}{HT_{max} - HT_{min}}$$

where HT_{mean} is the mean height across the constituent 1-meter pixels, HT_{88} is the dominant canopy height, and HT_{min} and HT_{max} are the minimum and maximum heights 1-meter pixel heights, respectively.

We defined our primary rugosity measure as the ratio of the local 3-cell canopy slope distance to the horizontal distance, summed in both north-south and east-west directions and standardized by the vegetation height at the center cell. Horizontal distance can be eliminated from the equation since it is determined only by the pixel resolution and is invariant across the image, leaving:

$$Rugosity = \frac{|HT_C - HT_N| + |HT_C - HT_S| + |HT_C - HT_E| + |HT_C - HT_W|}{HT_C}$$

where HT_C represents the vegetation height at the center pixel and HT_N , HT_S , HT_E , and HT_W represent the vegetation heights at the pixel immediately to the north, south, east and west respectively. We calculated the rugosity metric at four different resolutions to reveal different scales of horizontal canopy structure. Rugosity at 2-meter, 4-meter, and 8-meter resolutions were calculated by first degrading vegetation height, setting the coarser resolution cells to the maximum of the finer constituent cells. Aggregating by maximum eliminates many small gaps and increasingly focuses analysis on the upper levels of the canopy. The finer scale versions are quite affected by small breaks in canopy.

We created an alternative measure of canopy roughness by following Parker and Russ (2004) to calculate the normalized height standard deviation:

$$HTASD = \frac{\sigma_H}{HT_C}$$

where σ_H represents the 3x3-cell moving window standard deviation of the vegetation height, and HT_C represents the vegetation height at the center pixel. We calculated this metric at 4-meter and 8-meter resolutions, aggregating by mean instead of by maximum. Only coarser resolution versions of this metric differed substantially from the primary rugosity metric.

We generated three canopy cover predictor layers. Tree canopy cover (CC_{8F}) was defined as the fraction of the local 1-meter cells with height values over eight feet, while woody canopy cover (CC_{3F})

was the same but with a threshold of three feet. The top layer canopy cover (*CCTOP*) was defined as the fraction of 1-meter cells with height values greater than 90% of the corresponding 10-meter *HT88*. This predictor attempts to estimate the overall canopy cover of the dominant layer of vegetation.

2.3.3. Aerial Photography

The predictors developed from the 2012 NAIP aerial photography focused on texture-based attributes that exploit the high-resolution information not available from the satellite imagery. Translating elements of spatial patterning into predictive metrics allows mapping of fine-grained vegetation types, even when the mapping itself is done at a coarser resolution than the individual plants.

Table 4. Characteristics of aerial photography predictors.

Metric Name	Label	Computation Resolution	Description
NAIP Red Band	<i>R1</i>	1m	NAIP red band response
NAIP NDVI	<i>V1</i>	1m	NDVI from NAIP red and near-IR bands
NAIP N2VI	<i>N1</i>	1m	Product of NAIP near-IR band and NDVI
Red Band T5 Texture	<i>R1T5, R2DT5, R3DT5, R5DT5, R9DT5</i>	1m, 2m, 3m, 5m, 9m	Absolute value of difference between red band center cell and median of eight surrounding cells, calculated at 1m, 2m, 3m, 5m, and 9m resolution, aggregated by median
Red Band Normalized T5 Texture	<i>R1T5N, R2DT5N, R3DT5N, R5DT5N, R9DT5N</i>	1m, 2m, 3m, 5m, 9m	Ratio of red band T5 texture to red band value, aggregated by median
NDVI T5 Texture	<i>V1T5, V2DT5, V3DT5, V5DT5, V9DT5</i>	1m, 2m, 3m, 5m, 9m	Absolute value of difference between NDVI center cell and median of eight surrounding cells, calculated at 1m, 2m, 3m, 5m, and 9m resolution, aggregated by median
NDVI Normalized T5 Texture	<i>V1T5N, V2DT5N, V3DT5N, V5DT5N, V9DT5N</i>	1m, 2m, 3m, 5m, 9m	Ratio of NDVI T5 texture to red band value, aggregated by median
N2VI T5 Texture	<i>N1T5, N2DT5, N3DT5, N5DT5, N9DT5</i>	1m, 2m, 3m, 5m, 9m	Absolute value of difference between N2VI center cell and median of eight surrounding cells, calculated at 1m, 2m, 3m, 5m, and 9m resolution, aggregated by median
N2VI Normalized T5 Texture	<i>N1T5N, N2DT5N, N3DT5N, N5DT5N, N9DT5N</i>	1m, 2m, 3m, 5m, 9m	Ratio of N2VI T5 texture to red band value, aggregated by median

It is difficult to use air photos for automated vegetation mapping because of inconsistent radiometric properties between flight lines due to changes in sun angle, atmospheric conditions, vegetation phenology, and sensor calibration issues. However, using metrics based on texture (variance) rather than radiometric attributes can provide a more consistent means of object identification. Textural measures also can vary extraneously within and between photos, due to variability in view angle, sun-surface-sensor geometry, and atmospheric conditions, but these issues are more prevalent with tall (tree-sized) vegetation; most vegetation types at PCCA should not be strongly affected. We developed two texture measures that appear to respond strongly and consistently to spatial patterning, and ran them at various resolutions to pick up signals corresponding to vegetation patterned at differing scales.

The texture metrics must be calculated from a single-band image; the resulting characteristics can vary considerably depending on the input measure chosen. We used three different source images at 1-meter resolution, each of which seemed to respond well to at least one of the land-cover categories of interest. The red band, which responds strongly to the contrast of illumination and shadow, or dark woody material and bright soil backgrounds, was extracted from the 4-band NAIP imagery. The second source image used was NDVI, calculated from the near-infrared and red band responses, which strongly discriminates vegetated from unvegetated areas:

$$NDVI = \frac{nir - red}{nir + red}$$

where *nir* and *red* represent the near-infrared and red band responses, respectively. The third source image, N2VI, was created by multiplying *NDVI* by *nir*, allowing a clearer discrimination of vegetation crowns from their cast shadows, which can be easily confused in either of the other metrics.

We experimented with many possible moving window measures of high frequency contrast; the most effective at PCCA was created by subtracting the median of each cell's eight nearest neighbors from its own value, taking the absolute value of the result. We called this metric *T5* (it was the fifth texture tested):

$$T5 = | e - \text{median}(a, b, c, d, f, g, h, i) |$$

where the values of the pixels in the 3x3-cell computation window are named according to:

$$\begin{pmatrix} a & b & c \\ d & e & f \\ g & h & i \end{pmatrix}$$

We generated this metric at 1-meter resolution on each of the three source images (producing *R1T5*, *V1T5*, and *N1T5*). Then, we degraded each source image to various coarser resolutions (2-meter, 3-meter, 5-meter, and 9-meter) by aggregating to the coarser resolution based on the median. The *T5* metric was then produced at each of the coarser resolutions for each of the three source images (resulting in *R2DT5*, *R3DT5*, etc.).

Another version was made of each of the 15 texture metrics in which it was normalized by the local value of the source image from which it was computed (also aggregated by median to the coarser resolution), e.g.:

$$R1T5N = \frac{R1T5}{R1}$$

$$R2T5N = \frac{R2T5}{R2}$$

etc., where *R2* is determined by aggregating *R1* by median to 2-meter resolution. This process resulted in an additional 15 texture metrics, giving a total of 30 in addition to the three source images themselves.

2.3.4. Satellite Data

A range of predictive metrics were generated from the August 2010 and May 2012 SPOT-5 images. Metrics were either the raw band responses or spectral indices based on combinations of those responses.

The normalized difference vegetation index (NDVI), an index useful for discerning variations in vegetation vigor, was created from the near-infrared and red band responses, as described above. The normalized difference moisture index (NDMI), useful for discerning variations in vegetation structural attributes, was created by:

$$NDMI = \frac{nir - mir}{nir + mir}$$

where *nir* and *mir* represent the near-infrared and mid-infrared responses respectively. The normalized difference forestness index (NDFI, coined here) integrates characteristics of NDVI and NDMI, and is calculated by:

$$NDFI = NDVI + NDMI$$

Table 5. Characteristics of SPOT satellite data predictors.

Metric Name	Label	Computation Resolution	Description
Near-IR Band	<i>AU10B1, MA12B1</i>	10m	Near-IR band response from Aug. 2010 and May 2012
Red Band	<i>AU10B2, MA12B2</i>	10m	Red band response from Aug. 2010 and May 2012
Green Band	<i>AU10B3, MA12B3</i>	10m	Green band response from Aug. 2010 and May 2012
Mid-IR Band	<i>AU10B4, MA12B4</i>	10m	Mid-IR band response from Aug. 2010 and May 2012
NDVI	<i>AU10VI, MA12VI</i>	10m	Normalized Difference Vegetation Index from Aug. 2010 and May 2012
NDMI	<i>AU10MI, MA12MI</i>	10m	Normalized Difference Moisture Index from Aug. 2010 and May 2012
NDFI	<i>AU10FI, MA12FI</i>	10m	Normalized Difference Forest Index from Aug. 2010 and May 2012
NDSI	<i>AU10SI, MA12SI</i>	10m	Normalized Difference Snow Index from Aug. 2010 and May 2012
NDRG	<i>AU10RB, MA12RB</i>	10m	Normalized difference of red and green bands from Aug. 2010 and May 2012

The normalized difference snow index (NDSI, Hall *et al.* 1995), an index useful not only for detecting snow cover but also various geological properties, was created by:

$$NDSI = \frac{grn - mir}{grn + mir}$$

where *grn* and *mir* represent the green and mid-infrared responses respectively. Finally, the normalized difference red-green index (NDRG, coined here), which is helpful in detecting changes in soil color, was created using:

$$NDRG = \frac{red - grn}{red + grn}$$

where *red* and *grn* represent the red and green responses respectively. Each metric was generated from both of the SPOT satellite images.

2.4. Hydrological Modeling

Because the predictive modeling process treats data aspatially, predictors related to landscape context must be provided explicitly. One aspect of landscape context that is key to understanding vegetation distribution is hydrological connectivity. In order to incorporate information related to hydrological connectivity into predictive models, local metrics describing the influence of hydrology must be generated through simulating flow processes.

We created a hydrological flow accumulation layer based on the LiDAR bare earth elevation, correcting for poorly modeled flow at road crossings due to lack of information on culvert locations. We used the flow accumulation layer to create a channel network, calibrated by field observations of the flow thresholds at which channel formation occurs at PCCA. We then used flow accumulation and slope data to delineate riparian zones, also calibrated locally through observations of patterns of occurrence of riparian woody vegetation.

2.4.1. Flow Accumulation Modeling

Modeling hydrological flow accumulation was important both as a step in the process of delineating channels and riparian zones, and also as a key input needed to generate several predictive hydrological

metrics. Although ArcGIS can be used for estimating flow accumulation, we found that its restriction to modeling flow in a single direction out of each pixel resulted in patterns that were not realistic in relatively flat areas. Instead we used SAGA, an open source software package that includes a variety of advanced topographic analysis functions (SAGA-GIS 2012), allowing a more accurate delineation of the extent of moist areas.

To make computation feasible, hydrological modeling was performed at 3-meter resolution rather than the full 1-meter resolution of the LiDAR elevation dataset. We reduced the resolution by aggregating based on the minimum, setting each 3-meter cell equal to the lowest value of the 9 constituent 1-meter cells. This resulted in a greatly reduced number of obstructed flow paths in subsequent modeling, as compared to aggregating based on the mean. We then used SAGA to fill sinks in the elevation grid (using the Wang & Liu method, with *minslope* = 0.01) and modeled flow accumulation using the SAGA Parallel Processing method (with multiple flow directions and *convergence* = 1.1).

This procedure resulted in flow paths running along the upslope sides of the roads along Pine Creek and on the east side of the John Day River, where flow paths down slopes were modeled as blocked by the elevated road prism. We manually digitized short line segments across roads in areas where substantial amounts of flow were being incorrectly routed along roadsides. We buffered each segment by 1.5 feet, and then set all elevation cells overlapping each buffered segment to the minimum elevation. We ran the sink filling and flow accumulation procedures again, and the flow path problems were resolved.

2.4.2. Field Calibration

During the 2012 field effort, we generated calibration data to guide the delineation of channel networks and riparian zones. Several stream channels with differing general flow directions were hiked in the downstream direction, starting above the point of initial channel formation. At 100-meter intervals, a GPS point was collected and the channel type and cover of riparian woody vegetation (RWV) were assessed. Channels were coded as either permanent (with flowing water around July 1), seasonal (clearly with regular flow for at least a portion of the year, and consolidated alluvial substrate), intermittent (apparently flowing in brief but not rare episodes, with substrate composed of loose sand and rock), and gullies (only flowing after extreme events). RWV was defined as any woody vegetation differing from that found on surrounding slopes; we estimated the proportion of the 30-meter linear interval surrounding each sample point that had RWV, and the maximum horizontal and vertical distance from the channel that RWV was found. We also noted if RWV had been observed along the channel since the last sample location. Similar assessments were made on the lower portion of each tributary channel encountered, above the area influenced by the main channel.

In the office, the modeled channel flow accumulation was extracted for each sample point, and the relationships between flow accumulation, channel type, and occurrence of RWV were compiled separately for channels generally flowing in the four cardinal directions. The horizontal and vertical distances at which RWV was observed from channels of various sizes were used to generate a channel size-dependent envelope within which RWV can potentially occur, by keeping only the occurrences with the maximum distances observed along the spectrum of channel sizes. A regression was created linking the logarithm of flow accumulation with a function taking the form of the slope cost distance described in section 2.4.4, and this was used to parameterize the delineation of riparian zones.

2.4.3. Channel Network Delineation

Intermittent channels and seasonal/permanent channels were delineated in SAGA. The flow accumulation thresholds at which these two channel types were observed to initiate were used to parameterize the network delineation procedure. Each channel section was attributed by SAGA with its stream order (Shreve 1966), a system in which whenever two streams join, the resulting channel order is equal to the sum of the orders of the tributaries.

2.4.4. Riparian Zones Delineation

We started with the assumption that riparian zones should occur adjacent to channels, and should monotonically increase in their horizontal and vertical dimensions with increases in channel flow. The first step was therefore to determine the flow quantity associated with each section of the channel network. The channel network was broken into discrete channel reaches defined by network intersections. Many channel segments were composed of anastomosing flow pathways, in which flow was modeled in several adjacent parallel paths; it was necessary to consider the several paths as all contributing to a single total flow value. Determining this effective flow required first associating each flow accumulation cell with the nearest channel reach. For this purpose, distance was measured in terms of the cumulative slope across each cell separating the flow accumulation cells from the channel reaches. Average reach flow was then calculated by dividing the summed flow accumulation of the cells associated with the reach by the length of the reach.

In order to properly model the extent of riparian zones on different size channels, we needed to classify the channels into size classes. We determined that using nine channel classes represented a good compromise between the ability to accurately represent riparian extents across the wide range of channel sizes and the constraints posed by the time-intensive cost distance modeling process, which required an independent run for each class. Channels were assigned to one of the nine classes on the basis of average reach flow, with thresholds between the classes spaced in a regular geometric progression ranging from the minimum reach flow at which RWV was observed to the highest occurring reach flow in the mapping area.

We used a cost function to determine the distance riparian zones would stretch away from the associated channel. The cost function was based on the square of slope in order to emphasize sudden breaks in slope and produce boundaries corresponding to physiographic features such as fluvial terraces and natural levees. The least cost distance from each cell to each of the nine channel size classes was calculated using this squared slope cost function.

Riparian zones were demarcated by thresholds of cost distance that were a function of channel size class. We used the occurrences of RWV in the hydrological field calibration data to select appropriate thresholds. These observations were used to fit a mathematical model to describe cost distance threshold in terms of the geometric mean reach flow for each of the channel size classes. We found that a logarithmic model best fit the data, and used this to generate the shape of the function relating reach flow to cost distance thresholds for RWV occurrence. We then corrected for the fact that the limits on riparian zones are fixed by sudden breaks in slope by matching the generated curve to the floodplain boundaries observable in LiDAR elevation data for a moderate-sized channel at PCCA, and applying a linear correction to the cost distance thresholds based on this.

All cells with a least cost distance to any of the nine channel size classes less than the cost threshold for that class were flagged as riparian. We then ran a series of 3x3-cell focal majority filters, slightly modified to favor basin-filling, to remove speckle. Finally, we enforced a rule that all riparian cells must be contiguously connected through other riparian cells to a channel network cell. Although the delineated riparian zones were not used in the predictive cover modeling, several of the associated intermediate process results were used to generate predictive metrics (section 2.4.5).

The riparian zones spatial layer provided with the deliverables was restricted to the PCCA property boundary. The hydrological metrics are less reliable at any location lacking complete LiDAR coverage in the upstream contributing area, including much of the area outside of the PCCA boundary. Restricting the riparian layer to the PCCA boundary also allowed us to generate cumulative area estimates, as it excluded the large amounts of open water on the John Day River modeled as riparian.

2.4.5. Hydrological Predictive Metrics

Metrics describing hydrological processes and features were produced from the outputs of the hydrological modeling performed in SAGA. For computational feasibility, all hydrological metrics were derived from the 3-meter resolution elevation grid created from the 1-meter dataset by aggregating based on the minimum.

Table 6. Characteristics of hydrological predictors derived from LiDAR elevation data.

Metric Name	Label	Computation Resolution	Description
Vertical distance to permanent stream	<i>VDISTP</i>	3m	SAGA vertical distance above permanent channel network
Vertical distance to intermittent stream	<i>VDISTI</i>	3m	SAGA vertical distance above intermittent channel network
Horizontal distance to permanent stream	<i>HDISTP</i>	3m	Horizontal distance to permanent channel network
Horizontal distance to intermittent stream	<i>HDISTI</i>	3m	Horizontal distance to intermittent channel network
Highest stream order within 100m	<i>MAXORD</i>	10m	Highest order SAGA channel within 100m
Wetness index	<i>SAGAWET</i>	3m	SAGA wetness index
Uplandness index	<i>UPLAND</i>	3m	Log-scaled cost distance to channel network, produced in riparian delineation procedure

SAGA was used to determine the vertical distance of each cell above the two channel networks (intermittent and seasonal/permanent) delineated earlier (*VDISTP*, *VDISTI*). These predictors were included because of their likely correlation to the relative impacts of cold air drainage, which can significantly influence vegetation distribution in steep terrain. We used ArcGIS to determine the horizontal distance of each cell to the nearest channel in each network (*HDISTP*, *HDISTI*), as well as the highest Shreve stream order within 100 meters, if any were present (*MAXORD*).

The Compound Topographic Index (CTI) is a steady state soil wetness index based on local slope and upstream contributing area (Moore 1991), with useful properties for expressing landscape position and integrating hydrological processes. The CTI was modeled in ArcGIS but was found to inadequately represent the extent of moist areas away from channels in low gradient areas. Instead we used the SAGA Wetness Index (*SAGAWET*), a close analog to CTI, the behavior of which we found more realistic in low gradient areas.

An “uplandness” index was created based on a log-scaled version of the riparian zones cost distances computed above during the riparian zone modeling procedure. For each cell, the ratio of the slope-based cost distance to the riparian threshold for each stream size class was calculated. The uplandness index was defined as:

$$UPLAND = \log_{10} \left[1 + \min \left(\frac{C_1}{T_1}, \frac{C_2}{T_2}, \frac{C_3}{T_3}, \frac{C_4}{T_4}, \frac{C_5}{T_5}, \frac{C_6}{T_6}, \frac{C_7}{T_7}, \frac{C_8}{T_8}, \frac{C_9}{T_9} \right) \right]$$

where $C_{1..9}$ represent the slope-based cost distance to each of the nine stream size classes, and $T_{1..9}$ represent the cost distance threshold used to define the riparian zone associated with each size class. Higher values of the index are associated with decreasing hydrological influence.

2.5. Modeling

After the initial predictor data summarization steps (section 2.5.1), the remainder of the modeling procedures were implemented in the R programming language (R Development Core Team 2012).

2.5.1. Predictor Data Summarization

All predictor metrics were aggregated or resampled to a 10-meter resolution grid of fixed extent established by the NAIP data. Considerable care was taken to avoid unnecessary resampling and to ensure that no pixel shifts occurred during processing of any of the layers, which would diminish the highly accurate image coregistration needed to extract appropriate predictor data for small plots. All of the LiDAR-based canopy metrics were occasionally impacted by the missing LiDAR height data resulting from the artifact discussed in section 2.1.2.1. During the process of aggregating these metrics to the 10-meter modeling resolution, if at any step less than half the finer resolution cells contained valid data, the result was marked invalid also. After all 10-meter metrics had been created, a mask was created for each predictor group (LiDAR topography, NED topography, LiDAR canopy, aerial photography, and SPOT data) indicating which cells contained valid data for all metrics in the group.

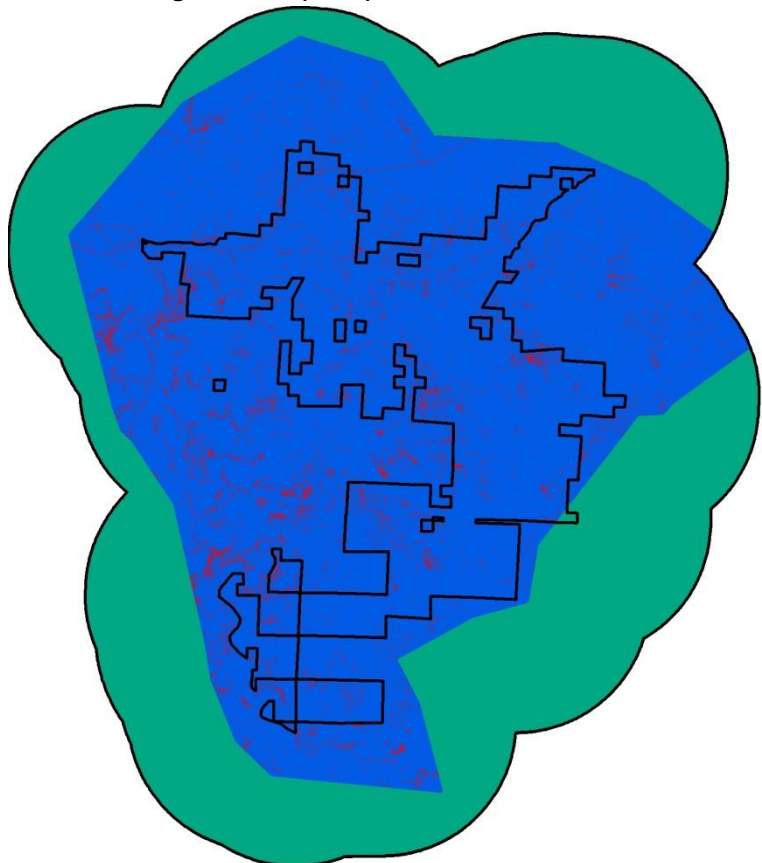
Predictor data was created for each training data plot by summarizing the metrics by their zonal mean values across the 443 training data polygons. For each predictor group, the percentage of 10-meter cells with valid data was calculated over each polygon. The summarized predictor values and percent valid information were exported into tables and joined to the training polygon shapefile with cover data that was produced in section 2.2.

The validity of the merged cover/predictor dataset was checked by testing the associations between the cover values for each land-cover category and the predictor data values. We calculated Spearman's ρ for each pairwise combination of the cover and predictor datasets. This statistic is a rank-based measure of association appropriate in cases where data do not come from a bivariate normal distribution.

Figure 2. Areas corresponding to the three model runs based on different subsets of predictors. The blue area (run 1) has all predictors available, the red area (run 2) lacks valid LiDAR height data, and the green area (run 3) lacks all LiDAR data.

2.5.2. Predictor Subsets

Not all the predictor groups are available in all parts of the mapping area. The LiDAR collection did not cover the full mapping area, and the height data was invalid in some places. In order to create a seamless map with the maximum possible accuracy in all areas, it was necessary to do three independent model runs using different subsets of the predictive variables. The primary model run was based on the first predictor subset, and was applied wherever all datasets were available. This run used predictors from the canopy, hydrology, LiDAR topography, aerial photography, and SPOT groups. The second run was applied in areas where LiDAR elevation data were available, but canopy metrics were invalid; it used predictors from the hydrology, LiDAR topography, aerial photography, and SPOT groups. The third run was



applied where there was no LiDAR coverage, and used predictors from only the NED topography, aerial photography, and SPOT groups. The portions of the mapping area where each of the predictor subsets were applied are shown in Figure 2.

2.5.3. Presence/Absence Modeling

2.5.3.1. Classification Models Development

Predicting species cover is actually a two-fold problem. The first step is to determine whether the species is present or absent; this is a classification problem. If it is present, its cover can be estimated in a second, quantitative modeling step. The predictive modeling algorithm that we used, Random Forests (Breiman 2001), can be run in two different modes corresponding to the two steps in the cover modeling process. The first step, predicting land-cover category presence and absence, was accomplished by using Random Forests in its classification mode.

First, the shapefile containing plot data and predictor summaries was imported into R, with the help of the *rgdal* R package (Keitt *et al.* 2012). For each of the three runs, any plots with less than 50% valid data for any of the predictor groups included in the predictor subset were dropped. Then, each of the land-cover category cover values were recoded to presence and absence by treating values of 1% and less as absent. We made this decision because it resulted in higher classification accuracy, and seemed to be a reasonable compromise considering that many plots where categories were marked with zero cover may well have had small amounts within the 90-by-90 meter assessment area. Our absence class therefore allows the possibility of trace amounts of cover.

The remaining steps were performed for each of the 19 land-cover categories in three separate runs using the different predictor subsets. A Random Forests classification model consisting of 2,500 unique decision trees was built for each land-cover category, specifying an equal sample size selected at random from both the presence and absence classes. We found that using an equal sample size is critical for creating a model that balances errors of omission and commission, especially for rare or undersampled vegetation types. A table detailing plots that were commonly mispredicted for each category was compiled and those plots were subject to further examination and quality control (section 2.2.3). After completing the quality control work, the modeling process was repeated and the presence/absence models generated for each of the three runs and 19 land-cover categories were saved for later use, along with variable importance values generated during the model construction.

2.5.3.2. Determining Optimal Probability Thresholds

When classes to be predicted are unbalanced (with the number of presences and absences unequal), and particularly if the training dataset does not accurately reflect the proportion of class occurrences in the landscape, it is important to have some criteria by which to ensure that they are not grossly overpredicted or underpredicted. This can easily result when basing the classification process on some naive measure (such as total overall accuracy of predicting a training set). To address this issue, we did an additional round of presence/absence modeling using the same training dataset as before. For each run and land-cover category, we determined an optimized probability threshold above which an unknown data point would be labeled as an occurrence. We found this threshold by creating 100 bootstrapped Random Forest models, holding out 5% of the samples during each iteration. Since the 5% sample was not used in model generation, it could be treated as independent test data. During each iteration, we determined the confusion matrix that would result from using any given probability as a threshold for presence prediction, ranging from 0.01 to 0.99 in intervals of 0.01. A running total confusion matrix was kept for each probability threshold through the 100 model iterations. The threshold value that generated the cumulative confusion matrix best matching the prevalence of occurrences in the training set (ideally, where the number of false negatives and false positives were equal) was selected as the optimal threshold. Use of this probability threshold should result in maps where land-cover categories are mapped in

proportion to their actual prevalence, even if the fraction of occurrences in the training data are not proportional to their representation over the full landscape. We deemed this a more important goal in creating maps useful for management than simply maximizing overall accuracy.

2.5.3.3. Map Creation

We used the presence/absence models generated for each predictor subset run and land-cover category to predict a floating-point presence probability at each 10-meter pixel in the mapping area. The import of predictor values from each cell and the output of the resulting probability was facilitated by the raster R package (Hijmans and van Etten 2012). We then merged the three predictor subset runs, correcting each predicted probability with reference to the determined optimal threshold, using:

$$p_{out} = \begin{cases} \frac{p_{in}}{2t}, & \text{if } p_{in} < t \\ 0.5 + \frac{(p_{in} - t)}{2(1 - t)}, & \text{otherwise} \end{cases}$$

where p_{in} represents the Random Forests predicted probability, t represents the optimized threshold, and p_{out} represents the standardized probability, with $p = 0.5$ corresponding to the minimum probability value representing category presence at the pixel.

In general, the predictions from the first predictor subset run were used if available because they were based on the complete set of predictors. Otherwise, the second run predictions, based on all predictors other than the vegetation canopy group, were used if available. The third run predictions were only used outside of the LiDAR coverage area. The only exceptions to this rule were for the mountain mahogany and bedrock land-cover categories (see section 2.5.4.3).

2.5.4. Cover Modeling

2.5.4.1 Regression Models Development

The quantitative modeling of land-cover category percent cover was accomplished by running Random Forests in its regression mode, training models only using field data with positive occurrences. Removing absence data prior to regression modeling avoids zero-inflation bias which can seriously compromise measures of best fit that are key to establishing a reliable regression. For this phase, we treated any amount of cover above zero as reflecting an occurrence. Apart from this altered threshold, the process was similar to the classification models creation. No sample sizes were specified; all presence data for each of the land-cover categories were used in developing each model. Rather than outputting a table of mispredicted plots, we saved the out-of-bag R-squared value that resulted from each model fit. The regression models were saved, along with the corresponding variable importance values.

2.5.4.2. Regression Models Correction

Random Forests regression tends to overpredict low values and overpredict high values. This can be partially corrected by performing a regression correction to fit values predicted from the training dataset back to the original collected data. The regression models created in the previous step were loaded and used to repredict the cover training values. A linear least-squares regression was then performed to fit the predicted values to the actual plot cover values. The slope and intercept characterizing the best fit regression line were saved and used during the subsequent cover prediction phase.

2.5.4.3. Map Creation

We used the regression models generated for each predictor subset run and land-cover category to predict a floating-point cover prediction at each 10-meter pixel in the mapping area. We then merged the

three predictor subset runs, correcting each predicted cover value using the slope and intercept determined in the previous step:

$$c_{out} = \max (0, \min(100, c_{in} * m + b))$$

where c_{in} represents the Random Forests predicted cover value, m represents the correction slope, b represents the correction intercept, and c_{out} represents the corrected cover value, constrained to between zero and 100 percent.

For the mountain mahogany and bedrock land-cover categories, we had insufficient training data available in valid LiDAR height areas to produce a reliable regression for the first predictor subset run, resulting in much poorer predictive strength than was possible without using the canopy predictors. For these two categories, merged results were based only on the cover values predicted in the second and third runs. Otherwise the predictive runs for all categories were merged as described in section 2.5.3.3.

2.5.5. Post-Processing

Several steps were taken to make the produced maps more reliable and useful. Where possible, we smoothed the predicted presence probabilities by using a 3x3-cell focal mean on the 10-meter pixels. For most land-cover categories, the smoothed probabilities are more reliable because they compensate for minor registration errors between datasets and remove other sources of noise from the predictions. However, for some land-cover categories—types that can occur in linear strips (e.g., riparian woody vegetation along streams, exotic grasses along livestock trails, exotic forbs along channels and roads, bare soil along roads) or in isolated small occurrences (e.g., individual conifers, exotic grasses in hotspots of livestock disturbance)—smoothing probability values diminishes the chance of detection. We therefore used unsmoothed probability values for these land-cover categories.

As discussed earlier, the regression approach is not well-suited to discontinuities such as that represented by presence vs. absence. Combining the classification and regression results by constraining the predicted cover values to locations where occurrence is found to be likely remedies this problem. We therefore set predicted canopy cover to zero in areas with adjusted presence probability less than 0.5 (i.e., less than the optimized occurrence threshold).

2.6. Model Accuracy Assessment

2.6.1. Presence Model

The field data collected in 2012 were needed for additional training data for many of the land-cover categories, and at any rate were inadequate in number to support a full map-based accuracy assessment. Instead, we performed a bootstrap sample-based approach to assess the accuracy of the presence/absence models for each of the land-cover categories. 5% of the plots were withheld from the model construction phase, and the withheld plots were predicted using the models built without them. The predicted plots were assessed against the observed data associated with them. This process was repeated 100 times for each land-cover category, compiling a cumulative confusion matrix. For purposes of this assessment, all predictions for plots with trace amounts of cover (greater than 0% and less than or equal to 1%) were considered correct because our absence class allows the possibility of trace amounts. Only the first predictor subset model run (the model run applied over most of PCCA, incorporating all predictor types) was assessed.

2.6.2. Cover Model

We used a similar bootstrap approach to assess the accuracy of the cover regression models. Again, 5% of the plots were withheld from each model during its construction, and the cover percent was predicted on them and saved along with the corresponding field data. The process was repeated at least 25 times and until at least 100 points had been accumulated. We calculated the R^2 and root-mean-square

error (RMSE) describing the fit of the predictions to the observed data for each land-cover category. The first predictor subset model run was used to assess for all land-cover categories other than mountain mahogany and bedrock, which were assessed using the second subset model run, the main model used for prediction of those categories.

2.7. Analysis

2.7.1. Land-Cover Category Area Totals

The total area occupied by each land-cover category was estimated from the resulting maps for the Pine Creek Conservation Area, for the adjacent Department of Interior lands, and for the full mapping area (PCCA buffered by 5 kilometers). Two estimates were made, one based on the number of 10-by-10 meter cells predicted with over more than a trace amount of cover, and one created by summing the actual cover predictions over all cells. The estimates may differ substantially, especially for those land-cover categories often occurring at low density.

2.7.2. Predictor Importance

The predictor importance values produced during the classification and regression modeling phases were compiled and assessed for the first predictor subset run, which used all predictor types. For the mountain mahogany and bedrock categories, the importance values were taken from the second predictor subset run because the first run was not used for these categories. For the classification modeling phase, an index of variable importance was created by dividing the mean decrease in accuracy associated with removing each variable from the model by the maximum mean decrease in accuracy for any variable. For the regression modeling phase, the ratio was made using the percent increase in root mean square error. Variable importances were compared within each model, and between the classification and regression phases.

3. RESULTS

3.1. Riparian Modeling

3.1.1 Field Calibration

Intermittent channels appeared to initiate at a flow accumulation threshold of approximately 25,000 9m² cells, representing an upslope contributing area of 22.5 hectares (56 acres). In generally north-facing areas the threshold for intermittent channel formation seemed to be somewhat higher, probably due to greater soil water-holding capacities. Seasonal and permanent channels were lumped, and initiated at approximately 200,000 9m² cells, an upslope contributing area of 180 hectares (445 acres), in both north and south-facing areas. Riparian woody vegetation also first appeared in any significance along channels with a contributing area of 180 hectares, so riparian zones were generated only along seasonal and permanent channels.

3.1.2. Channel Network Delineation

The resulting permanent and seasonal channel network is shown in Figure 3. Channels were not delineated outside the LiDAR coverage area, as the NED elevation dataset was not of sufficient resolution to produce comparable results. The channel networks were generated primarily to support the riparian zone and cover predictive modeling, and are most suitable for viewing as broad overviews. There are duplicate adjacent flow pathways present on some very low gradient channels (primarily in the Pine Creek floodplain). A total of 263 kilometers of permanent/seasonal stream channels and 595 kilometers of intermittent stream channels were delineated within the PCCA boundary; however, these estimates are probably high because of duplicated flow pathways. Stream channel data are not provided or analyzed

outside the PCCA boundary as they become less reliable when LiDAR coverage is lacking from the upstream contributing area to any location.

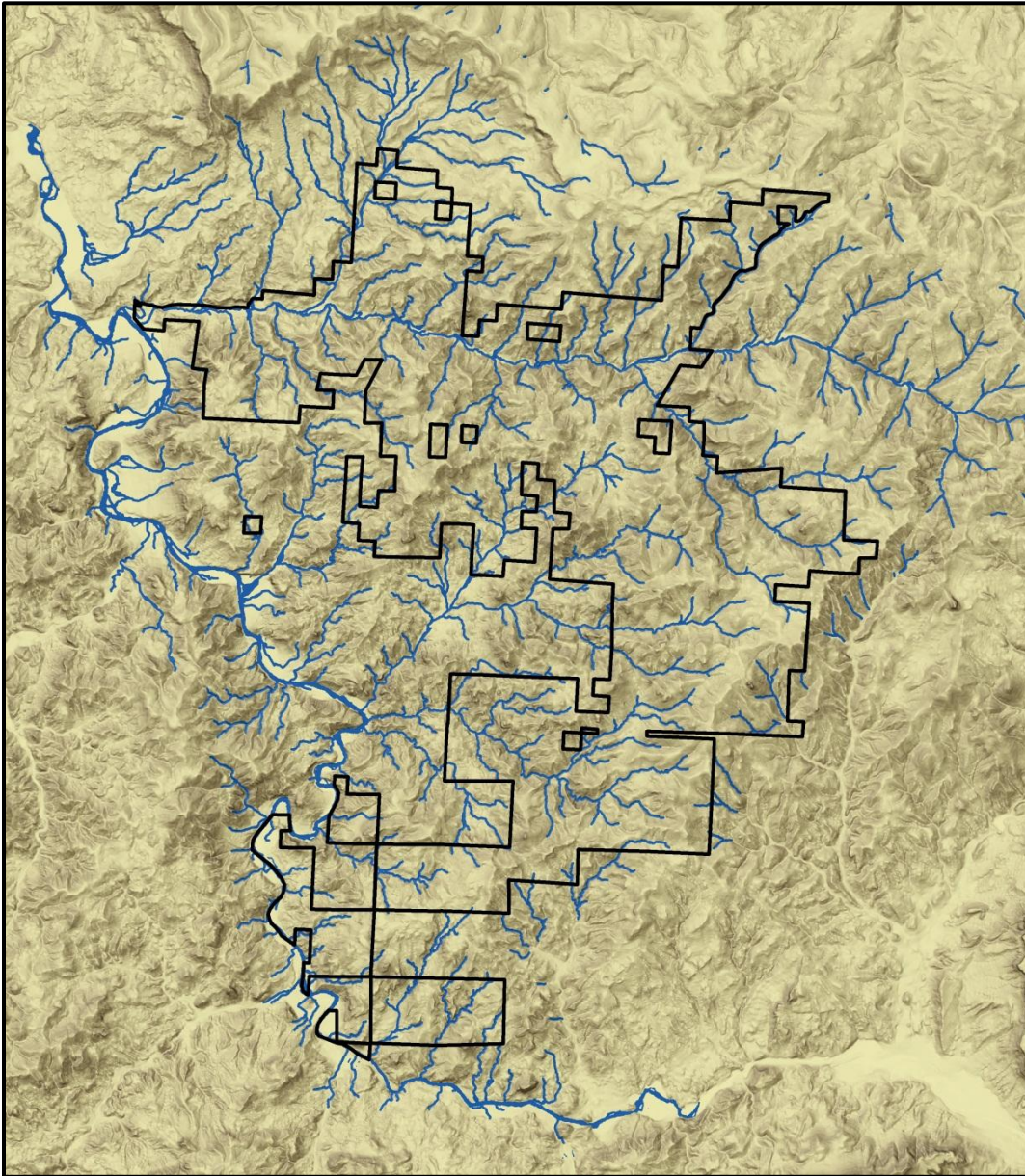


Figure 3. Delineated permanent and seasonal stream channels, with Pine Creek Conservation Area boundary superimposed (background is slope).

3.1.3. Riparian Zones Delineation

Riparian zones were generated only along seasonal and permanent channels, because the flow accumulation threshold for significant presence of RWV was similar to that for formation of these channels. The resulting riparian zones are shown in Figure 4. A total of 587 hectares (1450 acres) of riparian zones were delineated within PCCA boundary. Note that most of this area is not currently occupied by riparian woody vegetation, but it might represent past or future viable habitat. Riparian zones were not delineated outside the LiDAR coverage area, as the NED elevation dataset was not of sufficient resolution to produce comparable results, and are not provided or analyzed outside the PCCA boundary as

they become less reliable when LiDAR coverage is lacking from the upstream contributing area to any location.

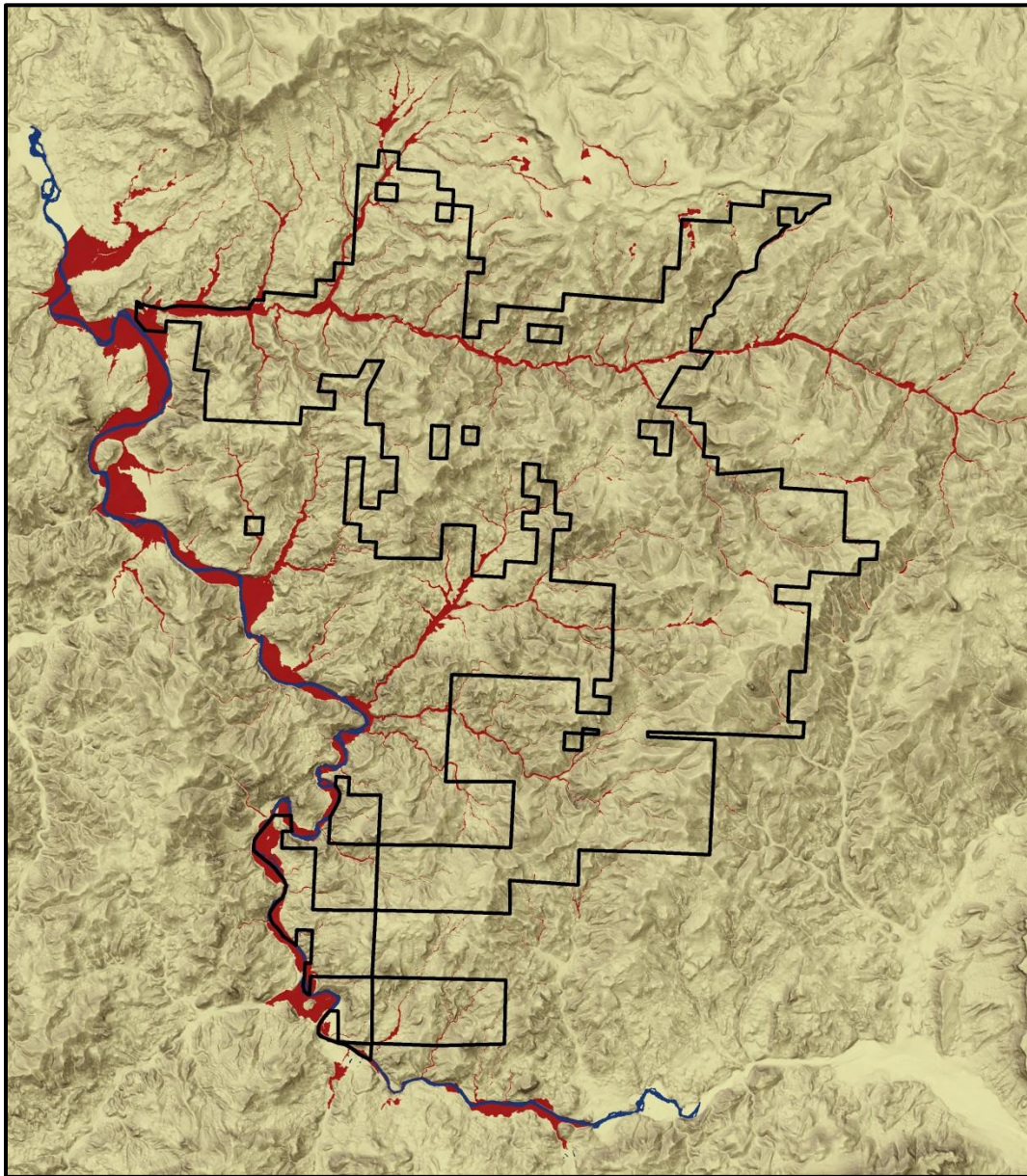


Figure 4. Delineated riparian zones, with Pine Creek Conservation Area boundary superimposed (background is slope).

3.2. Cover Modeling

3.2.1. Rank-based Associations

Table 7 contains a summary of the results of the Spearman's rank-based association test. For each land-cover category, the predictor with the highest association from each predictor group is shown with the corresponding ρ value. Strong associations are indicated by larger numbers (whether positive or negative), while for weak associations ρ is near zero. Positive relationships between the category's cover

and the predictor are indicated by positive values, while inverse relationships are indicated by negative values.

Table 7. Strongest predictor in each predictor group for each land-cover category, according to Spearman's rank-based association test, with corresponding value of ρ . Land-cover category names are defined in section 2.2.1.2, while predictor names and descriptions are in sections 2.3. and 2.4.5.

Land-cover Category	Air Photo	Canopy	Hydrology	LiDAR Topography	NED Topography	SPOT
CONIFER	R3DT5	CC8F	UPLAND	ELEV	ELEV	AU10RB
	0.662	0.802	0.095	0.303	0.303	-0.458
CERLED	V1T5N	FOLDY1	WET	SLD	SLD	AU10VI
	0.224	0.213	-0.258	0.275	0.234	-0.117
ARTTRI	R1T5	CCTOP	UPLAND	SLD	TPM600	MA12SI
	0.268	-0.334	-0.284	-0.230	-0.219	-0.182
ARTRIG	N3DT5	HT50	VDISTI	CUR30	CUR10	AU10SI
	-0.141	-0.097	0.220	0.249	0.232	-0.195
PURTRI	V1	FOLDY8	WET	SLD	RDIR	MA12RB
	-0.351	0.333	-0.421	0.414	0.356	0.404
RWV	R9DT5N	HT50	HDISTI	TPP200	TPP200	MA12FI
	0.465	0.401	-0.476	-0.463	-0.453	0.422
DRS	V1	MNNMAX	WET	ELEV	ELEV	AU10VI
	-0.145	-0.098	-0.093	-0.157	-0.156	-0.185
PSESPI	N1T5N	HT50	VDISTI	SLD	SLD	AU10B1
	0.220	0.358	0.569	0.532	0.531	-0.383
FESIDA	R1	HTTMD	UPLAND	RDIR	RDIR	AU10B3
	-0.409	0.299	0.306	-0.524	-0.522	-0.575
ACHSPP	V1	FOLDY8	WET	RDIR	RDIR	AU10VI
	-0.345	0.293	-0.309	0.292	0.291	-0.391
SPOCRY	V5DT5	CC8F	UPLAND	ELEV	ELEV	AU10FI
	-0.275	-0.256	-0.302	-0.417	-0.420	-0.274
POANAT	N1T5N	HTTMD	UPLAND	ELEV	ELEV	AU10B2
	0.396	0.424	0.358	0.386	0.384	-0.398
EXOGRASS	N1	HT50	WET	SLD	RDUR	AU10B1
	0.453	-0.511	0.443	-0.478	0.264	0.567
EXOFORB	N1	HT50	WET	SLD	SLD	AU10B1
	0.498	-0.488	0.477	-0.458	-0.402	0.507
MOSSCRYP	N1	HTTMD	UPLAND	ELEV	ELEV	AU10B1
	-0.371	0.456	0.311	0.253	0.247	-0.575
BEDROCK	V1	FOLDY8	WET	SLD	SLD	AU10VI
	-0.334	0.314	-0.436	0.420	0.370	-0.374
TALUS	V1	FOLDY8	WET	RDIR	RDIR	AU10VI
	-0.606	0.311	-0.458	0.502	0.492	-0.615
SOIL	N1	FOLDY4	VDISTI	CPR30	HL	MA12SI
	-0.192	0.258	0.083	0.133	-0.110	0.227
ASH	V1	HT50	MAXORD	CUR150	CPL150	MA12VI
	-0.342	0.079	-0.154	0.149	0.171	-0.389

The strength and sign of the associations found all appear reasonable. The strengths vary greatly by land-cover category, with some categories (e.g., mountain mahogany, shrubs tolerant of disturbed rangelands) showing only weak relationships to any of the predictors, while others (e.g., conifers, bluebunch wheatgrass) have strong associations with many predictors.

3.2.2. Accuracy Assessment

3.2.2.1. Presence Model

The confusion matrices resulting from the bootstrapped accuracy assessment are shown in Table 8. The producer accuracies are the only figures that are intrinsic to the model itself; the other figures (predictive value and total accuracy) are dependent on the true prevalence of each land-cover category, which are unknown. These values for predictive value and total accuracy given here assume that the training data accurately reflects the true prevalence, which is unlikely. The producer accuracy for presence is equivalent to sensitivity, the likelihood of correctly detecting a given positive occurrence (the false negative or omission error rate is equal to $1 - \text{sensitivity}$). The producer accuracy for absence is equivalent to specificity, the likelihood of correctly detecting a given negative occurrence (the false positive or commission error rate is equal to $1 - \text{specificity}$).

Summed across all categories, the average producer's accuracy for presence was 82.2%, corresponding to an omission error of 17.8%. This means that, overall, a category that is present in any location is mapped as absent 17.8% of the time. The average producer's accuracy for absence across all categories was 7.4%, corresponding to a commission error of 7.4%. This signifies that, overall, a category that is absent in any location is mapped as present 7.4% of the time. Obviously, these numbers vary greatly between categories. Planning of management activities based on the maps should always incorporate a consideration of the model accuracy for presence and absence of the categories in question.

Some of the rarer categories have high rates of omission error. Reduced omission errors for these categories could have been achieved if that had been the aim. However, that would have come at the expense of overpredicting the category in locations where it is not present. The thresholds chosen create a more informative map.

The reasons for the poorer performance for some land-cover categories vary. Some less well-predicted land-cover categories lacked adequate amounts of training data, due to either their rarity or inaccessibility in the training area (e.g., mountain mahogany, rigid sagebrush). Others may have been inconsistently identified by crews in the field (e.g., sand dropseed, ash deposits), or may often occur at low densities where they are difficult to map correctly (e.g., shrubs tolerant of disturbed rangelands).

The actual map accuracy for any land-cover category may be different than the model-based accuracies presented here. For some of the categories, accuracy in the field should be higher than that shown in the table. This is a consequence of the non-random locations of training data. Negative training data were frequently used in areas immediately adjacent to occurrences (e.g., RWV, rigid sagebrush) in order to train the model to more clearly recognize the difference. In addition, Random Forests is insensitive to some noise in the training dataset, and in some cases map outputs can be more accurate than cross-validated accuracy assessments, as performed here. In the end, the quality of the map will be determined by its usefulness in supporting management activities rather than by these model-based assessment figures.

Table 8. Confusion matrices resulting from the 100 bootstrapped AA runs for each of the 19 land-cover categories. Producer's accuracy for presence is equivalent to sensitivity; for absence it is equivalent to specificity. Predictive value and total accuracy are dependent on the true prevalence in the field, which are unknown.

Land-Cover Category	Actual	Mapped PRES	Mapped ABS	Producer's Accuracy	Omission & Commission Error	Predictive Value [†]	Total Accuracy [†]
Conifers	PRES	849	112	88.3%	11.7%	92.2%	90.4%
	ABS	72	881	92.4%	7.6%	88.7%	
Mountain Mahogany	PRES	21	22	48.8%	51.2%	58.3%	98.0%
	ABS	15	1755	99.2%	0.8%	98.8%	
Big Sagebrush	PRES	272	178	60.4%	39.6%	73.3%	84.3%
	ABS	99	1217	92.5%	7.5%	87.2%	
Rigid Sagebrush	PRES	31	26	54.4%	45.6%	62.0%	97.6%
	ABS	19	1835	99.0%	1.0%	98.6%	
Antelope Bitterbrush	PRES	161	93	63.4%	36.6%	76.7%	91.3%
	ABS	49	1337	96.5%	3.5%	93.5%	
Riparian Woody Vegetation	PRES	192	19	91.0%	9.0%	86.9%	97.7%
	ABS	29	1843	98.5%	1.5%	99.0%	
Disturbed Rangeland Shrubs	PRES	277	275	50.2%	49.8%	62.1%	73.1%
	ABS	169	930	84.6%	15.4%	77.2%	
Bluebunch Wheatgrass	PRES	1166	81	93.5%	6.5%	95.3%	91.7%
	ABS	58	378	86.7%	13.3%	82.4%	
Idaho Fescue	PRES	426	115	78.7%	21.3%	79.6%	86.4%
	ABS	109	993	90.1%	9.9%	89.6%	
Needlegrasses	PRES	246	116	68.0%	32.0%	71.5%	79.3%
	ABS	98	574	85.4%	14.6%	83.2%	
Sand Dropseed	PRES	62	58	51.7%	48.3%	54.9%	89.7%
	ABS	51	889	94.6%	5.4%	93.9%	
Native Bluegrasses	PRES	215	104	67.4%	32.6%	84.0%	85.7%
	ABS	41	656	94.1%	5.9%	86.3%	
Exotic Grasses	PRES	1393	82	94.4%	5.6%	96.3%	91.8%
	ABS	53	110	67.5%	32.5%	57.3%	
Exotic Forbs	PRES	577	155	78.8%	21.2%	84.1%	84.3%
	ABS	109	836	88.5%	11.5%	84.4%	
Moss & Crust	PRES	533	79	87.1%	12.9%	88.5%	85.4%
	ABS	69	330	82.7%	17.3%	80.7%	
Bedrock	PRES	238	137	63.5%	36.5%	69.2%	85.3%
	ABS	106	1174	91.7%	8.3%	89.5%	
Talus	PRES	782	142	84.6%	15.4%	88.9%	85.6%
	ABS	98	645	86.8%	13.2%	82.0%	
Bare Soil	PRES	1431	81	94.6%	5.4%	94.6%	90.0%
	ABS	82	41	33.3%	66.7%	33.6%	
Ash Deposits	PRES	51	55	48.1%	51.9%	48.6%	90.2%
	ABS	54	948	94.6%	5.4%	94.5%	
CUMULATIVE	PRES	8923	1930	82.2%	17.8%	86.6%	88.8%
	ABS	1380	17372	92.6%	7.4%	90.0%	

3.2.2.2. Cover Model

The R^2 and RMSE resulting from the bootstrapped test of the regression models are shown in Table 9. R^2 ranges from zero to one and indicates the strength of the prediction, while the RMSE represents the typical error in percent cover associated with predictions for each land-cover category. The significance of the RMSE can be assessed by comparing it to the typical percent cover at which each category occurs, given in Tables 10-12.

Table 9. R^2 and RMSE resulting from the bootstrapped cover model runs for each of the 19 land-cover categories.

Land-Cover Category	R^2	RMSE (%)
Conifers	0.760	5.0
Mountain Mahogany	0.185	6.9
Big Sagebrush	0.559	6.6
Rigid Sagebrush	0.019	11.7
Antelope Bitterbrush	0.075	2.7
Riparian Woody Vegetation	0.682	12.1
Disturbed Rangeland Shrubs	0.251	5.1
Bluebunch Wheatgrass	0.301	9.0
Idaho Fescue	0.416	11.6
Needlegrasses	0.092	6.1
Sand Dropseed	0.266	6.7
Native Bluegrasses	0.131	0.7
Exotic Grasses	0.683	15.0
Exotic Forbs	0.443	10.3
Moss & Crust	0.069	4.5
Bedrock	0.528	12.5
Talus	0.641	12.8
Bare Soil	0.213	11.4
Ash Deposits	0.784	15.5

3.2.3. Maps

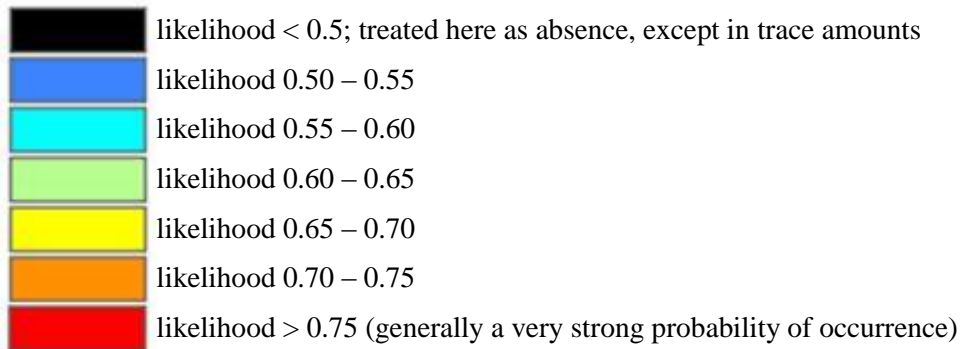
The resulting maps for cover are reproduced in Appendix C. Those for presence probability are not reproduced in the report but images in JPG format for both presence probability and percent cover have been provided separately. GIS versions of both datasets have also been provided in raster format so that they can be integrated into the Warm Springs GIS system and used for planning and directing management activities at PCCA. In general we recommend using the provided GIS datasets to create customized maps for management rather than using the snapshot images we have provided.

3.2.3.1. Presence Likelihood

The presence likelihood datasets have been provided in ArcGIS floating-point grid format, projected in UTM Zone 11 (NAD83 datum). Larger values indicate more likely occurrences of the land-cover category in question. Simple presence/absence maps can be created by thresholding the likelihood value at any desired cutoff. Values less than 0.5 have been treated as absences here, but for some applications it

may be useful to adjust that threshold, or to work with the actual likelihood value rather than a classified map.

The presence likelihood images, provided separately in JPG format, are color-coded as follows:



3.2.3.2. Percent Cover

The predicted percent cover datasets have been provided in ArcGIS floating-point grid format, projected in UTM Zone 11 (NAD83 datum). Percent cover values range from zero to one hundred. Zero values represent predicted absence (where presence likelihood is less than 0.5).



The cover maps are also shown in Appendix C. For each image, the land-cover category is predicted to be absent or present only in trace amounts in all areas colored white. Otherwise predicted covers range across the spectrum shown to the left, with darkest blue representing trace amounts of cover and orange-red representing a maximum cover value that varies by category and is shown on each map.

The cover maps have also been provided separately in JPG format. This version uses a similar color bar, except that predicted areas of absence are shown in black instead of white.

3.2.4. Land-Cover Category Area Totals

The total mapped area of each land-cover category is given in Tables 10-12 for woody vegetation, herbaceous vegetation, and ground cover types respectively. The presence area given is the total area in hectares of all the 10-meter pixels on which each land-cover type is predicted to be present in greater than trace amounts; the percent present column gives the proportion of the total land area that this figure represents. The cover area estimates the actual total cover occupied by each land-cover type, it is generally much lower than the presence area because most types occur at cover values well below 100%. The percent cover column gives the proportion of the land area that the cover area represents. The final column, the typical percent cover, gives the average cover value for each type at locations where it is predicted to occur. All the figures are given for four zones: Pine Creek Conservation Area itself (13,923 ha), the adjacent Department of Interior lands (7266 ha), the area over which training data was collected (the sum of PCCA and DOI; 21,189 ha), and the total mapping area including the five-kilometer buffer around PCCA (66501 ha).

Table 10. Mapped area of the woody vegetation land-cover categories over various portions of the mapping area, in order of prevalence at PCCA.

Category	Zone	Presence Area (ha)	Cover Area (ha)	Pct Present	Pct Cover	Typical Pct Cover
Conifers	PCCA	7255.2	1232.3	52.11	8.85	17.0
	DOI	2233.9	307.6	30.74	4.23	13.8
	Train Area	9489.1	1540.0	44.78	7.27	16.2
	Map Area	28260.6	4644.6	42.50	6.98	16.4
Disturbed Rangeland Shrubs	PCCA	4696.0	358.3	33.73	2.57	7.6
	DOI	4340.0	379.3	59.73	5.22	8.7
	Train Area	9036.0	737.6	42.64	3.48	8.2
	Map Area	24399.9	2068.6	36.69	3.11	8.5
Big Sagebrush	PCCA	950.7	94.6	6.83	0.68	9.9
	DOI	608.0	57.8	8.37	0.79	9.5
	Train Area	1558.7	152.3	7.36	0.72	9.8
	Map Area	6286.7	666.5	9.45	1.00	10.6
Mountain Mahogany	PCCA	193.8	34.4	1.39	0.25	17.7
	DOI	51.9	8.0	0.71	0.11	15.4
	Train Area	245.7	42.4	1.16	0.20	17.2
	Map Area	698.2	124.6	1.05	0.19	17.8
Riparian Woody Vegetation	PCCA	72.2	22.2	0.52	0.16	30.7
	DOI	4.4	1.1	0.06	0.02	25.4
	Train Area	76.6	23.3	0.36	0.11	30.4
	Map Area	509.3	172.5	0.77	0.26	33.9
Antelope Bitterbrush	PCCA	431.2	22.1	3.10	0.16	5.1
	DOI	319.3	16.5	4.39	0.23	5.2
	Train Area	750.5	38.6	3.54	0.18	5.1
	Map Area	2482.8	117.1	3.73	0.18	4.7
Rigid Sagebrush	PCCA	104.6	20.1	0.75	0.14	19.3
	DOI	5.2	0.9	0.07	0.01	16.8
	Train Area	109.8	21.0	0.52	0.10	19.1
	Map Area	275.9	55.8	0.41	0.08	20.2

Table 10 gives the mapped area figures for the woody vegetation categories. The most common woody vegetation type at PCCA is the conifer category, consisting mostly of western juniper but also including some Douglas-fir and ponderosa pine at higher elevations. It is present over about 52% of PCCA, occurring at an average cover proportion of 17%, resulting in a total coverage of about 17%. The category representing shrubs tolerant of disturbed rangelands is widespread, over 34% of PCCA, but at lower typical covers, resulting in a total coverage of 2.6%. Cover of the remainder of the woody vegetation categories accounts for only small amounts of the total land area.

Table 11 gives the mapped area figures for the herbaceous vegetation categories. The most commonly occurring herbaceous type at PCCA is bluebunch wheatgrass, but because it typically occurs at lower covers than exotic grasses where they are present, exotic grasses actually occupy more of the land area. Idaho fescue has the next highest total cover at PCCA, followed by exotic forbs. The other herbaceous vegetation categories occur at low total covers.

Table 11. Mapped area of the herbaceous land-cover categories over various portions of the mapping area, in order of prevalence at PCCA.

Category	Zone	Presence Area (ha)	Cover Area (ha)	Pct Present	Pct Cover	Typical Pct Cover
Exotic Grasses	PCCA	11872.9	2896.3	85.28	20.80	24.4
	DOI	6595.1	1741.4	90.76	23.97	26.4
	Train Area	18468.0	4637.7	87.16	21.89	25.1
	Map Area	60757.6	18267.6	91.36	27.47	30.1
Bluebunch Wheatgrass	PCCA	12620.3	2163.8	90.64	15.54	17.1
	DOI	5824.7	1116.4	80.16	15.36	19.2
	Train Area	18445.0	3280.3	87.05	15.48	17.8
	Map Area	51931.0	9003.3	78.09	13.54	17.3
Idaho Fescue	PCCA	6397.1	1075.3	45.95	7.72	16.8
	DOI	1612.9	334.6	22.20	4.60	20.7
	Train Area	8010.0	1409.9	37.80	6.65	17.6
	Map Area	19824.1	3368.4	29.81	5.07	17.0
Exotic Forbs	PCCA	3272.7	310.1	23.51	2.23	9.5
	DOI	2481.2	220.1	34.15	3.03	8.9
	Train Area	5753.9	530.2	27.16	2.50	9.2
	Map Area	23259.4	2774.4	34.98	4.17	11.9
Native Bluegrasses	PCCA	3134.9	70.4	22.52	0.51	2.2
	DOI	494.7	10.8	6.81	0.15	2.2
	Train Area	3629.6	81.2	17.13	0.38	2.2
	Map Area	6949.3	155.2	10.45	0.23	2.2
Sand Dropseed	PCCA	559.2	67.8	4.02	0.49	12.1
	DOI	1078.7	132.6	14.85	1.82	12.3
	Train Area	1637.9	200.4	7.73	0.95	12.2
	Map Area	4869.2	613.8	7.32	0.92	12.6
Needle-grasses	PCCA	986.7	65.1	7.09	0.47	6.6
	DOI	508.9	42.1	7.00	0.58	8.3
	Train Area	1495.6	107.2	7.06	0.51	7.2
	Map Area	4909.8	365.2	7.38	0.55	7.4

Table 12 gives the mapped area figures for the ground cover categories. The most commonly occurring and highest cover ground cover type is bare soil. The next highest cover amounts at PCCA are associated with talus, moss and cryptobiotic crust, and bedrock. Ash deposits occupy a comparatively small amount of the landscape.

Overall, the most commonly occurring land-cover categories at PCCA are bare soil, bluebunch wheatgrass, exotic grasses, moss and cryptobiotic crust, talus, and conifers; all occur at greater than 50% of sites. The same categories are most dominant by cover, but in a slightly different order due to variations in the typical percent cover values at which they occur.

PCCA is somewhat different than the mapping area as a whole. In the woody vegetation group, it has a bit more western juniper, and less big sagebrush and shrubs tolerant of disturbed rangelands than the surrounding area. It has less riparian woody vegetation, but this is likely due to the greater habitat available at higher elevations to the east. There appears to be substantially more rigid sagebrush at PCCA

than on the surrounding lands. In terms of herbaceous vegetation, PCCA appears to be in good condition compared to the surrounding area, with more bluebunch wheatgrass and Idaho fescue, less exotic grasses and forbs, and possibly more cryptobiotic crust.

Table 12. Mapped area of the ground cover categories over various portions of the mapping area, in order of prevalence at PCCA.

Category	Zone	Presence Area (ha)	Cover Area (ha)	Pct Present	Pct Cover	Typical Pct Cover
Bare Soil	PCCA	13105.8	2749.3	94.13	19.75	21.0
	DOI	6960.4	1556.2	95.79	21.42	22.4
	Train Area	20066.2	4305.5	94.70	20.32	21.5
	Map Area	59866.2	12253.2	90.02	18.43	20.5
Talus	PCCA	9872.9	1940.7	70.91	13.94	19.7
	DOI	6154.9	1316.7	84.70	18.12	21.4
	Train Area	16027.7	3257.4	75.64	15.37	20.3
	Map Area	44172.5	9187.8	66.42	13.82	20.8
Moss & Crust	PCCA	11610.7	1109.8	83.39	7.97	9.6
	DOI	4786.6	421.7	65.87	5.80	8.8
	Train Area	16397.3	1531.6	77.39	7.23	9.3
	Map Area	43484.1	4094.1	65.39	6.16	9.4
Bedrock	PCCA	2760.2	452.6	19.82	3.25	16.4
	DOI	1497.2	289.1	20.60	3.98	19.3
	Train Area	4257.4	741.6	20.09	3.50	17.4
	Map Area	10645.2	1790.3	16.01	2.69	16.8
Ash Deposits	PCCA	314.5	110.4	2.26	0.79	35.1
	DOI	378.3	131.2	5.21	1.81	34.7
	Train Area	692.8	241.6	3.27	1.14	34.9
	Map Area	2921.0	1022.4	4.39	1.54	35.0

3.2.5. Relative Importance of Predictors

The strength of the relationship between the importance values for the classification and modeling phases was tested by regressing them against one another. The resulting scatterplot and R-squared value of 0.052 indicated the lack of any significant relationship. In other words, there is generally no connection between the variables that are most important for predicting presence and absence and those for predicting the cover amount in areas where the category is known to be present. This is an interesting result.

The most significant predictors are shown in Appendix B for each of the land-cover category classification and regression models. All values refer to the first predictor subset run except for the mountain mahogany and bedrock categories, for which the second predictor subset run was the primary one. All predictors which ranked in the top ten predictors in either model are shown; the relative importance values for the top ten for each category are highlighted. Predictor names are the same as those introduced in sections 2.3 and 2.4.5, with the two letter prefix indicating whether they come from the LiDAR topography (li), NED topography (ne), LiDAR canopy (ca), aerial photography (ap), SPOT satellite (sp) or hydrological (hy) predictor groups.

APPENDIX A: FIELD SAMPLING FORMS

The protocols used during the 2011 and 2012 field sampling efforts differed because the 2012 effort was originally intended to generate additional samples to use for map accuracy assessment. In addition, it became clear at the end of 2011 that higher resolution SPOT satellite imagery would be available for the project instead of Landsat TM imagery, so subsequent plot data was collected assuming the use of finer scale data. The two field forms are shown below.

2012 Field Form

PCCA AA v2	Plot ID: AA	Region:	Ob:	Date:	Obs Type: On / Dist	Bear/Dist: / m
GPS acc ± m	Pt moved? Y/N	New ID:	Unit:	UTM E:	UTM N:	
Match pt description? Y/N	If not: Slope deg	Aspect deg	H88 ht ft	Canopy cover > 8': %		
Check/modify location with imagery? Y/N	Check/assign class using imagery? Y/N					
Interp #	Code/Desc	Notes			% rep	
best? <input type="checkbox"/> A						
best? <input type="checkbox"/> B						
best? <input type="checkbox"/> C						
best? <input type="checkbox"/> D						
Description (incl. disturbance or successional process):						
Shrb: 1) _____ 2) _____ 3) _____ 4) _____ 5) _____ Herb: 1) _____ 2) _____ 3) _____ 4) _____ 5) _____						
COVER	CAN - SUB - REGEN	Heterogeneity: L / M / H		Full sample? Y / N		Cover represents: -A / B / C / D
CONIFERS	- -	SHRUBS		NATIVE HERB-SUBSHRUB		EXOTIC HERB
JUNOCC - live junip.	- -	ARTRI - big sage		PSESPI - bluebunch wheatgrs		BROTEC - cheatgrass
JUNOCC - dead junip.	- -	PURTRI - bitterbrush		FESIDA - Idaho fescue		TAECAP - medusahead
PSEMEN - Doug-fir	- -	CERLED - mtn mahogany		ACHSPP - needlegrasses		VENDUB - ventenata
PINPON - ponderosa	- -	ERINAU+CHRVIS+TETCAN-rabbitbrush+horsebrush		SPOCRY - sand dropseed		Other exotic grasses
	- -			Other native grasses		Exotic forbs
DECIDUOUS TREES	- -	PRUVIR - chokecherry				GROUND
CELRET - hackberry	- -	SALIX - willows		ARTRIG - rigid sage		bedrock
AMEALN - servicebry	- -	Other shrubs		GUTSAR - broom snakeweed		loose rock (bigger than a silver dollar)
POPBAL - cottonwd	- -			Other native subshrubs		soil + litter + tiny rocks
POPTRE - aspen	- -					moss/crust
PRUEMA - cherry	- -			Native forbs		ash
	- -					
Nearby Trace 1 (1-2%) 1 (2-4%) 1+ (4-6%) 2 (6-10%) 2 (10-20%) 2+ (20-26%) 3 (26-36%) 3 (36-70%) 3+ (70-100%) <input type="checkbox"/> sheet entered <input type="checkbox"/> sheet verified						
Nearby opportunistic point name & description:						

2011 Field Form

PINE CREEK DATASHEET v2		Map Product		Base Map - Change		Plot Type		Nav - Opp		Plot #		Map #											
Date				Observers				Cluster #															
Polygon drawn?		Y - N		Obs Type		Onsite - Distance		Plot Size		Large-Narrow-Small		Coordinate Source		GPS - Map									
GPS?		Y - N		Unit		UTM E		UTM N		Notes													
POSITION		Slope		%		<input type="checkbox"/> ridge shoulder		<input type="checkbox"/> upper 1/3 slope		<input type="checkbox"/> middle 1/3 slope		<input type="checkbox"/> lower 1/3 slope		<input type="checkbox"/> toeslope									
		Aspect				<input type="checkbox"/> ridge top		<input type="checkbox"/> bench/flat		<input type="checkbox"/> drainage (concave)		<input type="checkbox"/> river bottom		<input type="checkbox"/> wetland									
Site description:																							
Unsampled vegetation in 90x90m area:																							
Disturbance evidence		<input type="checkbox"/> successful fire		<input type="checkbox"/> unsuccessful fire		<input type="checkbox"/> cattle grazing		<input type="checkbox"/>															
		Pre-fire juniper cover estimate		_____ %																			
Change evidence		<input type="checkbox"/> juniper seedlings		<input type="checkbox"/>																			
Imagery notes:																							
COVER AND CLASSIFICATION																							
Center Plot Radius		10m - 45m - _____ m		Plot Dimension Notes																			
Special Classes		<input type="checkbox"/> scab		<input type="checkbox"/> mtn mahogany		<input type="checkbox"/> salt desert shrub		<input type="checkbox"/> hackberry		<input type="checkbox"/> G.B. wildrye		<input type="checkbox"/>											
CATEGORY		CENTER		NW 37m		NE 37m		SE 37m		SW 37m		CATEGORY		CENTER		NW 37m		NE 37m		SE 37m		SW 37m	
Same as ---->												Same as ---->											
JUNIPER COUNT		live / dead		live / dead		live / dead		live / dead		live / dead		NATIVE HERB / SUB-SHRUB											
old growth		/ /		/ /		/ /		/ /		/ /		bluebunch											
> 10'		/ /		/ /		/ /		/ /		/ /		wheatgrass											
3-10'		/ /		/ /		/ /		/ /		/ /		Idaho fescue											
< 3'		/ /		/ /		/ /		/ /		/ /		needlegresses											
TREE-overstory												juniper (old)											
juniper > 10'												juniper > 10'											
juniper 3-10'												juniper 3-10'											
Douglas-fir												Douglas-fir											
ponderosa pine												ponderosa pine											
mtn. mahogany												mtn. mahogany											
hackberry												hackberry											
TREE-understory												Douglas-fir											
Douglas-fir												Douglas-fir											
SHRUB												big sage											
big sage												big sage											
rigid sage												rigid sage											
antel. bitterbrush												antel. bitterbrush											
serviceberry												serviceberry											
chokecherry												chokecherry											
other riparian												other riparian											
rabbitbrush												rabbitbrush											
other =												other =											
PHOTOS		CAMERA		IMAGE #		LOCATION		DIREC		DESCRIPTION													
<input type="checkbox"/> polygon created		<input type="checkbox"/> datasheet entered		<input type="checkbox"/> datasheet verified																			

APPENDIX B: PREDICTOR IMPORTANCE VALUES

CATEGORY	PREDICTOR	PRESENCE IMPORTANCE	COVER IMPORTANCE	CATEGORY	PREDICTOR	PRESENCE IMPORTANCE	COVER IMPORTANCE
ACHSPP	li_cpl150	0.4184	1	ARTTRI	ca_cc8f	0.638	0.2115
ACHSPP	ap_v1	1	-0.0344	ARTTRI	li_elev	0.5974	0.0835
ACHSPP	sp_au10vi	0.9773	0.0816	ARTTRI	hy_wet	0.5934	0.2206
ACHSPP	hy_vdistp	0.2168	0.8282	ARTTRI	ca_hta8sd	0.5805	0.0589
ACHSPP	li_rdir	0.8226	-0.0493	ARTTRI	ca_hta4sd	0.5285	0.2272
ACHSPP	ap_r1	0.7747	0.2741	ARTTRI	sp_au10b4	0.5084	0.2935
ACHSPP	li_cur150	0.3653	0.7238	ARTTRI	ap_n1t5n	0.5008	0.2271
ACHSPP	sp_ma12vi	0.7172	0.0231	ARTTRI	ap_r1t5	0.3212	0.2776
ACHSPP	li_sld	0.7064	0.456	ARTTRI	ap_v5dt5	0.0768	0.2649
ACHSPP	sp_ma12rb	0.6649	0.1874	ARTTRI	ap_v9dt5	-0.0096	0.2533
ACHSPP	ap_v2dt5n	0.0099	0.6159	ASH	sp_ma12rb	0.496	1
ACHSPP	ap_v9dt5n	0.2324	0.612	ASH	sp_ma12vi	1	0.279
ACHSPP	hy_upland	0.5606	0.4859	ASH	li_cpr5	0.2881	0.8639
ACHSPP	sp_au10fi	0.5406	0.0775	ASH	li_cpr10	0.3667	0.7363
ACHSPP	hy_wet	0.4172	0.5374	ASH	ap_v2dt5	0.1852	0.6174
ACHSPP	sp_au10rb	0.5337	0.1658	ASH	ap_r2dt5	0.2005	0.6108
ACHSPP	li_elev	0.5275	0.5084	ASH	ap_r5dt5n	0.6017	0.1015
ACHSPP	ca_88nmax	0.2329	0.4268	ASH	ap_n2dt5	0.2385	0.5984
ARTRIG	sp_ma12si	0.2595	1	ASH	ca_ht75	0.0804	0.5891
ARTRIG	sp_au10b3	1	-0.1681	ASH	ca_foldy2	0.2257	0.5831
ARTRIG	li_elev	0.9441	0.263	ASH	ap_v3dt5	0.2659	0.5815
ARTRIG	li_cur5	0.8542	0.2974	ASH	ca_foldy4	0.1233	0.5756
ARTRIG	li_cpr10	0.854	0.1614	ASH	sp_ma12si	0.541	0.5299
ARTRIG	li_cur10	0.7027	0.181	ASH	sp_ma12b4	0.5159	0.2682
ARTRIG	li_tpp200	0.6987	0.2353	ASH	ap_v1	0.4298	0.5092
ARTRIG	sp_au10b2	0.696	-0.1859	ASH	ap_r9dt5	0.4744	0.081
ARTRIG	li_rdir	0.6353	0.2965	ASH	sp_au10vi	0.4368	0.1246
ARTRIG	li_cpr5	0.5972	0.1322	ASH	sp_au10si	0.4224	0.0097
ARTRIG	li_tpm200	0.5361	0.006	ASH	ap_r5dt5	0.3847	-0.0619
ARTRIG	sp_ma12b2	0.4023	0.2883	BEDROCK	li_sld	0.9391	1
ARTRIG	li_cpl10	0.4016	0.2443	BEDROCK	hy_wet	1	0.466
ARTRIG	li_cpl5	0.2845	0.3211	BEDROCK	li_rdir	0.8633	0.2153
ARTRIG	ca_mnnmax	-0.1915	0.2682	BEDROCK	sp_ma12rb	0.7998	0.1548
ARTRIG	ap_n1	-0.1353	0.2519	BEDROCK	sp_au10vi	0.7692	0.1717
ARTTRI	ca_foldy1	0.7901	1	BEDROCK	ap_r9dt5	0.7302	0.0658
ARTTRI	ca_mnnmax	1	0.1322	BEDROCK	li_cpr10	0.7153	0.29
ARTTRI	ca_cctop	0.893	0.4482	BEDROCK	ap_n9dt5n	0.6903	0.0322
ARTTRI	ca_foldy2	0.7784	0.475	BEDROCK	ap_v1	0.6765	0.1103
ARTTRI	li_sld	0.6771	0.4149	BEDROCK	sp_ma12fi	0.4337	0.646
ARTTRI	ca_htwmd	0.644	0.2058	BEDROCK	li_cpr5	0.6261	0.2197

Appendix B, Variable Importance Values, cont.

CATEGORY	PREDICTOR	PRESENCE IMPORTANCE	COVER IMPORTANCE	CATEGORY	PREDICTOR	PRESENCE IMPORTANCE	COVER IMPORTANCE
BEDROCK	sp_ma12vi	0.5699	0.229	DRS	hy_hdisti	0.1102	0.6268
BEDROCK	sp_au10fi	0.5062	0.2765	DRS	hy_upland	0.6023	0.4691
BEDROCK	sp_ma12mi	0.3272	0.484	DRS	ca_ht88	0.342	0.5833
BEDROCK	sp_au10si	0.4538	0.4121	DRS	sp_ma12vi	0.5786	0.3417
BEDROCK	li_tpm200	0.4006	0.2621	DRS	sp_au10si	0.5764	0.3201
BEDROCK	sp_au10b1	0.1916	0.2366	DRS	sp_ma12b4	0.218	0.5473
CERLED	ap_v1	-0.0999	1	DRS	li_sld	0.5056	0.2919
CERLED	li_sld	1	0.1531	DRS	sp_ma12si	0.5054	0.1617
CERLED	hy_wet	0.9353	-0.019	DRS	sp_au10b1	0.4681	0.1612
CERLED	sp_au10si	0.0221	0.909	DRS	ca_ht75	0.3554	0.4462
CERLED	sp_au10vi	0.3952	0.7659	DRS	hy_vdistp	0.4398	0.4296
CERLED	sp_ma12vi	-0.0567	0.7515	DRS	ca_htmd	0.3605	0.4345
CERLED	ap_n1t5n	0.1906	0.7251	EXOFORB	ca_ht75	0.863	1
CERLED	ap_r3dt5	0.1143	0.6791	EXOFORB	hy_wet	1	0.2142
CERLED	sp_ma12si	0.0312	0.6317	EXOFORB	sp_au10b1	0.9451	0.535
CERLED	ap_r2dt5n	0.1764	0.6029	EXOFORB	ap_n1	0.8722	0.9322
CERLED	ap_n1t5	0.2996	0.594	EXOFORB	hy_vdisti	0.9218	0.1241
CERLED	ap_v1t5	0.2194	0.5848	EXOFORB	ca_foldy1	0.8924	0.1548
CERLED	li_cpr5	0.5224	-0.2247	EXOFORB	ca_ht50	0.8746	0.5029
CERLED	li_cur5	0.4407	-0.1099	EXOFORB	ca_ht88	0.7959	0.8314
CERLED	li_cur10	0.4397	0.1809	EXOFORB	hy_upland	0.8252	0.389
CERLED	ap_v9dt5n	0.4227	-0.0787	EXOFORB	hy_vdistp	0.8226	0.2333
CERLED	li_cpl5	0.4191	-0.2155	EXOFORB	sp_ma12si	0.8224	0.1754
CERLED	sp_au10fi	0.3963	-0.0462	EXOFORB	ap_v1	0.8031	0.8025
CERLED	li_cpl10	0.3918	0.0174	EXOFORB	hy_maxord	0.5421	0.6903
CONIFER	ca_cc8f	1	1	EXOFORB	ca_foldy2	0.5621	0.6155
CONIFER	ca_htmd	0.8708	0.6569	EXOFORB	ca_hta8sd	0.384	0.4618
CONIFER	ca_hta4sd	0.8665	0.7758	EXOFORB	ap_n1t5n	0.3478	0.4147
CONIFER	ca_hta8sd	0.8057	0.4598	EXOGRASS	ca_foldy1	0.4129	1
CONIFER	ap_v3dt5n	0.5436	0.7627	EXOGRASS	ca_8nmax	1	0.2795
CONIFER	ca_cc3f	0.7618	0.4406	EXOGRASS	sp_au10b2	0.9156	0.4935
CONIFER	ca_htwmd	0.7519	0.5463	EXOGRASS	sp_au10b3	0.9015	0.4125
CONIFER	ca_ht88	0.6875	0.7017	EXOGRASS	sp_ma12si	0.1917	0.8969
CONIFER	ca_ht75	0.568	0.5937	EXOGRASS	ca_ht50	0.5629	0.8667
CONIFER	ca_foldy4	0.5683	0.3128	EXOGRASS	sp_au10b1	0.5656	0.8229
CONIFER	ap_n1	0.5635	0.5027	EXOGRASS	ap_n1	-0.0083	0.8184
DRS	li_elev	1	1	EXOGRASS	li_rdur	0.7602	0.2602
DRS	hy_vdisti	0.2474	0.8446	EXOGRASS	ca_ht75	0.5399	0.7481
DRS	sp_au10vi	0.8201	0.3743	EXOGRASS	li_rdir	0.7138	0.1922
DRS	ca_cc8f	0.623	0.6529	EXOGRASS	sp_au10rb	0.6951	0.5088

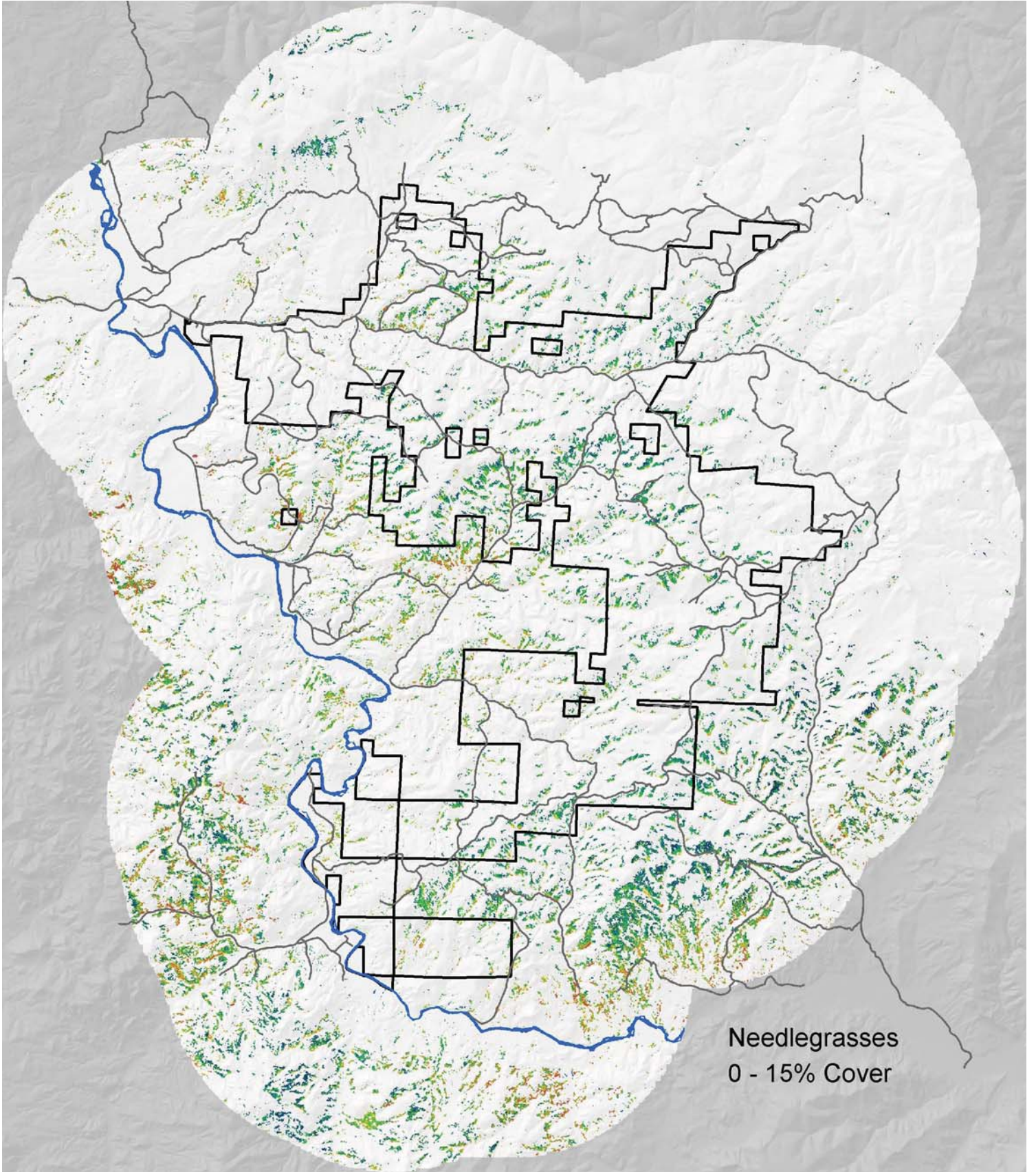
Appendix B, Variable Importance Values, cont.

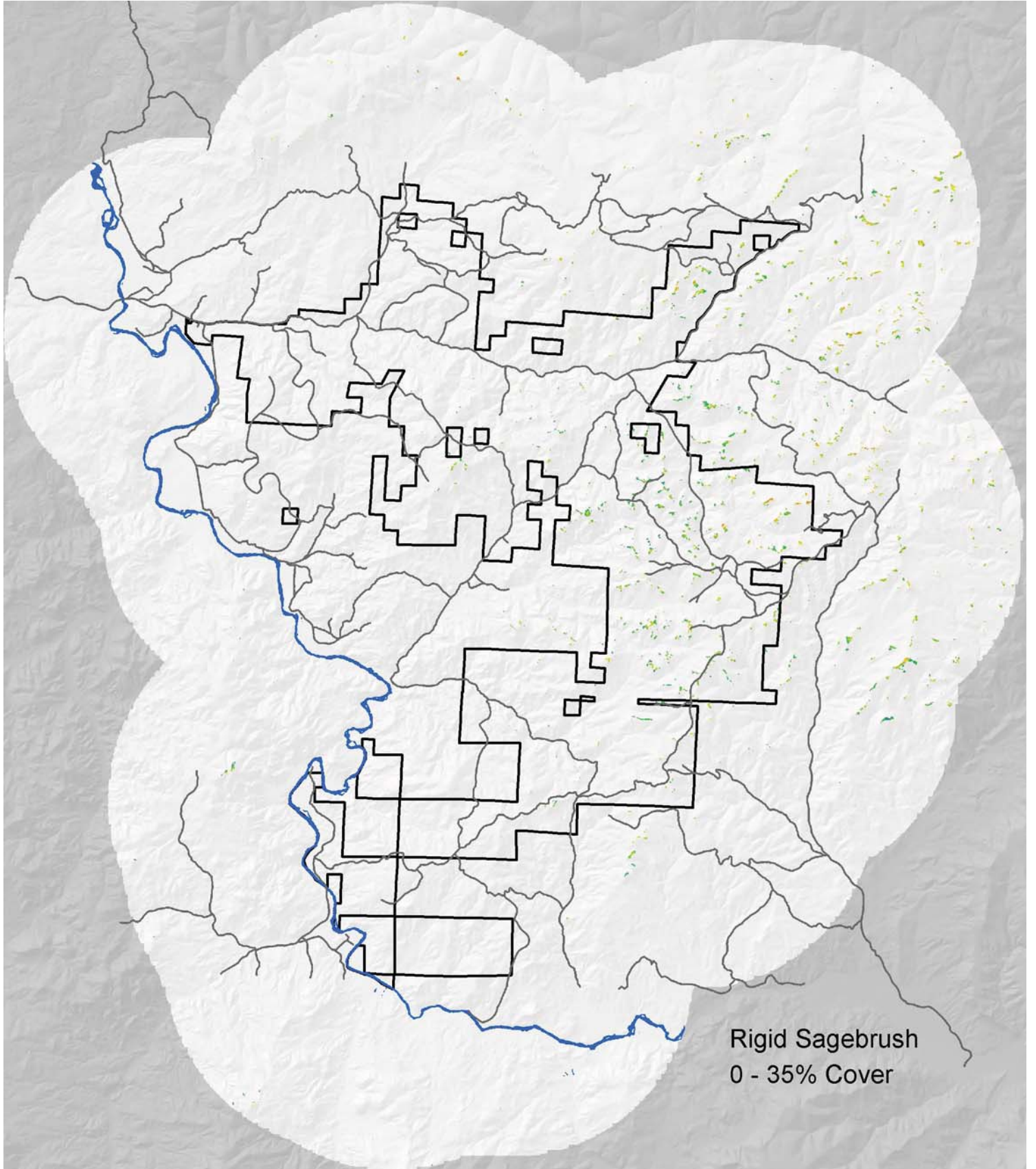
CATEGORY	PREDICTOR	PRESENCE IMPORTANCE	COVER IMPORTANCE	CATEGORY	PREDICTOR	PRESENCE IMPORTANCE	COVER IMPORTANCE
EXOGRASS	sp_ma12vi	0.0831	0.6529	POANAT	sp_ma12b1	0.9113	0.7313
EXOGRASS	ca_foldy8	0.6475	0.1894	POANAT	sp_au10b2	0.8742	0.4242
EXOGRASS	ap_v1	0.4067	0.6445	POANAT	ca_cctop	0.809	0.2757
EXOGRASS	ca_ht88	0.4389	0.6344	POANAT	sp_au10b4	0.7962	0.1544
EXOGRASS	ca_foldy2	0.2142	0.5708	POANAT	sp_au10b1	0.7294	0.1026
EXOGRASS	li_cpl30	0.5678	0.1935	POANAT	ca_mnnmax	0.6215	-0.043
FESIDA	li_rdir	1	1	POANAT	li_elev	0.4482	0.608
FESIDA	sp_au10b3	0.8952	0.2451	POANAT	ca_hta8sd	0.5147	0.5702
FESIDA	sp_au10b2	0.8694	0.3386	POANAT	ap_n1t5n	0.5313	-0.0838
FESIDA	sp_ma12rb	0.7255	0.3098	POANAT	sp_au10rb	0.5151	0.2782
FESIDA	sp_au10rb	0.7162	0.3109	POANAT	ca_htwmd	0.4486	0.3645
FESIDA	li_hl	0.7049	0.4045	POANAT	ca_cc8f	0.3141	0.4188
FESIDA	li_elev	0.6454	0.0185	POANAT	ap_r1t5	0.0333	0.3628
FESIDA	ca_hta8sd	0.6225	0.0262	POANAT	ap_r9dt5n	0.0097	0.3264
FESIDA	ap_r1	0.5693	0.1294	PSESPI	li_rdir	0.4426	1
FESIDA	sp_au10b1	0.5667	0.0727	PSESPI	hy_vdisti	1	0.5837
FESIDA	ap_v1	0.5413	0.2277	PSESPI	hy_vdistp	0.881	0.2496
FESIDA	hy_upland	0.4216	0.4292	PSESPI	hy_upland	0.8072	0.4167
FESIDA	ca_mnnmax	0.2126	0.2522	PSESPI	li_sld	0.7973	0.5435
FESIDA	ap_v1t5n	0.1415	0.2244	PSESPI	hy_wet	0.7896	0.4553
MOSSCRYP	sp_au10rb	0.9323	1	PSESPI	ca_ht50	0.7242	0.3924
MOSSCRYP	sp_au10b1	1	0.7459	PSESPI	li_elev	0.6484	0.2601
MOSSCRYP	hy_upland	0.8705	-0.0284	PSESPI	ca_ht75	0.6391	0.1961
MOSSCRYP	sp_ma12mi	0.7852	-0.1004	PSESPI	ca_ht88	0.6113	0.1692
MOSSCRYP	sp_au10b2	0.7797	0.3519	PSESPI	ca_foldy1	0.5677	0.285
MOSSCRYP	sp_au10mi	0.7632	0.0558	PSESPI	sp_ma12rb	0.2109	0.4448
MOSSCRYP	hy_wet	0.7053	0.2108	PSESPI	ap_r5dt5	0.2615	0.4426
MOSSCRYP	sp_au10fi	0.6139	0.0424	PSESPI	ca_mnnmax	0.2495	0.4077
MOSSCRYP	ca_cc3f	0.3838	0.611	PSESPI	ap_v5dt5	0.1961	0.3527
MOSSCRYP	sp_au10b3	0.6105	0.374	PURTRI	ap_n5dt5	0.0859	1
MOSSCRYP	sp_ma12fi	0.6042	-0.0283	PURTRI	li_rdir	1	-0.0455
MOSSCRYP	ap_v3dt5n	0.3289	0.5472	PURTRI	ca_foldy2	0.8123	-0.0293
MOSSCRYP	ca_cc8f	0.5357	0.5414	PURTRI	hy_wet	0.7388	0.0737
MOSSCRYP	sp_au10b4	0.4017	0.5189	PURTRI	li_elev	0.691	0.2042
MOSSCRYP	ap_n1	0.3161	0.5105	PURTRI	sp_ma12b1	0.6881	0.0908
MOSSCRYP	ca_hta4sd	0.474	0.4917	PURTRI	ca_88nmax	0.1677	0.6858
MOSSCRYP	ca_ht50	0.4228	0.4762	PURTRI	ca_ht50	0.661	0.3123
MOSSCRYP	sp_au10si	0.4008	0.4725	PURTRI	li_hl	0.6534	-0.1836
POANAT	ca_hta4sd	0.5769	1	PURTRI	hy_maxord	0.283	0.6447
POANAT	sp_au10b3	1	0.7031	PURTRI	ca_cc8f	0.5985	0.6305

Appendix B, Variable Importance Values, cont.

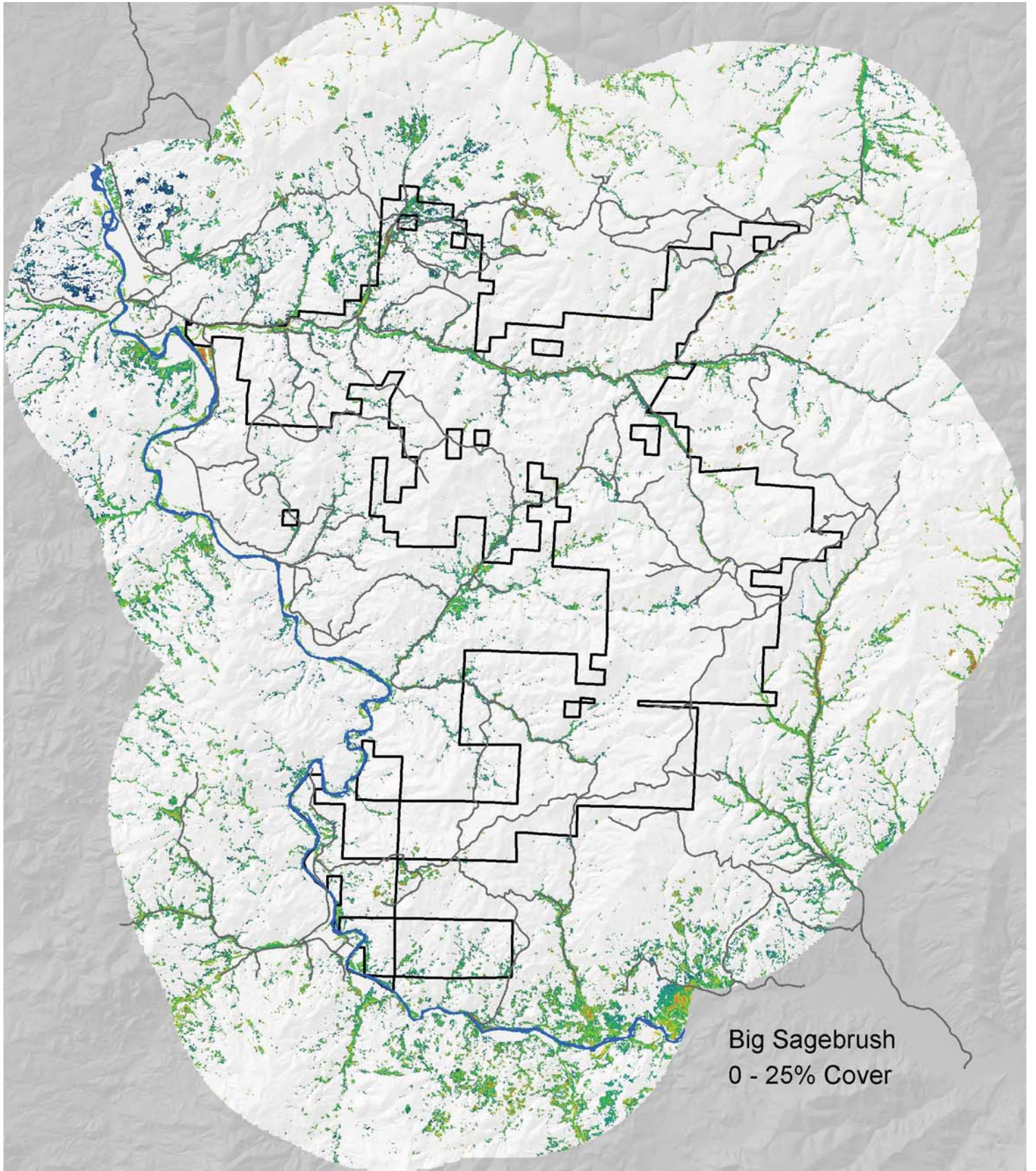
CATEGORY	PREDICTOR	PRESENCE IMPORTANCE	COVER IMPORTANCE	CATEGORY	PREDICTOR	PRESENCE IMPORTANCE	COVER IMPORTANCE
PURTRI	sp_ma12b2	0.6211	0.0424	SOIL	hy_hdisti	0.0611	0.4713
PURTRI	ca_htwmd	0.6153	0.0125	SOIL	ca_hta4sd	0.2068	0.4615
PURTRI	ca_foldy4	0.6046	-0.1104	SOIL	ca_mnnmax	0.0115	0.4508
PURTRI	ap_n9dt5	0.0367	0.4998	SOIL	ca_foldy4	0.2575	0.4278
PURTRI	ca_mnnmax	0.3731	0.4686	SOIL	ca_cctop	-0.2851	0.4262
PURTRI	ca_httmd	0.4622	0.4666	SPOCRY	ap_r2dt5	0.0447	1
PURTRI	li_tpp600	0.1474	0.4333	SPOCRY	li_elev	1	-0.0548
PURTRI	ap_n5dt5n	0.1685	0.3991	SPOCRY	ap_v1	0.9485	-0.0722
PURTRI	ca_foldy1	0.1504	0.3914	SPOCRY	hy_upland	0.9153	-0.0115
RWV	ap_v1	1	1	SPOCRY	ap_n1t5	-0.1542	0.8623
RWV	sp_ma12mi	0.5681	0.8757	SPOCRY	hy_vdisti	0.761	0.0269
RWV	ap_n1	0.8694	0.3792	SPOCRY	ap_n3dt5	0.1062	0.7324
RWV	hy_hdisti	0.8216	0.1103	SPOCRY	hy_vdistp	0.7087	0.1022
RWV	hy_hdistp	0.8053	0.1192	SPOCRY	ap_r1t5	-0.0471	0.7021
RWV	hy_wet	0.6602	0.1326	SPOCRY	ap_n1	0.6514	0.0756
RWV	li_tpp200	0.6097	0.3602	SPOCRY	sp_au10b1	0.6408	-0.1255
RWV	ca_htwmd	0.5626	0.0442	SPOCRY	sp_ma12mi	0.6296	0.07
RWV	sp_ma12fi	0.5588	0.5357	SPOCRY	sp_ma12b1	0.6038	0.3066
RWV	ap_v1t5n	0.5432	0.0903	SPOCRY	ap_r2dt5n	-0.019	0.5842
RWV	ap_r1t5n	0.46	0.5175	SPOCRY	ap_r3dt5	-0.3155	0.5721
RWV	sp_au10vi	0.3433	0.4725	SPOCRY	ap_r1t5n	0.3267	0.545
RWV	ap_v9dt5	0.2978	0.4233	SPOCRY	sp_ma12si	0.514	-0.1471
RWV	sp_ma12vi	0.3576	0.4196	SPOCRY	ca_foldy4	0.2333	0.4796
RWV	sp_au10fi	0.3365	0.4142	SPOCRY	ap_r3dt5n	-0.1127	0.4548
RWV	sp_au10mi	0.3631	0.4024	SPOCRY	ca_foldy2	-0.024	0.4079
SOIL	ap_n1	0.5082	1	TALUS	ap_v1	0.9606	1
SOIL	ap_v9dt5n	1	0.2665	TALUS	li_rdir	1	0.3857
SOIL	ap_v3dt5n	0.9814	0.251	TALUS	sp_au10vi	0.922	0.3174
SOIL	ap_v5dt5n	0.8795	0.306	TALUS	sp_ma12vi	0.822	0.6604
SOIL	ap_v2dt5n	0.8779	0.1886	TALUS	hy_wet	0.7892	0.1604
SOIL	ap_r3dt5	0.0368	0.7798	TALUS	sp_ma12rb	0.7756	0.5993
SOIL	sp_ma12vi	0.7416	0.3815	TALUS	li_sld	0.7308	0.6645
SOIL	ap_n5dt5n	0.7191	0.2166	TALUS	sp_au10fi	0.7148	0.2045
SOIL	ca_cc8f	0.6532	0.1746	TALUS	sp_ma12b1	0.3723	0.6759
SOIL	sp_ma12fi	0.6434	0.3042	TALUS	sp_ma12si	0.6698	0.499
SOIL	sp_ma12b4	0.6208	0.1423	TALUS	sp_ma12fi	0.4508	0.6155
SOIL	ap_v5dt5	0.6128	0.4172	TALUS	ap_r1	0.6037	0.342
SOIL	sp_ma12si	-0.262	0.5577	TALUS	li_hl	0.5415	0.6015
SOIL	li_sld	0.1536	0.543	TALUS	li_tpm600	0.1774	0.5031
SOIL	li_elev	0.5156	0.5261	TALUS	hy_hdisti	0.2203	0.4666

APPENDIX C: LAND-COVER CATEGORY COVER MAPS

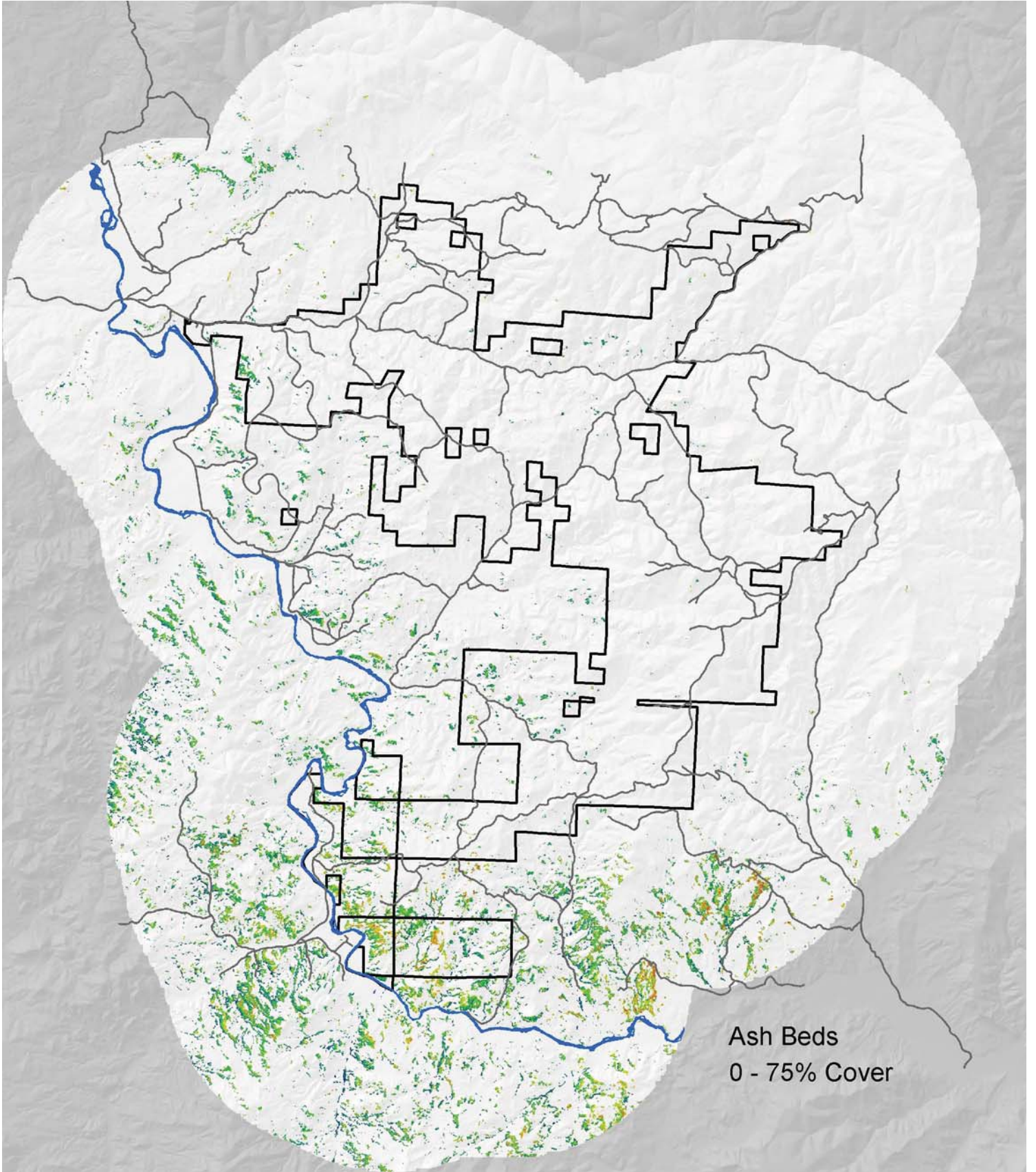




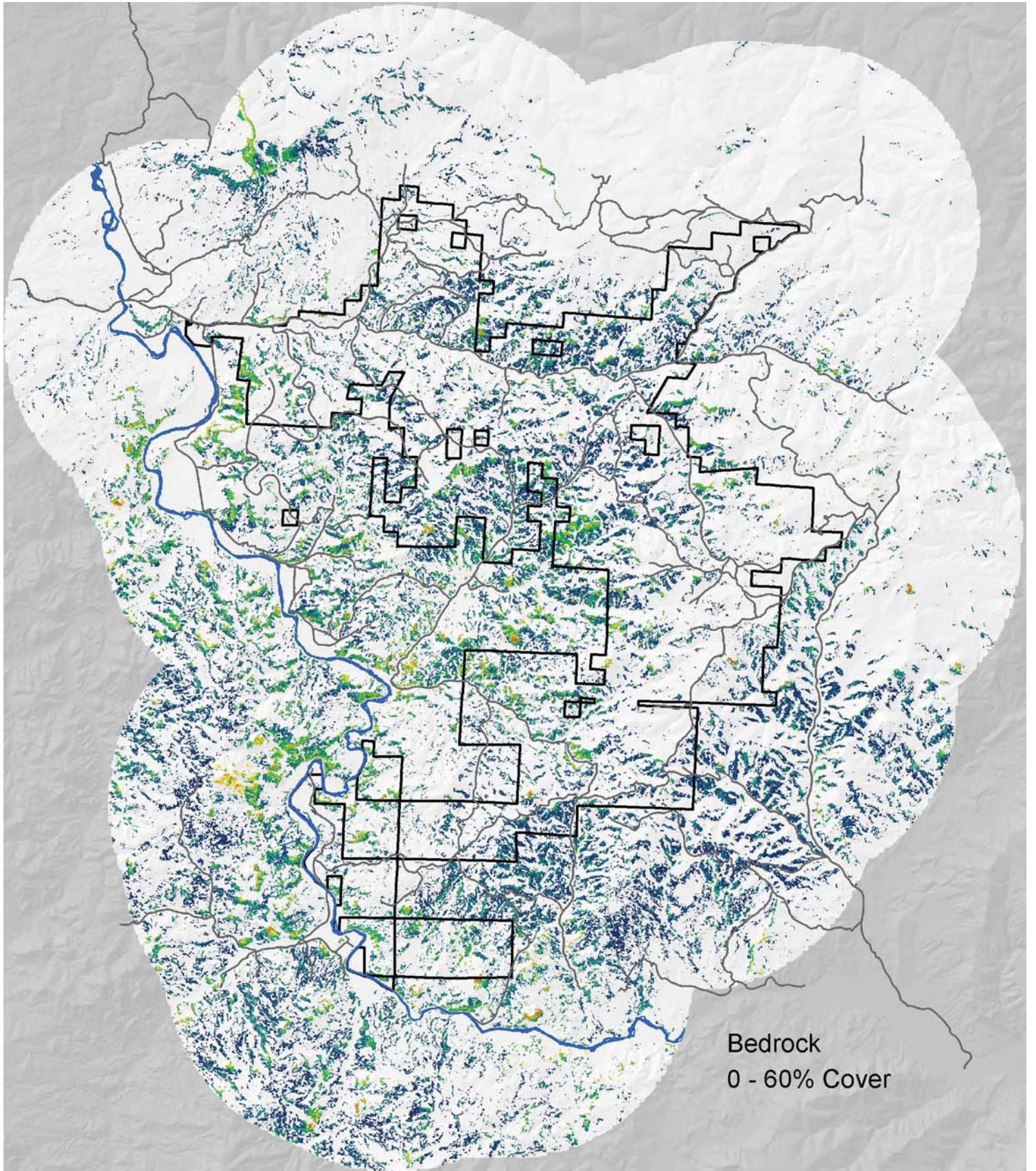
Rigid Sagebrush
0 - 35% Cover



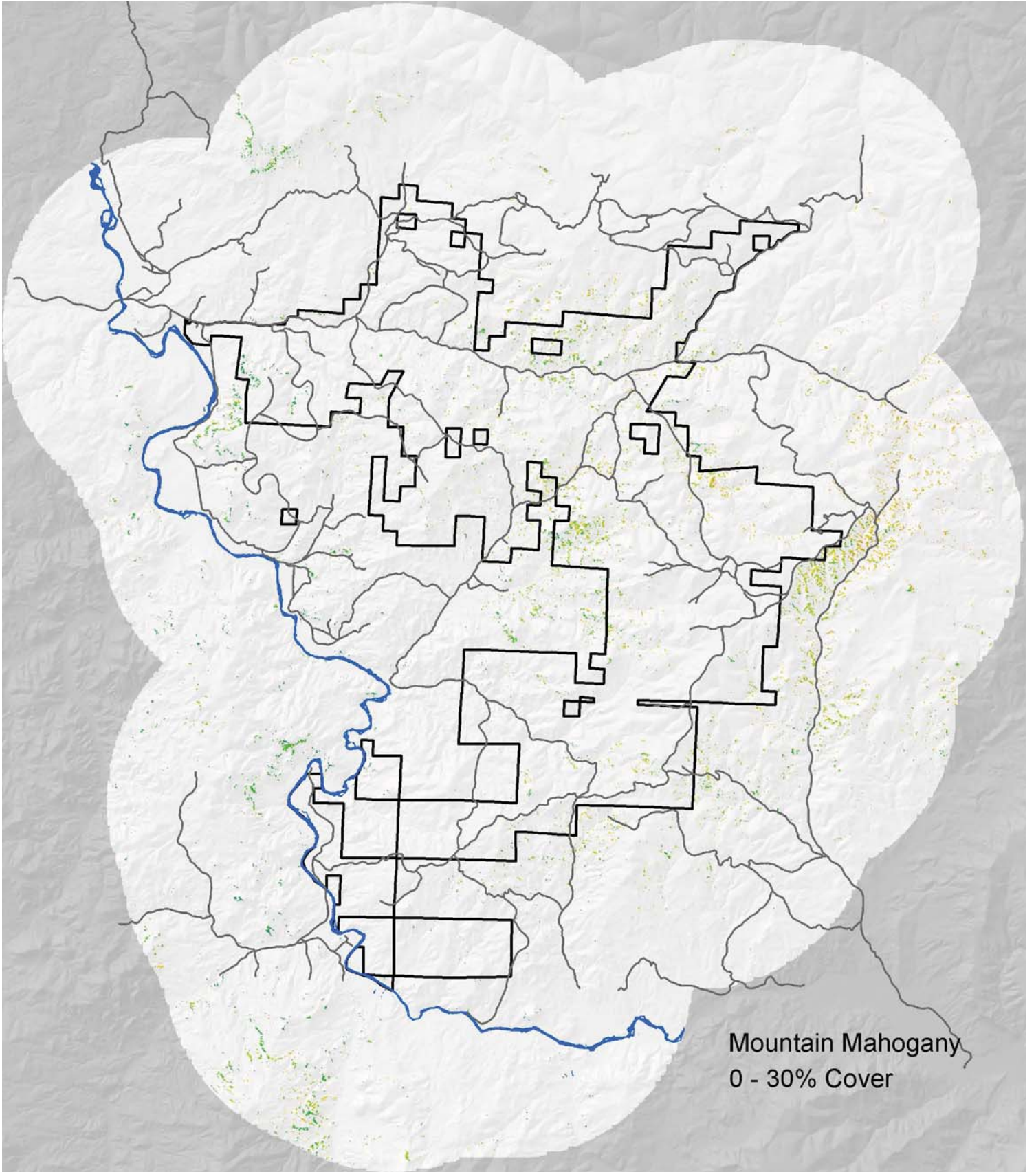
Big Sagebrush
0 - 25% Cover

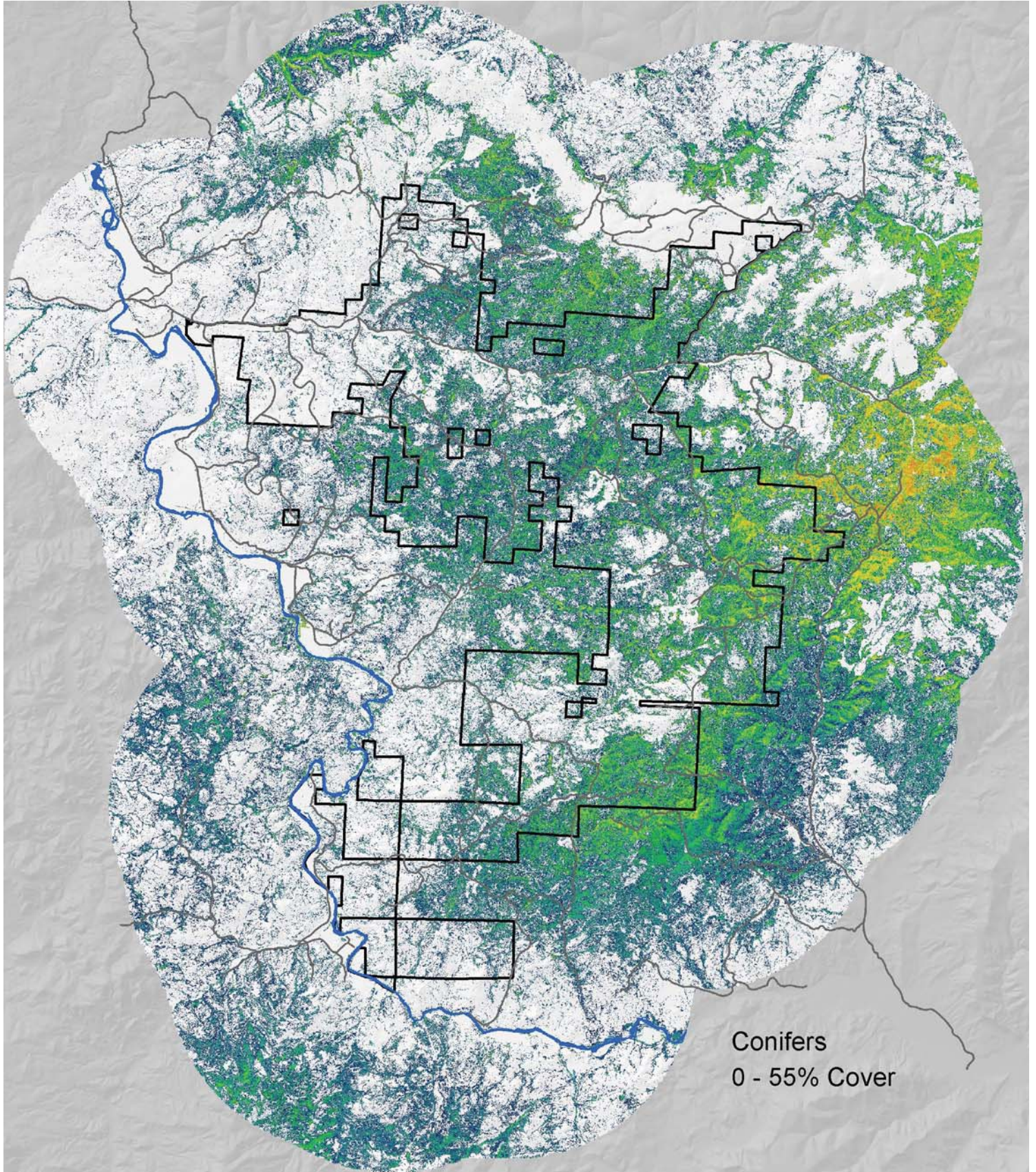


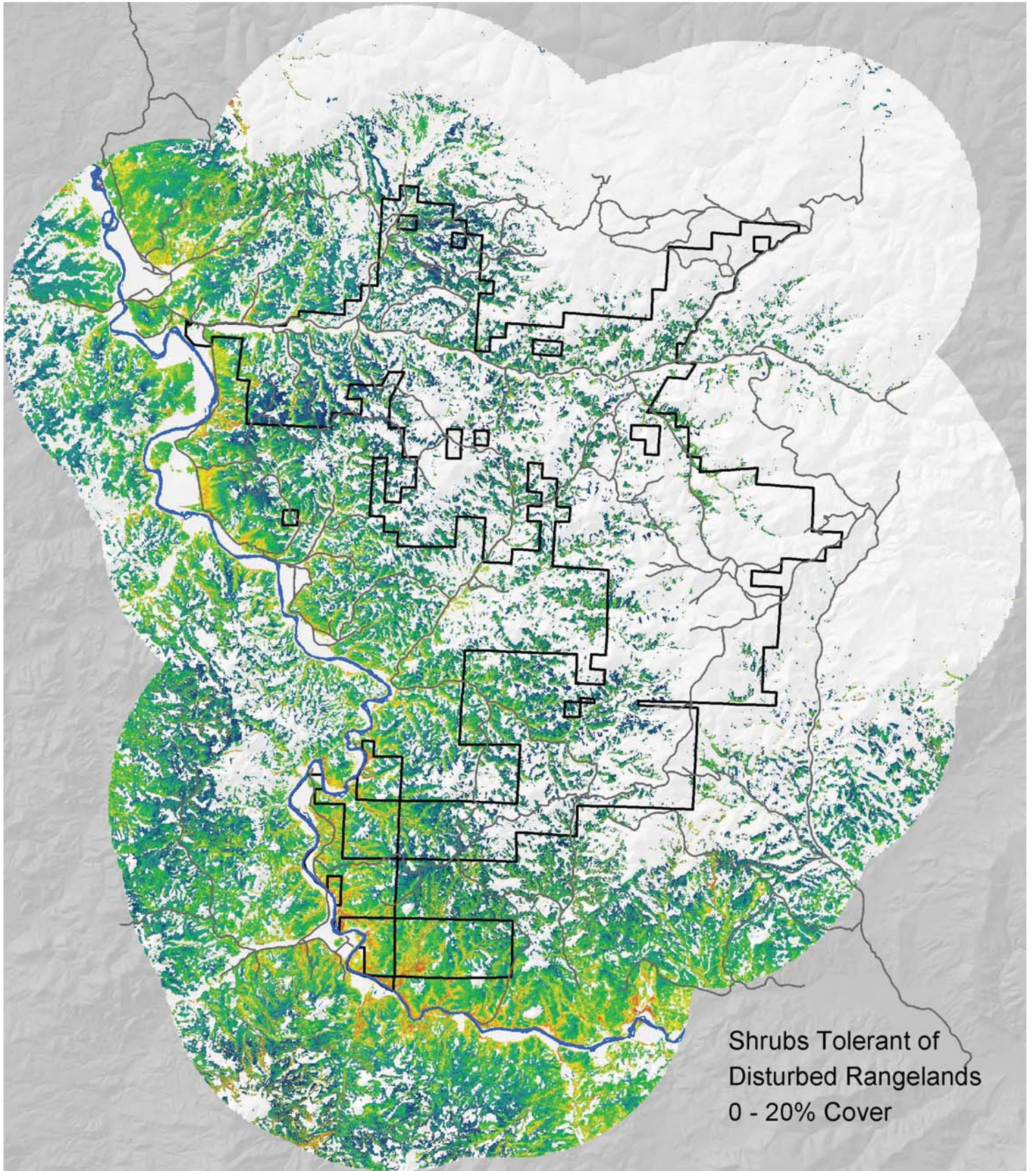
Ash Beds
0 - 75% Cover

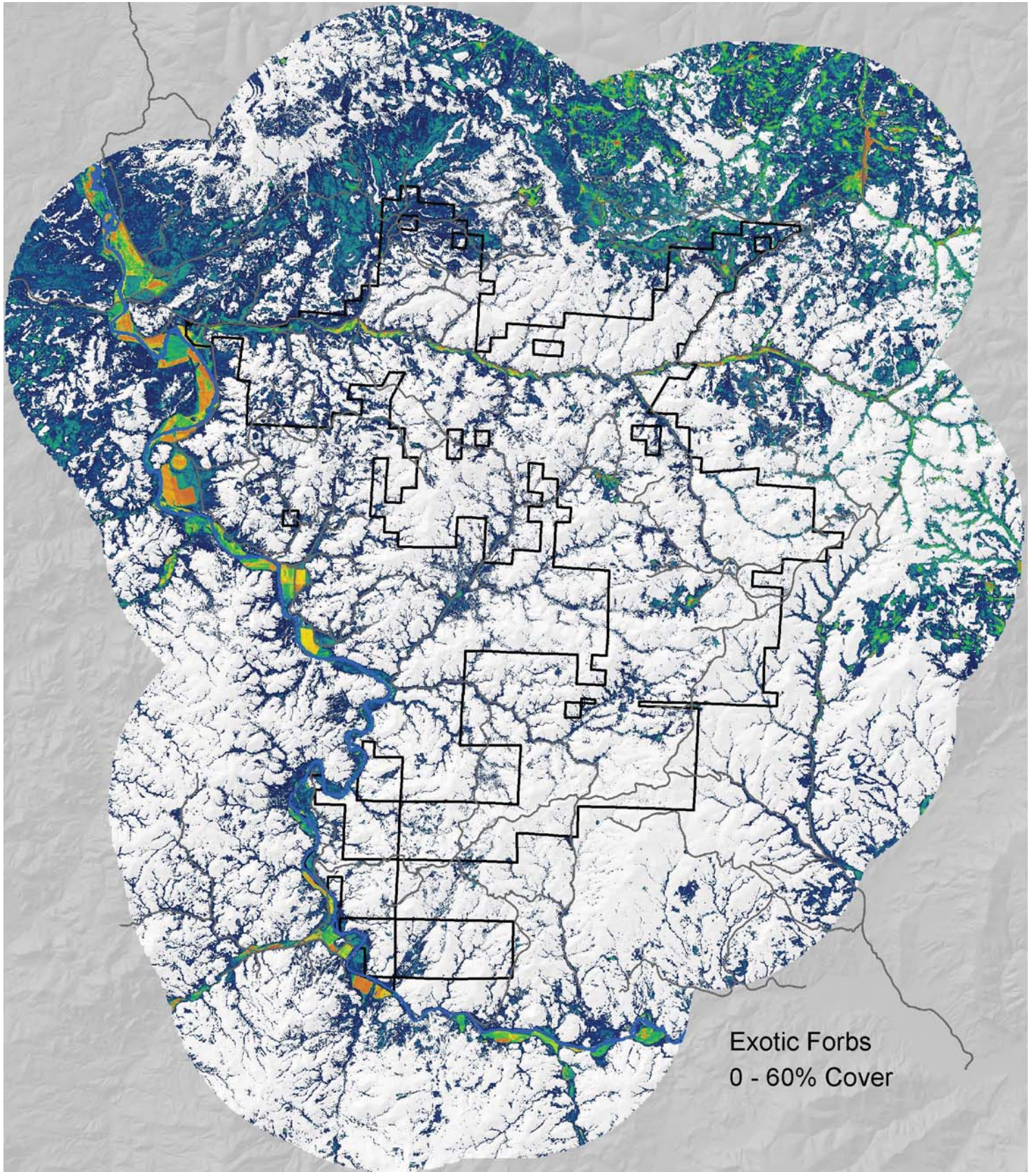


Bedrock
0 - 60% Cover

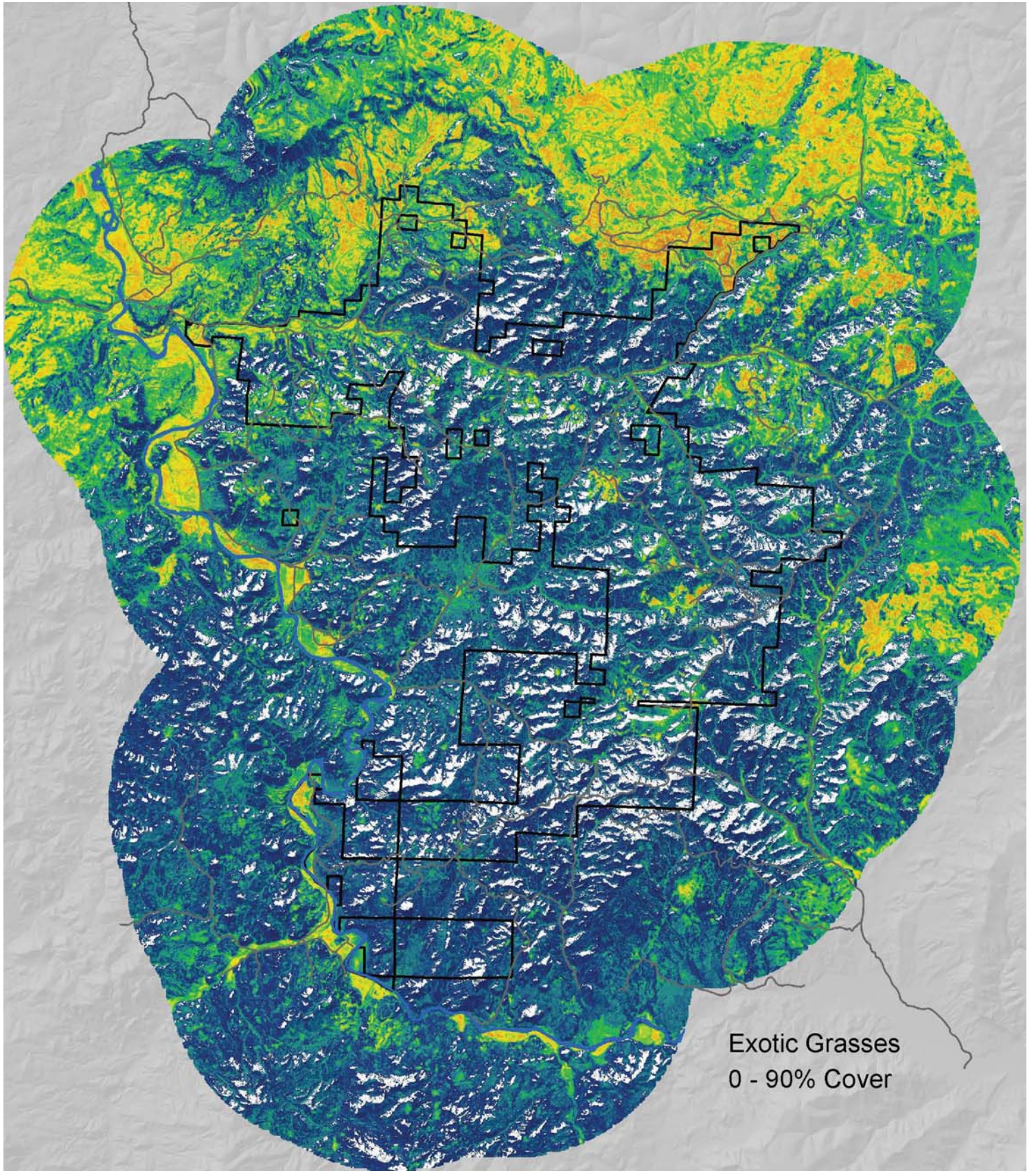




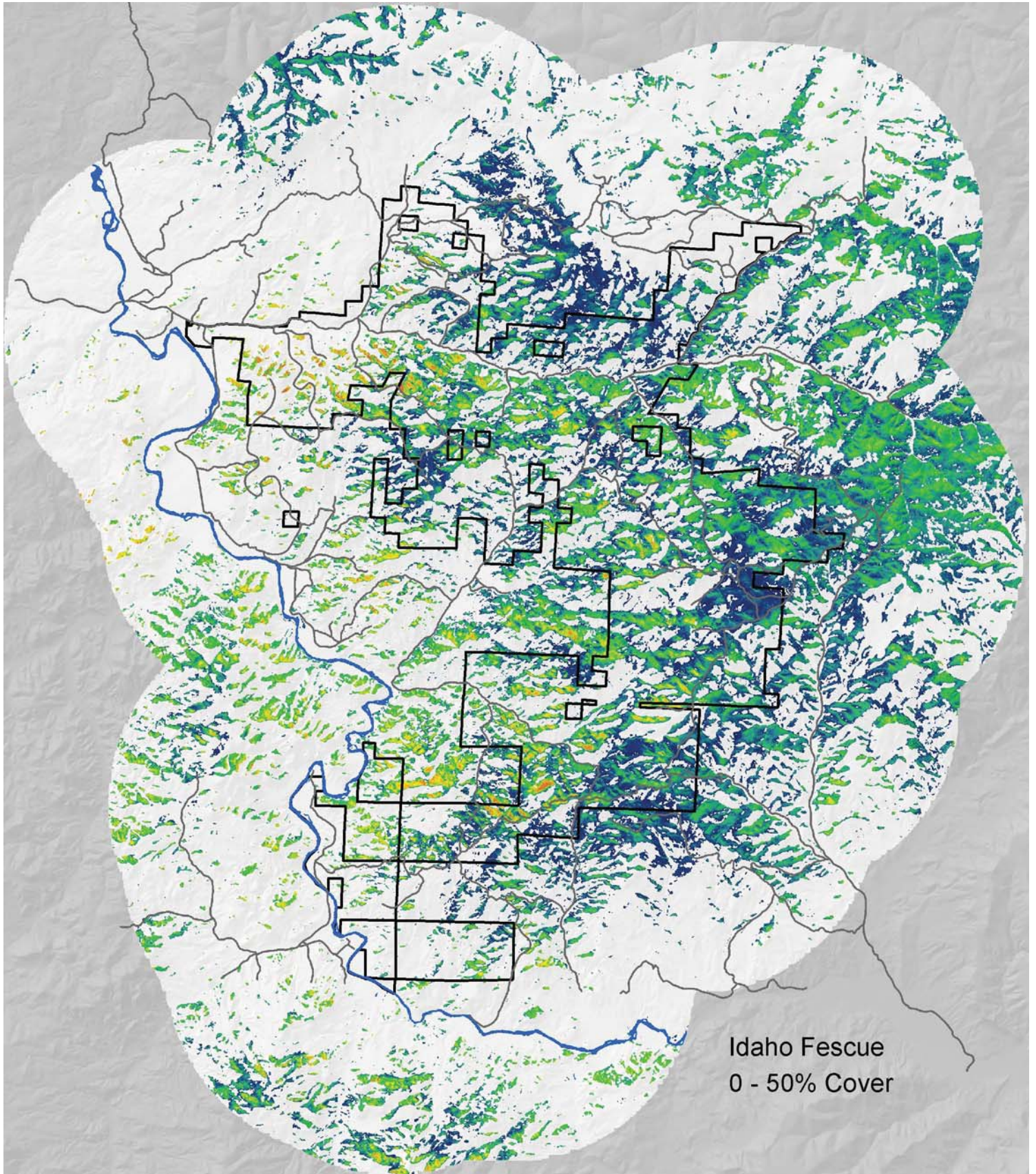




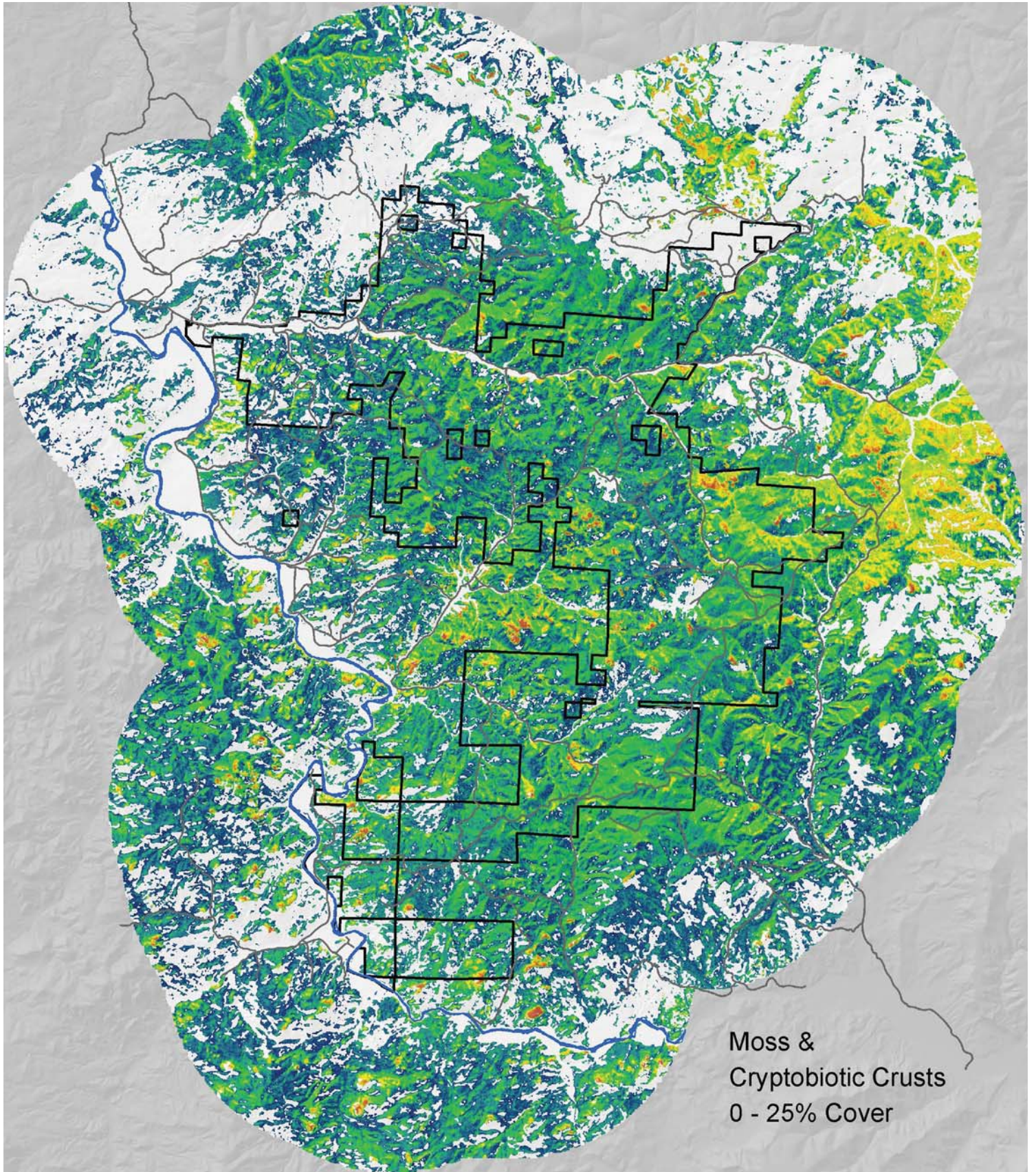
Exotic Forbs
0 - 60% Cover

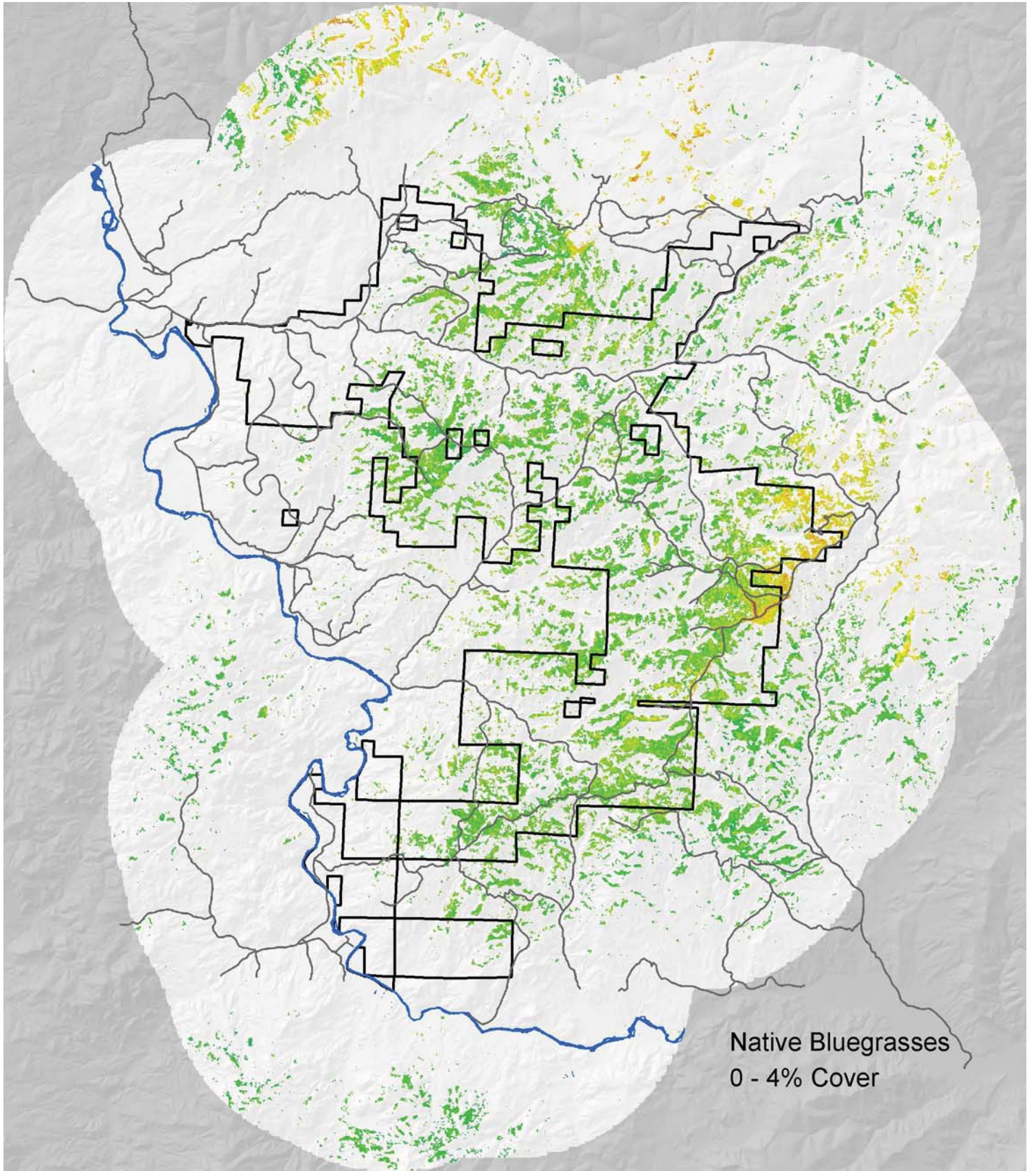


Exotic Grasses
0 - 90% Cover

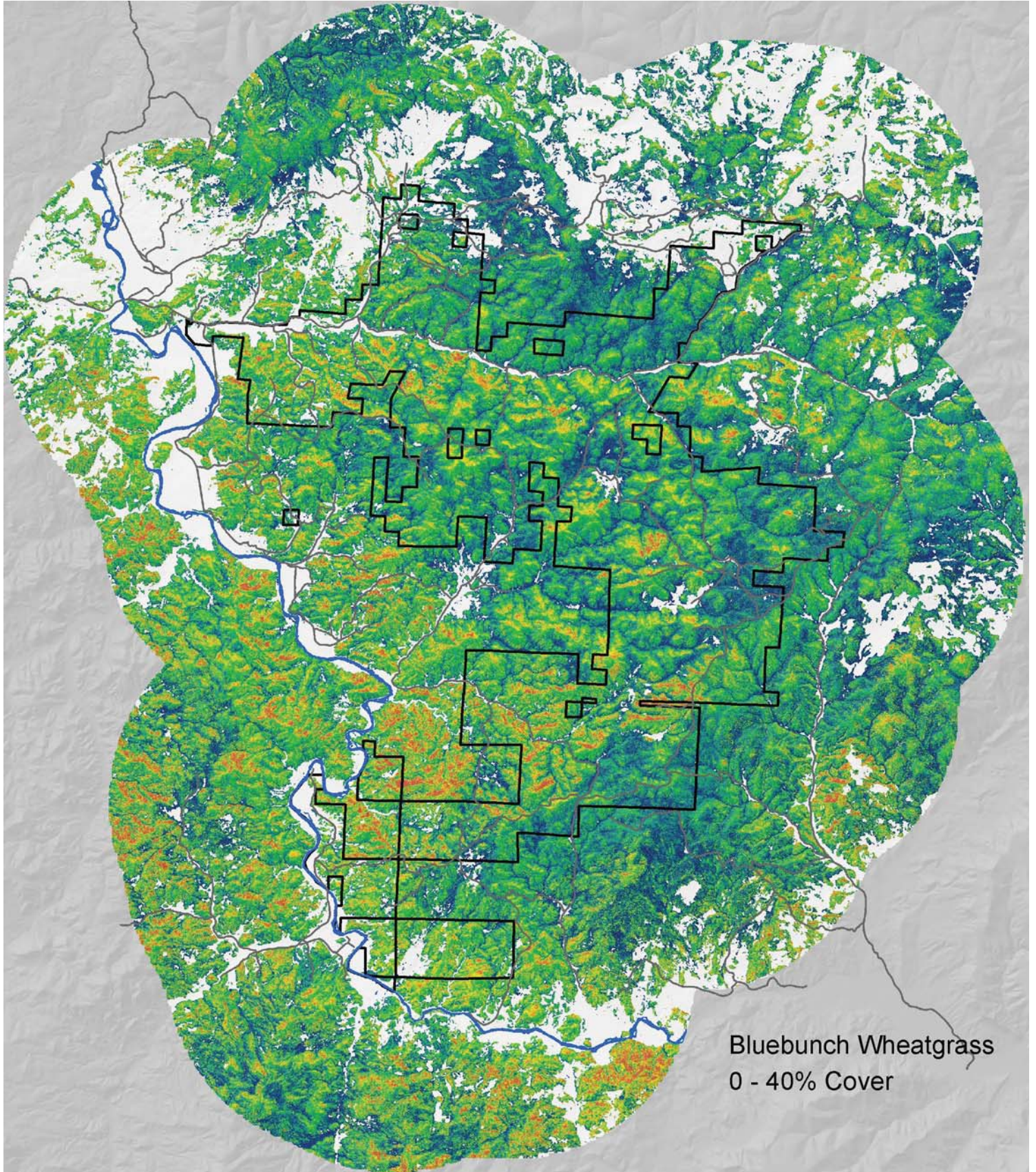


Idaho Fescue
0 - 50% Cover

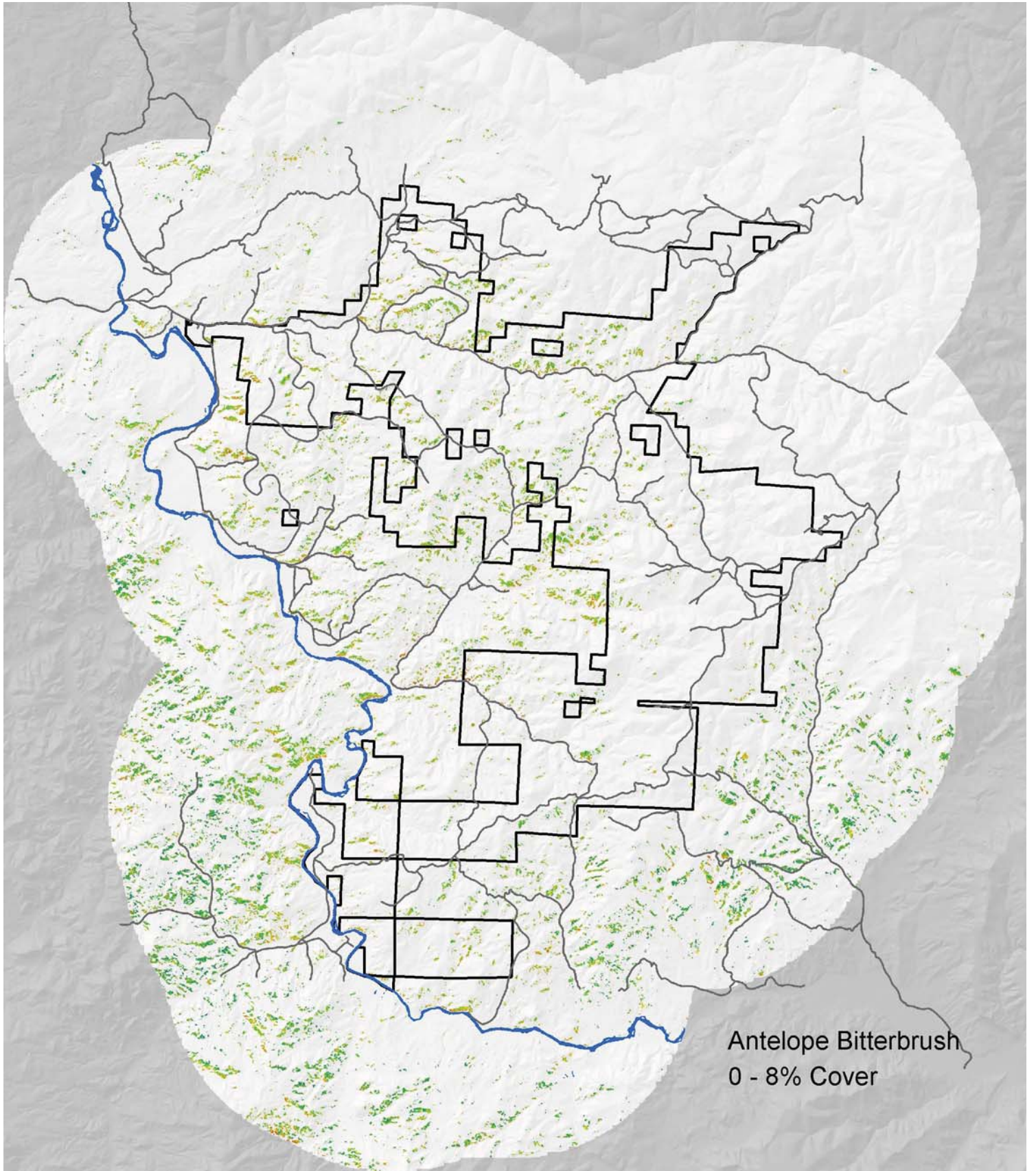




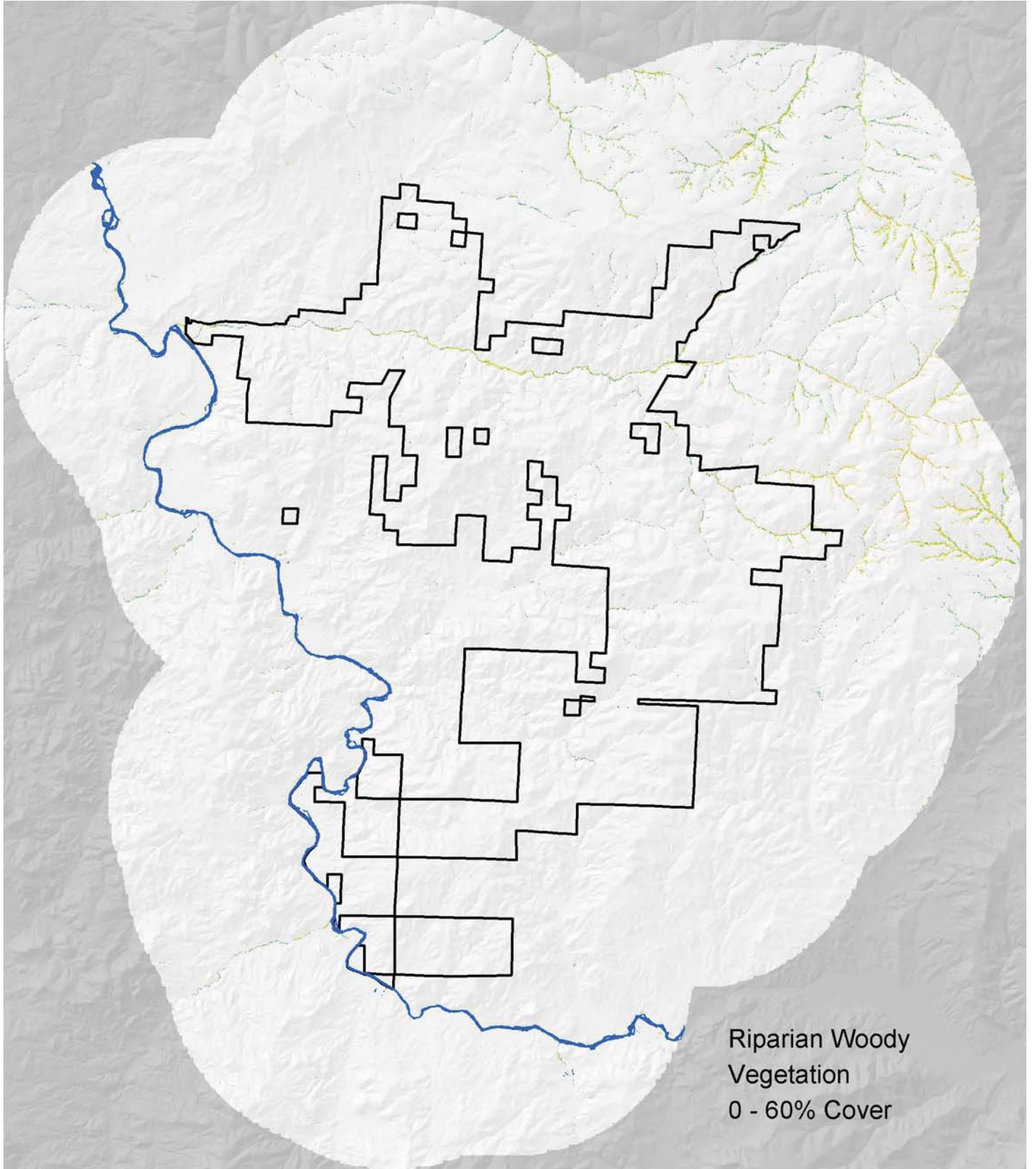
Native Bluegrasses
0 - 4% Cover

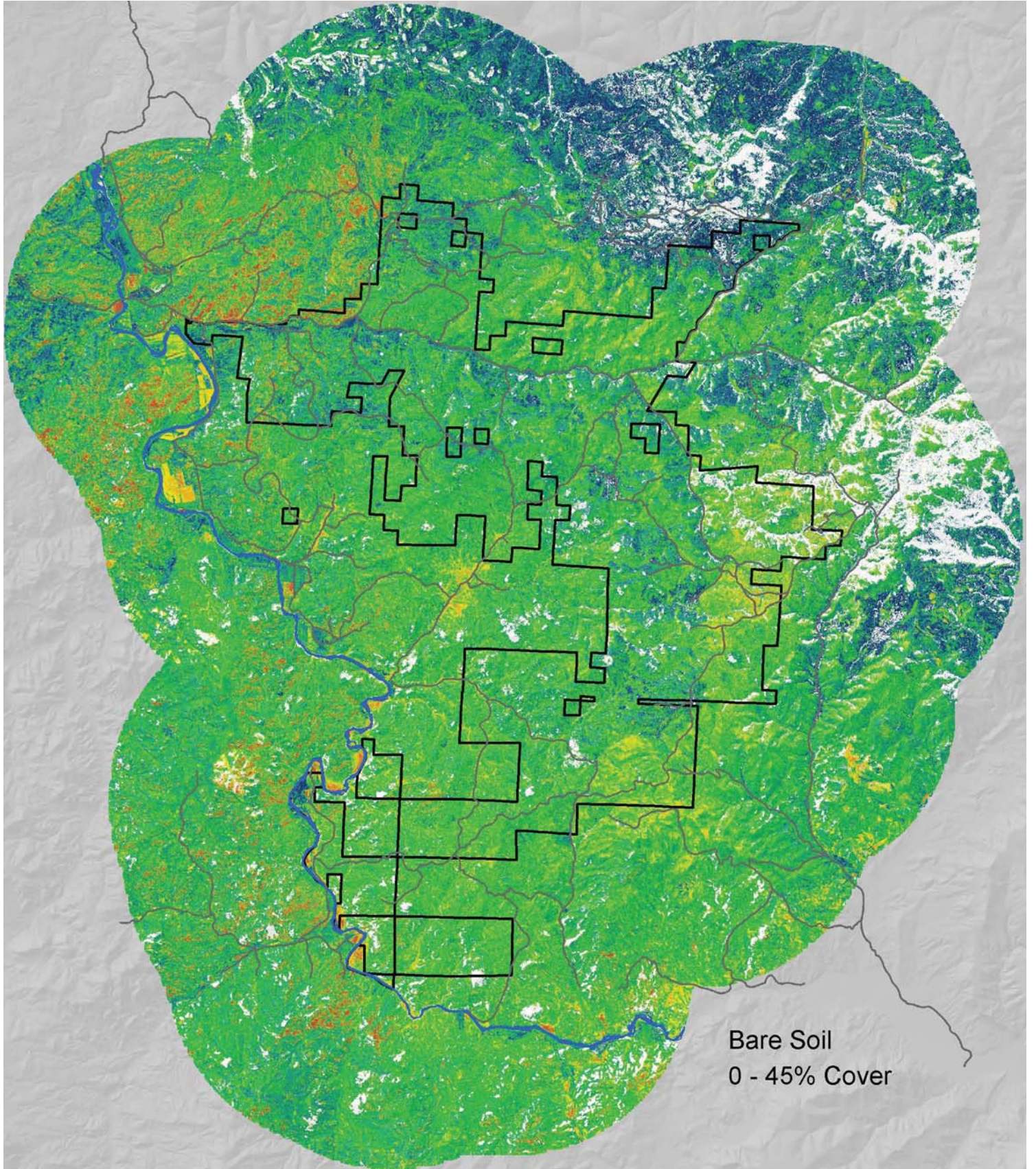


Bluebunch Wheatgrass
0 - 40% Cover

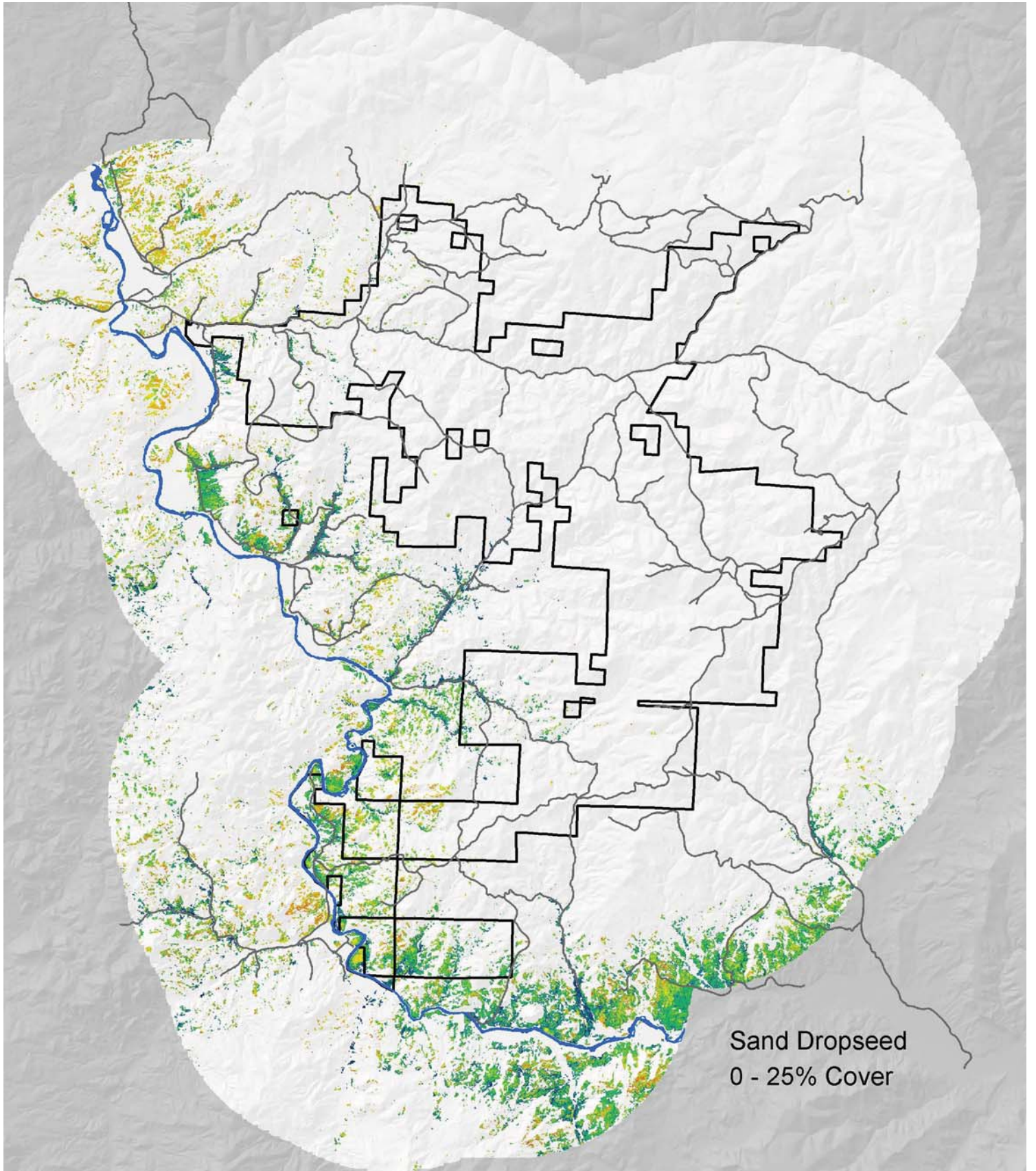


Antelope Bitterbrush
0 - 8% Cover

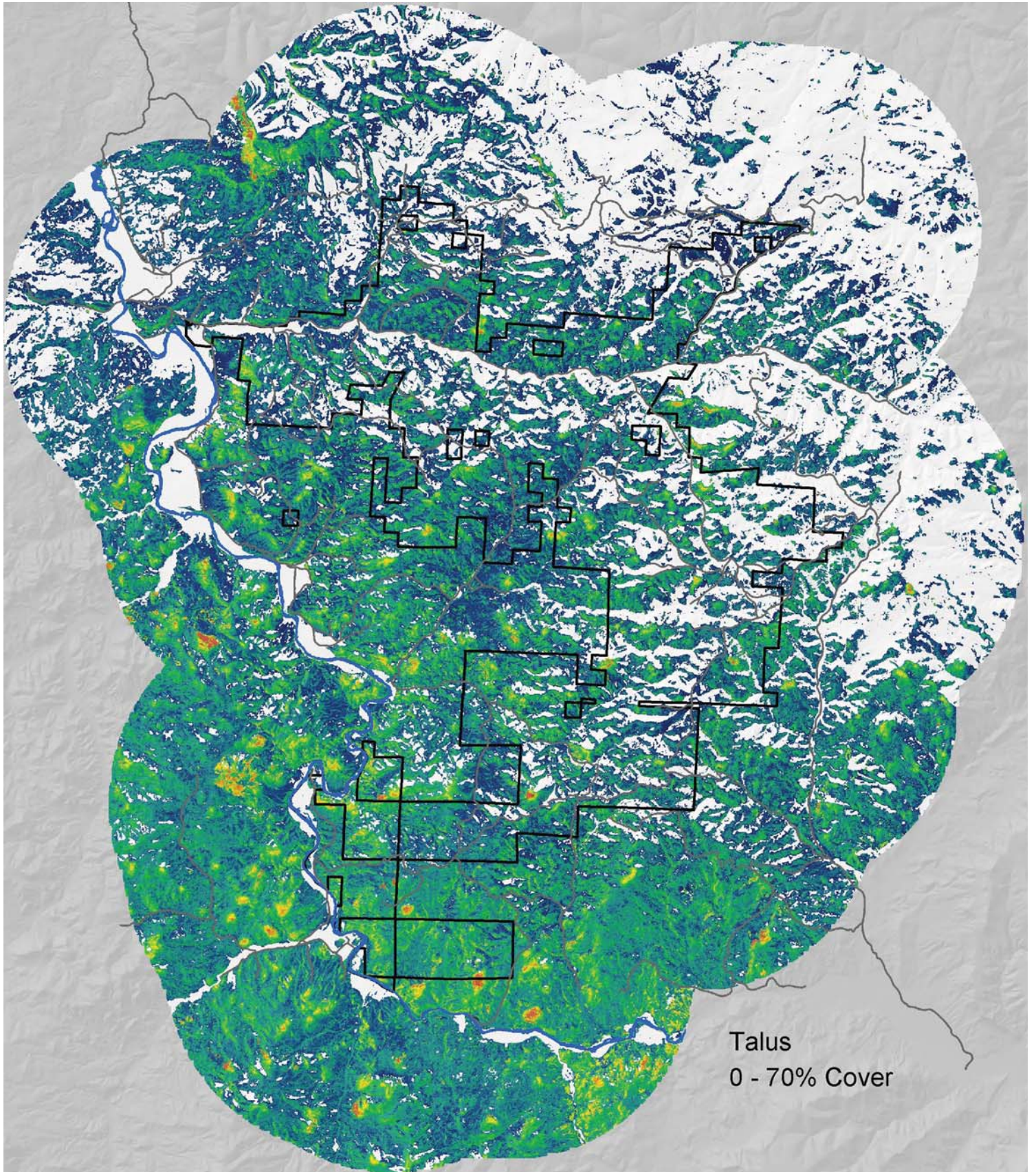




Bare Soil
0 - 45% Cover



Sand Dropseed
0 - 25% Cover



ATTACHMENT 2

WESTERN JUNIPER CHANGE DETECTION



Matt Noone and Eric Nielsen

Institute for Natural Resources, Portland State University

1. INTRODUCTION

The base mapping section of this report (Attachment 1) contains the highest quality map of the current distribution of western juniper at Pine Creek. This map was based on current LiDAR data, aerial photography, and other data sources. However, this map was not used in the juniper change detection process. Unbiased change detection between two dates requires that comparable data sources be used for each date. Because no LiDAR dataset was available for the historic time period, it could not be used for the current period either. Instead, our change detection modeling process for juniper cover relied only on comparable datasets available from each time period: a transform based on aerial photography, and Landsat TM satellite imagery. Note that while LiDAR data was not directly used in the change detection process, it was indirectly used as a training data source for building models to estimate juniper cover based only on air photo and TM imagery metrics.

Western juniper represents the vast majority of the vegetation over three feet in height within the project area. The exceptions are in riparian areas, where a variety of hardwood trees and shrubs occur, and at the highest elevations where Douglas-fir and ponderosa pine are present in small amounts. Because of the difficulty of reliably distinguishing juniper from riparian woody vegetation based only on satellite imagery and the lower quality air photos available historically, potentially riparian areas were excluded from the model-building process. Due to their similarity to juniper woodlands, the higher elevation conifers were not excluded nor distinguished from juniper in model-building. However, both riparian areas and Douglas-fir/ponderosa pine forests were removed from the final change estimations.

2. METHODS

2.1. Mapping

A map illustrating recent cover change in western juniper was created for a study area including lands from the Pine Creek Conservation Area (PCCA), Bureau of Land Management (BLM), and National Park Service (NPS) Clarno Unit (Figure 1). We used LiDAR data collected over the study area in 2011 to create a high-quality juniper canopy cover map that was used as reference data for training predictive models. Juniper canopy cover was modeled for the years 2000 and 2011 using predictor variables generated from aerial photography and satellite imagery. A change map identifying and quantifying juniper canopy cover decrease between the two time periods was then created by differencing the two independent maps. Due to the slow growth of young juniper trees, we determined that encroachment would be undetectable at an acceptable accuracy level over the short time period; therefore, only decreases in juniper canopy cover were mapped.

Given the size of the study area and that an individual juniper tree's crown diameter can occupy a substantial fraction of a 10-meter pixel, we determined that 10 meters was an appropriate mapping resolution. All maps and data layers produced are in the common projection of NAD 83, UTM Zone 11N. ERDAS Imagine was the main software package used for processing imagery and data layers while ArcGIS was primarily used to view and display the data. The user-sourced, statistical software package R (R Development Core Team 2012) was used for juniper canopy cover prediction.

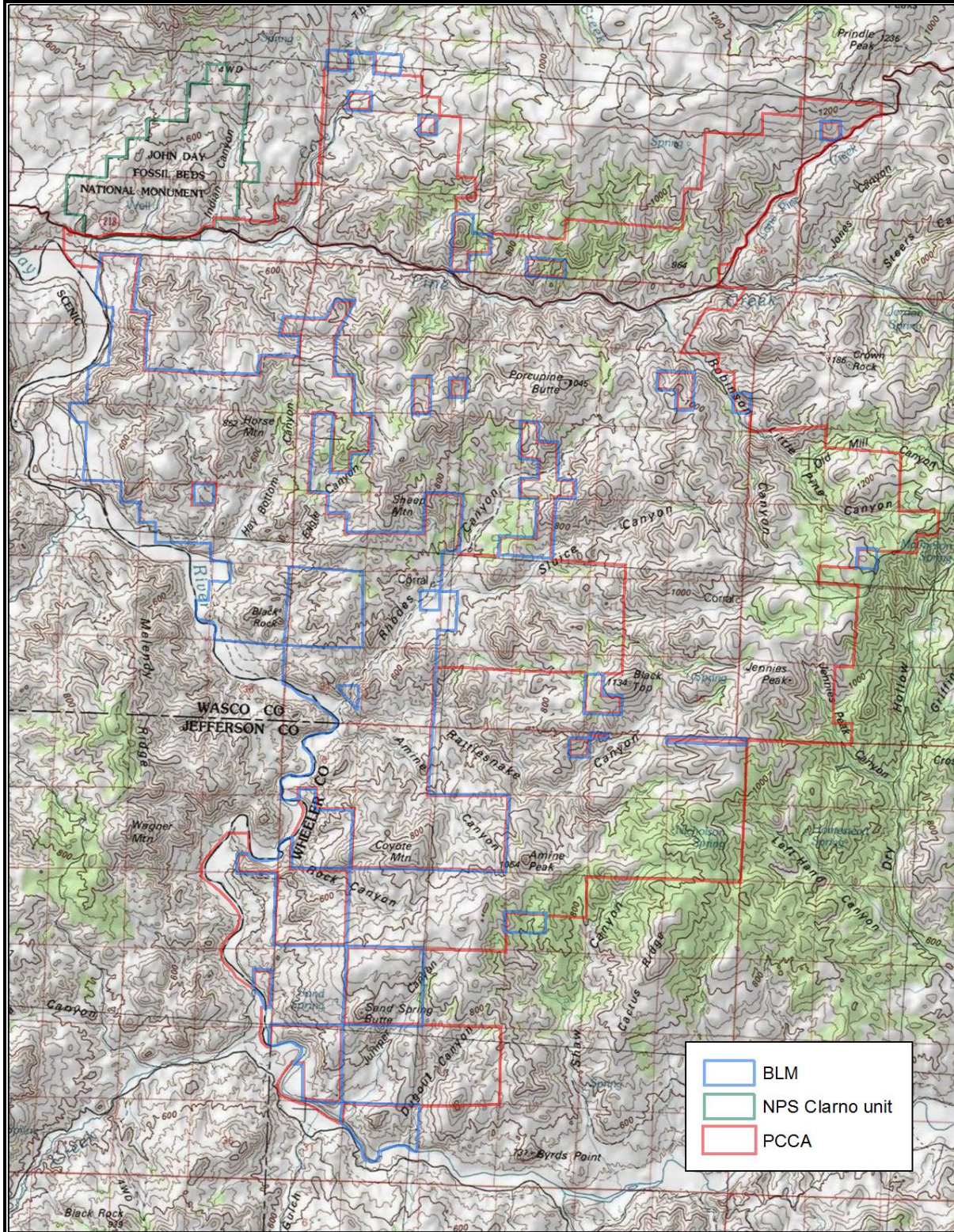


Figure 1. Map of the study area and land ownerships.

2.1.1. Data Acquisition and Preprocessing

2.1.1.1. LiDAR Training Data

Watershed Sciences collected LiDAR data in May 2011 for PCCA and the adjacent BLM and NPS land and the private inholdings. The original 3-dimensional point cloud dataset (Figure 2) was gridded to 3-foot resolution bare earth and highest hit elevation rasters. INR performed a variety of quality control steps on the Watershed Sciences deliverables, including removing the powerlines as well as artifacts in the highest hit raster that occurred on very steep slopes. The quality control process resulted in many very small areas of missing data, which were unavailable for use in training juniper cover models. The highest hit and bare earth elevation grids were then differenced to produce a vegetation height layer. In addition, an initial riparian area mask was produced from the bare earth elevation via a hydrological flow modeling procedure developed in Nielsen *et al.* (in press).

All 3-foot resolution LiDAR pixels representing vegetation over three feet in height, and lying outside the modeled riparian areas, were treated as fully occupied by juniper (more precisely, by upland conifers). A moving window was then used to estimate the mean juniper canopy cover at a 10-x-10-meter scale. The mean canopy cover value corresponding to the extent of each 10-meter cell in the image-based predictor layers was then extracted, resulting in a highly accurate percent canopy layer at 10-meter resolution.

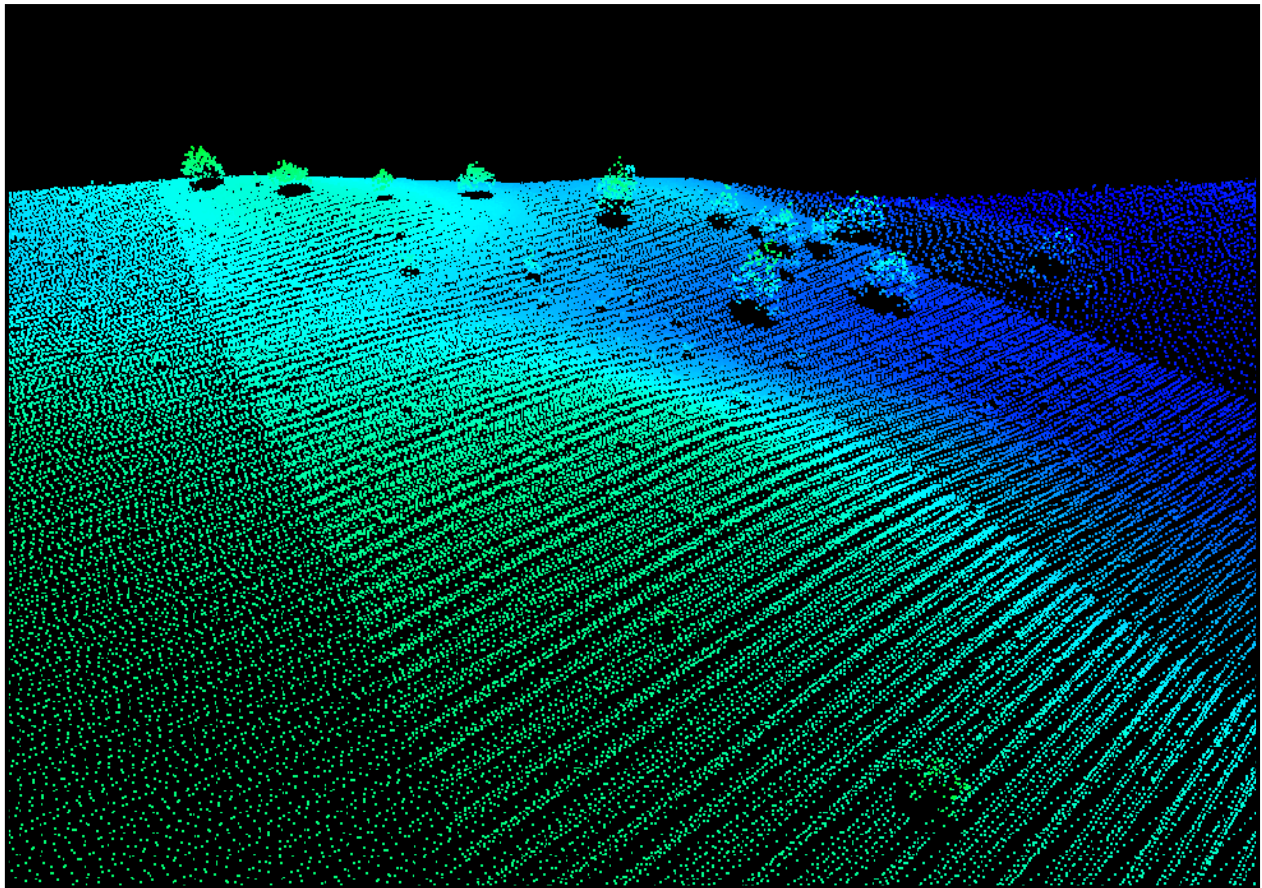


Figure 2. A 3D visualization of the LiDAR point cloud depicting juniper.

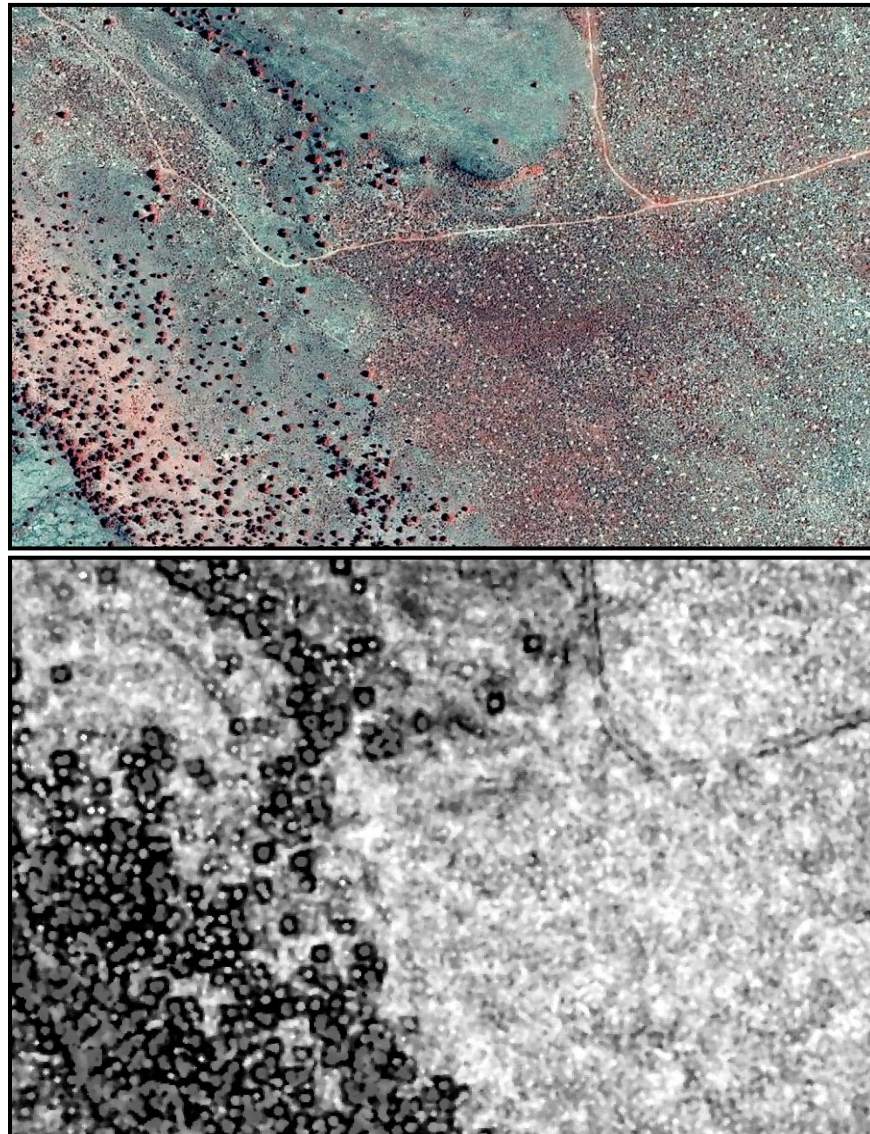
2.1.1.2. Aerial Photography Predictor Data

National Agricultural Inventory Program (NAIP) aerial photography was flown in 2011 at 1-meter resolution with four spectral bands (red, green, blue, and near-infrared); this imagery was obtained as uncompressed quarter quad TIFF tiles and then mosaicked. Black and white National Aerial Photography

Program (NAPP) photos at 1:40,000 scale were collected in 2000 and 2001. These aerial photos were digitally orthorectified into quads (DOQs) at 1-meter resolution, and made publicly available at the [Oregon Geospatial Enterprise Office \(GEO\)](#).

In order to provide equivalent predictor layers for juniper cover modeling for the two time periods, the 4-band 2011 NAIP was simplified to a single band image by calculating the first principal component, resulting in an image comparable to the 2000 black and white DOQ imagery. A variety of high resolution texture metrics developed at INR, including Normalized Difference Texture Index (NDTI) at 1m/3m and 2m/6m (see Figure 3 for texture example) and maximum-normalized standard deviation were produced from the 2000 DOQ and 2011 NAIP first principal component (see Nielsen *et al.* in press). The texture metrics and base imagery were then degraded to the 10-meter modeling resolution.

Figure 3. NAIP air photo (above) and Normalized Difference Texture Index at 2m/6m resolution (below).



2.1.1.3. Satellite Imagery Predictor Data

The Landsat archive was searched for cloud-free, late summer imagery. Landsat 5 Thematic Mapper (TM) satellite data for 1999 and 2011 was then downloaded from the USGS GLOVIS website, <http://glovis.usgs.gov/>. The Landsat imagery was reprojected to NAD 83, UTM Zone 11N to match the other data layers. A Landsat image from 1999 was chosen over a 2000 image to better match the late summer acquisition time of the 2011 image. The one year difference between the aerial photo flights and the satellite image collection is not expected to significantly affect results.

The TM images were converted to top-of-atmosphere reflectance values based on the Julian day and sensor and solar elevation at the time of image acquisition. A dark-object subtraction was then applied to provide a basic atmospheric correction. A topographic normalization algorithm modified from Twele (2006) was applied to correct for the influence of differential illumination with topographic aspect. Several vegetation indices, which can aid in identifying landcover characteristics that may not be identifiable in the raw spectral bands (Coppin and Bauer 1994), were calculated from each of the images. The Normalized Differenced Vegetation Index (NDVI), Normalized Differenced Moisture Index (NDMI; Jin and Sader 2005) and Tasseled Cap Wetness (TCW; Crist and Cicone 1984) were produced, and then all indices and individual band reflectances were resampled to the 10-meter modeling resolution.

2.1.2. Juniper Canopy Cover Modeling

Random Forests is a non-parametric inductive modeling technique based on CART (Classification and Regression Tree) modeling methodologies. CART modeling evaluates predictive input variables and partitions them based upon their ability to explain variance in a training dataset. In Random Forests, many separate trees are produced, each from a random selection of observations and predictor variables. When predictions are made on an independent dataset, each independently-generated tree receives a single vote, and the predicted class (or quantity, in the case of regression) is determined by the most popular outcome. Random Forests has become a popular modeling tool because it makes no assumptions regarding the statistical distributions of variables and has a very low tendency to overfit to the training data. It also generates estimates of model accuracy that tend not to be inflated as with many other CART techniques.

A random sample of 20,000 points was generated over the LiDAR coverage. We eliminated the influence of possible non-juniper tree canopy cover on the modeling process by excluding sample selection from the riparian areas modeled above. Sample points were intersected with the juniper canopy cover training data and the 2011 air photo and TM predictor variables (Table 1), and a Random Forest model composed of 500 independent trees was generated and saved. The model was then applied to both the 2000 and 2011 predictor variable sets, resulting in a continuous raster output representing 0-100 percent juniper canopy cover. This continuous raster was then binned into classes of 5% canopy cover increments.

It was then necessary to restrict the modeled change results to areas corresponding to potential western juniper habitat. A Random Forests classification model was used to map water, wooded riparian areas and Douglas-fir/ponderosa pine forests, and herbaceous wetlands, based on approximately one hundred photo-interpreted training points per landcover class. Agricultural land was not modeled but was extracted from the USGS 2006 National Land Cover Dataset (NLCD). These areas of non-juniper habitat were then eliminated from the binned percent canopy cover change map. Table 2 contains additional information about the landcover classes eliminated.

Table 1. Predictor variables used in random forest model

Resolution	Sensor	Predictor Variable	2000 Imagery	2011 Imagery
30m	Satellite	Landsat TM Band 1	7/31/1999	8/17/2011
30m	Satellite	Landsat TM Band 2	7/31/1999	8/17/2011
30m	Satellite	Landsat TM Band 3	7/31/1999	8/17/2011
30m	Satellite	Landsat TM Band 4	7/31/1999	8/17/2011
30m	Satellite	Landsat TM Band 5	7/31/1999	8/17/2011
30m	Satellite	Landsat TM Band 6	7/31/1999	8/17/2011
30m	Satellite	Tasseled Cap Greenness	7/31/1999	8/17/2011
30m	Satellite	Tasseled Cap Wetness	7/31/1999	8/17/2011
30m	Satellite	Tasseled Cap Brightness	7/31/1999	8/17/2011
30m	Satellite	Normalize Difference Moisture Index	7/31/1999	8/17/2011
30m	Satellite	Normalize Difference Vegetation Index	7/31/1999	8/17/2011
1m	DOQ/NAIP	First Principal Component	2000/2001	2011
1m	DOQ/NAIP	NDTI 1m/3m	2000/2001	2011
1m	DOQ/NAIP	NDTI 2m/6m	2000/2001	2011
1m	DOQ/NAIP	SD Normalized	2000/2001	2011

Table 2. Landcover class descriptions and source.

Class	Description
Water	River/pond/lake bodies of water
Agriculture	Agricultural areas burnt in from NLCD
Wetland	Areas of high infrared reflectance, lush vegetation, riparian areas.
Forest	Modeled areas of deciduous or (non-juniper) coniferous trees
Sagebrush/Grasslands	Annuals, shrubs, sagebrush or grasslands
5-10% Juniper Canopy Cover	Modeled juniper class
10-15% Juniper Canopy Cover	Modeled juniper class
15-20% Juniper Canopy Cover	Modeled juniper class
20-25% Juniper Canopy Cover	Modeled juniper class
25-30% Juniper Canopy Cover	Modeled juniper class
30-35% Juniper Canopy Cover	Modeled juniper class
35-40% Juniper Canopy Cover	Modeled juniper class
>40 % Juniper Canopy Cover	Modeled juniper class

2.1.3. Accuracy Assessment

To be able to utilize a map in an appropriate way, its strengths and weakness must be quantified and evaluated. Accuracy assessments were carried out on the 2000 and 2011 canopy cover maps, as well as the juniper change map.

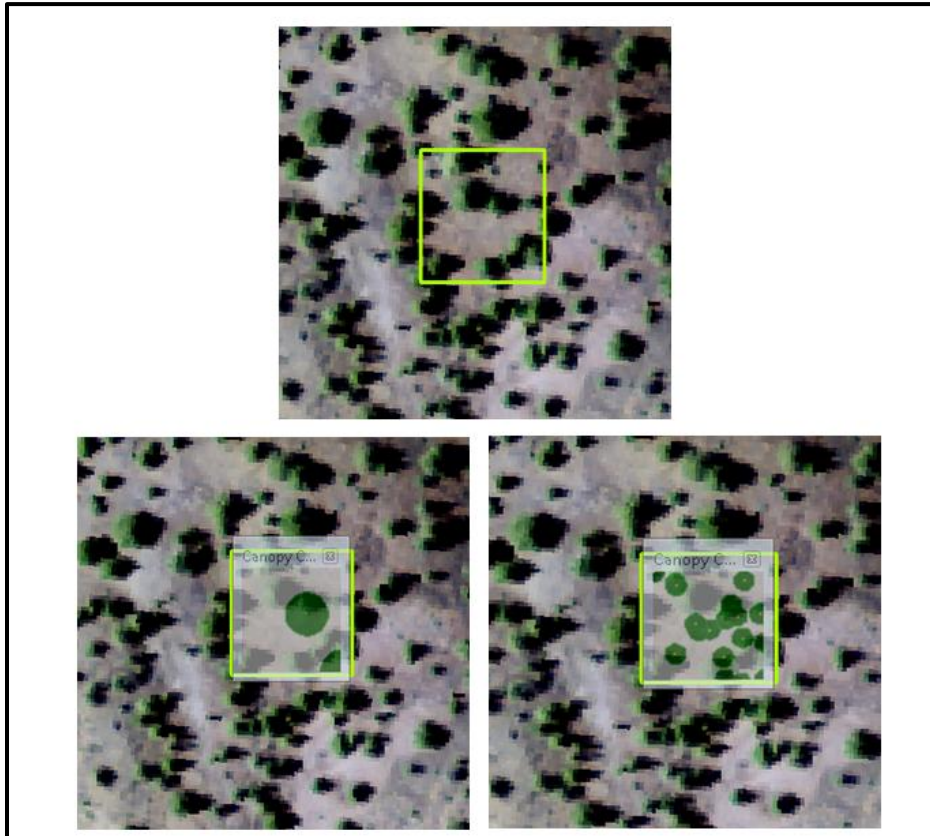
Stratified random points were generated throughout the map for each of the canopy cover map classes. At each of these points polygons were created around a 3 by 3 10m, pixel block resulting in a 30m by 30m polygon. A trained image interpreter familiar with the eastern Oregon landscape then evaluates and assigns the polygon an estimated juniper percent canopy cover based on aerial photography from the appropriate time period. Bias in the accuracy assessment can be minimized when interpretation samples are randomly selected within map class strata, which is unknown (blind) to the image interpreter.

For the cover type maps of 2000 and 2011 Digital Mylar was utilized to aid in canopy cover interpretations. The U.S. Forest Service Remote Sensing Applications Center (USFS RSAC) has developed an ArcGIS extension (<http://www.fs.fed.us/eng/rsac/digitalmylar/>) called Digital Mylar that provides digital templates of various percentages of canopy cover over a selected area that can be overlaid on digital aerial photograph. This template provides a frame of reference to more accurately estimate (via photo interpretation) canopy cover for each 30m square sample polygon (see Figure 4 for Digital Mylar template example). A zonal histogram function using the polygons as the zone of interest is then run on

the canopy cover map to determine the nine modeled estimates (one estimate for each 10m pixel) of juniper canopy cover within the polygon. The canopy cover of the map is then compared with the canopy cover estimate from the aerial photography determined by the image interpreter. A sample was considered in agreement with the photo interpreter's call as long as one of the nine pixels within the 30 by 30m polygon matched the photo interpretation canopy cover.

The juniper change map was evaluated somewhat differently, because only decreases in juniper cover were being evaluated. A total of 400 stratified random points were generated, 200 in each the change and no change classes. Once again, 30 by 30m polygons were generated from these randomly generated points. If any juniper trees in the polygons in 2000 were not identified in the 2011 photography the polygon was labeled as juniper change. If there were no junipers in either year or the same amount of live juniper in both years, polygons were labeled as no change. The new attributed polygons were intersected with the mapped juniper change data layer. If there were any change pixels in the polygon the polygon was considered to have changed, otherwise the sample area was considered as no change.

Figure 4. Example of Digital Mylar templates representing 15% canopy cover with two different crown diameter sizes.



The results from the comparison were then put into an error matrix. The error matrix represents statistics about the sources of error and the reliability of individual map classes in the landcover map (Congalton 1991, Congalton and Green 1999). The statistics are represented by the overall agreement, representing the correctly classified interpretation points divided by the total number of interpretation points. The statistics produce both omission error, related to the producer's agreement and commission error, related to the user's agreement. Commission error indicates if a particular map class is over mapped while omission error represents the likelihood a class is under mapped (see Figure 5 for error matrix formulas).

Figure 5. Equations used to calculate user's, producer's and overall accuracies for maps.

Equation A.1. Overall agreement

$$= \frac{\sum_{i=1}^k n_{ii}}{n} \text{ where } n_{ii} = \text{the points correctly classified}$$

Equation A.2. Producer's agreement

$$= \frac{n_{jj}}{n_{(j+)}} \text{ where } n_{jj} = \text{value in diagonal and } n_{(j+)} = \text{column total}$$

Equation A.3. User's agreement

$$= \frac{n_{ii}}{n_{(i+)}} \text{ where } n_{ii} = \text{value in diagonal and } n_{(i+)} = \text{row total}$$

3. RESULTS AND ACCURACY ASSESSMENT

3.1. Juniper Canopy Cover

The study area included a total of 50,862 acres, of which as of 2011, had 27,557 acres of juniper occupying 54% of the landscape (Table 4). Between 2000 and 2011, acres of western juniper were similar on south facing aspects but significantly lower on north facing aspects in 2011 (Figure 5). Juniper stands with higher canopy cover typically occurred on north facing aspects (Figure 6 and Figure 7).

The lower juniper canopy cover classes were typically more common at lower elevations rather than higher elevations (Figure 8). Stands with a high canopy cover classes more frequently occurred over 700 m elevation. There was no or very little juniper occurring below 500 m or above 1300 m elevation (Figure 9 and Figure 10).

Table 4. Acres of landcover classes mapped by ownership, 2011

Class	NPS	PCCA	BLM	Total	% of All Landcover
Wetland/Agriculture	8	98	31	137	0%
Forest	-	179	6	185	0%
Sagebrush/Grasslands	1,696	12,406	8,840	22,942	45%
5-10% Juniper Canopy Cover	191	4,225	1,852	6,269	12%
10-15% Juniper Canopy Cover	89	4,654	1,480	6,224	12%
15-20% Juniper Canopy Cover	23	4,179	1,039	5,240	10%
20-25% Juniper Canopy Cover	5	3,576	661	4,242	8%
25-30% Juniper Canopy Cover	1	2,656	353	3,009	6%
30-35% Juniper Canopy Cover	-	1,367	119	1,486	3%
35-40% Juniper Canopy Cover	-	541	31	572	1%
>40 % Juniper Canopy Cover	-	496	20	516	1%
Total Juniper Acres	308	21,693	5,556	27,558	54%

The 2011 juniper canopy cover map had an overall accuracy of 77% (Table 5). Producer's and user's accuracies were fairly balanced, meaning particular landcover classes were not being significantly over- or under-mapped. The no juniper (>1% landcover) class had a high producer's accuracy of 85% and user's accuracy of 93%, both quite high indicating areas are not being falsely called juniper. The forested class also had very high accuracies. The other canopy cover classes typically had fairly balanced accuracies of around 70%. Although 70% accuracy sounds fairly low, it must be kept in mind that the misclassified canopy covers were very rarely more than 10% off from the mapped classification. In fact there were only 16 instances where the mapped class was more than 10% different from the canopy cover class above or below it.

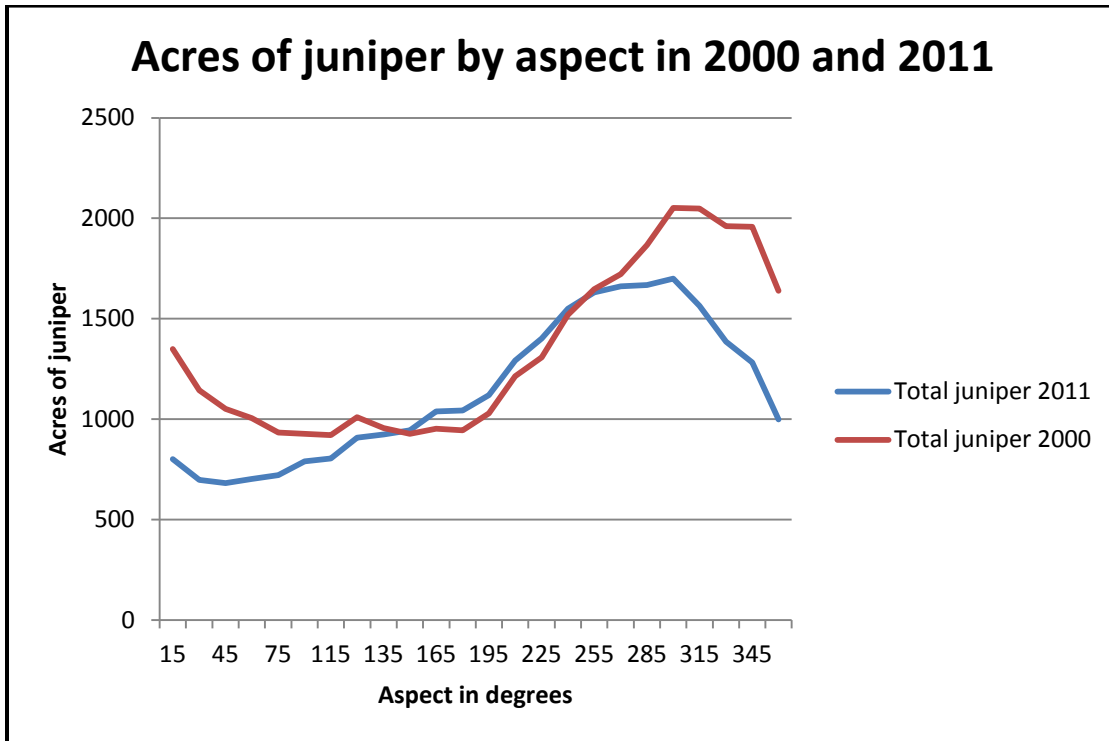


Figure 5. Juniper acres in 2000 vs 2011 by aspect intervals.

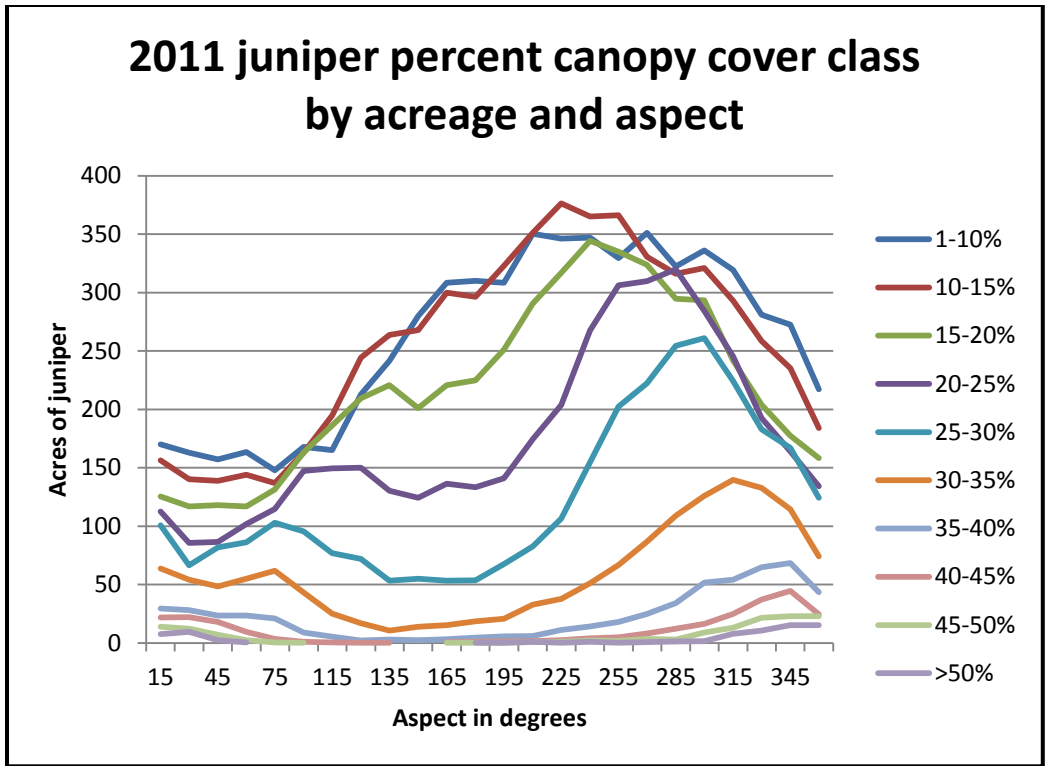


Figure 6. 2011 juniper canopy cover class acres by aspect intervals.

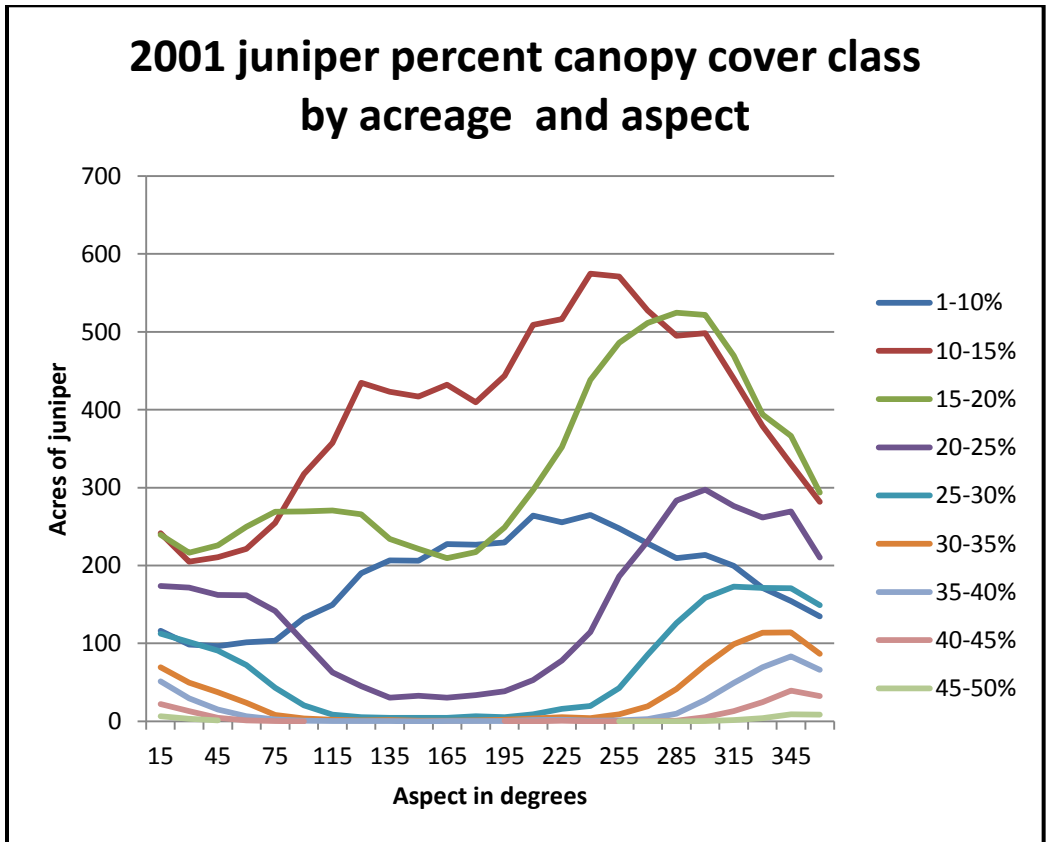


Figure 7. Juniper canopy cover class acres by aspect intervals.

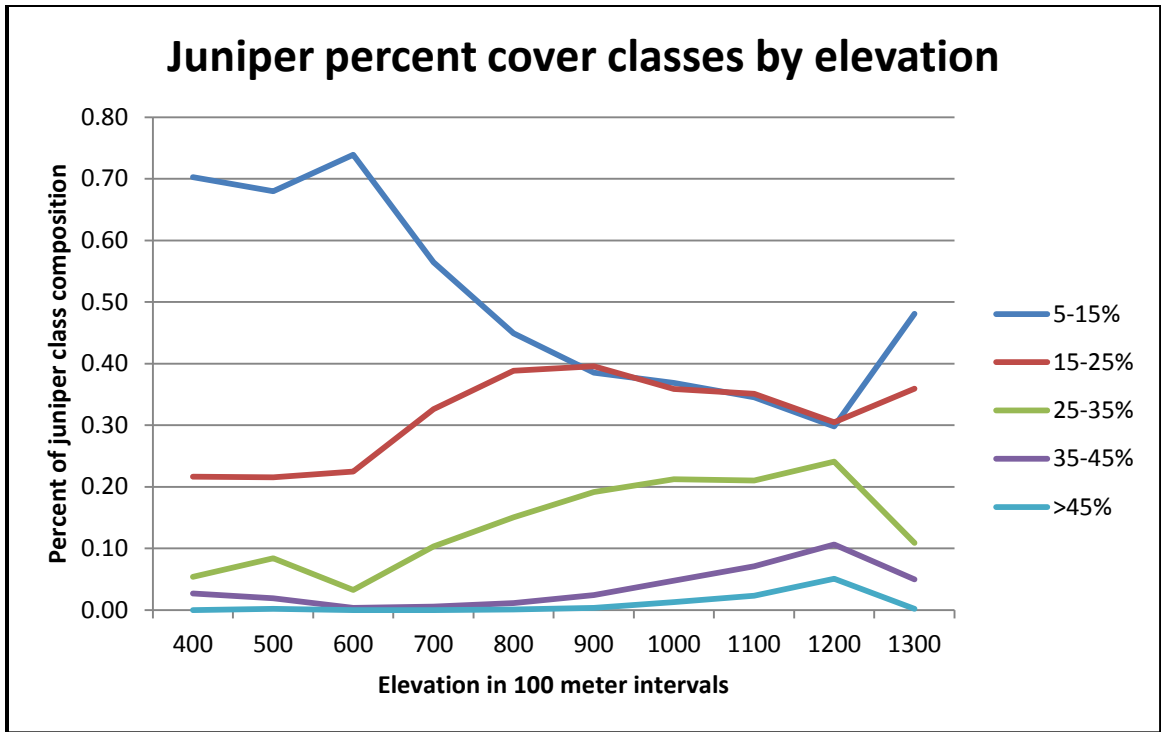


Figure 8. Juniper canopy cover class acres by elevation intervals.

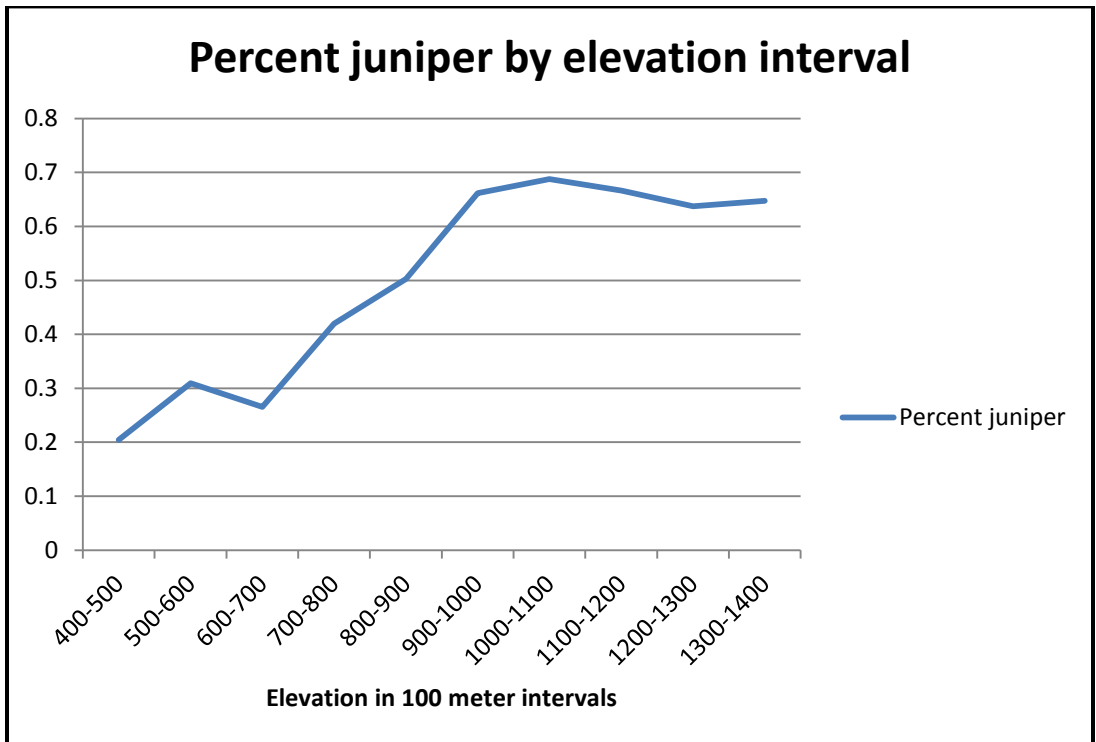


Figure 9. Percent of study area with juniper by elevation interval.

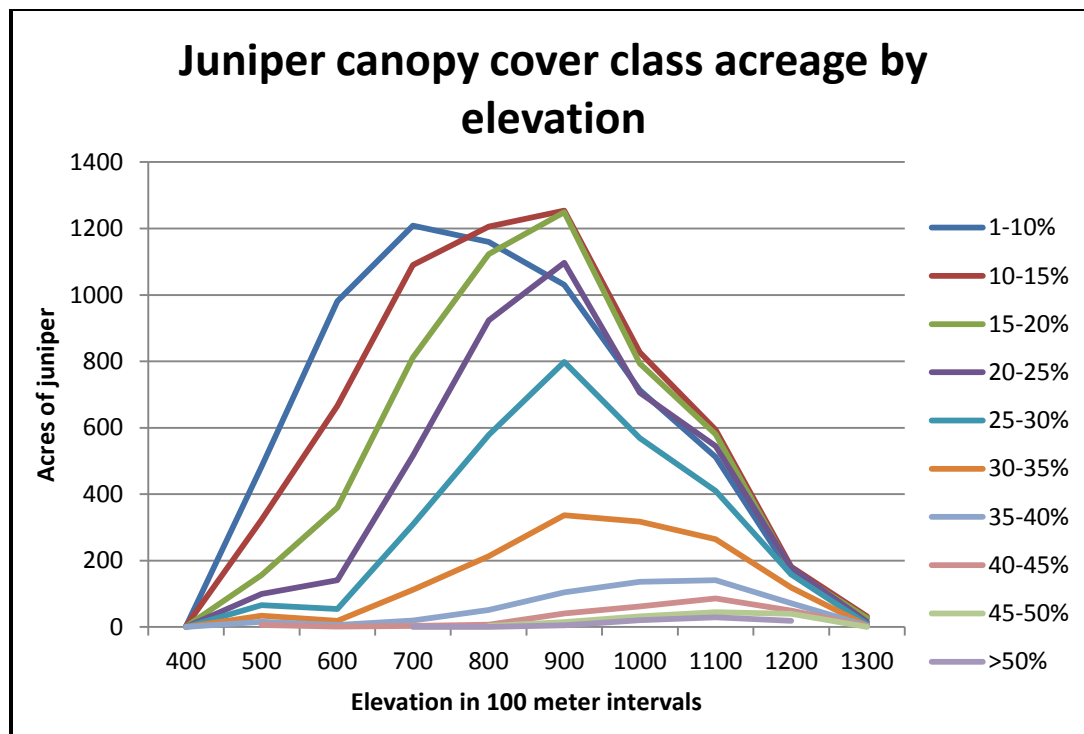


Figure 10. Juniper canopy cover class acreage by elevation interval.

Table 6. 2011 juniper canopy cover error matrix.

Mapped Class	Photo- Interpreted Class						Forest	Total	User's Accuracy
	<1%	1-10%	10-19%	20-29%	30-39%	>40%			
<1%	53	3	1				57	93%	
1-10%	4	23	4				31	74%	
10-19%	5	4	36	5			50	72%	
20-29%		3	10	34	8	3	58	59%	
30-39%				8	36	5	49	73%	
>40%			1	3	7	36	49	73%	
Forest							31	100%	
Total	62	33	52	50	51	44	325		
Producer's Accuracy	85%	70%	69%	68%	71%	82%	94%	Overall Accuracy = 77%	

3.2. Juniper Canopy Cover Change

In total there were 4,297 acres mapped showing juniper declines (Table 7). PCCA had the most (2,485 acres) acres of juniper decreasing while BLM had 1,766 acres that decreased. BLM had a greater percent decrease (32%) in acres than PCCA (11%). Overall, juniper acreage decreased by 16%. There was an insignificant amount of juniper decline mapped on the NPS lands.

The majority of juniper acres that decreased occurred on north facing aspects (those between 270-90 degrees). Overall, 77% of all juniper declines or 3,286 acres occurred on north facing aspects, while only 973 acres occurred on south facing aspects (Figure 11). The greatest percentage (31%) of juniper decrease occurred between 600 and 700 meters in elevation. The 800-900 m interval had the greatest

decrease in acres of juniper (~1000 acres or ~ 21%). Throughout the project area, the percentage of juniper decreases declined as elevation increased (Figure 12 and Figure 13).

Of the 400 points that were photo interpreted for juniper change 335 points were correctly classified resulting in an overall accuracy of 85%. User and producer accuracies were balanced around 84% (Table 8). The overall accuracy of the juniper change map was 85%, an accuracy considered more than sufficient.

Table 7. Acres of juniper as of 2011, and juniper decrease between 2000-2011

Property	Total Acres	Juniper Acres	Juniper Acres Decrease	Landscape Percent Change	Percent Decrease in Juniper Acres
Pine Creek Conservation Area	34,403	21,693	2,485	7%	11%
BLM	14,446	5,556	1,766	12%	32%
NPS Clarno unit	2,013	308	46	2%	15%
All Properties	50,862	27,557	4,297	8%	16%

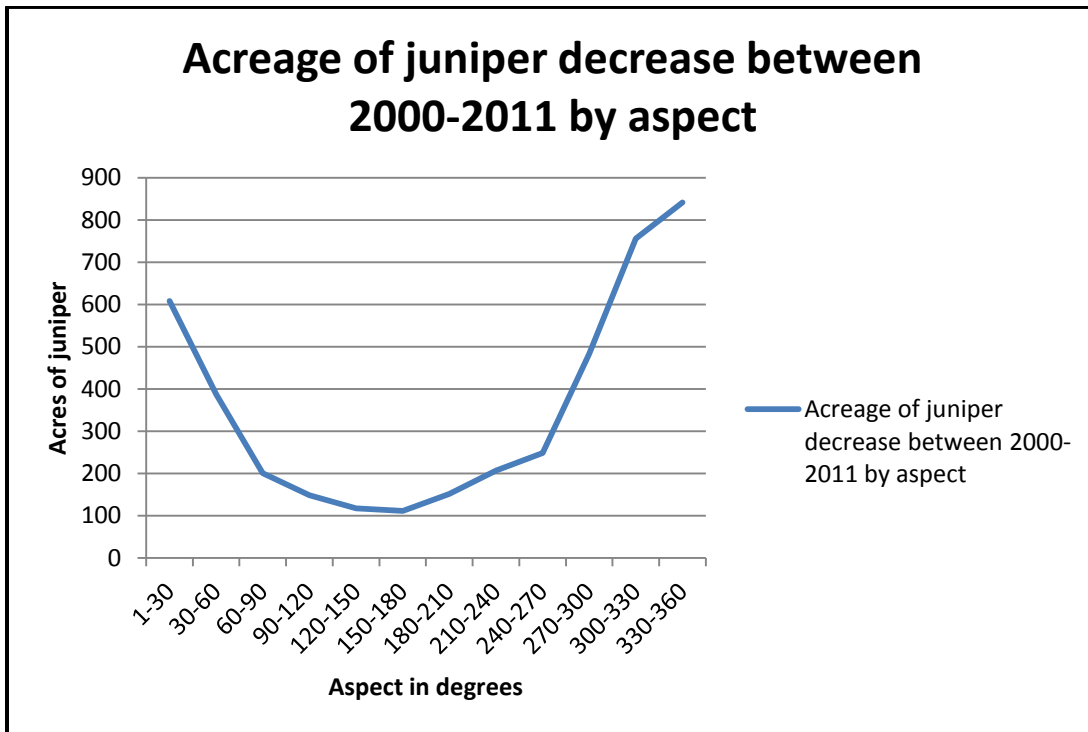


Figure 11. Juniper acres decreased between 2000 and 2011 by elevation interval.

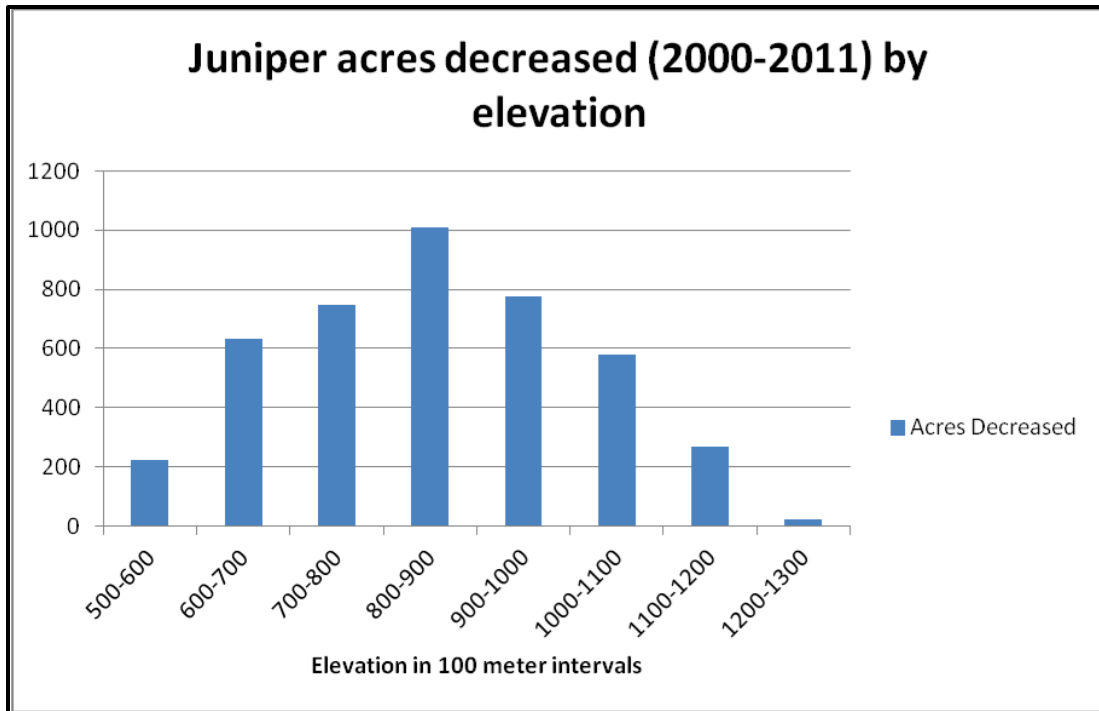


Figure 12. Juniper acres decreased between 2000 and 2011 by elevation intervals.

Table 7. Juniper Change Detection Error Matrix

Photo- Interpreted Class				
Mapped Class	No Change	Juniper Decrease	Total	User's Agreement
No Change	164	33	197	83.2%
Juniper Decrease	29	171	200	85.5%
Total	193	204	397	
Producer's Agreement	85.0%	83.8%		Overall Agreement = 84.4%

APPENDIX 1: OUTPUT MAPS

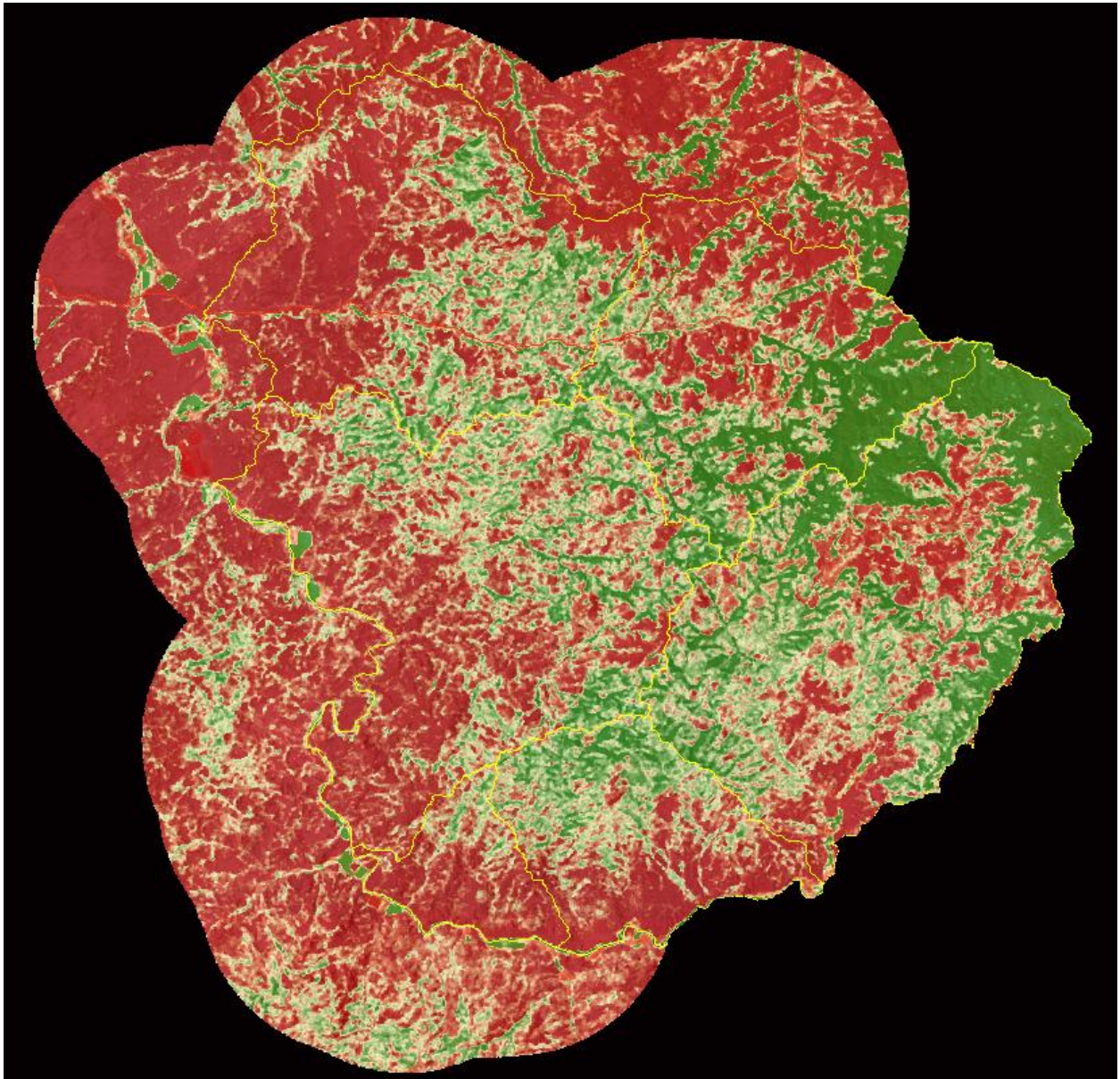


Figure 13. Percent juniper canopy cover in 2000 displayed in a red and green gradient. Dark green represents >40% canopy cover, red represents >1% canopy cover.

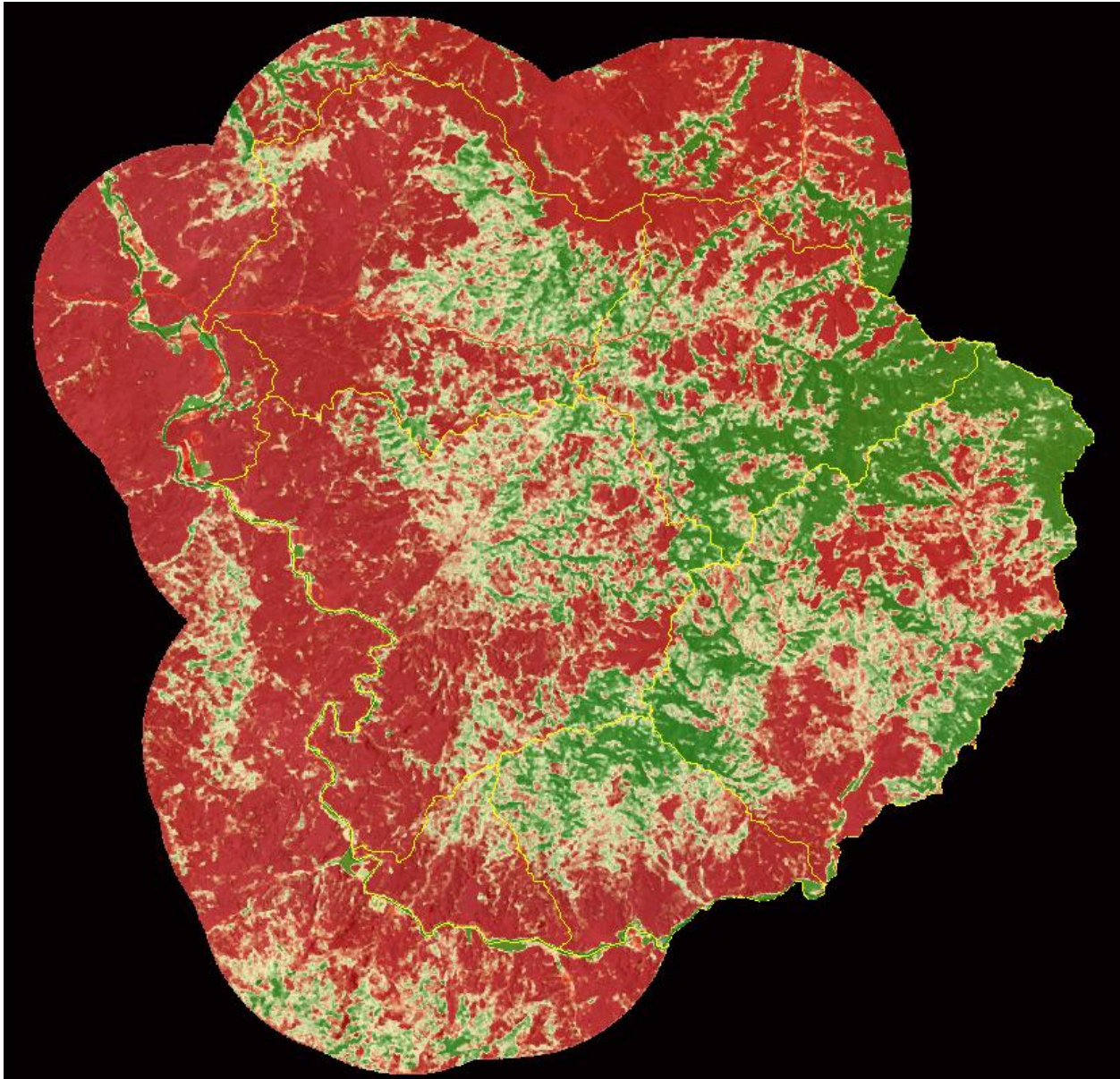


Figure 14. Percent juniper canopy cover in 2011 displayed in a red and green gradient. Dark green represents >40% canopy cover, red represents >1% canopy cover.

ATTACHMENT 3

PHOTO-INTERPRETATION SAMPLING



Eric Nielsen and Matt Lee

Institute for Natural Resources, Portland State University

1. INTRODUCTION

Recent high-quality color-infrared aerial photography and LiDAR data permit highly accurate mapping of western juniper and reasonable mapping of big sagebrush and riparian shrubs (see Attachment 1). However, mapping change over the 10-year period since the establishment of Pine Creek Conservation Area (PCCA) is a more difficult task, due to the lack of LiDAR imagery and the lower quality of air photos from the early 2000's. Automated change detection is one approach that is particularly applicable to western juniper, due to the presence of clear textural cues that are effective with even lower quality air photos (see Attachment 2). But small patches of sagebrush and riparian woody vegetation (RWV) can not be reliably modeled from those photos or from medium-resolution satellite imagery. Monitoring of permanent plots (see Attachment 4) is a useful approach for tracking change in plant diversity and investigating specific change processes, but the small number of transects and their non-random locations prohibit drawing conclusions on change in species-specific cover across the conservation area. We therefore performed several manual photo-interpretation exercises in order to provide estimates of change for big sagebrush and riparian shrubs, in addition to providing an alternative approach to estimating the current prevalence of western juniper, big sagebrush and RWV, and change in western juniper.

2. METHODS

All photo-interpretation was primarily performed using aerial photography for both historic and recent time periods. Conditions existing at the time of the establishment of PCCA were represented by pan-sharpening the true color air photos collected in 2002 over PCCA with 1:40000 scale panchromatic National Aerial Photography Program (NAPP) photos from 2000, which had a finer effective spatial resolution. Current conditions were represented by the four-band color-infrared National Agricultural Inventory Program (NAIP) imagery collected in 2011 at 1-meter resolution. In the case of big sagebrush, similarly specified NAIP imagery from 2009 was used instead, because it more clearly captured this species.

All assessments (other than historic sagebrush presence, see below) were made by having an experienced analyst familiar with the project area determine whether or not the land cover type of interest was present or not at each of a large number of randomly selected points, in both current and historic imagery. Minor local registration errors between the imagery datasets were ignored for purposes of determining whether land cover had changed, as this would otherwise have introduced a large additional source of variance into the change analysis process. The best judgment of the analyst was the final arbiter in all cases.

A vegetation height raster derived from LiDAR data collected in 2011 was occasionally used to aid in interpretation. Photo-interpretation of the historic imagery relied heavily on ascertaining whether conditions differed from recent imagery, rather than on making a completely independent interpretation, which would have been biased by the lower quality of the older datasets. All work was performed in ESRI ArcGIS.

2.1. Western Juniper

One thousand randomly located points were generated across the full extent of PCCA and adjacent DOI lands shown in Figure 1. Land ownership at each point was extracted and associated with the point. This permitted separate estimates of both current conditions and change to be produced on PCCA lands vs. Department of Interior lands (DOI; representing Bureau of Land Management lands and the Clarno Unit of the John Day Fossil Beds National Monument), as well as overall estimates incorporating all land combined (see Figure 2). Each point was assessed for live juniper presence in both dates of imagery. The percent cover estimates were then corrected for systematic bias by deriving a correction factor with reference to the coniferous tree cover map produced in the base mapping work (see Attachment 1). The

normal approximation to the binomial distribution was used to produce a 95% confidence interval (CI) for an estimate of the total area occupied by juniper in 2011. McNemar's test, a nonparametric statistic appropriate for testing for change on resampled plots with a dichotomous trait (Elzinga *et al.* 2001, p. 156) was run on the paired samples to produce a 95% CI for an estimate of the change in occupied area between 2002 and 2011.

2.2. Riparian Woody Vegetation

Because the total area occupied by RWV at PCCA is quite small, we first restricted the sampling area to portions of the study area that could conceivably be occupied by riparian vegetation. A riparian areas delineation produced from the LiDAR bare earth elevation data via a procedure developed in Nielsen *et al.* (in press) was used for this purpose. A list of stream channels along which RWV was of interest was provided by PCCA management. These channels were extracted from high resolution data from the National Hydrography Dataset, buffered, intersected with the riparian areas delineation, and then restricted to PCCA and DOI land. The streams and resulting sampling areas generated from them are shown in Figure 3. The delineation version used here represents a liberal interpretation of riparian areas and is unlikely to exclude any RWV. Even over the reduced sampling area, we anticipated significantly lower cover of RWV than in the western juniper sampling exercise, so a larger number of points were generated.

2450 randomly located points were generated across the full sampling area. The channel most closely associated with each point was extracted and saved, with the objective of producing separate estimates of current conditions and change for the western and eastern portions of Pine Creek and for all other channels in the study area considered cumulatively. We determined that it was relatively easy to further reduce the sampling area for the Pine Creek segments by hand-delineating a smaller polygon along the stream containing all the RWV and excluding none of it. An additional 317 randomly located points were generated across this reduced area, and combined with the 140 points selected across the full sampling area that fell within this area. Estimates of current conditions and change for the Pine Creek segments were made based only on the points within the hand-delineated area containing all RWV. Estimates for the remainder of the streams and the cumulative estimates for the entire study area were based on all points.

Each point was assessed for presence of RWV in both dates of imagery (Figure 4 shows the appearance of a representative area along Pine Creek in both air photo datasets). The fraction of points corresponding to RWV was determined for both dates. The normal approximation to the binomial distribution was used to produce a 95% CI for an estimate of the total area occupied by RWV in 2011. Again, McNemar's test was run on the paired samples to produce a 95% CI for an estimate of the change in occupied area between 2002 and 2011.

2.3. Big Sagebrush Stands

Due to the small size of individual plants and variety of other species that could be confused, it proved impossible to address big sagebrush at the scale of the individual plant, as had been possible with juniper and RWV. Instead, we took an approach focused at the stand level. Our estimates, both for current extent and for change since historic conditions, are therefore expressed in terms of the area occupied by coherent stands of big sagebrush rather than by individual plants. In addition, an alternative methodology for change estimation was necessitated by the fact that the historic photography was not of adequate quality to permit a confident assessment of whether or not sagebrush stands were present at any given location. Because the methods for estimating current extent and change differ, they are discussed separately here.

2.3.1. Estimation of Current Extent

The small total area occupied by big sagebrush stands required a restriction of the sampling area similar to that needed for RWV. Although there were no landscape features we could use to definitively restrict the sampling area, we determined that the likelihood of sagebrush stands existing in areas occupied by over 10% mature juniper cover was minimal. Therefore we created a 10-meter resolution LiDAR-derived 8-foot-plus juniper cover layer and eliminated all pixels with over 10% cover from the sampling area. Two successive focal majority filters were used to eliminate speckle from the result.

2000 randomly located points were generated across the PCCA portion of the sampling area; using a similar sampling density on DOI land resulted in an additional 1397 points. Each point was assessed for sagebrush stand presence in the 2009 aerial photography, which was the only air photo collection in which sagebrush stands could be reliably interpreted. The fraction of points corresponding to sagebrush stands was determined, and the sampling area were used to produce confidence intervals for the total area occupied by sagebrush stands in 2009 at 90% and 95%.

2.3.2. Estimation of Change

The appearance of sagebrush stands in the 2002 imagery seemed to be affected greatly by view angle, solar incidence angle, and soil background variation. Only some sagebrush stands were recognizable, and even then only some portions of the stands could be clearly delineated. It was therefore impossible to perform the change sampling similarly to juniper and RWV. Instead, we took the approach of reducing the sampling universe to a set of sagebrush stands (or portions thereof) that could be confidently assigned as such in 2002 imagery, delineated them in a set of polygons, and then examined the same polygons in 2009 imagery, reducing them in size where portions had been lost in the intervening years. This approach is not able to detect expansion in sagebrush stands; the only goal was to assess the likelihood of sagebrush stands that existed in 2002 continuing to exist in 2009. We have no basis for assuming that the stands identifiable in 2002 represent an unbiased sample of all sagebrush, but there seemed to be no alternative.

148 stands of sagebrush were delineated using 2002 imagery, composed of 90 stands on PCCA land and 58 on DOI land. The polygons were copied to a new ArcGIS layer and photo-interpreted in 2009 imagery, either leaving them unchanged, reducing their size, or eliminating them where necessary. Figure 5 shows an example area where a significant amount of sagebrush elimination appears to have occurred. The 2002 polygons were then shrunk by applying a negative five meter buffer to their perimeters, to reduce the impact of image registration errors or other edge effects causing an artificial reduction in area in the 2009 version. The 2009 polygons were also reduced by intersecting them with the buffered 2002 polygons, to maintain compatibility between the two datasets. Area statistics were then created for all polygons in both the 2002 and 2009 layers, and exported for analysis.

The fractional reduction in sagebrush stand area occurring between 2002 and 2009 was determined across the full PCCA and DOI polygon layers. This quantity was used to reconstruct PCCA and DOI sagebrush stand area in 2002 based on the 2009 sagebrush stand extent estimations determined previously. In addition, it was necessary to account for possible expansion of stands into new areas in the intervening time period. We had no basis for estimating the rate at which this expansion would occur, and instead produced three estimates for net sagebrush stand area change, making alternative assumptions about the fraction of total 2009 stand area resulting from expansion since 2002 (0%, 10%, and 20%).

3. RESULTS

3.1. Western Juniper

Comparison of the 2011 cover estimates with the coniferous tree base map cover gave a correction factor of 0.32 for conversion of photointerpreted cover to actual cover. After scaling the cover estimates by this correction factor, the sample point analysis for juniper yielded the results shown in Table 1 (see the map in Figure 6 for illustration of where the changed locations were).

The initial juniper tree cover in 2002 was estimated at 8.6% over the entire project area, 10.0% on PCCA land and 5.9% on DOI land (the disparity is likely due to the overall higher suitability of PCCA land for western juniper, due to its higher elevation). Juniper trees were eliminated on an estimated 1.5% of all land (~800 acres), but expanded on 0.3% (~170 acres), for a net decrease of 1.2% (~640 acres) over the entire project area. Junipers were eliminated at roughly the same rate on DOI and PCCA land (1.6% vs. 1.5%, ~290 acres vs. ~520 acres), but appeared to expand more slowly on DOI than PCCA land (0.2% vs. 0.4%, ~34 acres vs. ~130 acres).

A relative reduction of approximately 14.2% net live juniper cover occurred between 2002 and 2011 over the entire project area, corresponding to a loss estimate of ~640 acres. McNemar's test indicated a definite decrease in juniper over the full project area ($p < 0.0001$, 95% CI: net loss 400 - 805 acres). On PCCA land, net loss definitely occurred ($p = 0.0004$), with an estimated relative reduction of 11.2%, or a net loss of ~380 acres (95% CI: 176 - 529 acres). On DOI land, net loss very likely occurred ($p = 0.0013$), with an estimated relative reduction of 24.2%, or a net loss of ~250 acres (95% CI: 109 - 314 acres).

Table 1. Results of paired juniper point sampling using 2002 and 2011 air photos.

Owner	Total samples	Samples with juniper (2002)	Samples with juniper (2011)	Percent juniper (2002)	Percent juniper (2011)	Relative percent change	Acres of juniper (2011), 95% CI	Acres of juniper decrease, 95% CI
PCCA	661	206	183	9.97	8.86	-11.2	3048 ± 745	(176, 529)
DOI	339	62	47	5.85	4.44	-24.2	797 ± 394	(109, 314)
Total	1000	268	230	8.58	7.36	-14.2	3854 ± 847	(400, 805)

3.2. Riparian Woody Vegetation

The results of the sample point analysis for RWV are shown in the map in Figure 7 and in Table 2. A relative increase of approximately 35.6% was observed in the acreage occupied by RWV across the entire project area, corresponding to an increase of 37.5 acres (95% CI: 29.8 - 39.2 acres). Increases of RWV were indicated in each of the three sampling units: Pine Creek West ($p < 0.0001$), Pine Creek East ($p < 0.0001$), and the other riparian areas all considered cumulatively ($p = 0.0004$). RWV gains in Pine Creek West were estimated at 5.2 acres (95% CI: 3.2 - 5.7 acres). In Pine Creek East, gains were estimated at 4.6 acres (95% CI: 2.6 - 5.3 acres). In all other riparian areas considered cumulatively, gains were estimated at 14.8 acres (95% CI: 7.5 - 16.6 acres)

Table 2. Results of paired RWV point sampling using 2002 and 2011 air photos.

Sampling unit	Total samples	Samples with RWV (2002)	Samples with RWV (2011)	Est. acres of RWV (2002)	Acres of RWV (2011), 95% CI	Relative percent change	Acres of RWV increase, 95% CI
Pine Creek W (hand-delin)	187	43	64	10.6	15.8 ± 3.1	+48.8	(3.2, 5.7)
Pine Creek E (hand-delin)	270	102	123	22.2	26.7 ± 3.5	+20.6	(2.6, 5.3)
All other streams	1706	53	69	48.9	63.6 ± 14.7	+30.2	(7.5, 16.6)
Entire project area	2447	118	160	105.3	142.8 ± 21.4	+35.6	(29.8, 39.2)

3.3. Big Sagebrush Stands

3.3.1. Estimation of Current Extent

The results of the sample point analysis for big sagebrush stands are shown in the map in Figure 8 and in Table 3. Approximately 1.6% of all land in the project area was occupied by sagebrush stands in 2009, representing a total of from 678 - 983 acres (90% CI). The fraction of land occupied is similar on PCCA and DOI lands.

Table 3. Results of sagebrush stand point sampling using 2009 air photos.

Owner	Total samples	Samples with sagebrush stand (2009)	Acres of sagebrush stands (2009), 90% CI	Percent of all land (2009), 90% CI
PCCA	2000	51	533.0 ± 121.6	1.55 ± 0.35
DOI	1397	28	297.3 ± 91.8	1.66 ± 0.51
Total	3397	79	830.3 ± 152.5	1.59 ± 0.29

3.3.2. Estimation of Change

The fractional reduction in sagebrush stand area determined from the analysis of the delineated polygons is shown in Table 4. By this estimation, approximately 30% of the sagebrush stand area that existed in 2002 did not remain in 2009. The loss appeared to be concentrated on PCCA lands; DOI lands were much less affected. Sagebrush loss appeared to primarily result from fires. In the southern portion of PCCA, a significant decrease in stand area was observed; a fire in 2004 in this area was the likely cause. Smaller decreases in sagebrush cover in some delineated polygons resulted from juniper encroachment, which appeared to gradually exclude sagebrush in some areas. It is possible that the difference in image quality between the two collections resulted in some false change. It is important to remember that the samples were not randomly chosen. Although an effort was made to delineate most clearly identifiable sagebrush stands across the entire project area, there may be bias toward either particular geographic areas or toward environmental settings where sagebrush loss was more severe than it was as a whole.

Table 4. Fate of the sagebrush stands delineated from 2002 imagery.

Owner	Stands delineated (2002)	Stands remaining (2009)	Acres delineated (2002)	Acres remaining (2009)	Percent of area remaining (2009)	Percent of area lost (2009)
PCCA	90	74	140.7	88.2	62.7	37.3
DOI	58	51	65.9	55.7	84.5	15.5
Total	148	125	206.6	143.9	69.7	30.3

Net sagebrush stand area change across the project area was estimated by using the current extent estimates derived above, and assuming that the reduction in occupied area seen in the delineated stands was representative of the reduction in area of sagebrush stands as a whole. To account for expansion into new areas, we produced three estimates for net change; one assumed that no measurable expansion occurred, while two others assumed that expansion since 2002 was responsible for 10% and 20% of the total existing 2009 stand area, respectively. The results are shown in Tables 5-7.

Assuming that expansion was responsible for 10% of the 2009 stand area, which is likely generous, sagebrush stands went from occupying 2.3% of all land in 2002 to 1.6% in 2009. On PCCA land only, the decline was steeper, from 2.5% in 2002 to 1.6% in 2009, while on DOI lands the change was from 2.0% in 2002 to 1.7% in 2009.

Table 5. Estimated net sagebrush stand area change, assuming no expansion.

Owner	Acres (2002)	Acres (2009)	Acres lost	Percent of area remaining (2009)	Percent of area lost (2009)
PCCA	849.6	533.0	316.6	62.7	37.3
DOI	352.0	297.3	54.7	84.5	15.5
Total	1201.6	830.3	371.3	69.1	30.9

Table 6. Estimated net sagebrush stand area change, assuming 10% of 2009 stand area from expansion.

Owner	Acres (2002)	Acres (2009)	Acres lost	Percent of area remaining (2009)	Percent of area lost (2009)
PCCA	764.6	533.0	231.6	69.7	30.3
DOI	316.8	297.3	19.5	93.8	6.2
Total	1081.4	830.3	251.1	76.8	23.2

Table 7. Estimated net sagebrush stand area change, assuming 20% of 2009 stand area from expansion.

Owner	Acres (2002)	Acres (2009)	Acres lost	Percent of area remaining (2009)	Percent of area lost (2009)
PCCA	679.7	533.0	146.7	78.4	21.6
DOI	281.6	297.3	-15.7	105.6	-5.6
Total	961.2	830.3	131.0	86.4	13.6

APPENDIX A: FIGURES

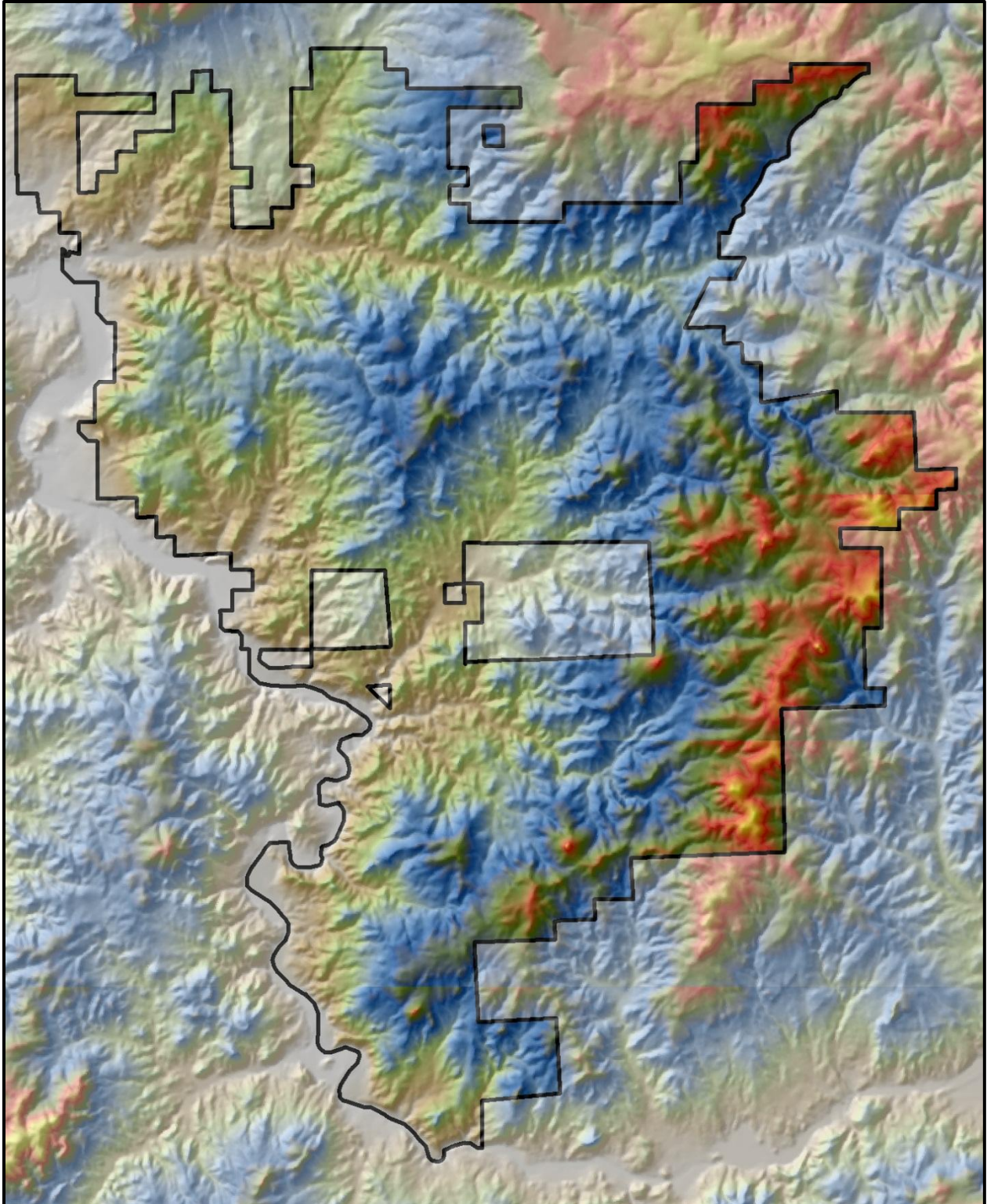


Figure 1. Pine Creek Conservation Area and adjacent Department of Interior lands are shown within the black outline, overlaid on a digital elevation model. Washed-out elevation colors represent private inholdings and other land not included in the analysis.

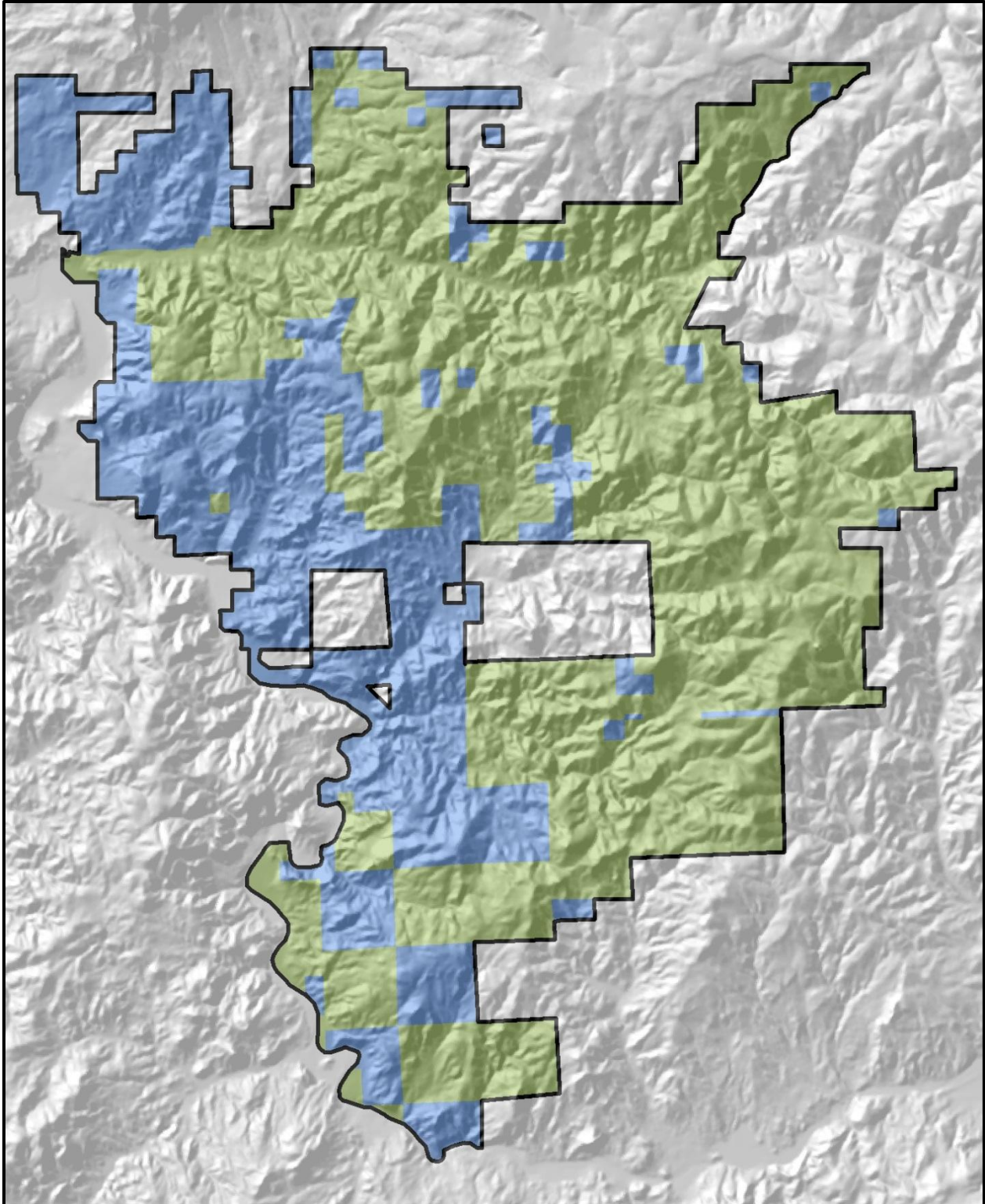


Figure 2. Pine Creek Conservation Area lands are shown in green, while adjacent Department of Interior lands are shown in blue. Other land is privately owned or otherwise not included in the analysis.

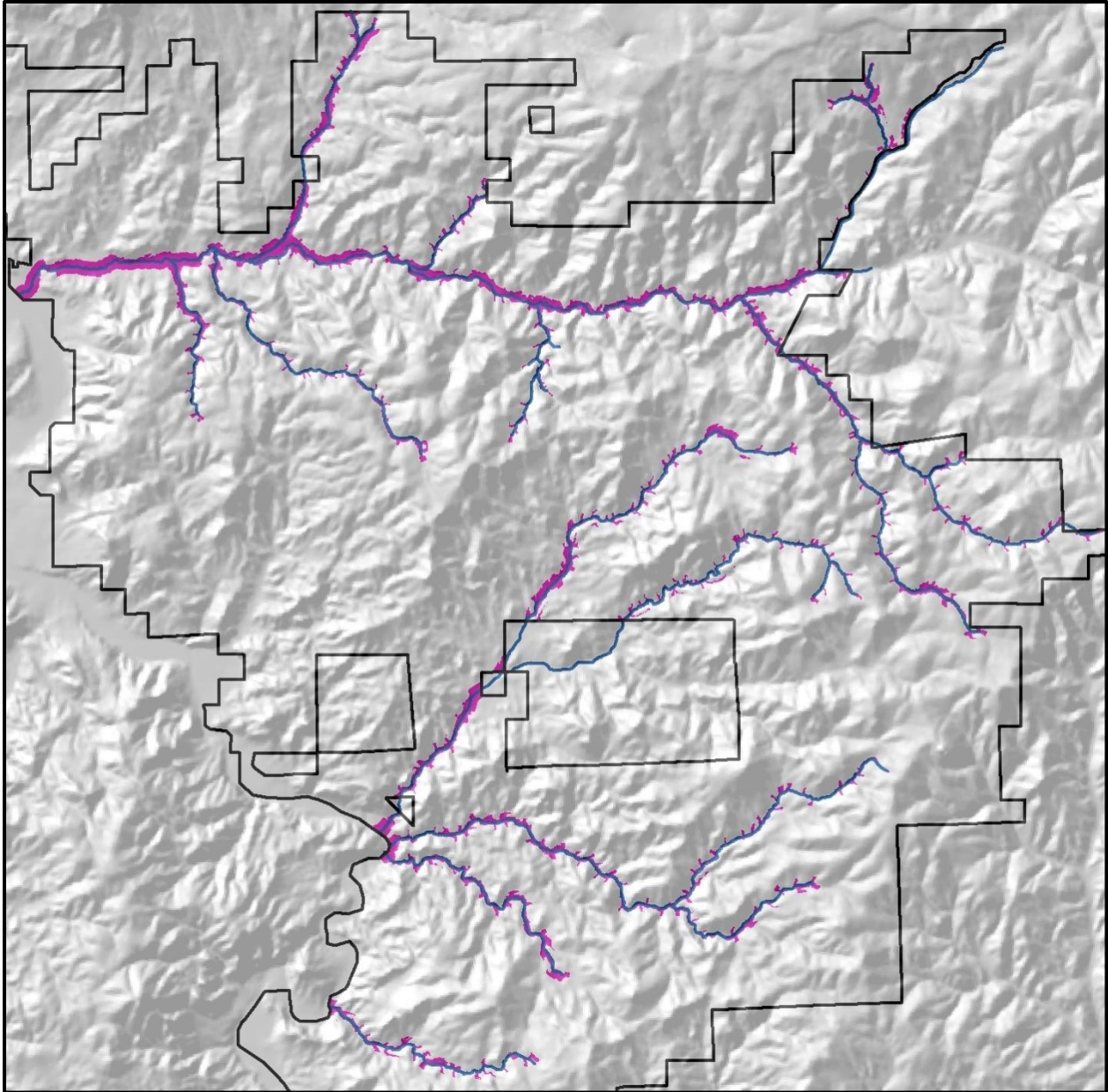
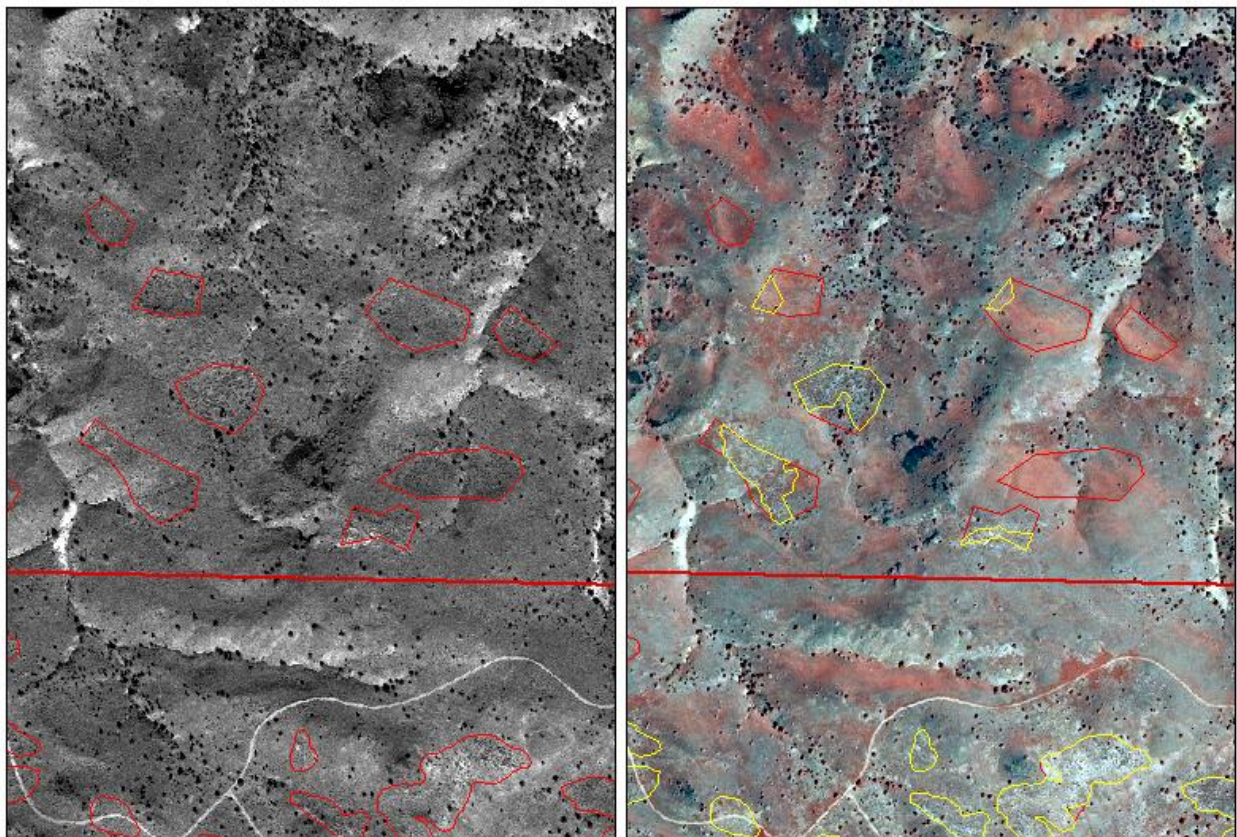


Figure 3. Streams included in riparian woody vegetation analysis are shown in blue; the sampling area generated around these streams is shown in pink.



Figure 4 (above). Comparison of the same riparian area in true-color 2002 air photo (left) and color-infrared 2011 air photo (right).

Figure 5 (below). Comparison of sagebrush stands delineated in 2002 air photo (left) with the same stands delineated in 2009 air photo (yellow polygons on right).



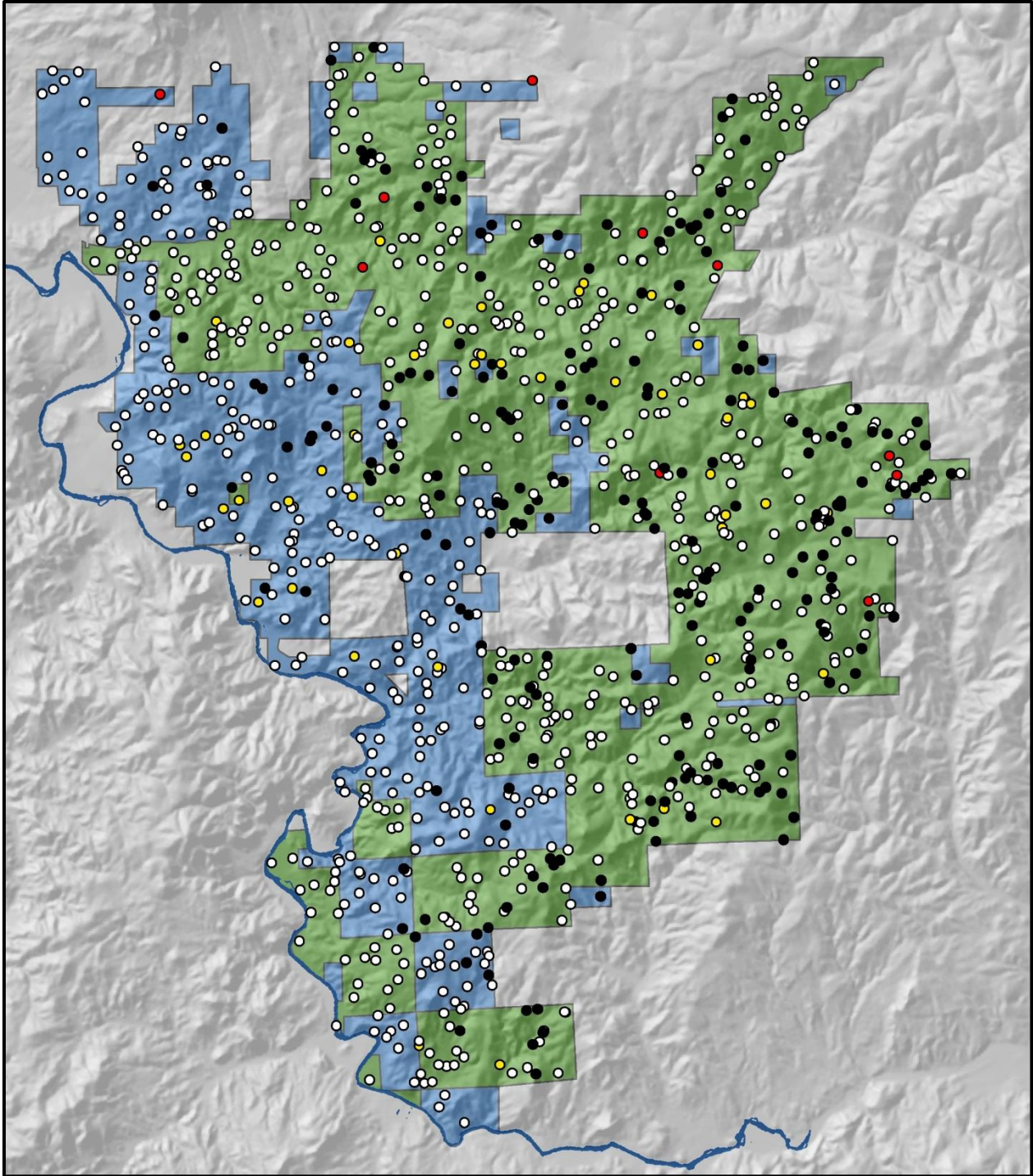


Figure 6. Western juniper sampling results. White represents juniper absence in both 2002 and 2011, black represents presence in both years, yellow represents elimination during the time period and red represents expansion. PCCA land is shown in green; BLM and NPS land are in blue.

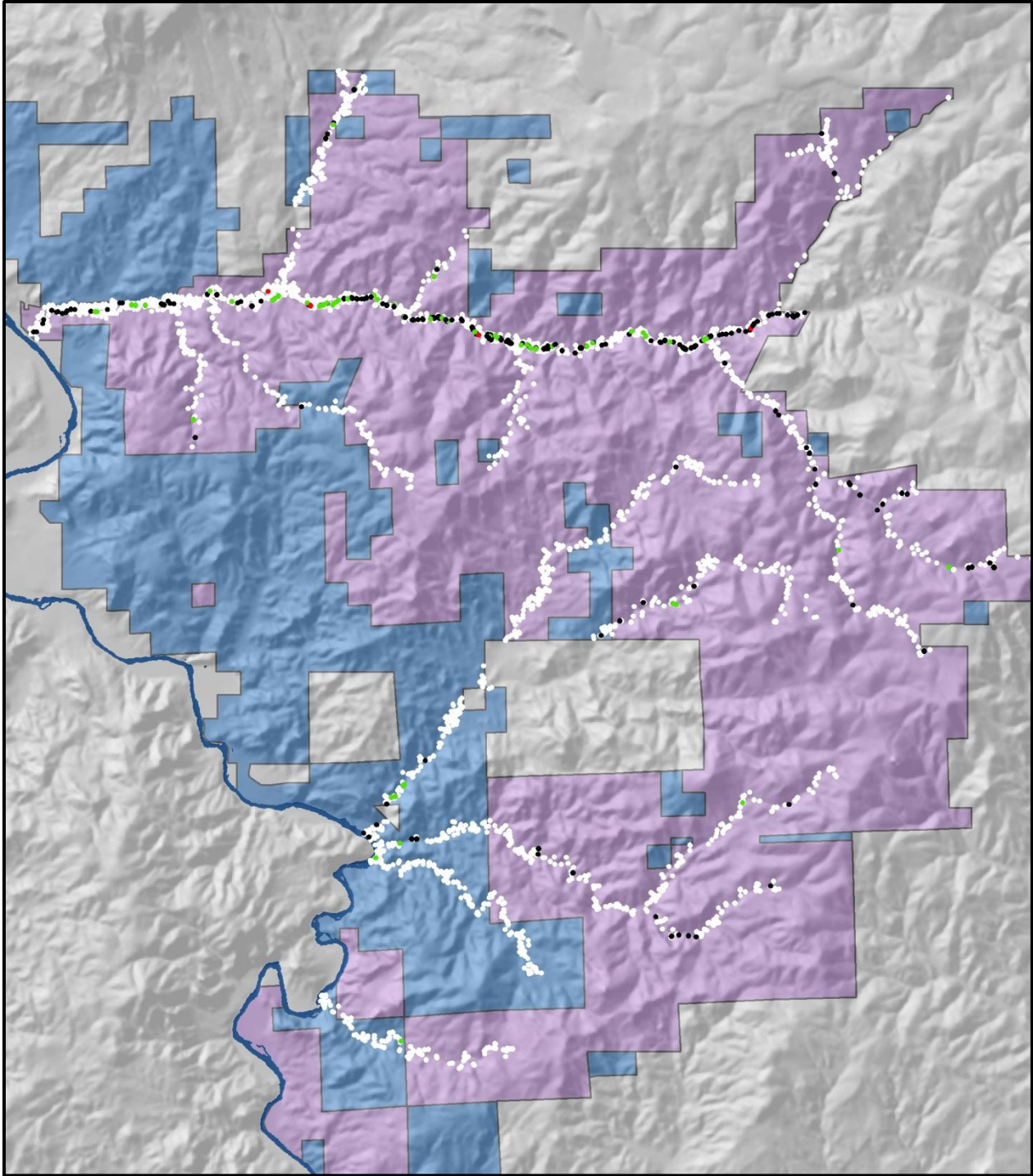


Figure 7. Riparian woody vegetation sampling results. White represents RWV absence in both 2002 and 2011, black represents presence in both years, red represents elimination during the time period and green represents expansion. PCCA land is shown in purple; BLM and NPS land are in blue.

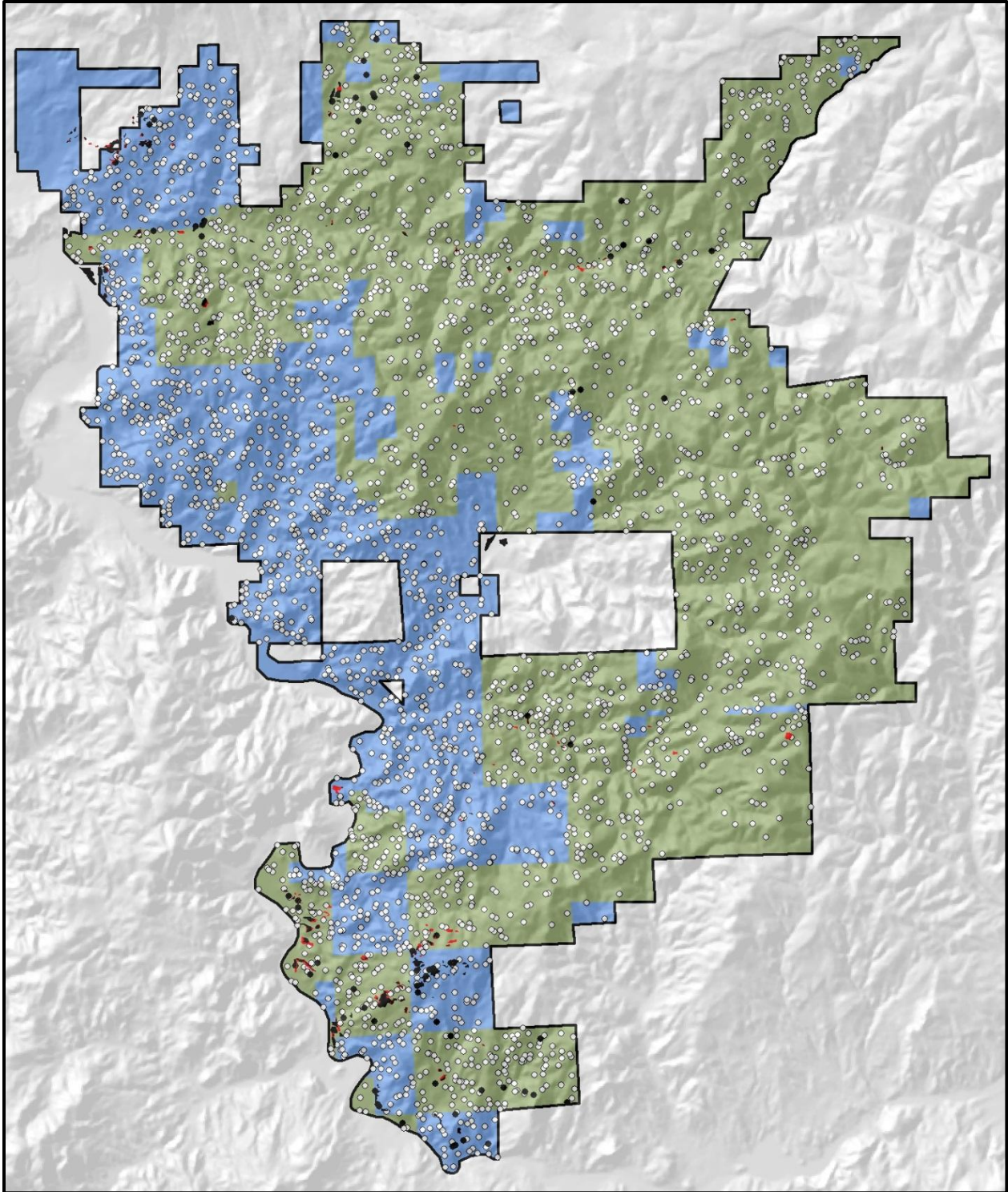


Figure 8. Big sagebrush stand sampling results. White dots represent absence of sagebrush stand in 2009, black dots represent presence in 2009. Red areas are portions of delineated 2002 stands that are no longer occupied by sagebrush. PCCA land is shown in green, while BLM and NPS land are in blue.

ATTACHMENT 4

VEGETATION TRANSECTS CHANGE MONITORING, 2002 - 2011



Jimmy Kagan

Institute for Natural Resources, Portland State University

1. INTRODUCTION

In the Pine Creek Conservation Area monitoring report to the Bonneville Power Administration, Berry (2006) reported that upland vegetation was probably the most important factor affecting wildlife habitat and watershed function. In order to evaluate changes in upland vegetation conditions occurring as a result of tribal management, staff at the Pine Creek Conservation Area (PCCA) worked with Oregon State University's Oregon Natural Heritage Information Center (ORNHIC) to establish permanent field vegetation monitoring plots in 2001. The objective of this work was to attempt to determine how different vegetation communities were changing over time.

A total of 65 detailed plots were established to provide a permanent baseline to measure vegetation change. The sites for the plots were selected to reflect the full range of diversity of the different plant communities or vegetation types located in the conservation area. Plots were either placed well within the "boundaries" of a particular community, or through the transition zones between communities. Plots were placed in representative areas chosen by the PCCA manager and ORNHIC's ecologist to represent community types that occurred frequently throughout the ranch. Plots were also selected to sample unusual community types that needed representation. The ability to relocate the detailed plots was a key requirement, so most were not very far from roads and clearly marked trails. However, care was taken to assure that plots were distributed across all areas of the conservation area.

As part of a project to assess changes over the first 10 years of tribal management, PCCA staff funded ORNHIC to revisit and resample these detailed vegetation plots again in 2011 and 2012. During the decade, ORNHIC had been transferred from OSU to Portland State University and renamed the Oregon Biodiversity Information Center, but the ecology staff remained unchanged, and resampling was undertaken along with an additional effort to provide a more accurate vegetation map, and to use LiDAR to accurately map the distribution of western juniper (*Juniperus occidentalis*) in the conservation area.

In our 2010 scoping report, it was noted that there were two primary problems with resampling this data. First, because the original plots were not selected randomly, changes for the entire plot set cannot be statistically generalized to represent changes for the entire PCCA. Comparisons of change could only be made between the different sampled vegetation types, to address the question of whether some plant communities are recovering or degrading faster or slower than other types, but generalizations about the status of the entire site may not be made using this data.

The second difficulty related to the marking of the plots so they could be relocated. Since much of the point sampling was based on the point intercept method to accurately measure vegetation cover, relocating the plots exactly was critical. As a result, both ends of the permanent transects were marked with tall (but slender) white posts, and GPS coordinates were collected at both ends. All of the transects ran exactly from north to south (0 – 180°), so that if either of transect ends could be relocated, it would be possible to re-sample the plots. The PCCA manager and ORBIC selected large white fiberglass poles to mark both ends of the transects. These had been used successfully in the past at sites in western Oregon, and near Prineville, although mostly in areas with relatively deep soils. Because the Pine Creek Conservation Area was so rocky, frost heaving led to a significant number of posts being dislodged. However, the report also suggested that if only half of the plots can be relocated, the change in habitat quality information could be very useful.

Over the resampling period, 52 of the 65 plots were able to be relocated, for a total of 80%, which given the potential difficulties outlined above, was a better result than anticipated. At least 5 of the 13 plots not relocated were in areas where a relatively hot fire had burned after the plots were established, and both transect ends were likely destroyed in the fires. At one of these locations, small melted bits of fiberglass were recovered, although it was impossible to determine if these were at a transect end, since no evidence of the metal post tag could be recovered. However, at least 3 of the relocated transects appeared to survive fires, perhaps because the fires were fast-moving or not as hot.

2. METHODS

We attempted to revisit all permanent 50-meter line intercept plots that had been established in 2002. Transects had been marked with 5-foot, fiberglass electric fence posts at each end. For each plot, plant species cover was determined using the point intercept method, with points taken every meter at the right side of the half meter mark, starting at 0.5 and ending at 49.5. In addition to the point intercept cover information, a plant species list was gathered at each plot, which included all species found within a meter of the point intercept transect line. The plant species list was comprehensive for all perennial vascular plant species, and included any annual plant species which could be identified (i.e. had flowers and/or fruit). These lists should help determine if species richness is increasing or decreasing at these sites.

To best describe the changes, each of the plots was characterized by the plant community represented using the National Vegetation Classification System (NVC) (Jennings et al. 2009), and the major changes in cover of dominant species was briefly summarized. In addition, each of the plots was characterized as to whether the overall ecological condition had improved (+), declined (-) or stayed about the same (#), based the following factors:

1. Total native species cover and diversity (good)
2. Total bunchgrass cover (good)
3. Non-native species cover (bad)
4. Presence of noxious species (bad)
5. Cover of western juniper (not optimal)

Note that the condition rankings are only an evaluation of changes over the last ten years, not the current condition of the vegetation in these plots. These summaries are included as Appendix 1. Plant names in these summaries and graphs are represented by the 4-6 digit NRCS Plants Codes, found online at <http://plants.usda.gov/>. A list of the codes from this report can be found in Appendix 2.

In addition to the data noted above, additional plot-level data was collected, including topographic slope and aspect, GPS locational information, and descriptive notes on the location, soil types, and general botanical condition.

3. RESULTS

As expected, the changes found at the 52 resampled plots vary widely across the conservation area. Many plots showed significant ecological improvements, with declining cover of invasive species and expansion of native bunchgrasses. The series of managed and unmanaged wildfires occurring between 2002 and 2012 resulted in significant mortality of western juniper, a major management objective that should eventually facilitate diversity increases in other native plants. However, the fires also resulted in loss of cover of native shrubs and forbs. This is likely a short term effect only, as long as future juniper expansion is held in check.

The plots are then listed by the three major ecosystem types sampled: juniper woodlands, shrublands and shrub steppe, and grasslands. Then, within each of these major types, they are grouped into what formerly would have been considered an alliance in the NVC, the major dominance types. Since the alliance concept is currently being revised, these groupings are provided to help examine patterns in the different vegetation communities in the conservation area. Descriptions of the vegetation change within each of these types are found below, as are the summaries of each of the plots sampled.

3.1. Juniper Plots

A total of 22 of the 52 plots sampled were classified as western juniper (*Juniperus occidentalis* or JUOC) communities. Of these, 3 had unchanged juniper, 7 showed increases, 12 showed decreases of

which 5 decreased to no juniper. The declines were usually large, while the increases tended to be small, generally around 6%, representing increasing juniper growth rather than juniper reproduction. As described above, each of the western juniper community plots was characterized as to whether the overall ecological condition had improved, declined or stayed about the same. Half of the plots (11) showed improved ecological condition, 8 remained largely the same, and 3 declined. In the 3 plots that declined, fires had both reduced juniper cover and native perennial bunchgrasses, and increased non-natives, but it is possible that the native bunchgrasses and will recover.

Nine of the juniper plots had some shrubs present. One was established due to its high cover of the important wildlife species, curl-leaf mountain mahogany (*Cercocarpus ledifolius* or CELE3). And in this plot, mountain mahogany increased in cover by 8% to 32%, juniper increased slightly to 8%, and bunchgrass cover also improved. Three had significant amounts of bitterbrush (*Purshia tridentata* or PUTR2), a target species. Bitterbrush increased in one, remained the same in another, and vanished from the third. Another four juniper plots had sagebrush in the stands, and in all but one, the sagebrush disappeared from the samples during the study. The last of the nine juniper shrub plots was a western juniper / snowberry (*Symphoricarpos albus* or SYAL) community, in which a burn occurred, removing the juniper but allowing for an increase in snowberry, the addition of native roses, and the reduction in cover of annual grasses.

The remaining juniper plots had bunchgrass understories. One represented an unusual community with Great Basin wildrye (*Leymus cinereus* or LECI4) as one of the dominant grasses. The wildrye remained stable while other native bunchgrasses and native perennial forbs increased. Three plots had Idaho fescue – bluebunch wheatgrass (*Festuca idahoensis* or FEID – *Pseudoroegneria spicata* ssp. *spicata* or PSSPS) understories. Of these, two improved showing significant increases in fescue cover and decreases in juniper. In the third, most of the juniper was removed by a fire from an initial high cover (56%), but the fire's impact also set back the native bunchgrasses and forbs while increasing weeds. Western juniper / bluebunch wheatgrass communities represented the largest number of juniper plots sampled, at five. Of these, three showed improved conditions, one declined, and one showed no change. The last group is the western juniper / Sandberg bluegrass (*Poa secunda* or POSE) communities, of which four examples were sampled. These represent the shallow-soiled areas somewhat more resistant to change. Three of the four showed no significant change, while the fourth improved as a result of a fire which removed all of the juniper.

3.2. Shrubland and Shrub Steppe Plots

A total of 11 of the 52 plots sampled were classified as shrub or shrub steppe communities. These were dominated by some combination of basin or Wyoming big sagebrush (*Artemisia tridentata* ssp. *tridentata* or ARTRT and *A. t. ssp. wyomingensis* or ARTRW, merged in this report as ARTR2 or big sagebrush), rigid sagebrush (*Artemisia rigida* or ARRI), bitterbrush (*Purshia tridentata* or PUTR2), green rabbitbrush (*Chrysothamnus viscidiflorus* or CHVI8), or broom snakeweed (*Gutierrezia sarothrae* or GUSA2). The last two of these are native weedy shrubs which increase following disturbances, while the sagebrush and bitterbrush represent target species due to their importance for many wildlife species. Just under half of the plots (5 of the 11) showed improved ecological condition, 3 remained largely the same, and 3 declined. Two of the three plots that declined started in very poor condition and are part of the Pine Creek Valley bottom area currently in planning for restoration by the U.S. Forest Service.

Big sagebrush (both Wyoming and basin) declined in six of the 8 shrubland plots in which it had been found in 2002, completely disappearing from 4 of these plots. The other two shows modest (4% and 6%) increases in sagebrush cover. Bitterbrush was found in only two plots, but increased cover in both. And the only rigid sagebrush plot that was relocated had burned, leading to the disappearance of the rigid and Wyoming sagebrush plants that had been present and a potential issue in assuring the exact area was resampled. Because all of the sagebrush species native to the Pine Creek Conservation Area are killed by almost any wild fire, however hot, and since none resprout, the large fires continue to reduce sagebrush

cover throughout the conservation area. However, the almost total exclusion of livestock has resulted in improving conditions throughout most of the shrublands.

3.3. Grassland Plots

The remaining 19 plots were initially classified as grasslands, dominated by sand dropseed (*Sporobolus cryptandrus* or SPCR), Thurber's needlegrass (*Achnatherum thurberiana* or ACTH7), Idaho fescue, bluebunch wheatgrass, and Sandberg's bluegrass. Most had no juniper or shrubs present, although plots are classified as grasslands if their shrub or tree cover is below 10%, and small amounts of juniper (at 2%) were found in 5 of these plots in 2002, although only in 2 in 2012. Of the 19 plots, 12 showed improved conditions, 2 declined, and 5 showed no meaningful change. Two of the 5 plots that showed no change actually got both better and worse at the same time, both with lower weeds and more bunchgrasses, but significant new juniper invasions which turned them from grasslands into juniper woodlands. They are organized below by their dominant grasses, which basically correspond to the NVC alliance.

The two sand dropseed plots both improved. Interestingly, this is the only dominant C4 grass, and it does respond favorably to increases in atmospheric CO₂ as well as summer moisture, both of which have been available over the last three years. These plots were at the lower elevations in areas close to water that had historically been more heavily impacted by livestock use and are probably responding to the decade long livestock exclusions. There were four plots dominated by Thurber's needlegrass with bluebunch wheatgrass. Two of these plots improved, one did not change, and one improved in condition but was invaded by juniper. There were also four Idaho fescue dominated plots, all of which got better, probably because they are the most mesic of the types and responded especially well to the increased late summer moisture in 2011 when most of the resampling took place. The most common type is dominated by bluebunch wheatgrass, representing 9 of the 19 grassland plots. Of these, 5 improved, 2 got worse, and one did not change, and one got better while becoming a western juniper plot.

3.4. Species Richness Data

The species richness was measured by recording all of the species found within a meter of either side of the point intercept transect line, or all species in a 50 by 2 meter area. A total of 145 vascular plant species were identified within the 52 resampled transects in 2002, while only 139 were found in 2011. These include native and non-native species, and annual and perennial plants. A summary of the plants found in each sampled year in each of the different major plant groups is given in Table 1.

The grass found in the 2002 plot samples and not in 2011 was needle-and-thread (*Heterostipa comata*), which remains common at PCCA but was replaced in the sampled plot by sand dropseed, which significantly expanded its cover in this area. However, it does appear likely that the cover of both needle-and-thread, and Indian ricegrass (*Achnatherum hymenoides*) have declined at PCCA, as have the cover of Sandberg's bluegrass and squirreltail (*Elymus elymoides* or ELEM5). These are all native grasses that tend to increase with disturbance or occur in open, sandy disturbed areas. So, what is probably happening is that the more robust or larger grasses such as Thurber's needlegrass, Idaho fescue, Junegrass (*Koeleria macrantha* or KOMA), sand dropseed and bluebunch wheatgrass which had been reduced by livestock, are expanding since livestock was removed, and now are outcompeting these other native grasses.

Table 1. Summary of species richness data from 2002 and 2011.

Plant Group	Species Richness (2002)	Species Richness (2011)
Native perennial grasses	10	9
Native annual grasses	2	2
Native annual forbs	14	13
Native perennial forbs	90	81
Native shrubs and trees	10	12
Exotic annual grasses	5	6
Exotic perennial grasses	2	5
Exotic annual forbs	7	4
Exotic perennial forbs	5	7

There were two new shrubs found in 2012 in the plots. While this is not a significant increase, it appears to be an indication of increased shrub cover in the areas of PCCA that have not burned. The two new species included spineless horsebrush (*Tetradymia canescens*), a bottomland shrub now found in some lowland areas, which are improving, both through restoration activities and recovery. These areas were the most intensively impacted by livestock, and other bottomland species often associated with salt-desert scrub habitats, such as black greasewood (*Sarcobatus vermiculatus*), spiny hopsage (*Grayia spinosa*) and shadscale (*Atriplex confertifolia*) also appear to be increasing in the area. While none of these are targets for conservation, they do represent habitats that were formerly much more abundant in the Columbia Basin and along the Columbia River floodplain. The other new shrub found in 2011 was oceanspray (*Holodiscus discolor*), now found at the western juniper/snowberry plot. This also represents an indication of the increase in all the shrubs from mesic habitats at the higher elevations in the conservation area, almost certainly the result of the removal of livestock.

The majority of the small decline in the diversity of native perennial forbs is probably an artifact of the sampling time in 2011. The months of May and June were exceptionally wet in 2011 (and in 2010 and somewhat in 2012). As a result, the roads at PCCA were impassable in the early spring of 2011, and the sampling had to be postponed until late June and early July rather than May through early June which were the months that sampling that took place in 2002. Therefore, some very early spring, relatively common forbs, including a number of onion (*Allium*) species, the yellow fritillary (*Fritillaria pudica*) and bitter root (*Lewisia rediviva*) were found in 2002 but not in 2011. In 2002, four species of flowering daisy's (*Erigeron*) were found, while only one was recorded in 2011. In addition, some of the later flowering plants, such as the buckwheat (*Eriogonum*) species were found to be slightly more diverse in 2011, with 6 species found in the plots, rather than the 5 from 2002. As a result, the study was probably not very effective at looking at changes in species richness, other than providing an indication that the diversity of the site appears not to have changed nearly as much as the composition and cover of the dominant species.

Most of the annual forbs found at the Pine Creek Conservation Area are ephemeral, flowering for just a few weeks and remaining invisible when they are not in flower. As a result, the sampling method used, involving a single visit during each field season, results in the numbers of annual forbs found being dependent on the time of year each plot was visited and the spring rainfall, more than any actual changes occurring at the site. Therefore, the fact that only one fewer species was found in 2011, in spite of the late sampling, is somewhat surprising. However, it appears that when looking at change between 2002 and 2011, what is most relevant is the diversity of native perennial grasses, perennial forbs and shrubs. And for purposes of this study, the only meaningful numbers are those of the native species, which represented 110 of the taxa found in 2001 and 102 of the taxa found in 2011.

The figures on the following pages illustrate change in dominant species abundance at the sampled plots across the conservation area. Four different species groups are summarized (native bunchgrasses, exotic species, woody vegetation, and perennial forbs). Three figures are shown for each group. The first

is a chart that shows the actual changes in sampled point data for each species, summarized across all 52 resampled plots. The second shows how the percent cover has changed for each of these species across all the plots in the conservation area. The third shows the relative change in abundance for each species. For species that were rarely found, small increases and decreases in cover can lead to very large changes in relative abundance, but for the more abundant species, this can be the best indicator for how species abundances have changed since 2002.

4. CONCLUSIONS

Overall, comparing individual plots, the areas sampled showed improved conditions, and increases in the cover and distribution of the species and habitats targeted when the property was acquired for restoration. It is important to keep in mind that the changes in species cover across the entire dataset do not necessarily represent changes across the Pine Creek Conservation Area, since they were located to cover the diversity of habitats, rather than being randomly located. However, since they are distributed across the entire conservation area, they probably do a good job representing many of the changes that have occurred.

The bunchgrass data shows increases in the grasses that are more sensitive to livestock, such as Idaho fescue, bluebunch wheatgrass, and especially Thurber's needlegrass. As discussed above, sand dropseed increases may be a result of its C4 photosynthetic pathway, its occurrences at lower elevations where it is more accessible to livestock, or other unknown reasons. The only significant declines were in Sandberg bluegrass, the very small and livestock resistant native bunchgrass, which does not appear to compete as well with the larger native grasses in the absence of livestock grazing.

The exotic species data shows declines in most of the species, with the notable exception of medusahead (*Taeniatherum caput-medusae*, TACA8). This grass has increased in cover across the sampled area from 2.35% cover to 3.4% cover as it has become established across the conservation area. The other exotic species that have been expanding are actually biennials including teasel (*Dipsacus fullonum*, DIFU2) and mullein (*Verbascum thapsus*, VETH), that are characteristic of seasonal riparian habitats. So their appearance in plots for the first time may indicate rising water tables and late season flooding, since they rarely occur in totally upland habitats. It is apparent from the fieldwork that ventenata (*Ventenata dubia*, VEDU) has also been increasing, although it only showed up once, in a single plot. The only widespread perennial exotic grass is bulbous bluegrass (*Poa bulbosa*, POBU), which declined from 3.3% cover to 0.8% cover across all the plots. Annual bromes including cheatgrass remain the most widespread exotics at 24% cover in 2011, but declined across the plots, as did the introduced perennial thistles (*Cirsium*) species, dropping from 0.15% to 0.04% cover.

Western juniper showed more than a 2.5% change in cover across the plots, down from 7.4% to below 5%, representing a 34% decline. While these declines were almost entirely due to the wildfires occurring across Pine Creek Conservation Area, a primary management goal was met. Unfortunately, these fires also resulted in major declines in the already low cover of big sagebrush, which dropped from 2.2% cover to 1.3% cover across the samples. Other shrubs, including curl-leaf mountain mahogany, bitterbrush, snowberry and rose all increased in the samples. The change in broom snakeweed and green rabbitbrush may be a result of plant identification confusion, so it is probably best to merge these data points, and look at them together as weedy, small native shrubs. In this case, there was a small decline, from 2.5% cover to 1.5% cover in these disturbance related shrubs.

The cover of most of the forbs declined to some extent. This is likely primarily due to the fact that sampling occurred later in the season in 2011 than in 2002, because of access difficulties resulting from the extremely cool and wet spring in 2011. However, increasing bunchgrass cover and variation in seasonal rainfall may also be partly responsible for the observed changes.

Figure 1. Changes in Native Bunchgrass hits.

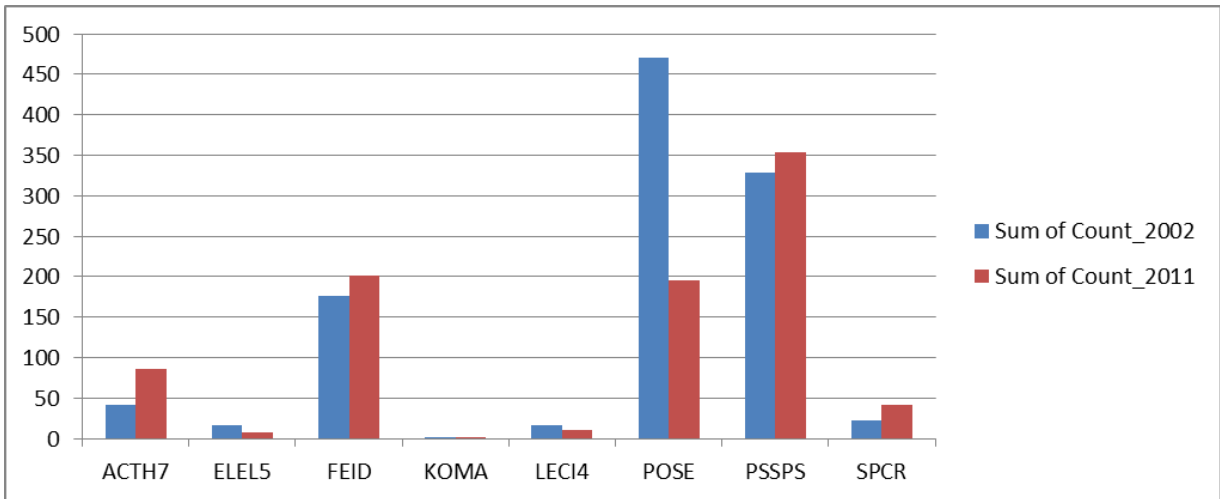


Figure 2. Changes in bunchgrass cover across all transects.

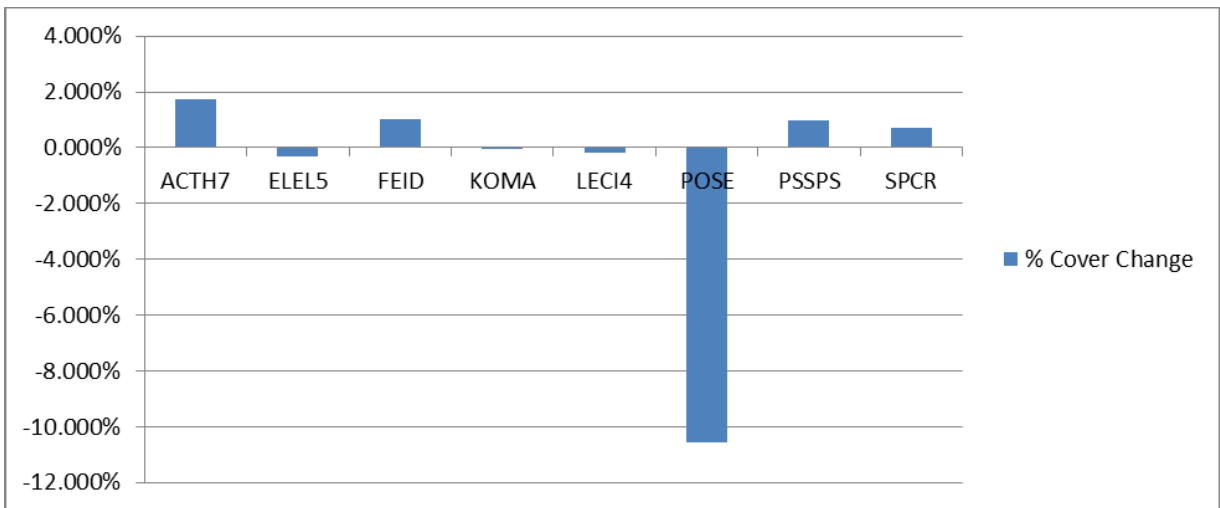


Figure 3. Relative change in individual bunchgrass species cover.

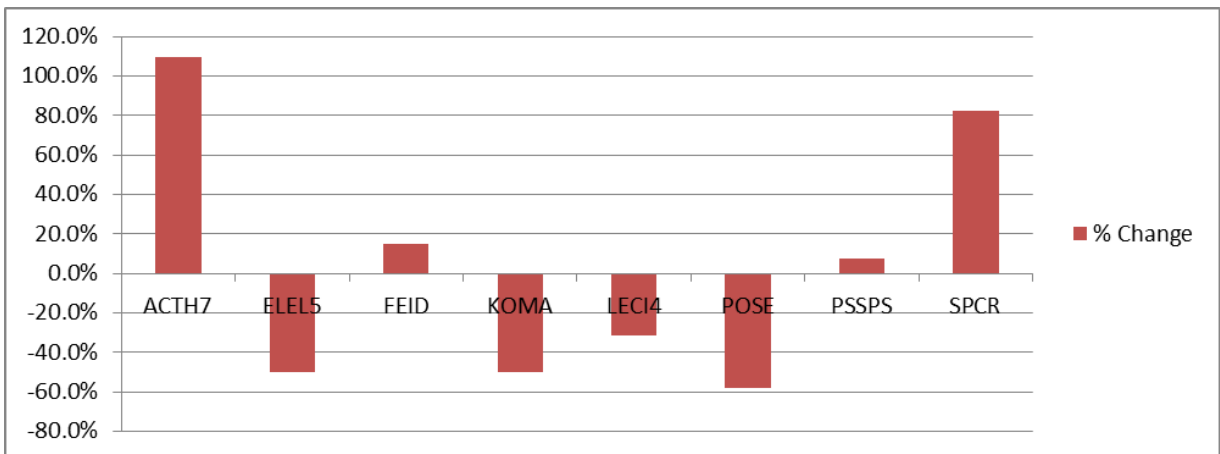


Figure 4. Changes in Exotic Species.

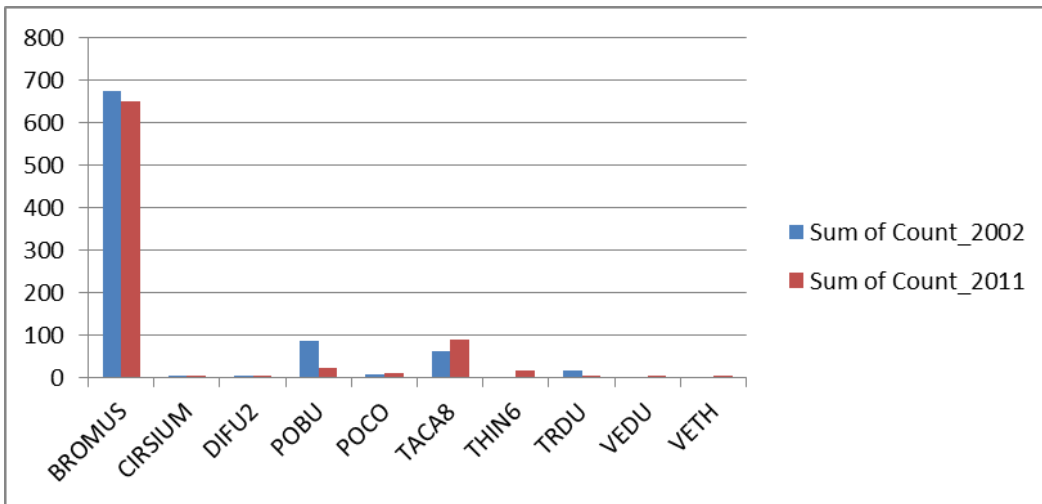


Figure 5. Changes in exotic species cover across all transects.

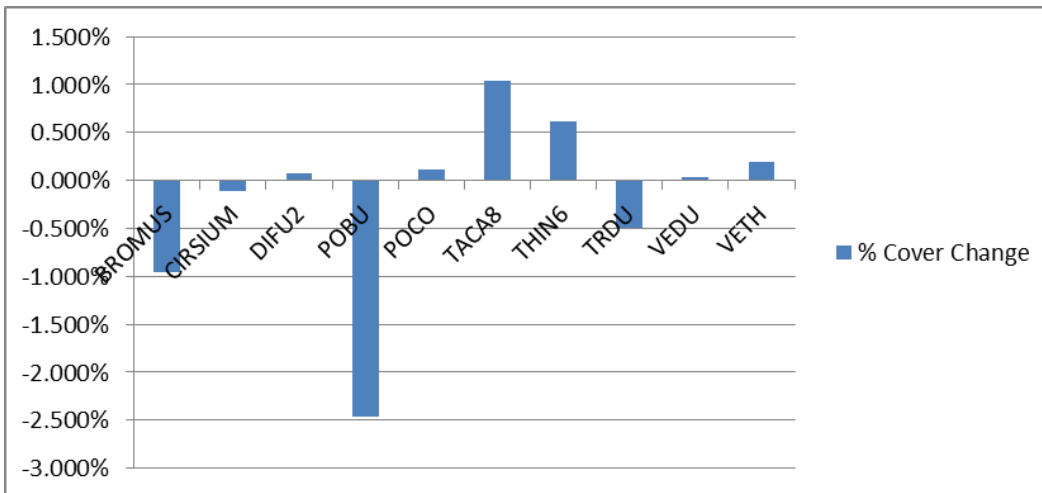


Figure 6. Relative change in individual exotic species cover.

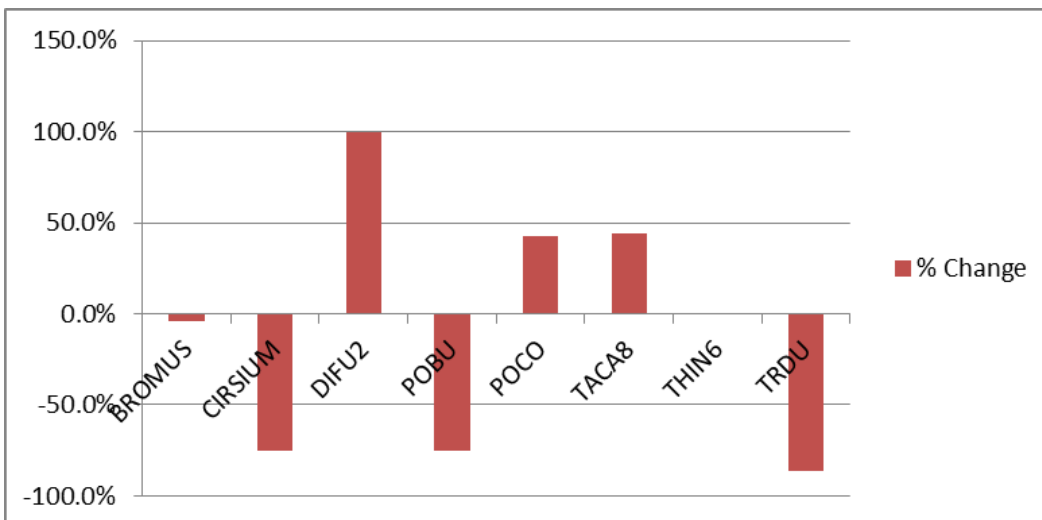


Figure 7. Changes in western juniper and shrub species.

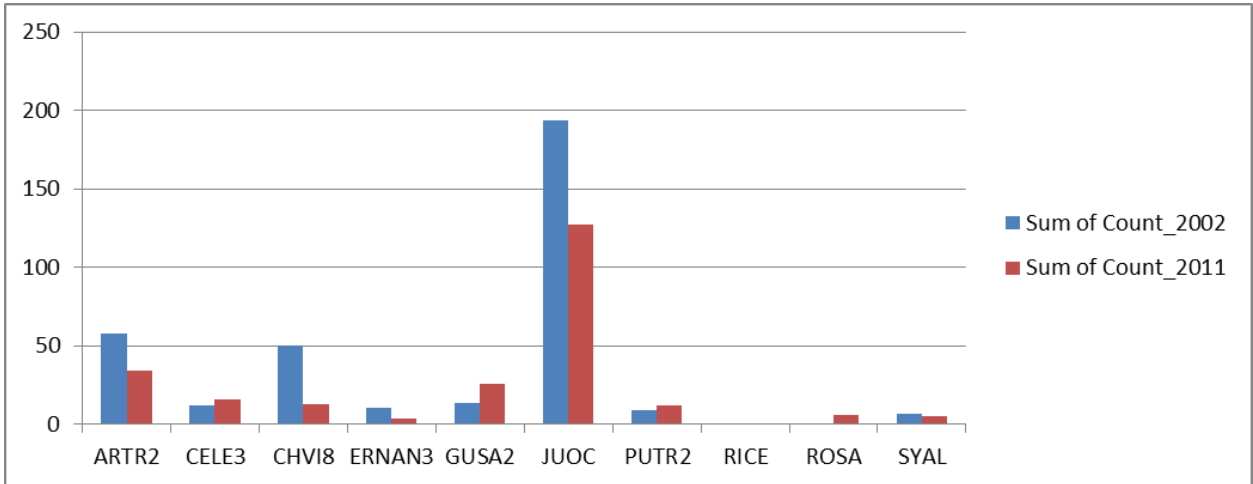


Figure 8. Changes in juniper and shrub species cover across all transects.

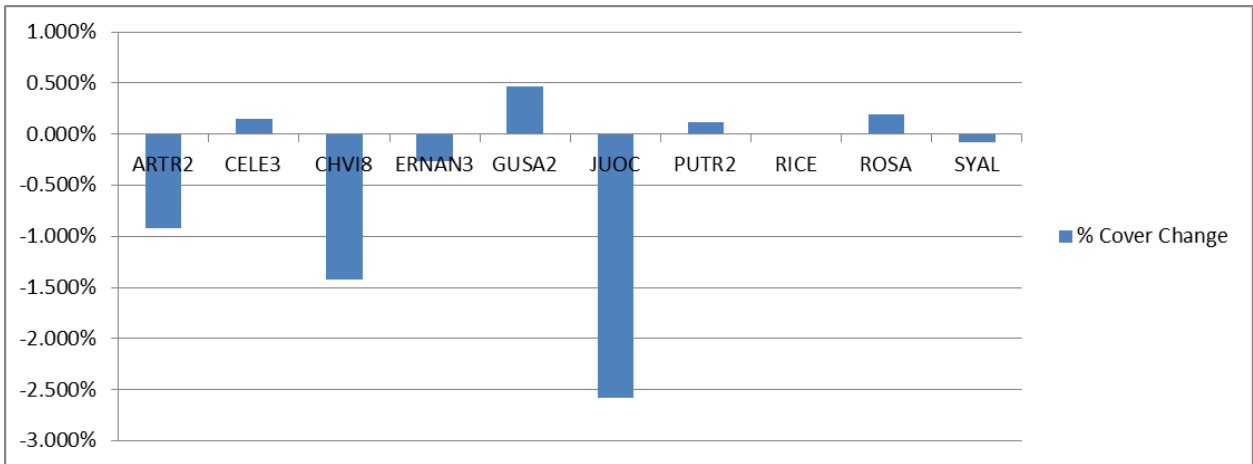


Figure 9. Relative change in juniper and individual shrub species cover.

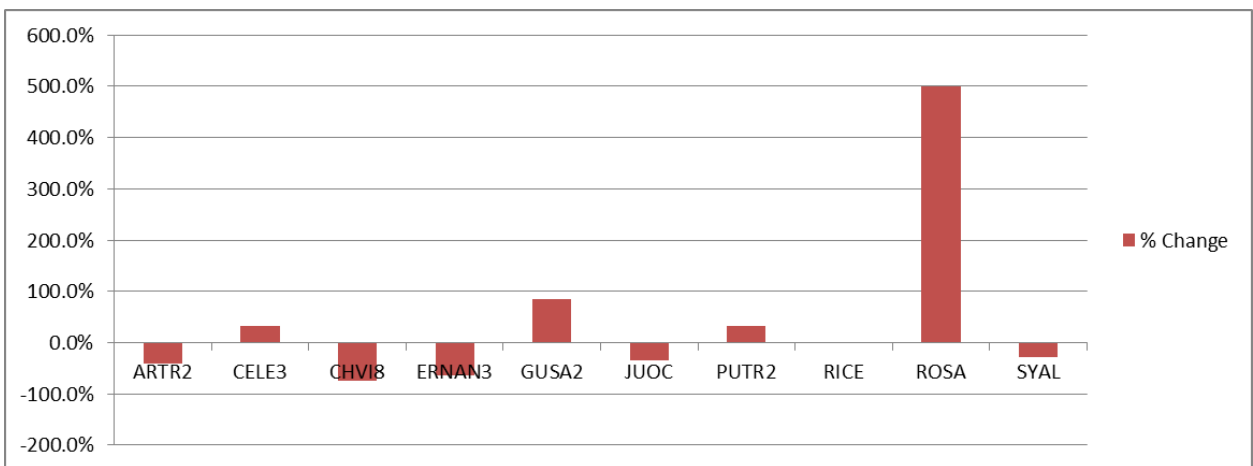


Figure 10. Changes in native perennial forb species.

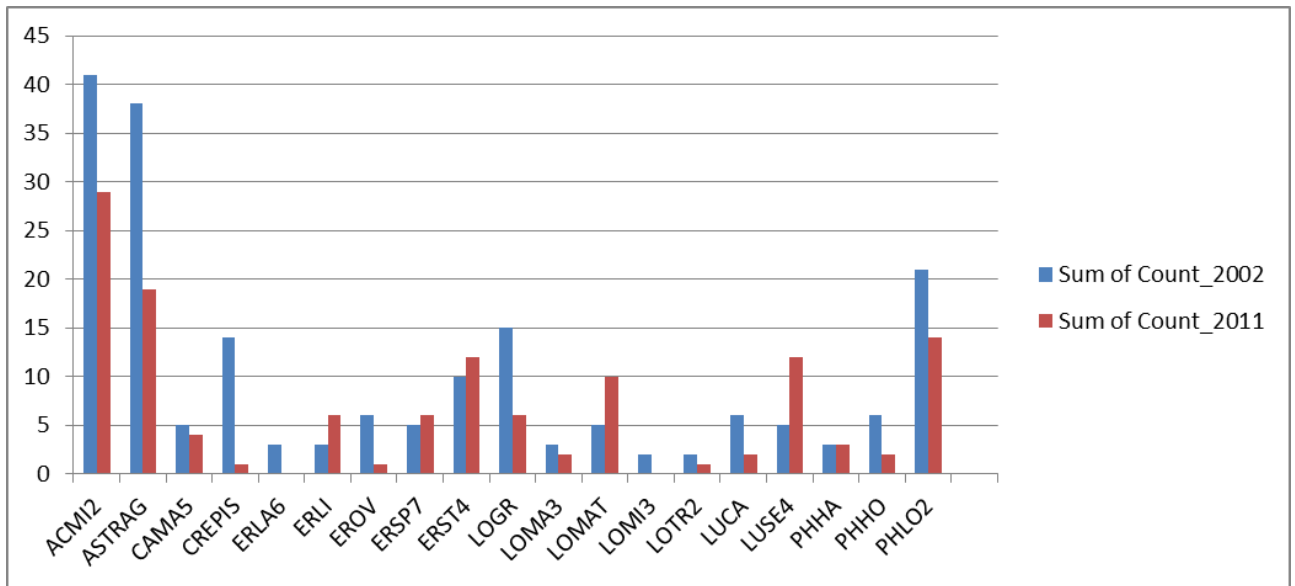


Figure 11. Changes in native perennial forb species cover across all transects.

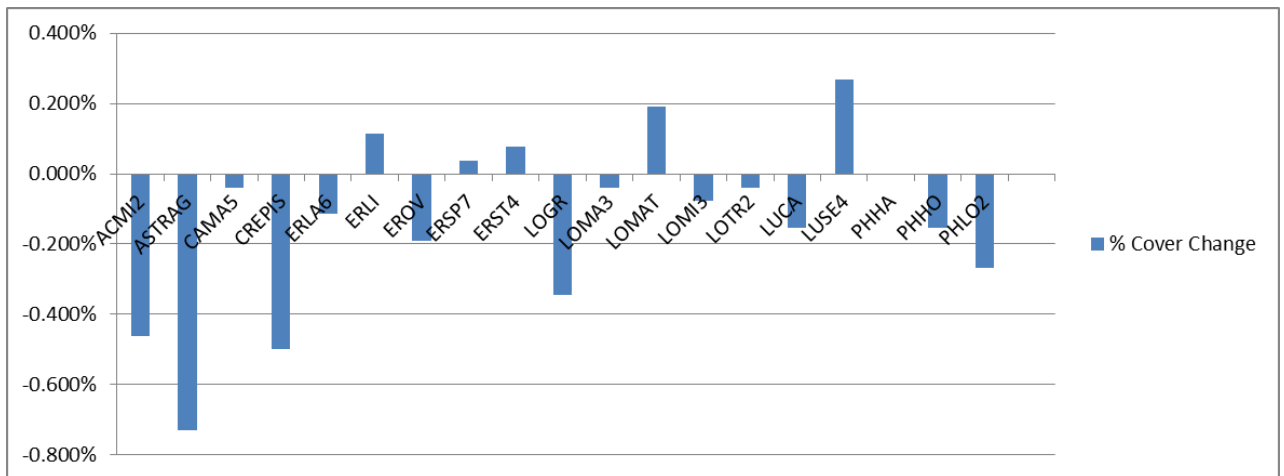
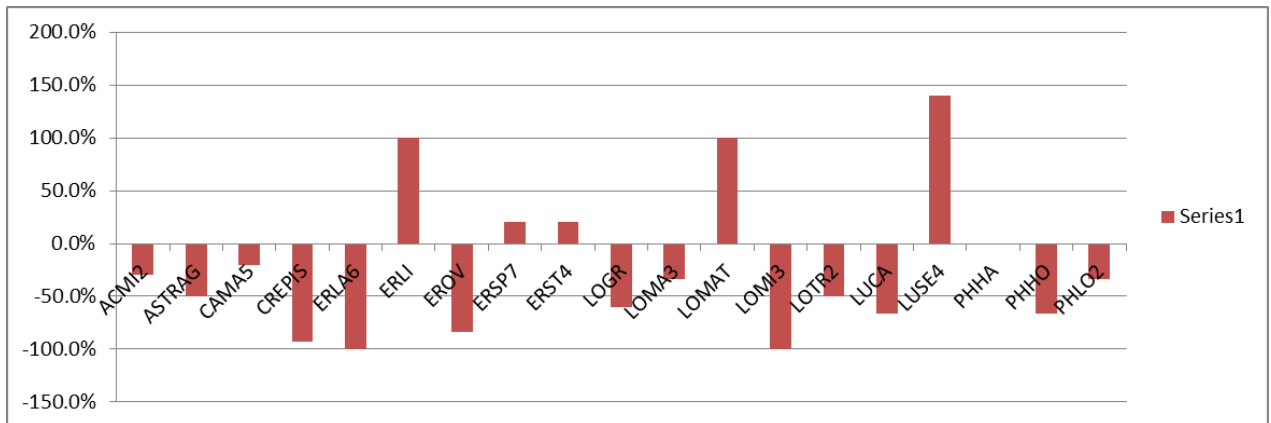


Figure 12. Relative change in native perennial forb species cover.



APPENDIX 1: PLOT CHANGE SUMMARIES

The changes in each of the plots sampled are described below. Plant names are represented by the 4 digit NRCS Plants Database Codes, found online at <http://plants.usda.gov/>. Only the dominant plants and important native species or introduced weeds are included in the summaries. The plot numbers are listed first. These numbers are from the tags used to mark the two transect ends, and are meaningless, apart from linking the plot summaries to the plot database and spreadsheets. The evaluation of the change as improved (+), declined (-) or the same (#) is included at the end of each plot.

Juniper / Shrub Plots

- 9-30: JUOC/CELE/POSE plot. CELE3 up from 24% to 32% cover. JUOC up from 6 to 8%. POSE down from 18% to 6%, but ACTH7 (2%) and PSSPS (4%) are new. BRTE down from 10 to 8% cover (the only weed). +
- 00-17: JUOC/PUTR2/POSE plot. PUTR2 gone (was 6%). JUOC up 2% to 4%. Bunchgrasses increased (POSE (24 to 28%), (PSSPS, FEID, ACTH7 together 18%). BRTE down from 6 to 2% cover. (Now a PSSPS-POSE plot). +
- 14-15: JUOC/PUTR2 plot. Minor changes only. Non-significant declines in Juniper. POSE up from 10 to 20%, PSSPS down from 30 to 12%. Increases in PUTR2 & ARTR2 (up 2%) & Native forbs. Small increase in BRTE (2% to 12%). #
- 93-94: JUOC/PUTR2/PSSPS-POSE plot. JUOC and PUTR2 the same (at 14 and 8%). PSSPS down 6% but ACTH7 up 8%. BRTE down from 36 to 32% cover. Minor changes. #
- 1-2: JUOC/ARTR2/PSSPS plot. JUOC (10%), ARTR2 (2%), and POSE (22%) gone. Increases in ACTH7 (2 to 10%) and PUTR2 (now at 2%) Declines in PSSPS (30 to 4%), BRTE (100% to 32%), but POBU (6%) and TACA8 (2%) new. +
- 16-21: JUOC/ARTR2/POBU plot. Increases in JUOC (2 to 8%), ARTR2 (8 to 12%), SPCR (2 to 6%), ACTH7 (0 to 6%) and PSSPS (0 to 2%). Large declines in POBU (68 to 20%) & CHVI8 gone (was 8%). First (2%) appearance of TACA8. BRTE from 6 to 26%. #
- 89-90: JUOC/ARTR2/POSE plot. Weedy plot. JUOC & ARTRW gone (from only 2%). TACA8 went from 60% cover to 18% cover, annual bromes from 29 to 44% cover, POBU vanished (10% to 0%) and ERCI6 (38% to 6%). Native perennial forbs about the same. ELEL5 gone (from 4%). #
- 95-96: JUOC/ARTR2/PSSPS-POSE plot. JUOC down from 6% to 2%. ARTR2 gone (was 34%). PSSPS down from 12% to 4%, FEID from 6 to 4%. Annual bromes from 12% to 62%, TACA8 new at 2%, but POBU gone (was 16%). -
- 5-6: JUOC/SYAL/PSSPS plot. JUOC gone (was 10%). PSSPS, FEID, POSE all with 6-8% declines, bunchgrass @ 22%. Rose + 2 to 8%, SYAL - 14 to 10%. BRTE down from 50 to 22%. +

Juniper / Bunchgrass Plots

- 41-42: JUOC/LECI4 plot. Increases in JUOC (12-16%), native bunchgrass (16-25%, with increased diversity, from 2 to 4 species), sagebrush (2-14%) and native forbs (+9%). +
- 37-38: JUOC/FEID-PSSPS plot. Declines (40%-20%) in JUOC, with increases (24 to 40%) of FEID. Small declines (~15% in PSSPS and POSE). BRTE stable at 2%. +
- 85-86: JUOC/FEID-PSSPS plot. JUOC down from 20% to 12% cover. FEID up from 34% to 56% cover. POSE down from 22 to 8% cover, Annual bromes down from 10 to 6% cover, other changes minor. +
- 3-4: JUOC/FEID-PSSPS plot. Burned, JUOC down from 56% to 8%, PSSPS from 36% to 2% & FEID from 44% to 2%. Significant increases in litter (from fire). 4% TACA8 (new) cover, BRTE increased from 4% to 34%. -
- 22-23: JUOC/PSSPS plot. Large increases in native bunchgrass cover and diversity (now FEID, ACTH7 present with more PSSPS, increases in native forbs. Hits of ARTRW & PUTR2 showing up. POBU (6%) gone. JUOC (22%) & Bromus (12%) stayed the same. +
- 51-52: JUOC/PSSPS plot. Almost no changes (none meaningful). #

- 61-62: JUOC/PSSPS plot. JUOC gone (was 24%). FEID up to 20% from 16%, PSSPS stays at 32%. BRTE new at 24%, ROWO new at 4%, native perennial forbs show small declines. +
- 59-60: JUOC/PSSPS plot. JUOC up 10 to 16%, POSE & PSSPS up 25% (to 18% cover), Forbs down a small amount. BRTE down from 16 to 6%. +
- 67-68: JUOC/PSSPS plot. JUOC down from 22% to 14%. TACA8 new at 8% and annual bromes from 16 to 50%. Bunchgrasses about the same. -
- 29-30: JUOC/POSE plot. JUOC increased by from 8% to 12% cover. VUMI went from 16 to 32%. POSE declined from 36 to 12%. Other native bunchgrasses about the same. Declines in native forbs. BRTE gone (was 2%). #
- 49-50: JUOC/POSE plot. JUOC (18 to 20%), CHVI8 (4 to 2%), POSE (28 to 14%); FEID (+6%) and PSSPS (+2%) new. Native forbs and introduced annual grasses +6%. #
- 65-66: JUOC/POSE plot. JUOC gone (was 14%). POSE & PSSPS down to 4% each. ACTH7 new at 8%. BRTE stable (30%). +
- 87-88: JUOC/POSE plot. JUOC down from 6 to 2% cover. POSE down from 10% to 8%, PSSPS up from 2% to 6%. TACA8 new at 2%, forbs about the same, BRTE up from 46% to 58% cover. #

Shrub-Dominated Plots

- 83-84: PUTR2/POSE plot. ARTRW down from 4% to 0%. PUTR2 up from 2% to 8%. ACHT7 new at 8%, POSE down from 20 to 14%, PSSPS down from 4 to 2%. Slight increases in native forbs, BRTE up from 40% to 50%. +
- 1-3: ARRI/POSE plot. ARRI and ARTRW gone. Increases in FEID (4, large decreases in POSE, Eriogonum species and PSSPS the same. (Changes here seem questionable and perhaps represent a plot not correctly relocated. A fire may have displaced one end of this transect). #
- 0-0. ARTR2/ACTH7 plot. ARTR2 gone (from 6%), but PUTR2 and SPCR both new at 4%, and ACTH7 up from 2% to 12%. BRTE down from 56% to 46%. +
- 91-92: ARTR2/LECI4 plot. Major changes, ARTR2 gone (was 36% cover). JUOC (at 2%) also gone. LECI4 down from 12% to 4%. POSE (10%), TACA8 (2%) and POBU (18%) gone. BRTE (down 58%). These replaced by THIN6 (at 20%). Other weeds include POPR (stable at 12%), DIFU2 up to 8% from 2%. (Sagebrush burned or cleared). Restoration needed. # (+ & -)
- 1-26: ARTR2/LECI4 plot. ARTR2 up (6 to 10%), LECI4 the same. Decreases in POBU (38 to 14%), BRTE (12 to 6%). +
- 31-32: ARTR2/POSE plot. Weedy, ARTR2 gone, was 2%, POSE down from 22 to 2%. Now dominated by annual forbs (28%). Intermediate wheatgrass (THIN8) new at 12%, noted near plot in 2001, now in the plot and medusahead (TACA8) up from 2 to 12%, BRTE stable at 10%. A restoration bottomland plot. (22% POSE to start with). -
- 6-7: ARTR2/FEID plot. ARTRW, forbs down, CHVI8 down from 4 to 2%. FEID from 60% cover to 48% cover, PSSPS new at 8%. Lots of juniper seedlings seen in 2002, none in 2011. *Poa bulbosa* @ 4% cover now gone, BRTE down from 4 to 2%. +
- 9-10: ARTR2/ACTH7-POSE plot. Changed to ARTR2/ACTH7-SPCR plot. ARTR2 up from 8 to 14%, ACTH7 up from 10 to 14%, SPCR (12%) and PSSPS (8%) new, POSE down from 16 to 10%. GUSA2 down from 4 to 2%, Bromus up from 42% to 70%, although *Erodium* gone (was 12%). +
- 3-18: CHVI8/POSE plot. Weedy; CHVI, bunchgrasses (FEID, POSE, & PSSPS at ~ 4%), and many perennial forbs gone. Annual bromes (58% to 36%) and TACA8 (36% to 22%) down, but it remains plenty weedy. -
- 3-4 Braille: CHVI8/PSSPS-POSE plot. CHVI8 & POSE gone. PSSPS and VUMI small declines. BRTE (6%) and TACA8 (22%) new invaders. Forbs about the same. -
- 4-19: GUSA2/VUMI plot. GUSA2 increased by 10%, increases in annual introduced grasses (Bromus, TACA, VEDU totaling 24%), and native forbs (6% increase) and some PSSP6 showing up. #

Grassland Plots

- 11-12: SPCR plot. Increases in SPCR (34 -52%) cover, decreases in POSE (22% to 2%) and ACTH7 (4% to 0). Some forb declines. One (new) TACA8 hit, but BRTE way down (50 to 16%). +
- 39-40: SPCR plot. Increases (6-24%) in ACTH7, minor forb changes, CHVI8 drops from 10- 4%. BRTE still high (42%, down from 44%). +
- 00-00 ACTH7-PSSPS plot. large increase in VUMI (meaningless), very minor changes (ACTH7 same, PSSP 25%, POSE tiny decline), BRTE down from 20% to 14%. #
- 63-64: ACTH7-PSSPS plot. ACTH7 up from 14 to 22%. PSSPS up from 4 to 16%. POSE down from 26 to 8%. Lupinus up from 2 to 22%. BRTE increased from 36 to 42%. +
- 69-70: ACTH7-PSSPS plot. ACTH7 up 8% to 24% cover, PSSPS up 18% to 22% cover. POSE down 20% to 10%. BRTE up from 24 to 34%. Forbs about the same. +
- 27-28: ACTH7-PSSPS plot. JUOC invading the plot, now 12% cover, leading to small declines in forbs and native bunchgrasses. Now a JUOC/ACTH7-PSSPS-POSE plot. BRTE down from 40% to 16%. # (+ & -)
- 43-44: FEID plot. Initial low cover (2%) of JUOC & ERNAN3 now gone. FEID totally dominant (54% to 82%). POSE from 30 to 16%, PSSPS from 6 to 4%. +
- 53-54: FEID-PSSPS plot. FEID up from 36% to 54%, POSE & PSSP down (36% to 10% & 36 to 12%). Forbs the same. BRTE down from 16 to 8%. +
- 30-33: PSSPS-FEID plot. FEID increased from 4 to 14%, while PSSPS and POSE declined slightly. JUOC and CHVI8 both disappeared. Forbs about the same, few weeds. +
- 12-3: FEID plot. Plot turned into a PSSPS-FEID plot...Significant increases in FEID (4 to 24%), PSSPS (2 to 50%), declines in forbs. BRTE from 2 to 14%, the only weed. +
- 1-2 Braille: PSSPS-POSE plot. declines in POSE, ELEL5 and CHVI8 (which was common and mostly vanished), PSSPS the same, Small (52 to 58%) increases in annual Bromes, plus TACA8 up from 6 to 18%. One new JUOC hit (none before). -
- 3-10: PSSPS-POSE plot. Declines in PSSPS (44 to 28%), POSE (26-8%). BRTE from 22 to 48%. Minor increase (2 to 4%) in ACTH7, 2% new TACA8, forbs the same. -
- 45-46: PSSPS-POSE plot. 8% increases in PSSPS & FEID cover, 18% declines in POSE. BRTE up from 12 to 20%. Other changes insignificant. +
- 47-48: PSSPS-POSE plot. 16% declines in POSE, 4% in PSSPS, no other real changes (2% JUOC, no change). #
- 71-72: PSSPS-POSE plot. PSSPS up from 38 to 50%. POSE down from 22 to 12%. Bromus up from 20 to 28%. Forbs the same. +
- 73-74: PSSPS-POSE plot. JUOC up from 2% to 12% cover, so this has become a JUOC/POSE woodland from its grassland state. PSSPS up from 28 to 36%, POSE down from 30 to 22%. Other bunchgrasses (FEID, ACTH7) up slightly 2% to 10%. BRTE up from 14 to 24%, forbs the same. # (+ & -)
- 77-78: PSSPS-POSE plot. PSSPS up from 32% to 62% cover. POSE down from 30% to 3%. TACA8 new at 8%, Bromus up from 24 to 42%, apparently annuals replacing POSE but not bluebunch. Forbs about the same. +
- 81-82: PSSPS-POSE plot. Turned into a PSSPS plot. POSE down from 68% to 20%, PSSPS new at 52%. Forbs the same. TACA8 up from 2 to 46%, BRTE up from 6 to 14%. +
- 55-56: PSSPS-Eriogonum plot. PSSPS up from 20 to 28%, Eriogonum up 4%, POSE up 2%. BRTE stable at 22%. +

APPENDIX 2: NRCS PLANTS CODES AND NAMES

Exotic Species

CODE	Scientific Name	Common Name	Species Group
BROMU	Bromus sp.	cheatgrass and annual bromes	exotic annual grass
CIRSI	Cirsium sp.	thistle	exotic perennial forb
DIFU2	Dipsacus fullonum	teasel	exotic perennial forb
POBU	Poa bulbosa	bulbose bluegrass	exotic perennial forb
POCO	Poa compressa	Kentucky/Canada bluegrass	exotic perennial grass
TACA8	Taeniatherum caput-medusae	medusahead	exotic annual grass
THIN6	Thynopyrum intermedium	intermediate wheatgrass	exotic perennial forb
TRDU	Tragopogon dubius	salsify	exotic perennial forb
VEDU	Ventenata dubia	ventenata	exotic annual grass
VETH	Verbascum thapsis	mullen	exotic perennial forb

Native Forbs

CODE	Scientific Name	Common Name	Species Group
ACMI2	Achillea millefolium	yarrow	native perennial forb
ASTRA	Astragalus sp.	milkvetch species	native perennial forb
CAMA5	Calochortus macrocarpus	sagebrush mariposa lily	native perennial forb
CREPI	Crepis sp.	hawksbeard	native perennial forb
ERLI	Erigeron linearis	desert yellow fleabane	native perennial forb
EROV	Eriogonum ovalifolium	cushion buckwheat	native perennial forb
ERSP7	Eriogonum sphaerocephalum	rock buckwheat	native perennial forb
ERST4	Eriogonum strictum	Blue Mountain buckwheat	native perennial forb
LOGR	Lomatium grayi	Gray's desert parsley	native perennial forb
LOMA3	Lomatium macrocarpum	bigseed biscuitroot	native perennial forb
LOMAT	Lomatium sp.	desert parsley species	native perennial forb
LOMI3	Lomatium minus	John Day Valley buckwheat	native perennial forb
LOTR2	Lomatium triternatum	nineleaf biscuitroot	native perennial forb
LUCA	Lupinus caudatus	tailcup lupine	native perennial forb
LUSE4	Lupinus sericeus	silky lupine	native perennial forb
PHHA	Phacelia hastata	silverleaf phacelia	native perennial forb
PHHO	Phlox hoodii	spiny phlox	native perennial forb
PHLO2	Phlox longifolia	longleaf phlox	native perennial forb

Native Perennial Bunchgrasses

CODE	Scientific Name	Common Name	Species Group
ACTH7	Achnatherum thurberianum	Thurber's needlegrass	native bunchgrass
ELEL5	Elymus elymoides	squirreltail	native bunchgrass
FEID	Festuca idahoensis	Idaho fescue	native bunchgrass
HECO26	Hesperostipa comata	needle-and-thread	native bunchgrass
KOMA	Koeleria macrantha	Junegrass	native bunchgrass
LECI4	Leymus cinereus	Basin wildrye	native bunchgrass
POSE	Poa secunda	Sandberg bluegrass	native bunchgrass
PSSPS	Pseudoroegneria spicata ssp. spicata	bluebunch wheatgrass	native bunchgrass
SPCR	Sporobolus cryptandrus	sand dropseed	native bunchgrass

Woody Vegetation

CODE	Scientific Name	Common Name	Species Group
ARRI2	<i>Artemisia rigida</i>	rigid sagebrush	native shrub
ARTR	<i>Artemisia tridentata</i>	big sagebrush	native shrub
ARTRT	<i>Artemisia tridentata</i> var. <i>tridentata</i>	Basin big sagebrush	native shrub
ARTRW8	<i>Artemisia tridentata</i> var. <i>wyomingensis</i>	Wyoming big sagebrush	native shrub
CHVI8	<i>Chrysothamnus viscidiflorus</i>	green or yellow rabbitbrush	native shrub
ERNAN3	<i>Ericameria nauseosa</i> ssp. <i>nauseosa</i>	grey rabbitbrush	native shrub
GUSA2	<i>Gutierrezia sarothrae</i>	broom snakeweed	native shrub
JUOC	<i>Juniperus occidentalis</i>	western juniper	native tree
ROSA	<i>Rosa</i> sp.	Rose	native shrub

ATTACHMENT 5

MAPPING AND MODELING PLANTS OF TRIBAL INTEREST



Matt Noone and Jimmy Kagan

Institute for Natural Resources, Portland State University

1. INTRODUCTION

One of the initial goals in the 2011-2012 Pine Creek Conservation Area (PCCA) assessment was to assist in identifying sensitive and important natural resources to engage tribal stakeholders and to assure support for site conservation. In particular, there is a strong interest by many tribal members in gathering native plants for food and fiber. The locations of these plants on the tribal lands around Warm Springs are well known, often closely held family knowledge. However, as PCCA was recently acquired for wildlife mitigation, the potential locations of these species is not well known.

Recent work has demonstrated the capacity of Random Forests modeling techniques to predict the distribution of rare plant species with a relatively small set of training points. Work in the Oregon Coast Range by the Oregon Natural Heritage Program, in northwestern California on serpentine habitats by the U.S. Forest Service, and in western New York by The Nature Conservancy have created very high resolution maps for very rare species with only a few positive locations. These maps were used in Oregon to help find new sites of recently described species, to great effect. Providing this data, in a secure fashion, could help tribal members find important cultural plants, and increase tribal interest in maintaining their populations and habitats.

Random Forests models require relatively few plots, but all models do better with more training plots. While successful maps have been created in Oregon with only 3-4 known positive sites, it is unlikely that reliable maps could be modeled with fewer. If important cultural species were only known from one or two sites, it might be possible to manually create the maps. Since much of the work in the other tasks involved widespread sampling of the vegetation on PCCA, the INR team anticipated that during these inventories, sufficient locations for many of the more significant cultural plant species would be located, and modeling their distributions could easily follow.

The results of this part of the project were less interesting than we anticipated, largely because it appears that the cultural species of greatest interest are not very abundant nor widely distributed on the PCCA. However, maps and models were generated for some species, and data has been compiled allowing additional maps to be fairly easily generated if sufficient new locations are discovered in the future.

2. METHODS

2.1. Identifying Cultural Species

An initial list of cultural species of interest was compiled from a comprehensive list of plants known or suspected from the Pine Creek Conservation Area by Briggette M. Whipple, then the Culture & Heritage Committee Chairperson and Tribal Anthropologist/Ethnographer for the Confederated Tribes of Warm Springs, along with Rick Hayes of PCCA. Species which do not occur on the PCCA were removed from the list, and those species of greatest interest were chosen to pursue for modeling. The total list, with those species identified by Whipple and Hayes is included as Appendix 1.

The list included 11 species of shrubs and small trees that produce berries, five of which are gooseberry (*Ribes*) species, and all of which occur primarily in riparian or streamside habitats. The list also included many of the other riparian trees and shrubs that occur at PCCA, including 6 species of willow (*Salix*), white alder (*Alnus rhombifolia*) red-osier dogwood (*Cornus stolonifera*) and aspen (*Populus tremuloides*). It also included the two main species of upland trees, western juniper and Ponderosa pine.

There were only four upland shrubs on the list, including purple sage (*Salvia dorrii*), curl-leaf mountain mahogany (*Cercocarpus ledifolius*) and big sagebrush (*Artemisia tridentata*). It also included 7 species of native graminoids (grasses, sedges, rushes and cattail), and 15 species of native forbs, 5 of which have edible roots.

2.2. Modeling and Mapping Methodology

Inductive species modeling tools such as DOMAIN, Maximum Entropy (MAXENT), and Random Forests (RF) have become widely used to predict suitable habitat and depict the probability of finding animal and plant species within their known distributions (Buechling and Tobalske 2011, Williams *et al.* 2009). These models also provide rich information about species-habitat relationships and habitat suitability. A wide range of models have been produced at various geographic scales (Franklin 2009).

However, not all modeling methods are suitable for all species. Models based only on presence data and environmental factors (which include all MAXENT and DOMAIN models) can produce output that over-predicts suitable habitat (Stohlgren *et al.* 2011), especially when predictions are extrapolated beyond the range of known occurrences. Models relying on absence data that are not properly applied may yield poor results. Absence does not always correlate with poor habitat potential (Royle *et al.* 2012). Other models may be limited by the resolution and accuracy of input layers. Species dependent on fine-scale habitat such as cliffs cannot be well-predicted using coarse-scale imagery such as Landsat satellite data.

We used Random Forests (Breiman 2001, Liaw and Wiener 2002), a machine learning technique that extends classification trees by leveraging the predictive power of multiple trees. It requires two types of input data: points of species presence and absence, and rasters describing environmental factors that constrain the species' distribution. The species presence locations were acquired during the two-year project inventory and sampling, and many fewer locations were identified than anticipated. Expected absence points were identified using sampled vegetation and plot data where suitable habitat and no plants were found, along with expert manual attribution for point in habitat that was clearly unsuitable.

For each species, we modeled the relationship between presence/absence points and environmental predictors. The technique yields a prediction that is analogous (but not identical) to a probability of habitat suitability. We built a prediction for each pixel in our map, and simplified the raster surface into categories relating to model certainty using the precision-recall F-measure (Sing *et al.* 2005). To integrate maps when multiple target species were found (such as cous biscuitroot and bitterroot, which often occur together), we simplified the single-species maps to presence-absence (0 or 1), and then summed them, highlighting areas likely to contain both endangered species.

2.2.1. Data Acquisition

2.2.1.1. Species Location Training Data

In the proposal, we anticipated collecting opportunistic positive training locations while doing fieldwork for other products. We took advantage of vegetation plots for use as negative training locations, although this could only be done when reasonable habitat affinities could be developed, which was one of the critical attributes we used to select species for modeling. Positive occurrences came from the resampled transect data, and when available from the 2011 vegetation analysis data. It was determined that sufficient training data was collected to model only two cultural species; *Lewisia rediviva* (bitterroot) and *Lomatium cous* (cous biscuitroot). In total 14 observations of *L. rediviva* and 10 of *L. cous* were observed in the field. In all but 4 observations both were observed occurring together. With the similarity in habitats affinity the potential distribution for the two species were modeled together. An additional 44 positive habitat training points were generated in areas identified through expert knowledge from an ecologist familiar with PCCA. 174 negative habitat training points were then generated in areas where the cultural species were known not to exist. The negative training points include areas such as water, agriculture, juniper woodlands, grasslands, and riparian areas.

2.2.1.2. Other Spatial Predictor Data

Any type of inductive or deductive species models require relatively comprehensive spatial data which to drive the model outputs. In the proposal, we anticipated that in addition to the detailed spatial data acquired for the vegetation analysis, it may be helpful to limit prediction of some targets by the mapped class from products 1 and 2. Attachment 1, which describes the creation of the vegetation map for the Pine Creek Conservation Area, contains a summary of all of the spatial data collected and used in the project. All available data described in the attachment was used to develop the species models, along with the products developed from the data. Data layers utilized were either provided by the CTWS or downloaded from <http://oregonexplorer.info>.

Predictor variables used in the modeling process were almost identical to those used in the Base Mapping section. Multiple vegetation indices were created from SPOT-5 satellite sensor imagery. Various high resolution texture metrics were calculated from 2012 NAIP aerial photos. The LiDAR flown over PCCA in 2011 provided the most accurate elevation information available for the area. All base mapping predictor variables were used except LiDAR heights because of missing data associated with steep cliffs.

All maps and data layers produced are in the common projection of NAD 83, UTM Zone 11N in ESRI grid raster format. ArcGIS was used for processing imagery and data layers and creating maps. The statistical software package R (R Development Core Team 2012) was used to run Random Forests, creating the potential distribution maps for the two cultural species. The two cultural species potential habitat maps were created for the PCCA and adjacent BLM and NPS lands.

2.3. Accuracy Assessment

Due to the irregular occurrence of the cultural plants, and the remoteness of the ranch, it was not possible to conduct a field accuracy assessment on the cultural distribution map. However, the randomForest model is able to conduct an ‘out of bag’ (OOB) estimate of the model accuracy by withholding a random subset of the training data through each tree classification, the withheld training points are then used to evaluate the modeled output accuracy for each iteration of trees grown. RandomForest also provides output showing the relative importance of input variables in determining the final prediction. The most important variables in deciding how the final prediction were geographic predictor variables developed from the LiDAR such as elevation, solar radiation, profile curvature, topographic position, and distance to intermittent and permanent streams. Spectral information had less influence on geographical characteristics. This lesser importance of the spectral bands in the modeled output is due to the weak phenological correlation between the cultural plants being modeled and the existing landscape. The modeled output results should be thought of as a potential vegetation distribution for the cultural plants rather than existing vegetation.

The overall map accuracy of 99% indicates high correlation between geographical variables and areas of training data where the species were observed (Table 1).

Table 1. Error matrix produced by model using out of bag estimation to evaluate map accuracy.

Model Accuracy		
	Absence	Presence
Absence	155	1
Presence	1	59

Overall Map Accuracy: 99%

3. MAPPING RESULTS

The majority of areas *L. cous* and *L. rediviva* were mapped tended to be higher elevation scablands in the northern portion of PCCA (Figures 1 and 2). The sites were characterized by exposed soils, moss and crust with clumps of scattered vegetation. Overall these sites were characterized with a light fuel load. Potential habitat seldom occurred in the dense juniper woodlands, although some scattered old growth juniper could occasionally be found in these areas.

Only three species models were completed, and only two of these using the inductive species methodology. As mentioned in the results section, in our proposal, we anticipated collecting opportunistic positive training locations while doing fieldwork for the various vegetation analysis. However, for the species of greatest interest, few occurrences were located, and some were not suitable for modeling. For example, wild celery (*Lomatium nudicaule*) was of great interest, but all the locations were along roads or in areas that couldn't be applied across the PCCA, and thus were not suitable for modeling. Only the edible plants, cous biscuitroot and bitterroot were modeled, although we were not able to find as many positive locations as we would have liked.

Many of the plants of interest were riparian shrubs and small trees, mostly willow shrubs or fruit and berry bearing shrubs and small trees. A number of the forbs and graminoids also represented occur exclusively in wetland and riparian habitats. At PCCA, all of the wetlands are associated with riparian habitats, and all are very limited. While modeling distribution of these species is possible, the results are not likely to be very accurate, since the riparian areas at PCCA are the most rapidly changing areas within the conservation area. Active restoration and planting, often of many of the target species, is occurring in Robinson Canyon, along Pine Creek, and natural recovery is occurring as the water table is appearing to rise throughout the site. While modeling is quite possible, the team decided that this should be postponed for three to five years, until more riparian areas have recovered, and the distribution of these species has stabilized.

Big sagebrush was listed as a cultural species, but is both so widely distributed and so driven by the pattern of historic fires and western juniper cover that making predictive map did not seem useful. In addition, the change in sagebrush cover was analyzed using the air photography for one of the change analysis, so areas with current sagebrush patches at the site are included in the final products.

Three upland shrub species, purple sage, bitterbrush and mountain mahogany, can be modeled. Bitterbrush is widely distributed across PCCA, and has been increasing in cover. The vegetation map shows the distribution sufficiently to identify locations for tribal members to identify collection locations.

There were 4 species of upland grasses on the list: Thurber's needlegrass (*Achnatherum thurberiana*), indian ricegrass (*Achnatherum hymenoides*), great basin wildrye (*Leymus cinereus*), and blue wildrye (*Elymus glaucus*). Of these, Thurber's needlegrass is very common in the PCCA, occurring as one of the dominant grasses in 7 of the 65 permanent plots, and in 15 of the 164 vegetation mapping plots, or about 10% of the sampled areas. In the plot change analysis, this species was increasing at PCCA, and it occurs widely enough through the site that a model does not appear necessary. Blue wildrye is limited to the very highest elevations and most mesic sites, general in and around the Ponderosa pine forests, and as a result, there is not sufficient data to model it. Indian ricegrass naturally occurs in dunes or unconsolidated ash, where soils are not stable. It was sampled at a number of sites in the initial 2002 inventory, but was not observed at all in the 2011 and 2012 resampling.

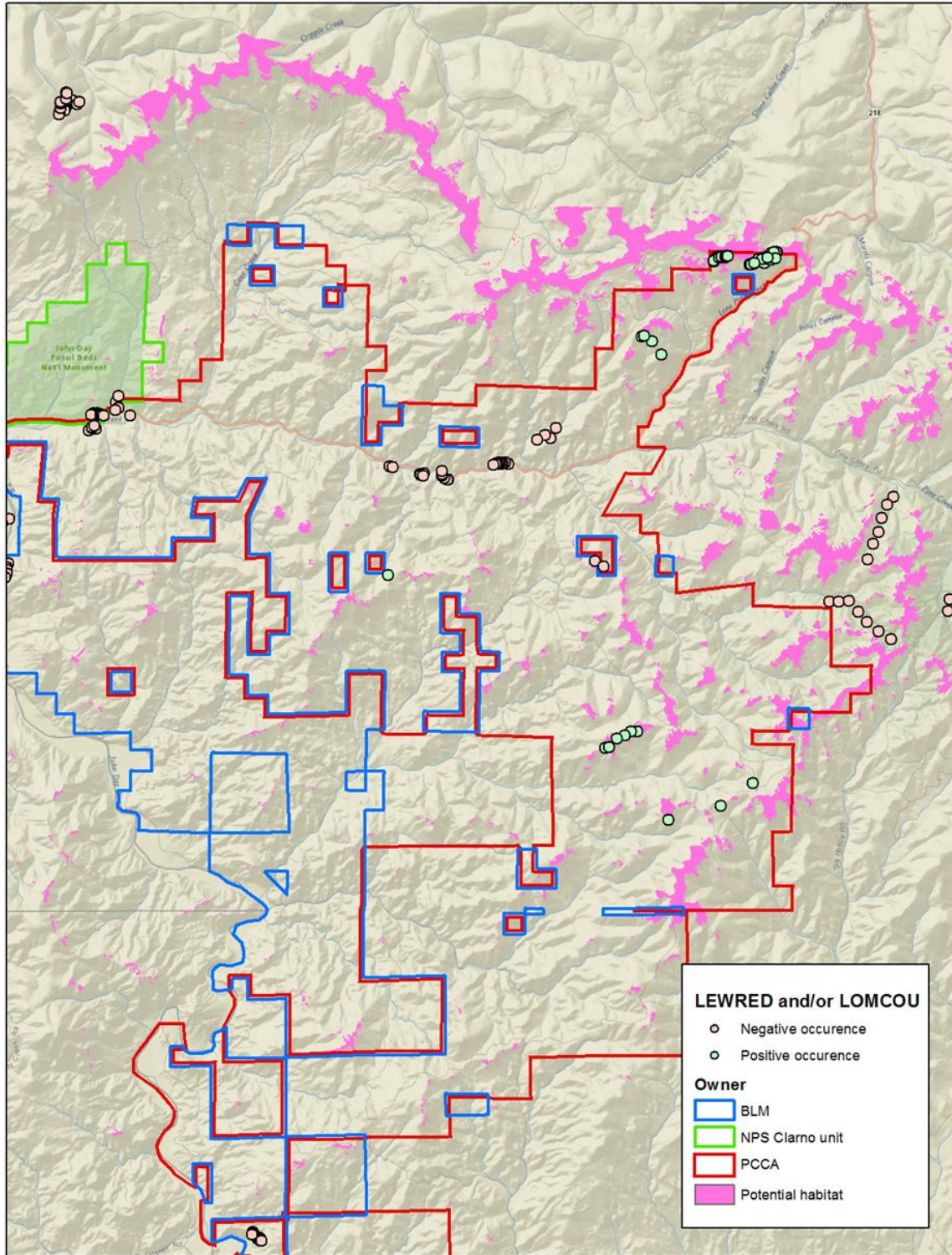


Figure 1. Modeled potential habitat of *L. rediviva* and *L. cous* (pink). Landownership boundaries are also displayed, green dots represent positive occurrences of cultural plants while yellow dots represent negative occurrences.

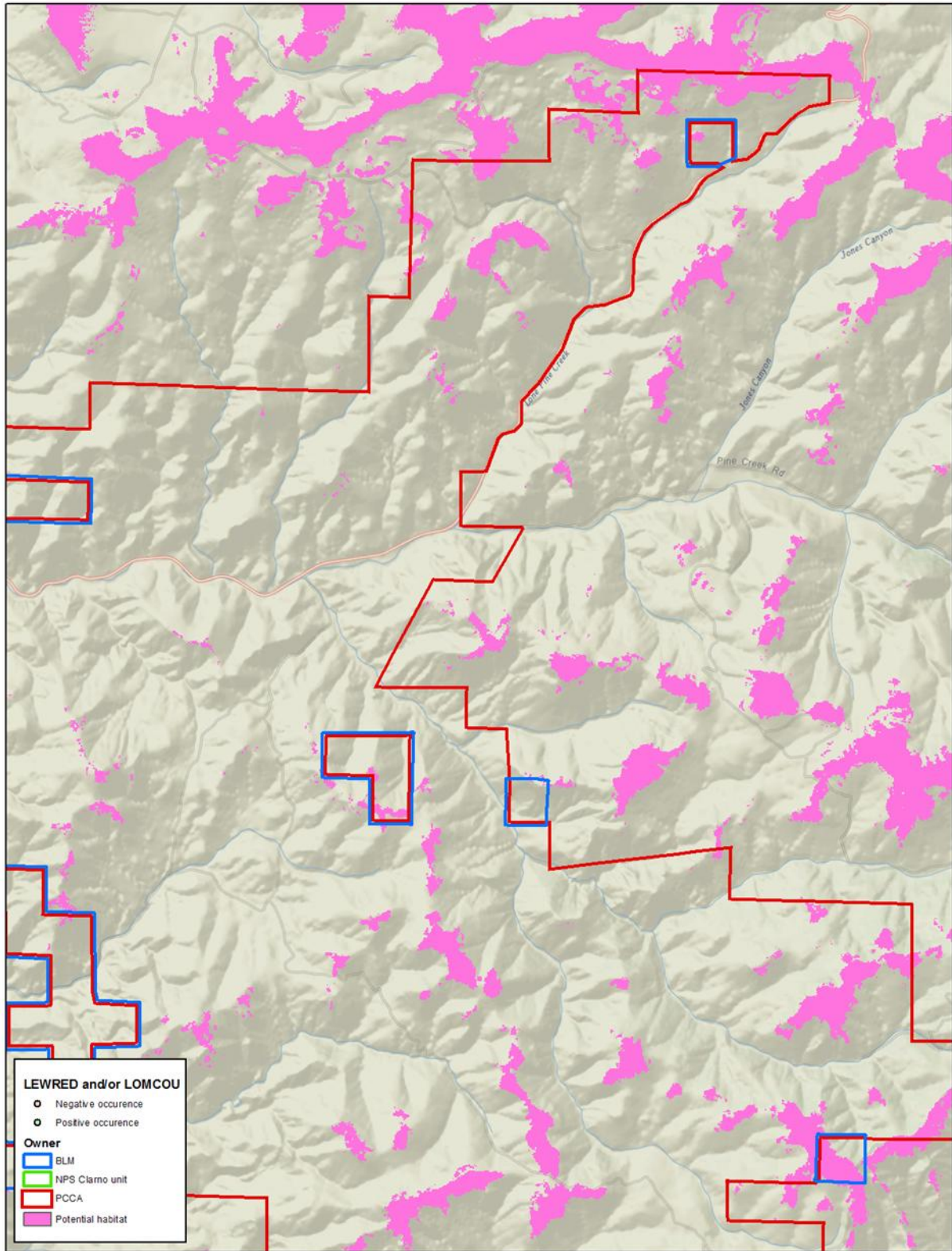


Figure 2. Close up of NE edge of the Pine Creek Conservation Area, the majority of predicted potential habitat for bitterroot and cous biscuitroot occur here.

APPENDIX A. CULTURAL PLANTS AT PINE CREEK CONSERVATION AREA

The following are the plants known or expected from PCCA and Warm Springs. Those highlighted in blue were selected by the Warm Springs Cultural /Heritage Chairperson, Brigitte Whipple, as being of cultural interest.

Family	Genus	Species	Common Name	Nat / Int	Ann/ Per	Form	Observed	Expected
Native Trees, Shrubs, and Vines								
1	Betulaceae	Alnus	incana	mountain alder	N	P	T	1
2	Betulaceae	Alnus	rhubifolia	white alder	N	P	T	1
3	Betulaceae	Betula	occidentalis	water birch	N	P	T	1
4	Cupressaceae	Juniperus	occidentalis	western juniper	N	P	T	1
5	Pinaceae	Pinus	ponderosa	ponderosa pine	N	P	T	1
6	Pinaceae	Pseudotsuga	menziesii	Douglas fir	N	P	T	1
7	Rosaceae	Prunus	emarginata	bittercherry	N	P	T	1
8	Rosaceae	Prunus	virginiana	chokecherry	N	P	T	1
9	Salicaceae	Populus	tremuloides	aspen	N	P	T	1
10	Salicaceae	Populus	balsamifera ssp. trichocarpa	black cottonwood	N	P	T	1
11	Ulmaceae	Celtis	reticulata	hackberry	N	P	T	1
12	Anacardiaceae	Toxicodendron	rydbergii	poison-ivy	N	P	S	1
13	Berberidaceae	Mahonia	repens	creeping Oregon grape	N	P	S	1
14	Caprifoliaceae	Sambucus	nigra ssp. cerulea	blue elderberry	N	P	S	1
15	Caprifoliaceae	Symphoricarpus	albus	snowberry	N	P	S	1
16	Chenopodiaceae	Atriplex	canescens	saltbush	N	P	S	1
17	Chenopodiaceae	Atriplex	confertifolia	shadscale	N	P	S	1
19	Chenopodiaceae	Grayia	spinosa	spiny hopsage	N	P	S	1
20	Chenopodiaceae	Sarcobatus	vermiculatus	black greasewood	N	P	S	1
21	Asteraceae	Artemisia	arbuscula	low sagebrush	N	P	S	1
22	Asteraceae	Artemisia	rigida	stiff sagebrush	N	P	S	1
23	Asteraceae	Artemisia	tridentata	big sagebrush	N	P	S	1
24	Asteraceae	Chrysothamnus	viscidiflorus	green rabbitbrush	N	P	S	1
25	Asteraceae	Ericameria	nauseosa	gray rabbitbrush	N	P	S	1
26	Asteraceae	Gutierrezia	sarothrae	matchbrush	N	P	S	1
27	Asteraceae	Haplopappus	macronema	discoid goldenwweed	N	P	S	1
28	Asteraceae	Haplopappus	resinosus	gnarled goldenweed	N	P	S	1
29	Asteraceae	Tetradymia	canescens	spineless horsebrush	N	P	S	1
30	Cornaceae	Cornus	sericea ssp. sericea	creek dogwood	N	P	S	1
32	Ericaceae	Vaccinium	membranaceum	thin-leaved huckleberry	N	P	S	1
34	Grossulariaceae	Ribes	aureum	golden currant	N	P	S	1
35	Grossulariaceae	Ribes	cereum	wax currant	N	P	S	1
36	Grossulariaceae	Ribes	oxyacanthoides	Umatilla gooseberry	N	P	S	1
37	Grossulariaceae	Ribes	inerme	whitestem gooseberry	N	P	S	1
38	Grossulariaceae	Ribes	niveum	snow gooseberry	N	P	S	1
39	Hydrangeaceae	Philadelphus	lewisii	mockorange	N	P	S	1
40	Labiatae	Salvia	dorrii	purple sage	N	P	S	1
41	Polemociaceae	Leptodactylon	pungens	granite prickly phlox	N	P	S	1
42	Polygonaceae	Eriogonum	heracleiodes	Wyeth buckwheat	N	P	S	1
43	Polygonaceae	Eriogonum	microthecum	slenderbush buckwheat	N	P	S	1
44	Rosaceae	Amelanchier	alnifolia	serviceberry	N	P	S	1
45	Rosaceae	Cercocarpus	ledifolius	mountain mahogany	N	P	S	1
46	Rosaceae	Crataegus	columbiana	Columbia hawthorn	N	P	S	1

	Family	Genus	Species	Common Name	Nat / Int	Ann/ Per	Form	Observed	Expected
47	Rosaceae	Crataegus	douglasii	Douglas' hawthorn	N	P	S	1	
48	Rosaceae	Holodiscus	discolor	ocean-spray	N	P	S	1	
49	Rosaceae	Holodiscus	dumosus	dwarf ocean-spray	N	P	S	1	
50	Rosaceae	Peraphyllum	ramosissimum	squaw apple	N	P	S		1
51	Rosaceae	Purshia	tridentata	bitterbrush	N	P	S	1	
52	Rosaceae	Rosa	woodsii var. ultramontana	Woods' rose	N	P	S	1	
53	Salicaceae	Salix	amygdaloides	peach-leaf willow	N	P	S	1	
54	Salicaceae	Salix	exigua	coyote willow	N	P	S	1	
55	Salicaceae	Salix	lasiolepis	arroyo willow	N	P	S	1	
56	Salicaceae	Salix	lucida ssp. caudata	greenleaf willow	N	P	S	1	
57	Salicaceae	Salix	melanopsis	dusky willow	N	P	S	1	
58	Salicaceae	Salix	monochroma	onecolor willow	N	P	S	1	
59	Ranunculaceae	Clematis	ligusticifolia	western clematis	N	P	V	1	

Native Graminoids

	Family	Genus	Species	Common Name	Nat / Int	Ann/ Per	Form	Observed	Expected
1	Cyperaceae	Carex	amplifolia	bigleaf sedge	N	P	G	1	
2	Cyperaceae	Carex	angustata	wide-fruit sedge	N	P	G		1
3	Cyperaceae	Carex	geyeri	elk sedge	N	P	G		1
4	Cyperaceae	Carex	hystricina	porcupine sedge	N	P	G	1	
5	Cyperaceae	Carex	nebrascensis	Nebraska sedge	N	P	G		1
8	Cyperaceae	Cyperus	squarrosus	flatsedge	N	P	G	1	1
9	Cyperaceae	Eleocharis	palustris	creeping spike-rush	N	P	G	1	
10	Cyperaceae	Schoenoplectus	americanus	American bulrush	N	P	G	1	
11	Cyperaceae	Schoenoplectus	tabernaemontani	softstem bulrush	N	P	G		1
12	Cyperaceae	Scirpus	acutus	hardstem bulrush	N	P	G		1
14	Juncaceae	Juncus	balticus	baltic rush	N	P	G		1
15	Juncaceae	Juncus	bufonius	toadrush	N	P	G		1
16	Juncaceae	Juncus	ensifolius	swordleaf rush	N	P	G	1	
17	Juncaceae	Juncus	torreyi	Torrey's rush	N	P	G		1
18	Juncaceae	Juncus	tenuis	field rush	N	P	G	1	
19	Poaceae	Achnatherum	hymenoides	Indian ricegrass	N	P	G	1	
20	Poaceae	Achnatherum	thurberianum	Thurber's needlegrass	N	P	G	1	
21	Poaceae	Agrostis	stolonifera	redtop	N	P	G	1	
22	Poaceae	Bromus	ciliatus	fringed brome	N	P	G		1
23	Poaceae	Danthonia	californica	California oatgrass	N	P	G	1	
24	Poaceae	Distichlis	spicata	alkali saltgrass	N	P	G	1	
25	Poaceae	Elymus	trachycaulus	slender wheatgrass	N	P	G		1
26	Poaceae	Elymus	glaucus	blue wildrye	N	P	G	1	
27	Poaceae	Elymus	elymoides	bottlebrush squirreltail	N	P	G	1	
28	Poaceae	Festuca	idahoensis	Idaho fescue	N	P	G	1	
29	Poaceae	Glyceria	striata	tall mannagrass	N	P	G	1	
30	Poaceae	Hesperostipa	comata	needle-and-thread	N	P	G	1	
31	Poaceae	Koeleria	macrantha	prairie Junegrass	N	P	G	1	
32	Poaceae	Leymus	cinereus	basin wildrye	N	P	G	1	
33	Poaceae	Muhlenbergia	asperifolia	rough-leaved dropseed	N	P	G	1	
34	Poaceae	Phragmites	australis	common reed	N	P	G	1	
35	Poaceae	Poa	secunda	Sandberg's bluegrass	N	P	G	1	
36	Poaceae	Pseudoroegneria	spicata	bluebunch wheatgrass	N	P	G	1	
37	Poaceae	Puccinellia	lemmonii	alkali grass	N	P	G		1
38	Poaceae	Sporobolus	airoides	alkali sacaton	N	P	G		1

	Family	Genus	Species	Common Name	Nat / Int	Ann/ Per	Form	Observed	Expected
39	Poaceae	Sporobolus	cryptandrus	sand dropseed	N	P	G	1	
40	Poaceae	Vulpia	microstachys	annual fescue	N	A	G	1	
42	Typhaceae	Typha	latifolia	cat-tail	N	P	G	1	
Native Forbs									
1	Aizoaceae	Mollugo	verticillata	carpetweed	N	A	F		1
2	Alismataceae	Sagittaria	cuneata	arumleaf arrowhead	N	P	F		1
3	Amaranthaceae	Amaranthus	albus	tumble pigweed	N	A	F	1	
4	Amaranthaceae	Amaranthus	retroflexus	pigweed amaranth	N	A	F	1	
5	Apocynaceae	Apocynum	androsaemifolium	spreading dogbane	N	P	F	1	
6	Apocynaceae	Apocynum	cannibinum	hemp dogbane	N	P	F		1
7	Asclepiadaceae	Asclepias	fascicularis	narrow-leaved milkweed	N	P	F	1	
8	Asclepiadaceae	Asclepias	speciosa	showy milkweed	N	P	F	1	
9	Boraginaceae	Amsinckia	menziesii var. intermedia	common fiddleneck	N	A	F	1	
10	Boraginaceae	Amsinckia	tesselata	tesselate fiddleneck	N	A	F	1	
11	Boraginaceae	Cryptantha	affinis	slender cryptantha	N	A	F		1
12	Boraginaceae	Cryptantha	flaccida	weakstem cryptantha	N	P	F	1	
13	Boraginaceae	Cryptantha	propria	Malheur cryptantha	N	A	F	1	
14	Boraginaceae	Cryptantha	pterocarya	winged cryptantha	N	P	F	1	
15	Boraginaceae	Lithospermum	ruderales	Columbia puccoon	N	P	F	1	
16	Boraginaceae	Myosotis	discolor	changing forget-me-not	N	A	F	1	
17	Cactaceae	Opuntia	fragilis	brittle cactus	N	P	F	1	
18	Cactaceae	Opuntia	polyacantha	prickly pear	N	P	F		1
19	Cactaceae	Pediocactus	simpsonii	hedgehog-cactus	N	P	F	1	
20	Capparidaceae	Cleome	platycarpa	golden cleome	N	A	F	1	
21	Chenopodiaceae	Chenopodium	leptophyllum	narrowleaf goosefoot	N	A	F	1	
22	Chenopodiaceae	Monolepis	nuttalliana	patata	N	A	F		1
23	Asteraceae	Achillea	millefolium	yarrow	N	P	F	1	
24	Asteraceae	Agoseris	glauca	pale agoseris	N	P	F	1	
25	Asteraceae	Agoseris	heterophylla	annual agoseris	N	A	F	1	
26	Asteraceae	Anaphalis	margaritacea	pearly-everlasting	N	P	F	1	
27	Asteraceae	Antennaria	dimorpha	low pussy-toes	N	P	F	1	
28	Asteraceae	Antennaria	luzuloides	woodrush pussytoes	N	P	F	1	
29	Asteraceae	Antennaria	microphylla	littleleaf pussytoes	N	P	F	1	
30	Asteraceae	Arnica	cordifolia	heart-leaved arnica	N	P	F	1	
31	Asteraceae	Artemisia	ludoviciana	western mugwort	N	P	F	1	
32	Asteraceae	Aster	modestus	few-flowered aster	N	P	F		1
33	Asteraceae	Balsamorhiza	sagittata	arrow-leaf balsamroot	N	P	F	1	
34	Asteraceae	Balsamorhiza	serrata	serrate balsamroot	N	P	F	1	
35	Asteraceae	Bidens	cernua	beggars-ticks	N	A	F		1
36	Asteraceae	Blepharipappus	scaber	blepharipappus	N	A	F	1	
37	Asteraceae	Chaenactis	douglasii	hoary chaenactis	N	P	F	1	
38	Asteraceae	Chaenactis	nevii	John Day chaenactis	N	P	F		1
39	Asteraceae	Cirsium	undulatum	wavy-leaved thistle	N	B	F	1	
40	Asteraceae	Conyza	canadensis	horseweed	N	A	F	1	
41	Asteraceae	Conyza	canadensis	horseweed	N	P	F	1	
42	Asteraceae	Coreopsis	atkinsoniana	Columbia coreopsis	N	A	F		1
43	Asteraceae	Crepis	acuminata	long-leaved hawksbeard	N	P	F	1	
44	Asteraceae	Crepis	atribarba	slender hawksbeard	N	P	F	1	
45	Asteraceae	Crepis	intermedia	gray hawksbeard	N	P	F	1	

	Family	Genus	Species	Common Name	Nat / Int	Ann/ Per	Form	Observed	Expected
46	Asteraceae	Crepis	occidentalis	western hawksbeard	N	P	F	1	
47	Asteraceae	Crocidium	multicaule	spring gold	N	A	F		1
48	Asteraceae	Erigeron	annuus	annual fleabane	N	A	F		1
49	Asteraceae	Erigeron	filifolius	thread-leaf fleabane	N	P	F	1	
50	Asteraceae	Erigeron	foliosus	leafy fleabane	N	P	F	1	
51	Asteraceae	Erigeron	linearis	linear-leaved daisy	N	P	F	1	
52	Asteraceae	Erigeron	philadelphicus	Philadelphia fleabane	N	P	F	1	
53	Asteraceae	Eriophyllum	lanatum	wooly sunflower	N	P	F	1	
54	Asteraceae	Euthamia	occidentalis	western goldenrod	N	P	F	1	
55	Asteraceae	Gaillardia	aristata	blanket flower	N	P	F	1	
56	Asteraceae	Gnaphalium	palustre	lowland cudweed	N	A	F	1	
57	Asteraceae	Grindelia	nana	low gumweed	N	A	F	1	
58	Asteraceae	Haplopappus	armerioides	thrift goldenweed	N	P	F		1
59	Asteraceae	Haplopappus	stenophyllus	narrow-leaf goldenweed	N	P	F		1
60	Asteraceae	Helianthus	annuus	common sunflower	N	A	F	1	
61	Asteraceae	Helianthus	cusickii	Cusick's sunflower	N	P	F	1	
62	Asteraceae	Helianthus	nuttalii	Nuttall's sunflower	N	P	F	1	
63	Asteraceae	Heterotheca	oregana	Oregon goldaster	N	P	F	1	
64	Asteraceae	Hieracium	albiflorum	white hawkweed	N	P	F		1
65	Asteraceae	Hieracium	cynoglossoides	houndstongue hawkweed	N	P	F	1	
66	Asteraceae	Hymenopappus	filifolius	Columbia cut-leaf	N	P	F		1
67	Asteraceae	Iva	axillaris	poverty-weed	N	P	F		1
68	Asteraceae	Iva	xanthifolia	tall marsh-elder	N	A	F	1	
69	Asteraceae	Lactuca	serriola	tall blue lettuce	N	A	F		1
70	Asteraceae	Lagophylla	ramosissima	slender hareleaf	N	A	F		1
71	Asteraceae	Layia	glandulosa	tidytips	N	A	F	1	
72	Asteraceae	Machaeranthera	canescens	hoary aster	N	A	F	1	
73	Asteraceae	Madia	gracilis	common tarweed	N	A	F		1
74	Asteraceae	Nothocalais	troximoides	false agoseris	N	P	F	1	
75	Asteraceae	Packera	cana	wooly groundsel	N	P	F	1	
76	Asteraceae	Senecio	serra	butterweed groundsel	N	P	F	1	
77	Asteraceae	Solidago	canadensis	Canada goldenrod	N	P	F		1
78	Asteraceae	Solidago	missouriensis	Missouri goldenrod	N	P	F	1	
79	Asteraceae	Solidago	occidentalis	western goldenrod	N	P	F	1	
80	Asteraceae	Stephanomeria	minor	narrow-leaved skeletonweed	N	P	F		1
81	Asteraceae	Uropappus	lindleyi	Lindley's silverpuffs	N	A	F	1	
82	Asteraceae	Xanthium	strumarium	common cocklebur	N	A	F	1	
83	Crassulaceae	Sedum	lanceolatum	lanceleaved stonecrop	N	P	F	1	
84	Crassulaceae	Sedum	stenopetalum	wormleaf stonecrop	N	P	F	1	
85	Brassicaceae	Arabis	cusickii	Cusick's rockcress	N		F	1	
86	Brassicaceae	Arabis	holboellii	Holboell's rockcress	N		F	1	
87	Brassicaceae	Arabis	sparsiflora or lemmonii	rockcress	N		F	1	
89	Brassicaceae	Descurainia	pinnata	tansy mustard	N	A	F	1	
90	Brassicaceae	Descurainia	incana	mountain tansy mustard	N	A	F	1	
91	Brassicaceae	Erysimum	capitatum	prairie rocket	N	B	F		1
92	Brassicaceae	Erysimum	inconspicuum	small wallflower	N	B	F	1	
93	Brassicaceae	Idahoia	scapigera	scalepod	N	A	F	1	
94	Brassicaceae	Lesquerella	occidentalis	western bladderpod	N	P	F	1	
95	Brassicaceae	Phoenicautis	cheiranthoides	daggerpod	N	P	F	1	
96	Brassicaceae	Physaria	oregona	Oregon twinpod	N	P	F	1	
97	Brassicaceae	Thelypodium	laciniatum	thickleaved thelypody	N	B	F	1	

	Family	Genus	Species	Common Name	Nat / Int	Ann/ Per	Form	Observed	Expected
98	Brassicaceae	Thysanocarpus	curvipes	sand fringe-pod	N	A	F	1	
99	Ericaceae	Pterospora	andromeda	woodland pinedrops	N	A	F		1
100	Euphorbiaceae	Chamaesyce	serpyllifolia	thyme-leaf spurge	N	A	F		1
101	Euphorbiaceae	Euphorbia	glyptosperma	ridge-seeded spurge	N	A	F		1
102	Gentianaceae	Centaurium	exaltum	western centauray	N	A	F		1
103	Geraniaceae	Geranium	viscosissimum	sticky purple geranium	N	P	F		1
104	Hydrophyllaceae	Hydrophyllum	capitatum	ballhead waterleaf	N	P	F	1	
105	Hydrophyllaceae	Phacelia	hastata	whiteleaf phacelia	N	P	F	1	
108	Hydrophyllaceae	Phacelia	linearis	narrow-leafed phacelia	N	A	F	1	
109	Hydrophyllaceae	Phacelia	lutea	yellow phacelia	N	A	F		1
110	Hydrophyllaceae	Phacelia	ramosissima	branched phacelia	N	P	F		1
111	Iridaceae	Iris	missouriensis	iris	N	P	F	1	
112	Iridaceae	Olsynium	douglasii v. inflatum	grass widow	N	P	F	1	
113	Labiatae	Agastache	urticifolia	nettle-leaved horse-mint	N	P	F	1	
114	Labiatae	Mentha	arvensis	field mint	N	P	F	1	
115	Labiatae	Mentha	spicata	spearmint	N	P	F	1	
116	Labiatae	Prunella	vulgaris	self-heal	N	P	F		1
117	Labiatae	Scutellaria	angustifolia	narrow-leaved skullcap	N	P	F	1	
118	Fabiaceae	Astragalus	collinus	hillside milkvetch	N	P	F	1	
119	Fabiaceae	Astragalus	conjunctus	stiff milkvetch	N	P	F	1	
120	Fabiaceae	Astragalus	diaphanous	John Day milkvetch	N	A	F		1
121	Fabiaceae	Astragalus	filipes	basalt milkvetch	N	P	F	1	
122	Fabiaceae	Astragalus	lentiginosus	freckled milkvetch	N	P	F	1	
123	Fabiaceae	Astragalus	misellus	pauper milkvetch	N	P	F	1	
124	Fabiaceae	Astragalus	purshii	wooly-pod milkvetch	N	P	F	1	
125	Fabiaceae	Astragalus	whitneyii	balloon milkvetch	N	P	F	1	
126	Fabiaceae	Dalea	ornata	western prairie-clover	N	P	F	1	
127	Fabiaceae	Glycyrrhiza	lepidota	licorice	N	P	F	1	
128	Fabiaceae	Lathyrus	rigidus	stiff peavine	N	P	F	1	
129	Fabiaceae	Lupinus	caudatus	tailcup lupine	N	P	F	1	
130	Fabiaceae	Lupinus	lepidus	Pacific lupine	N	P	F	1	
131	Fabiaceae	Lupinus	saxosus	rock lupine	N	P	F	1	
132	Fabiaceae	Vicia	americana	American vetch	N	P	F	1	
133	Lemnaceae	Lemna	minor	water lentil	N	P	F	1	
134	Lemnaceae	Spirodela	polyrhiza	great duckweed	N	P	F		1
135	Liliaceae	Allium	acuminatum	Hooker's onion	N	P	F	1	
136	Liliaceae	Allium	tolmiei	Tolmie's onion	N	P	F	1	
137	Liliaceae	Brodiaea	douglasii	Douglas' brodiaea	N	P	F	1	
138	Liliaceae	Calochortus	macrocarpus	sagebrush mariposa	N	P	F	1	
139	Liliaceae	Erythronium	grandiflorum	pale fawn-lily	N	P	F		1
140	Liliaceae	Fritillaria	pubida	yellow bell	N	P	F	1	
141	Liliaceae	Smilacina	racemosa	western Solomon-plume	N	P	F	1	
142	Liliaceae	Veratrum	californicum	California false hellebore	N	P	F		1
143	Liliaceae	Zigadenus	paniculatus	panicked death-camas	N	P	F		1
144	Linaceae	Linum	perenne	wild blue flax	N	P	F	1	
145	Loasaceae	Mentzelia	albicaulis	small-flowered blazing-star	N	A	F		1
146	Loasaceae	Mentzelia	laevicaulis	blazing-star	N	P	F	1	
147	Malvaceae	Sphaeralcea	grossularifolia	gooseberryleaf globemallow	N	P	F	1	
148	Malvaceae	Sphaeralcea	munroana	white-stemmed globemallow	N	P	F	1	
149	Onagraceae	Camissonia	tanacetifolia	tansy-leaved evening-primrose	N	A	F		1
150	Onagraceae	Clarkia	pulchella	deer horn	N	A	F	1	

	Family	Genus	Species	Common Name	Nat / Int	Ann/ Per	Form	Observed	Expected
151	Onagraceae	Clarkia	rhomboidea	common clarkia	N	A	F		1
152	Onagraceae	Epilobium	minutum	small-flowered willow-herb	N	A	F		1
153	Onagraceae	Epilobium	ciliatum	Watson's willow-herb	N	A	F	1	
154	Onagraceae	Oenothera	caespitosa	desert evening-primrose	N	A	F		1
155	Onagraceae	Oenothera	elata ssp. Hirsutissima	Hooker's evening-primrose	N	A	F	1	
157	Orobanchaceae	Orobanche	fasciculata	Clustered broomrape	N	P	F	1	
158	Orobanchaceae	Orobanche	uniflora	naked broomrape	N	P	F	1	
159	Paeoniaceae	Paeonia	brownii	Brown's peony	N	P	F	1	
160	Plantaginaceae	Plantago	major	common plantain	N	P	F		1
161	Polemoniaceae	Collomia	grandiflora	large-flowered collomia	N	A	F	1	
162	Polemoniaceae	Collomia	linearis	narrow-leaved collomia	N	A	F		1
163	Polemoniaceae	Navaretia	divaricata	mountain navaretia	N	A	F		1
164	Polemoniaceae	Phlox	gracilis	slender phlox	N	A	F	1	
165	Polemoniaceae	Phlox	hoodii	Hood's phlox	N	P	F	1	
166	Polemoniaceae	Phlox	hoodii	moss phlox	N	P	F	1	
167	Polemoniaceae	Phlox	viscida	sticky phlox	N	P	F	1	
168	Polemoniaceae	Polemonium	micranthum	annual polemonium	N	A	F	1	
170	Polygonaceae	Eriogonum	compositum	northern buckwheat	N	P	F	1	
171	Polygonaceae	Eriogonum	elatum	tall buckwheat	N	P	F	1	
172	Polygonaceae	Eriogonum	sphaerocephalum	round-headed eriogonum	N	P	F	1	
173	Polygonaceae	Eriogonum	strictum	strict buckwheat	N	P	F	1	
174	Polygonaceae	Eriogonum	umbellatum	sulfur-flower buckwheat	N	P	F	1	
175	Polygonaceae	Eriogonum	vimineum	broom buckwheat	N	A	F	1	
176	Polygonaceae	Polygonum	amphibium	water smartweed	N	P	F		1
177	Polygonaceae	Polygonum	coccineum	water smartweed	N	P	F		1
178	Polygonaceae	Polygonum	hydropiper	smartweed	N	A	F		1
179	Polygonaceae	Polygonum	sawatchense	sawatch knotweed	N	P	F		1
180	Polygonaceae	Rumex	venosus	veiny dock	N	P	F	1	
181	Portulacaceae	Claytonia	perfoliata	miner's lettuce	N	A	F	1	
182	Portulacaceae	Lewisia	rediviva	bitterroot	N	P	F	1	
183	Potamogetonaceae	Potamogeton	natans	broad-leaved pondweed	N	P	F	1	
184	Primulaceae	Dodecatheon	conjugens	Bonneville shootingstar	N	P	F	1	
185	Ranunculaceae	Aconitum	columbianum	Columbian monkshood	N	P	F		1
186	Ranunculaceae	Actaea	rubra	western baneberry	N	P	F		1
187	Ranunculaceae	Aquilegia	formosa	red columbine	N	P	F	1	
188	Ranunculaceae	Delphinium	barbeyi	tall larkspur	N	P	F	1	
189	Ranunculaceae	Delphinium	bicolor	little larkspur	N	P	F	1	
190	Ranunculaceae	Ranunculus	aquatilis	water buttercup	N	P	F	1	
191	Ranunculaceae	Ranunculus	glaberrimus	sagebrush buttercup	N	P	F	1	
192	Ranunculaceae	Ranunculus	sceleratus	celery-leaved buttercup	N	A	F	1	
193	Ranunculaceae	Ranunculus	uncinatus	hooked buttercup	N	P	F	1	
194	Rhamnaceae	Ceanothus	sanguineus	redstem ceanothus	N	P	F	1	
195	Rhamnaceae	Ceanothus	velutinus	mountain balm	N	P	F		1
196	Rosaceae	Geum	triflorum	old man's whiskers	N	P	F	1	
197	Rosaceae	Potentilla	glandulosa	sticky cinquefoil	N	P	F	1	
198	Rosaceae	Potentilla	gracilis	cinquefoil	N	P	F	1	
199	Rosaceae	Sanguisorba	occidentalis	annual burnet	N	A	F	1	
200	Rubiaceae	Galium	aparine	bedstraw	N	A	F	1	
201	Rubiaceae	Galium	mexicanum ssp. asperrimum	Mexican bedstraw	N	A	F	1	
202	Rubiaceae	Galium	watsonii	shrubby bedstraw	N	A	F	1	

	Family	Genus	Species	Common Name	Nat / Int	Ann/ Per	Form	Observed	Expected
203	Saxifragaceae	Heuchera	cylindrica	alumroot	N	P	F	1	
204	Saxifragaceae	Lithophragma	glabrum	bulbous woodlandstar	N	P	F	1	
205	Saxifragaceae	Lithophragma	parviflorum	smallflower woodlandstar	N	P	F	1	
206	Saxifragaceae	Saxifraga	integrifolia	wholeleaf saxifrage	N	P	F	1	
207	Scrophulariaceae	Castilleja	applegatei	wavy-leaved paintbrush	N	P	F	1	
208	Scrophulariaceae	Castilleja	linariaefolia	narrow-leaved paintbrush	N	P	F		1
209	Scrophulariaceae	Castilleja	xanthotricha	yellow-hairy indian painbrush	N	P	F	1	
210	Scrophulariaceae	Collinsia	parviflora	small-flowered blue-eyed mary	N	A	F	1	
211	Scrophulariaceae	Mimulus	cusickii	Cusick's monkeyflower	N	A	F	1	
212	Scrophulariaceae	Mimulus	floribundus	purple-stemmed monkeyflower	N	A	F		1
213	Scrophulariaceae	Mimulus	guttatus	yellow monkeyflower	N	P	F	1	
214	Scrophulariaceae	Mimulus	moschatus	musk flower	N	P	F		1
215	Scrophulariaceae	Mimulus	nanus	dwarf purple monkeyflower	N	A	F		1
216	Scrophulariaceae	Mimulus	washingtonensis	Washington monkeyflower	N	A	F		1
217	Scrophulariaceae	Orthocarpus	sp.	owl-clover	N	A	F		1
218	Scrophulariaceae	Penstemon	deustus	hot-rock penstemon	N	P	F	1	
219	Scrophulariaceae	Penstemon	eriantherus	fuzzytongue penstemon	N	P	F	1	
220	Scrophulariaceae	Penstemon	richardsonii	Richardson's penstemon	N	P	F	1	
221	Scrophulariaceae	Penstemon	speciosus	royal penstemon	N	P	F	1	
222	Scrophulariaceae	Veronica	americana	American brooklime	N	P	F	1	
223	Scrophulariaceae	Veronica	anagallis-aquatica	water speedwell	N	P	F	1	
224	Scrophulariaceae	Veronica	peregrina	purslane speedwell	N	A	F		1
225	Scrophulariaceae	Veronica	serpyllifolia	thyme-leaf speedwell	N	P	F	1	
226	Solanaceae	Datura	stramonium	stramonium	N	P	F		1
227	Solanaceae	Solanum	triflorum	cut-leaved nightshade	N	A	F		1
228	Apiaceae	Angelica	dawsonii	Dawson's angelica	N	P	F	1	
229	Apiaceae	Cicuta	douglasii	western water hemlock	N	P	F	1	
230	Apiaceae	Heracleum	lanatum	cow parsnip	N	P	F	1	
231	Apiaceae	Lomatium	cous	cous biscuitroot	N	P	F	1	
232	Apiaceae	Lomatium	dissectum	fern-leaved lomatium	N	P	F	1	
233	Apiaceae	Lomatium	gormanii	Gorman's lomatium	N	P	F	1	
234	Apiaceae	Lomatium	grayi	Gray's lomatium	N	P	F	1	
235	Apiaceae	Lomatium	bicolor v. leptocarpum	slender-fruited lomatium	N	P	F	1	
236	Apiaceae	Lomatium	macrocarpum	large-fruited lomatium	N	P	F	1	
	Apiaceae	Lomatium	tamanitchii	Yakama biscuitroot	N	P	F	1	
237	Apiaceae	Lomatium	minus	John Day valley desert-parsley	N	P	F	1	
238	Apiaceae	Lomatium	nudicaule	bare-stem biscuitroot	N	P	F	1	
239	Apiaceae	Lomatium	triternatum	nine-leaved lomatium	N	P	F	1	
240	Apiaceae	Osmorhiza	occidentalis	western sweet-cicely	N	P	F	1	
241	Apiaceae	Perideridia	gairdneri	yampah	N	P	F	1	
242	Urticaceae	Urtica	dioica	stinging nettle	N	P	F	1	
243	Valerianaceae	Plectritis	macrocera	white plectritis	N	A	F	1	
244	Violaceae	Viola	nephrophylla	northern bog violet	N	P	F	1	
245	Violaceae	Viola	nuttallii	yellow prairie violet	N	P	F	1	
Native Lycopods, Ferns, and Horsetails:									
1	Polypodiaceae	Cheilanthes	gracillima	lace lip-fern	N	P	C	1	
2	Polypodiaceae	Cryptogramma	acrostichoides	American rockbrake	N	P	C	1	
3	Polypodiaceae	Cystopteris	fragilis	brittle bladder-fern	N	P	C	1	
4	Equisetaceae	Equisetum	arvense	common horsetail	N	A	C	1	
5	Equisetaceae	Equisetum	hyemale	common scouring-rush	N	P	C		1

	Family	Genus	Species	Common Name	Nat / Int	Ann/ Per	Form	Observed	Expected
6	Equisetaceae	Equisetum	pratense	shady horsetail	N	A	C		1
7	Equisetaceae	Equisetum	variegatum	variegated horsetail	N	P	C		1
8	Marsileaceae	Marsilea	vestita	pepperwort	N		C	1	
9	Polypodiaceae	Polystichum	sp.	sword-fern	N	P	C	1	
10	Selaginellaceae	Selaginella	watsonii	Watson's club-moss	N	P	C	1	
Introduced Trees and Shrubs									
1	Aceraceae	Acer	negundo	box-elder	I	P	T	1	
2	Eleagnaceae	Eleagnus	angustifolia	Russian olive	I	P	T	1	
3	Fabiaceae	Robinia	pseudo-acacia	black locust	I	P	T	1	
4	Moraceae	Morus	alba	white mulberry	I	P	T	1	
5	Rosaceae	Pyrus	communis	pear	I	P	T	1	
6	Rosaceae	Pyrus	malus	apple	I	P	T	1	
7	Salicaceae	Populus	alba	white poplar	I	P	T	1	
8	Salicaceae	Populus	nigra v. italica	Lombardy poplar	I	P	T	1	
9	Ulmaceae	Ulmus	pumila	Siberian elm	I	P	T	1	
10	Rosaceae	Rosa	canina	dog rose	I	P	S		1
11	Rosaceae	Rosa	eglantaria	sweetbriar	I	P	S	1	
12	Rosaceae	Rubus	discolor	Himalayan blackberry	I	P	S	1	
13	Rosaceae	Rubus	laciniatus	evergreen blackberry	I	P	S	1	
14	Solanaceae	Lycium	barbarum	matrimony vine	I	P	S	1	
Introduced Graminoids									
1	Poaceae	Aegilops	cylindrica	jointed goatgrass	I	A	G	1	
2	Poaceae	Agropyron	cristatum	crested wheatgrass	I	P	G	1	
3	Poaceae	Agropyron	repens	quack grass	I	P	G	1	
4	Poaceae	Arrhenatherum	elatius	tall oatgrass	I	P	G	1	
5	Poaceae	Avena	fatua	wild oats	I	A	G	1	
6	Poaceae	Bromus	briziformis	rattlesnake grass	I	A	G	1	
7	Poaceae	Bromus	commutatus	hairy brome	I	A	G	1	
8	Poaceae	Bromus	diandrus	ripgut brome	I	A	G	1	
9	Poaceae	Bromus	japonicus	Japanese brome	I	A	G	1	
10	Poaceae	Bromus	hordeaceus	soft brome	I	A	G	1	
11	Poaceae	Bromus	rubens	foxtail brome	I	A	G		1
12	Poaceae	Bromus	tectorum	cheatgrass	I	A	G	1	
13	Poaceae	Crypsis	alopecuroides	Helechloa	I	A	G		1
14	Poaceae	Dactylis	glomerata	orchard-grass	I	P	G	1	
15	Poaceae	Echinochloa	crus-galli	barnyardgrass	I	P	G	1	
16	Poaceae	Eragrostis	cilianensis	candy grass	I	A	G	1	
17	Poaceae	Eremopyrum	triticeum	annual wheatgrass	I	A	G	1	
18	Poaceae	Hordeum	murinum	charming barley	I	P	G	1	
19	Poaceae	Hordeum	jubatum	foxtail barley	I	P	G	1	
20	Poaceae	Hordeum	vulgare	cultivated barley	I	A	G		1
21	Poaceae	Lolium	pratense	meadow fescue	I	P	G	1	
22	Poaceae	Panicum	capillare	witchgrass	I	P	G		1
23	Poaceae	Pascopyrum	smithii	western wheatgrass	I	P	G	1	
24	Poaceae	Pennisetum	glaucum	yellow bristlegrass	I	A	G		1
25	Poaceae	Phalaris	arundinacea	reed canarygrass	I	P	G	1	
26	Poaceae	Phleum	pratense	common timothy	I	P	G	1	
27	Poaceae	Poa	bulbosa	bulbous bluegrass	I	P	G	1	

	Family	Genus	Species	Common Name	Nat / Int	Ann/ Per	Form	Observed	Expected
28	Poaceae	Poa	compressa	Canada bluegrass	I	P	G	1	
29	Poaceae	Poa	pratensis	Kentucky bluegrass	I	P	G	1	
30	Poaceae	Polypogon	monospeliensis	rabbitfoot grass	I	A	G		
31	Poaceae	Secale	cereale	cereal rye	I	A	G	1	
32	Poaceae	Setaria	viridis	green bristlegrass	I	A	G		1
33	Poaceae	Taeniatherum	caput-medusae	medusahead	I	A	G	1	
34	Poaceae	Thinopyrum	ponticum	rush wheatgrass	I	P	G	1	
35	Poaceae	Triticum	asperum	cultivated wheat	I	A	G	1	
36	Poaceae	Ventenata	dubia	vententata	I	A	G	1	
37	Poaceae	Vulpia	myuros	foxtail fescue	I	A	G	1	
Introduced Forbs									
1	Boraginaceae	Asperugo	procumbens	madwort	I	A	F	1	
2	Boraginaceae	Cynoglossum	officinale	common hounds-tongue	I	B	F	1	
3	Caryophyllaceae	Cerastium	glomeratum	sticky chickweed	I	A	F	1	
4	Caryophyllaceae	Holosteum	umbellatum	jagged chickweed	I	A	F	1	
5	Caryophyllaceae	Saponaria	officinalis	bouncing bet	I	P	F	1	
6	Chenopodiaceae	Bassia	hyssopifolia	bassia	I	A	F		1
7	Chenopodiaceae	Chenopodium	album	lambsquarter	I	A	F	1	
8	Chenopodiaceae	Chenopodium	botrys	Jerusalem-oak	I	A	F		1
9	Chenopodiaceae	Kochia	scoparia	mock cypress	I	A	F	1	
10	Chenopodiaceae	Salsola	kali	Russian thistle	I	A	F	1	
11	Asteraceae	Acroptilon	repens	Russian knapweed	I	P	F	1	
12	Asteraceae	Ambrosia	tomentosa	skeletonleaf bursage	I	P	F	1	
13	Asteraceae	Anthemis	cotula	mayweed chamomile	I	A	F	1	
14	Asteraceae	Arctium	minus	common burdock	I	P	F	1	
15	Asteraceae	Centaurea	cyanus	bachelor's buttons	I	P	F	1	
16	Asteraceae	Centaurea	diffusa	diffuse knapweed	I	P	F	1	
17	Asteraceae	Centaurea	maculosa	spotted knapweed	I	P	F	1	
18	Asteraceae	Centaurea	solstitialis	yellow star-thistle	I	B	F	1	
19	Asteraceae	Cichorium	intybus	chicory	I	P	F	1	
20	Asteraceae	Cirsium	arvense	Canada thistle	I	P	F	1	
21	Asteraceae	Cirsium	vulgare	bull thistle	I	B	F	1	
22	Asteraceae	Lactuca	serriola	prickly lettuce	I	A	F	1	
23	Asteraceae	Onopordum	acanthium	Scotch thistle	I	B	F	1	
24	Asteraceae	Sonchus	asper	prickly sow-thistle	I	A	F	1	
25	Asteraceae	Tanacetum	vulgare	common tansy	I	A	F		1
26	Asteraceae	Taraxacum	officinale	dandelion	I	P	F	1	
27	Asteraceae	Tragopogon	dubius	yellow salsify	I	A	F	1	
28	Convolvulaceae	Convolvulus	arvensis	field morning-glory	I	P	F	1	
29	Brassicaceae	Alyssum	alyssoides	pale allysum	I	A	F	1	
30	Brassicaceae	Camelina	microcarpa	littlepod falseflax	I	A	F	1	
31	Brassicaceae	Capsella	bursa-pastoris	shepherd's-purse	I	A	F	1	
32	Brassicaceae	Cardaria	draba	whitetop	I	P	F	1	
33	Brassicaceae	Chorispora	tenella	blue mustard	I	A	F	1	
34	Brassicaceae	Draba	verna	spring whitlow-grass	I	A	F	1	
35	Brassicaceae	Lepidium	perfoliatum	clasping pepperweed	I	A	F	1	
36	Brassicaceae	Rorippa	nasturtium-aquaticum	water-cress	I	P	F	1	
37	Brassicaceae	Sisymbrium	altissimum	tumblemustard	I	A	F	1	
38	Brassicaceae	Sisymbrium	loeselii	small tumbleweed mustard	I	A	F	1	
39	Dipsacaceae	Dipsacus	sylvestris	teasel	I	B/P	F	1	

	Family	Genus	Species	Common Name	Nat / Int	Ann / Per	Form	Observed	Expected
40	Geraniaceae	Erodium	cicutarium	filaree	I	A	F	1	
41	Hypericaceae	Hypericum	perforatum	St.John's-wort	I	P	F	1	
42	Labiatae	Lamium	amplexicaule	common hen-bit	I	A	F	1	
43	Labiatae	Marrubium	vulgare	horehound	I	P	F	1	
44	Labiatae	Mentha	piperita	peppermint	I	P	F		1
45	Labiatae	Nepeta	cararia	catnip	I	P	F		1
46	Fabiaceae	Medicago	lupulina	black medic	I	A	F	1	
47	Fabiaceae	Medicago	sativa	alfalfa	I	P	F	1	
48	Fabiaceae	Melilotus	officinalis	white sweet-clover	I	B	F	1	
49	Fabiaceae	Trifolium	dubium	suckling clover	I	A	F	1	
50	Fabiaceae	Trifolium	repens	white clover	I	P	F	1	
51	Liliaceae	Asparagus	officinalis	asparagus	I	P	F	1	
52	Malvaceae	Malva	neglecta	cheeseweed	I	P	F	1	
53	Onagraceae	Epilobium	angustifolium	fireweed	I	A	F	1	
54	Plantaginaceae	Plantago	lanceolata	English plantain	I	P	F	1	
55	Polygonaceae	Rumex	acetosella	sheep sorrel	I	P	F	1	
56	Polygonaceae	Rumex	crispus	curly dock	I	P	F	1	
57	Portulacaceae	Portulaca	oleracea	common purslane	I	A	F	1	
58	Ranunculaceae	Ceratocephala	testiculatus	hornseed buttercup	I	A	F	1	
61	Scrophulariaceae	Linaria	dalmatica	Dalmatian toadflax	I	P	F	1	
62	Scrophulariaceae	Verbascum	blattaria	moth mullein	I	B	F	1	
63	Scrophulariaceae	Verbascum	thapsus	common mullein	I	B	F	1	
64	Solanaceae	Hyoscyamus	niger	black henbane	I	A	F		1
65	Solanaceae	Nicotiana	acuminata	wild tobacco	I	A/P	F	1	
66	Solanaceae	Nicotiana	attenuata	coyote tobacco	I	A/P	F	1	
67	Solanaceae	Physalis	longifolia	ground-cherry	I	P	F		1
68	Solanaceae	Solanum	dulcamara	bittersweet	I	P	F	1	
69	Apiaceae	Anthriscus	scandicina	bur chervil	I	A	F	1	
70	Apiaceae	Conium	maculatum	poison hemlock	I	P	F	1	
71	Apiaceae	Daucus	carota	Queen Anne's lace	I	B	F	1	
72	Apiaceae	Pastinaca	sativa	parsnip	I	P	F		1
73	Valerianaceae	Valerianella	locusta	European corn-salad	I	A	F		1
74	Zygophyllaceae	Tribulus	terrestris	puncture-vine	I	A	F	1	